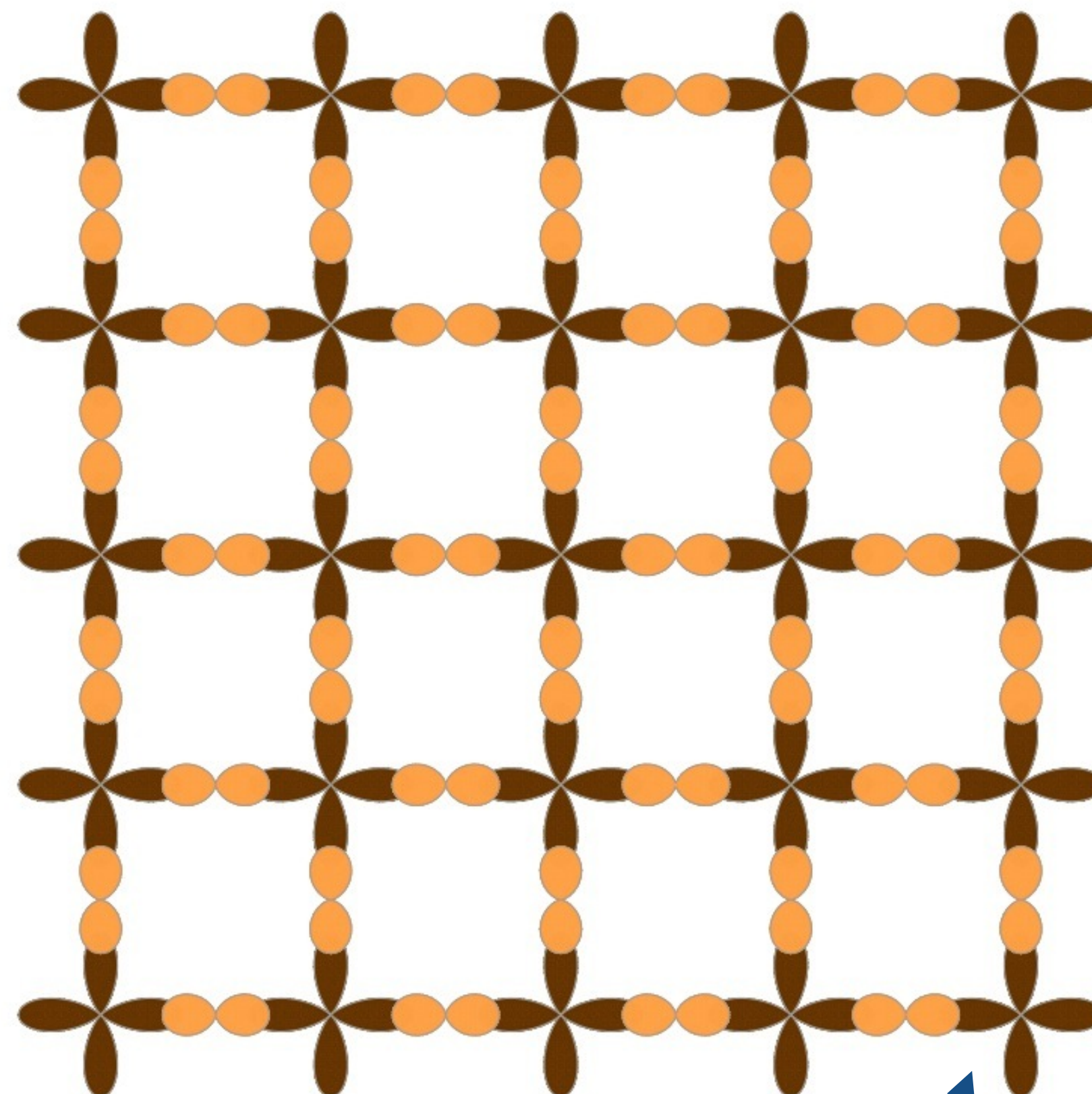
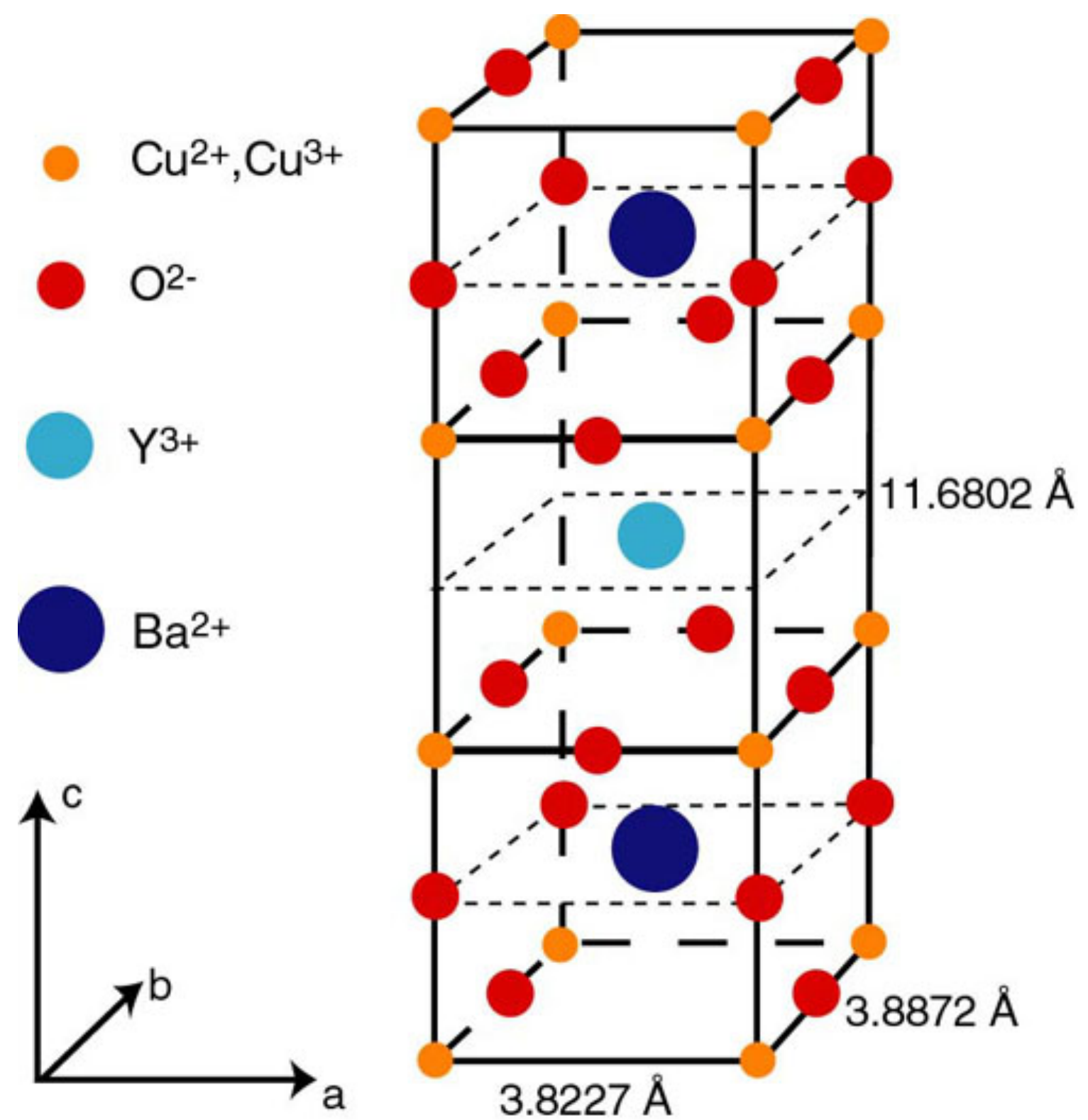


Detecting spin liquid quantum entanglement by measuring Fermi surfaces

Young Investigators Meet on Quantum Condensed Matter Theory 2025
Indian Institute of Science Education and Research, Tirupati
December 21, 2025

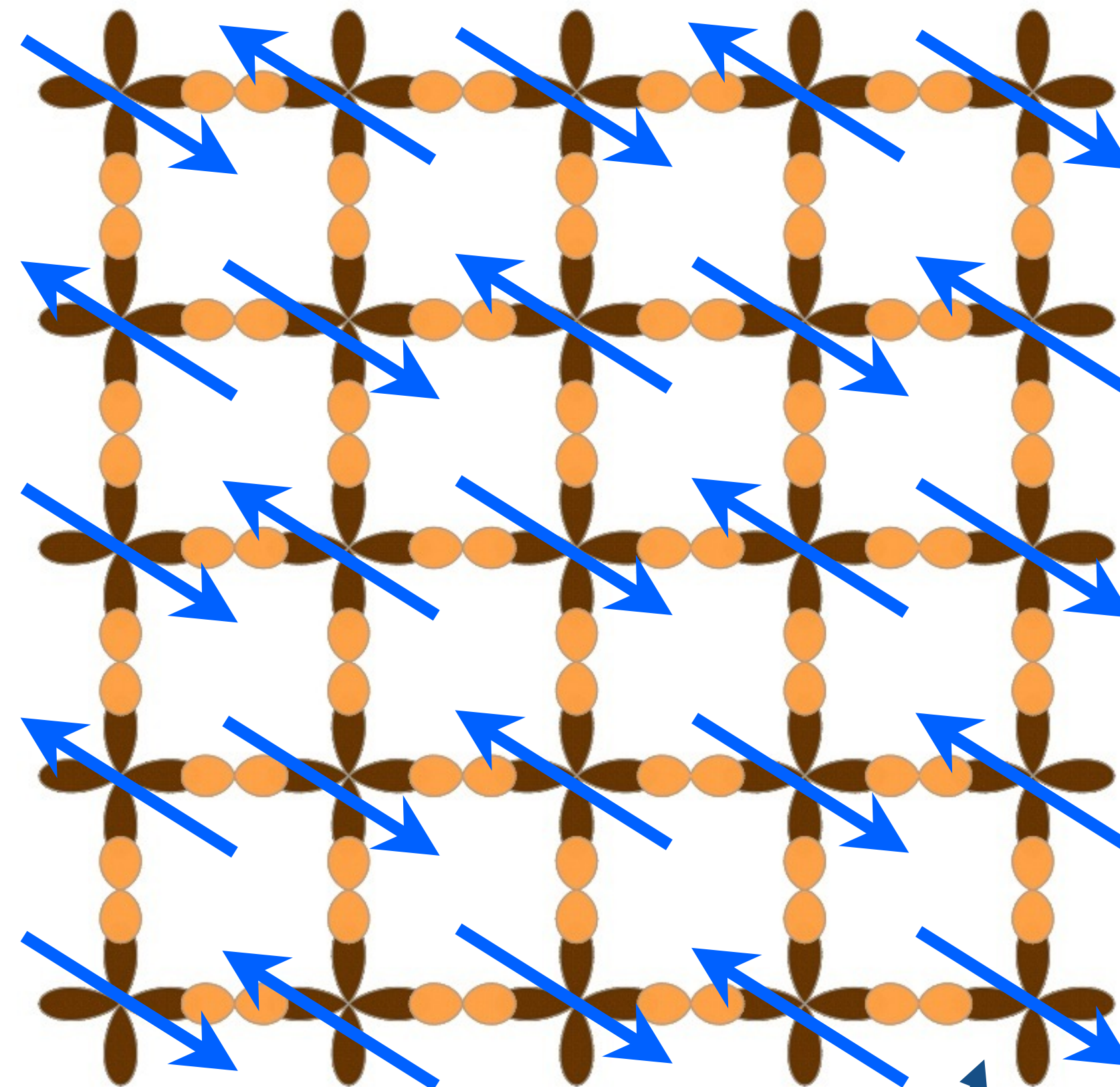
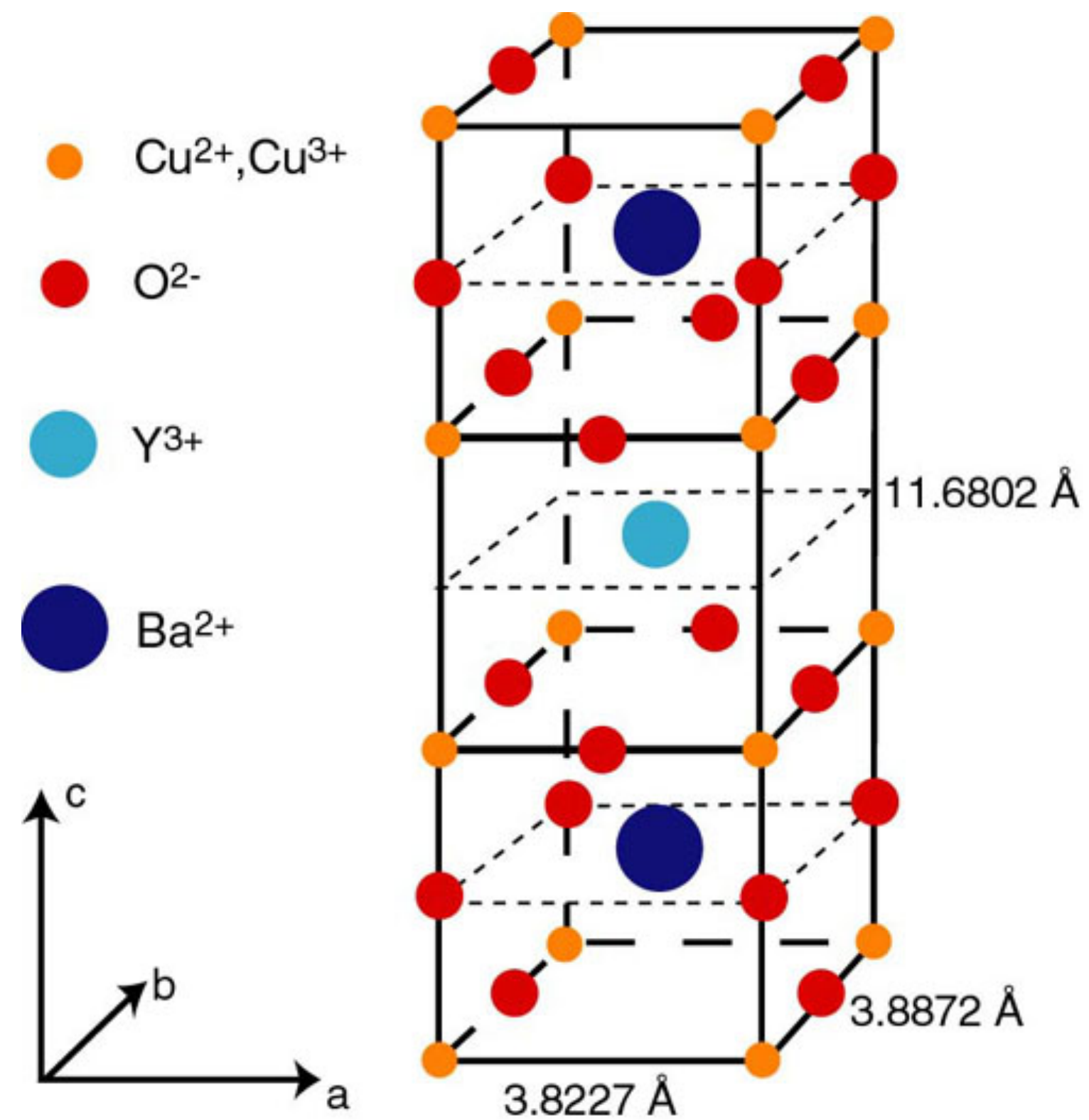
Subir Sachdev





Cu

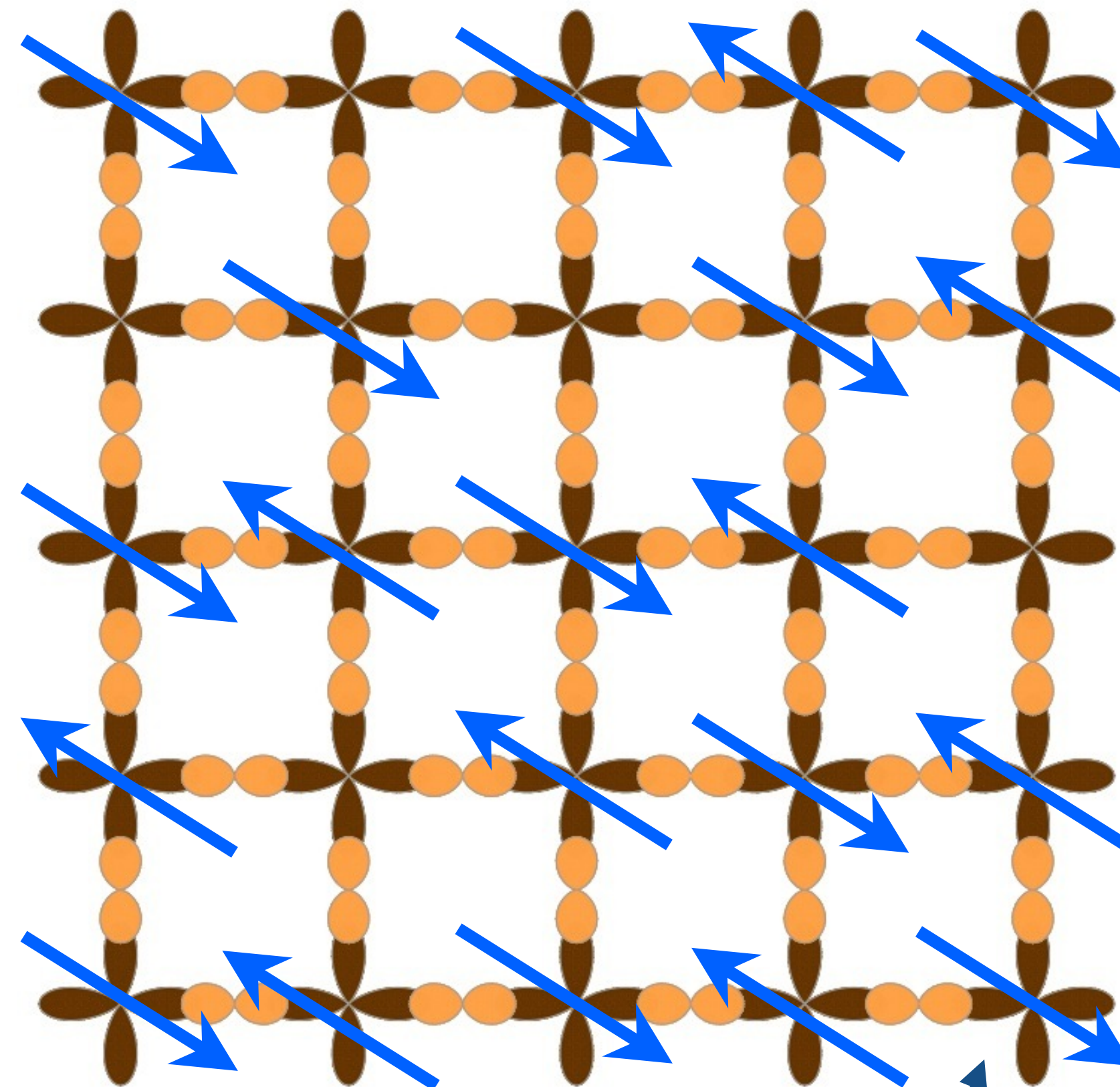
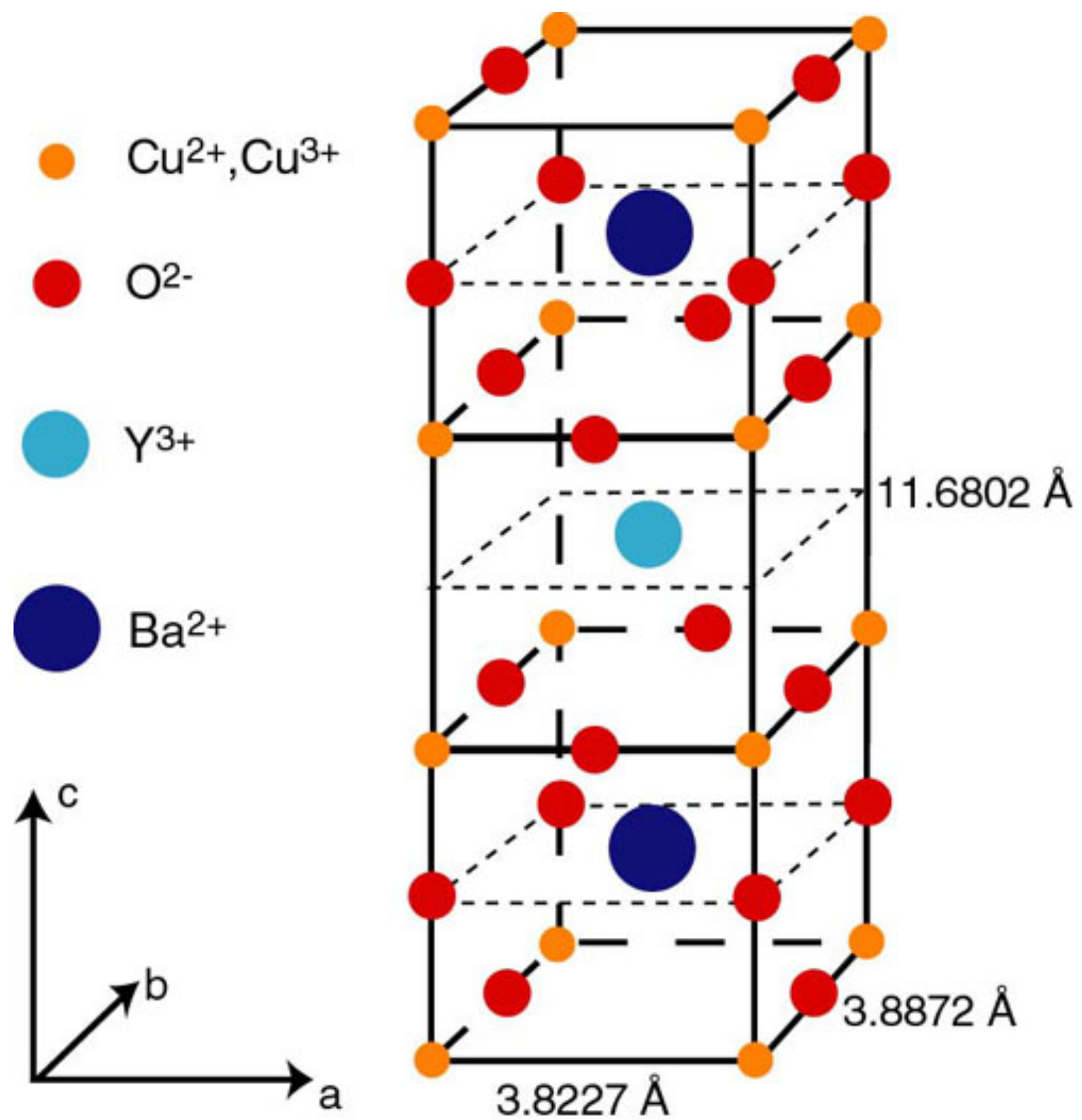




Cu

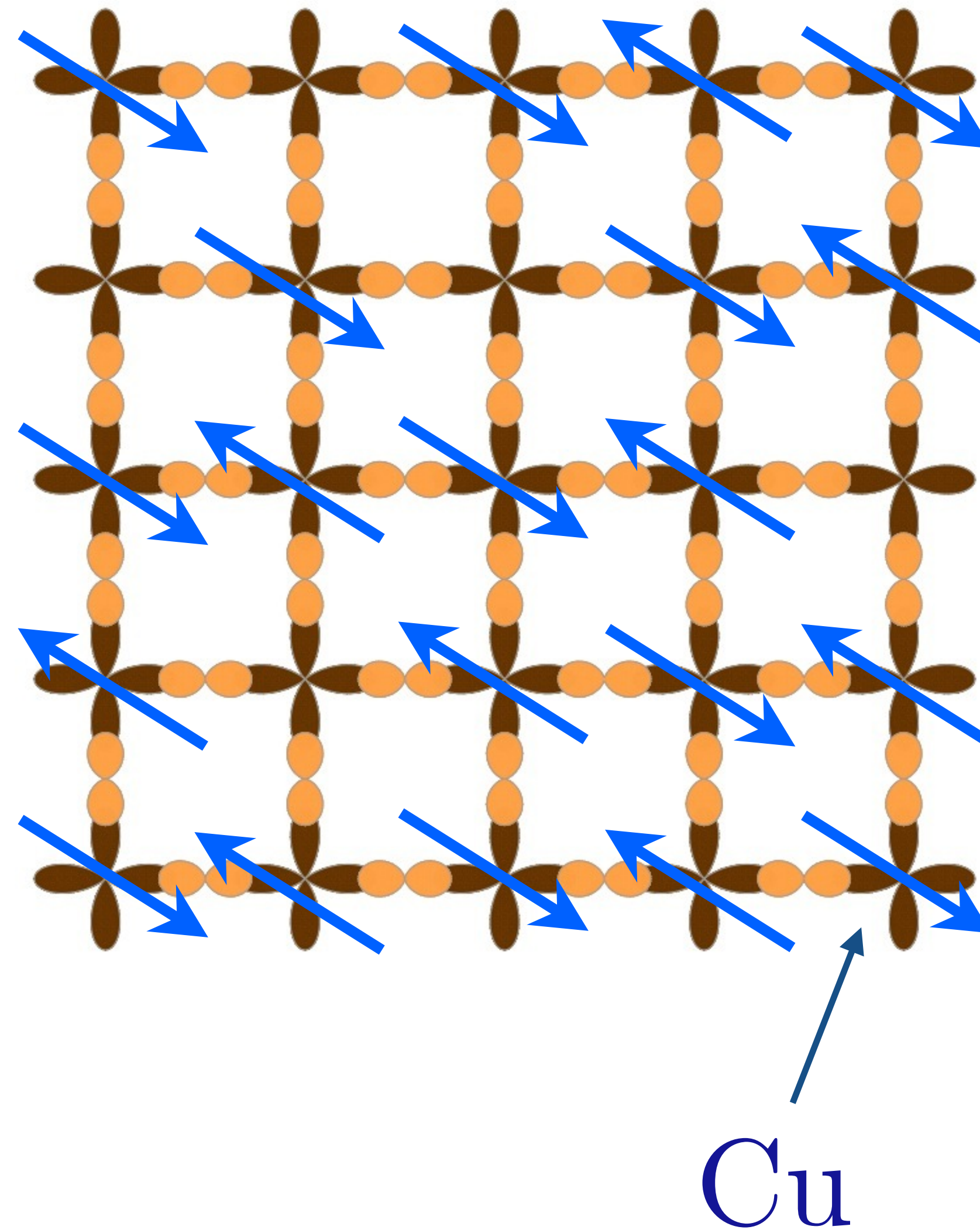
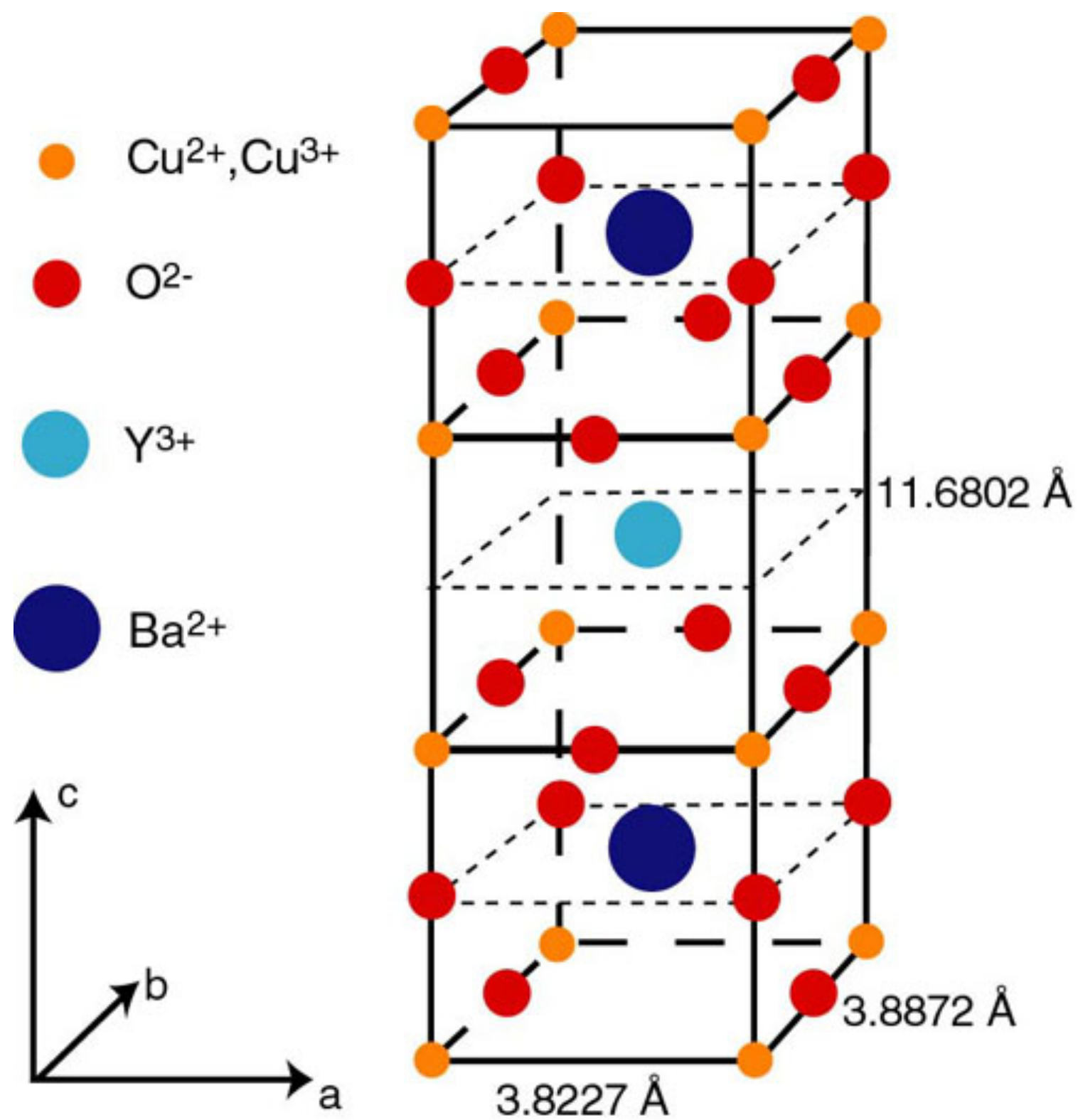


Insulating antiferromagnet with one electron per site

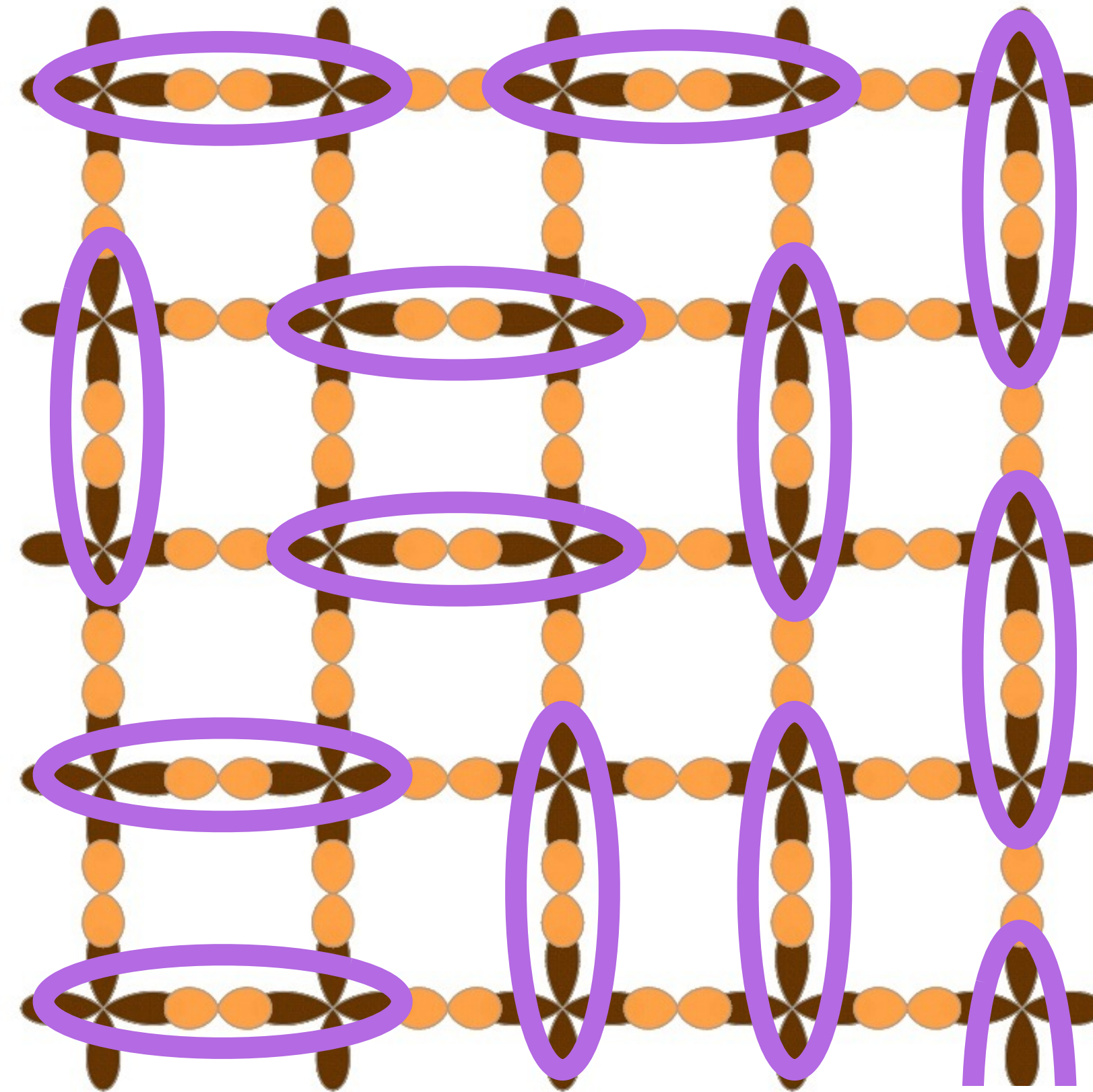
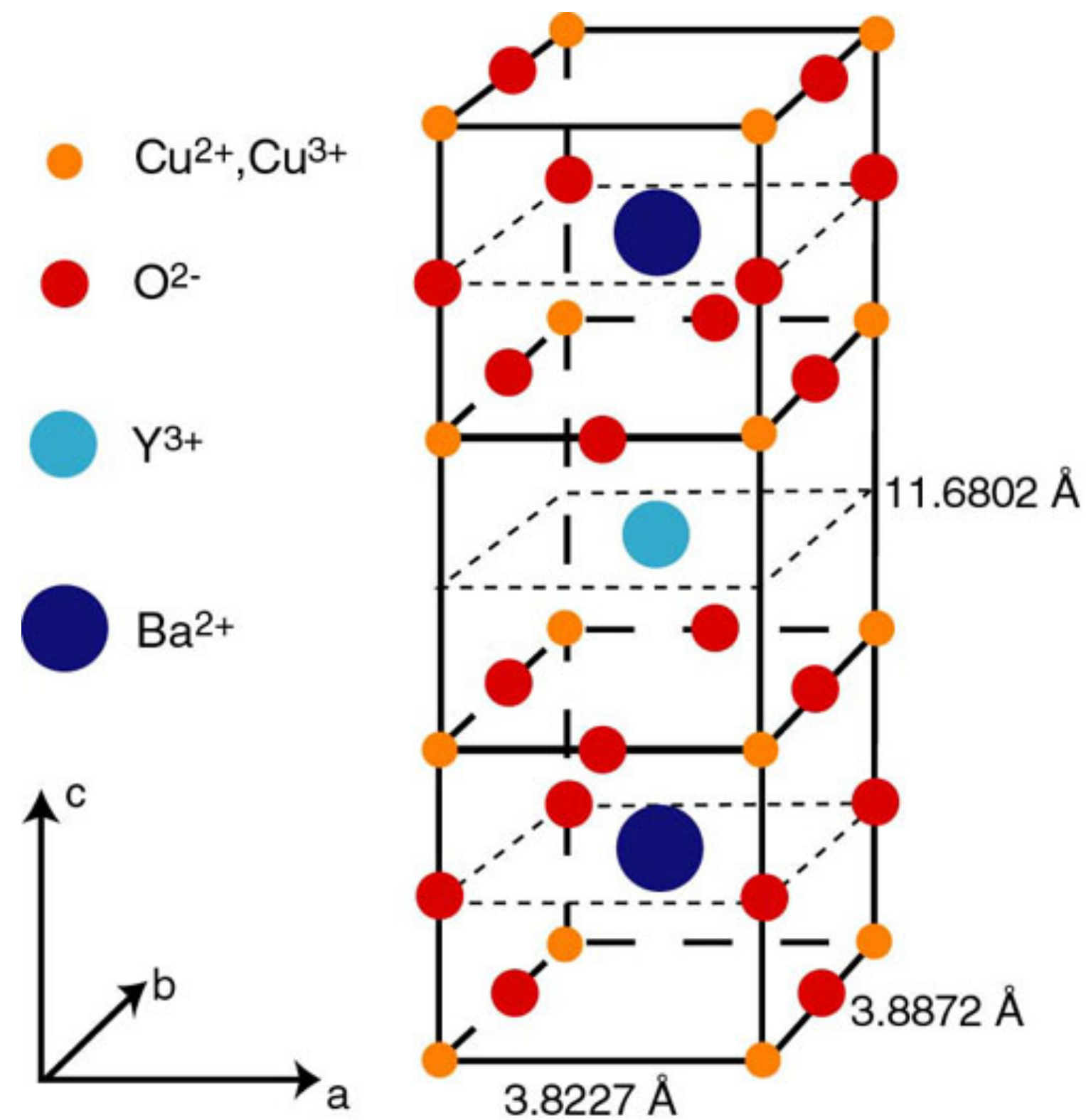


Cu

High
 temperature
 superconductor
 obtained upon
 doping the
 antiferromagnet
 with density p
 holes.



High
 temperature
 superconductor
 obtained upon
 doping the
 antiferromagnet
 with density p
 holes.
 Hole density
 relative to the
 filled band
 $\rho = 1 + p.$



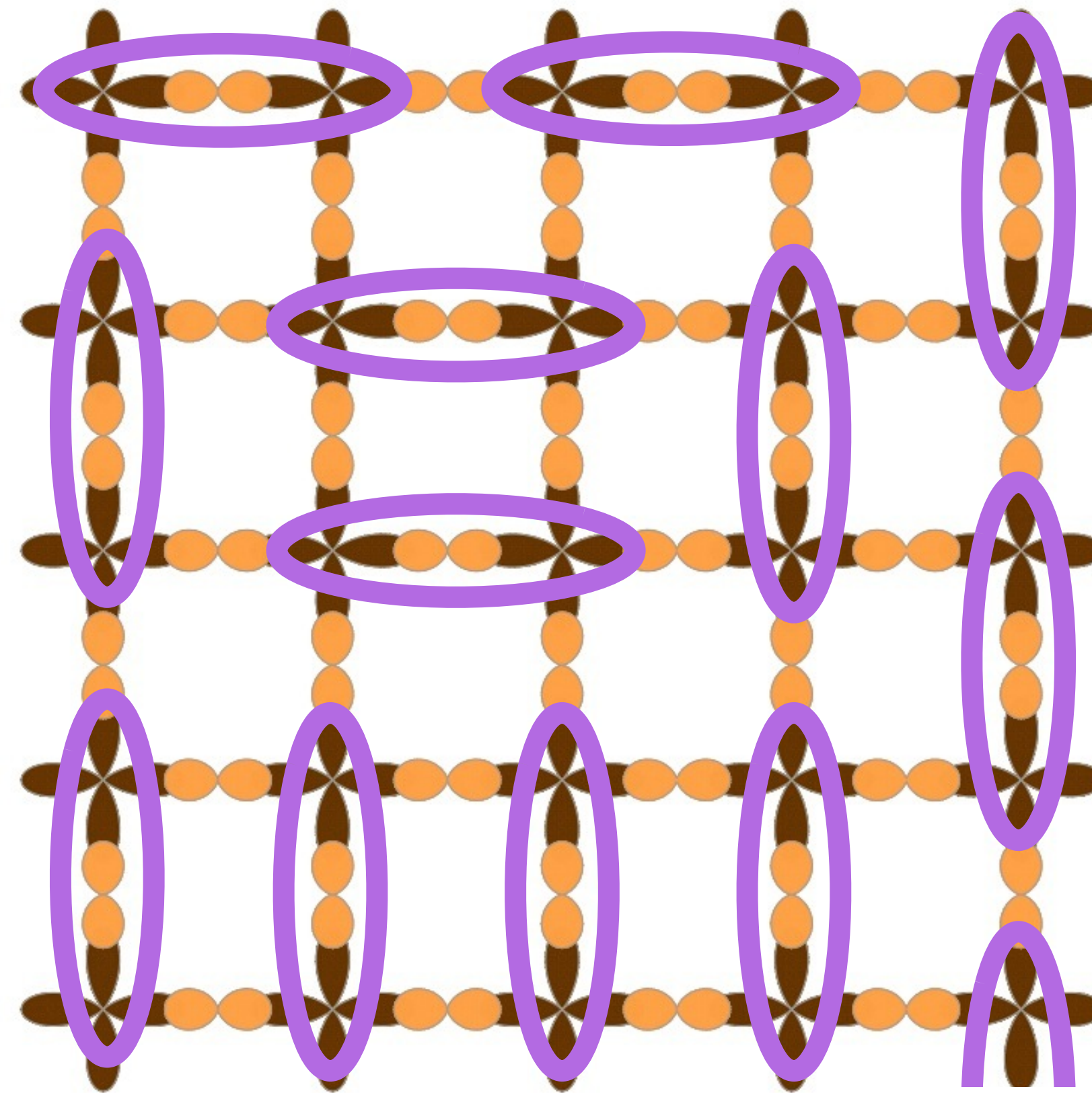
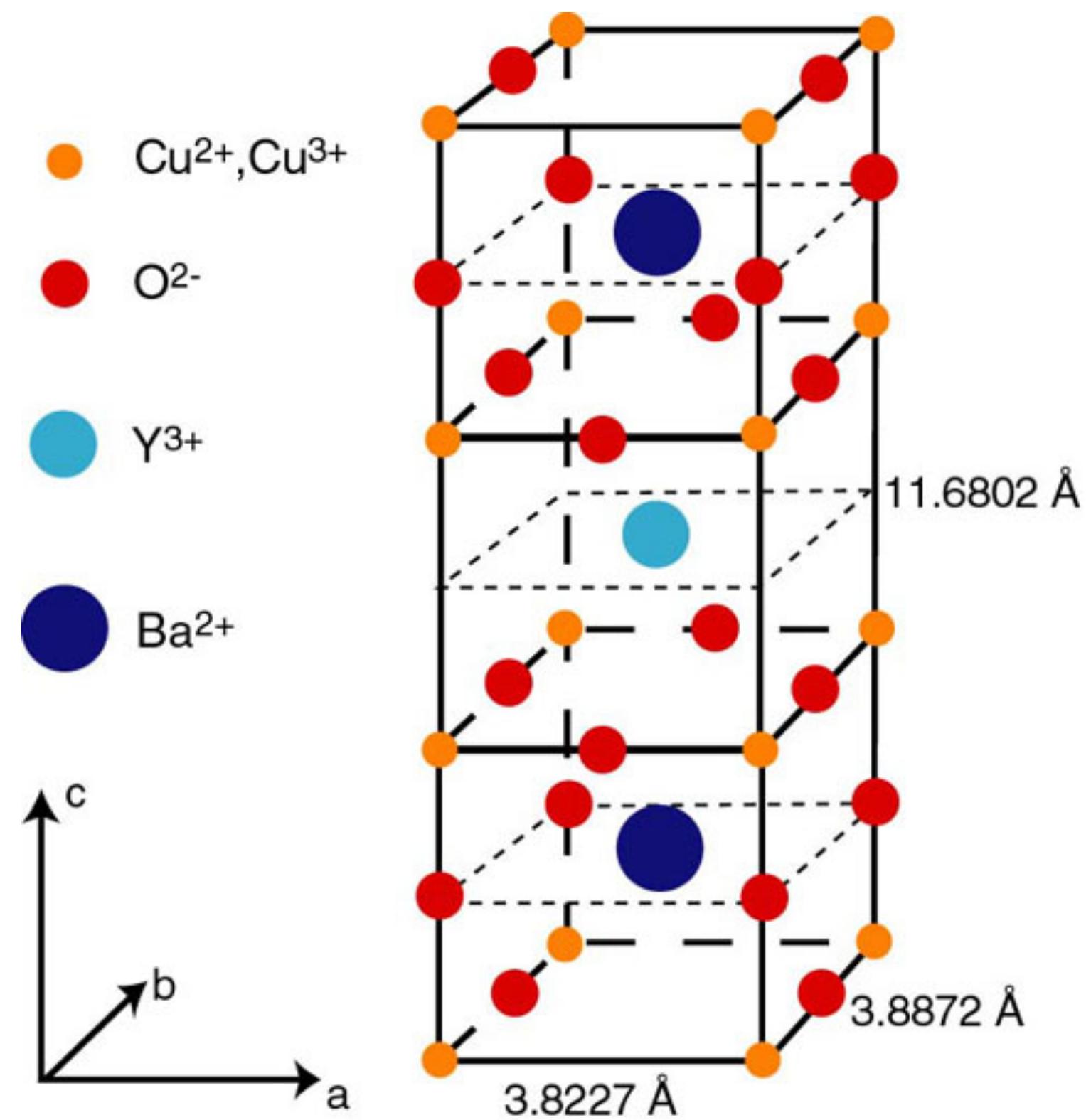
$$|G\rangle = \sum_{\mathcal{D}} c_{\mathcal{D}} |\mathcal{D}\rangle$$

$\mathcal{D} \rightarrow$ dimer covering
 of lattice



$$\text{Oval} = \frac{1}{\sqrt{2}} (|\uparrow\downarrow\rangle - |\downarrow\uparrow\rangle)$$

P.W.Anderson and G. Baskaran (1988): The key to high temperature superconductivity
 is the formation of a “resonating valence bond state”
 (a type of **quantum spin liquid**) which entangles the electrons on Cu



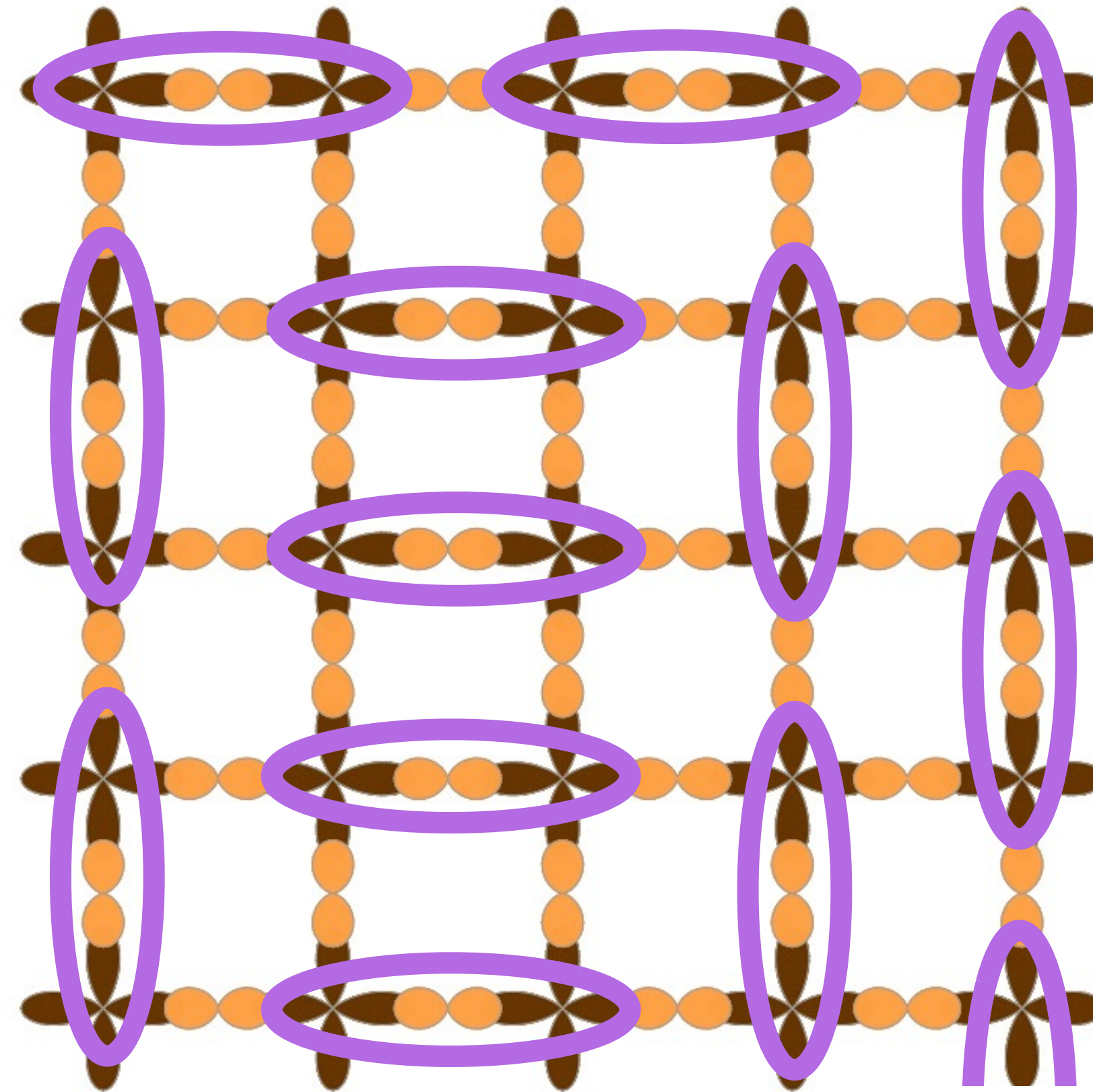
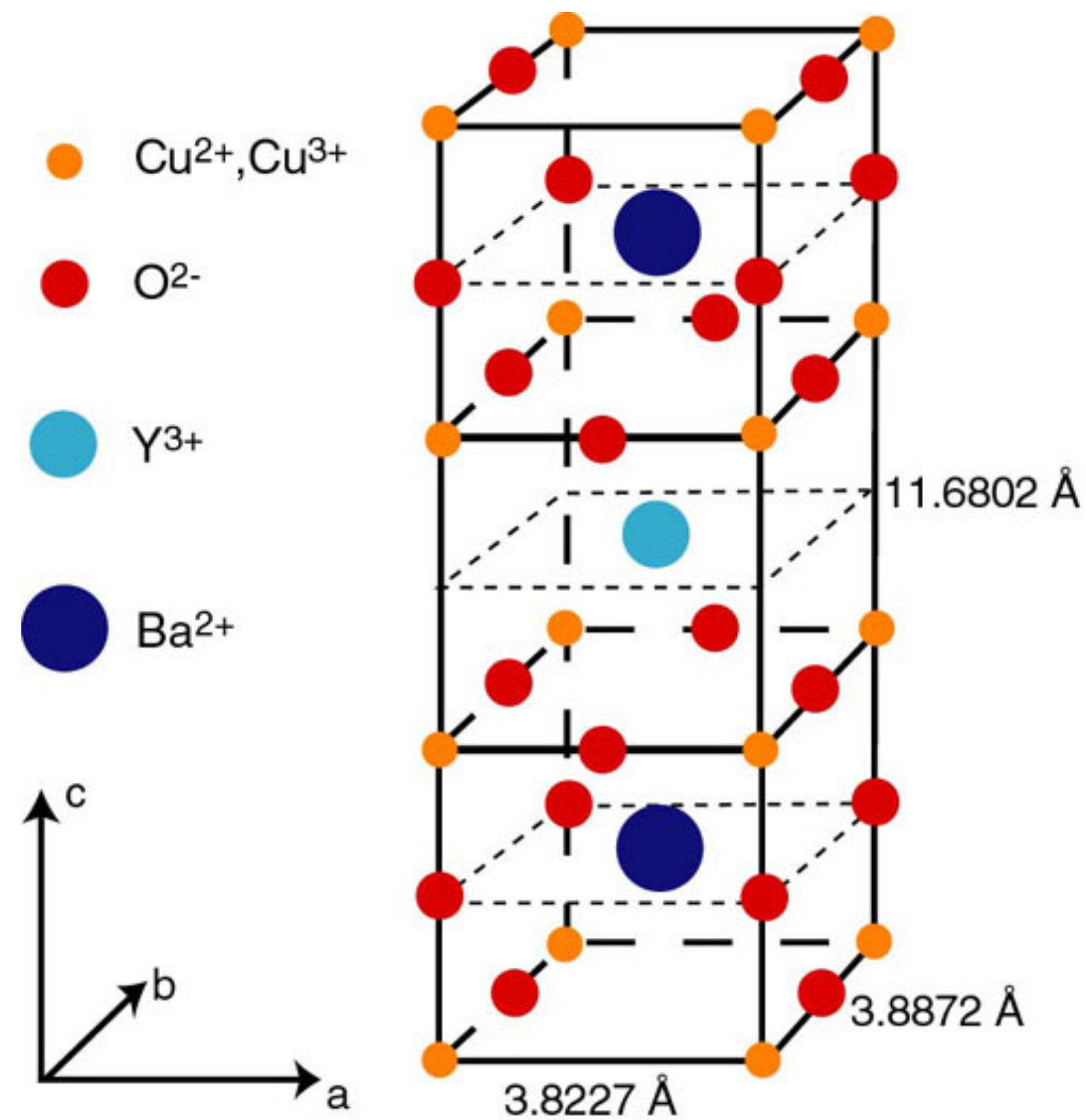
$$|G\rangle = \sum_{\mathcal{D}} c_{\mathcal{D}} |\mathcal{D}\rangle$$

$\mathcal{D} \rightarrow$ dimer covering
 of lattice



$$= \frac{1}{\sqrt{2}} (|\uparrow\downarrow\rangle - |\downarrow\uparrow\rangle)$$

P.W.Anderson and G. Baskaran (1988): The key to high temperature superconductivity
 is the formation of a “resonating valence bond state”
 (a type of **quantum spin liquid**) which entangles the electrons on Cu



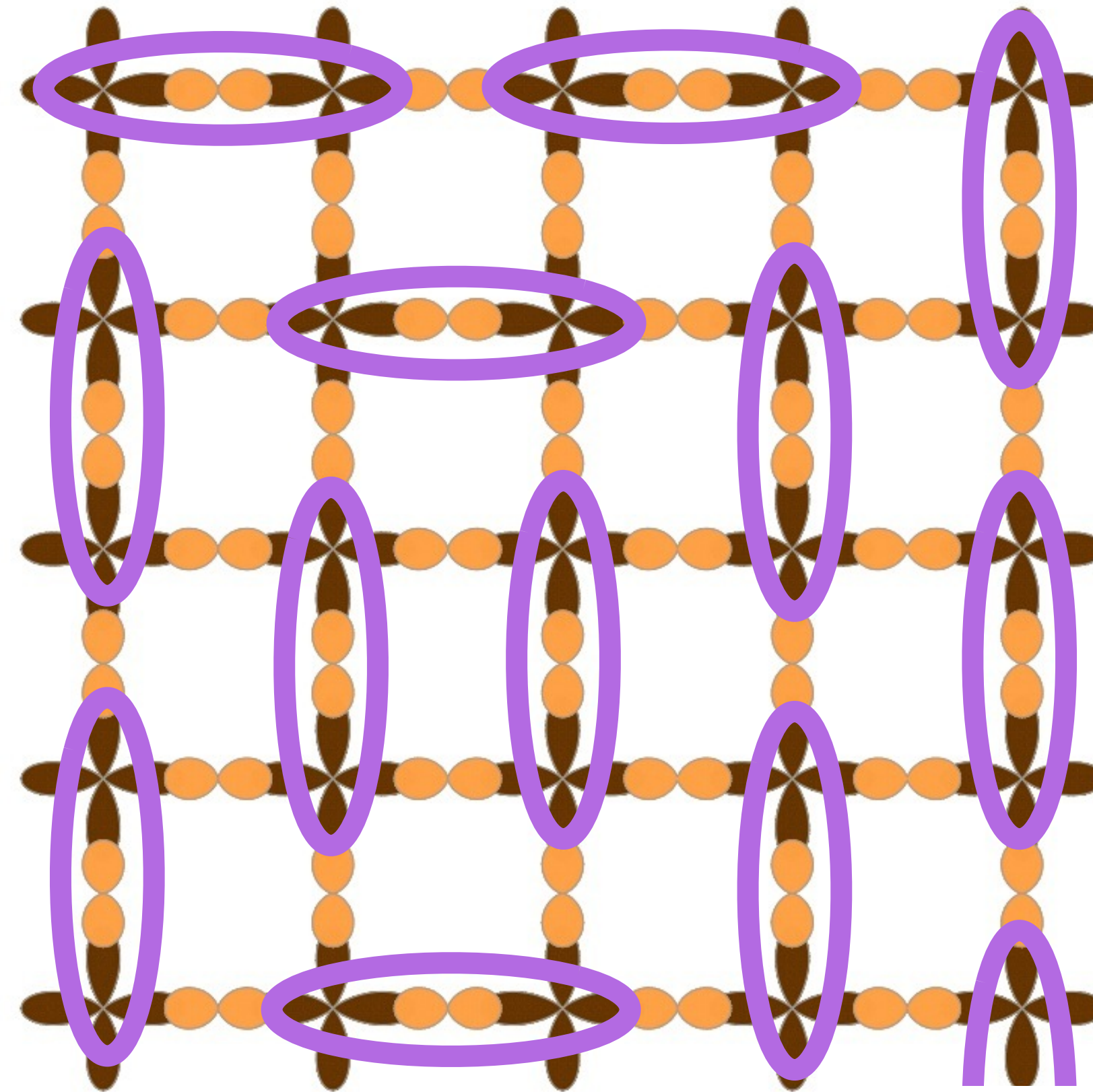
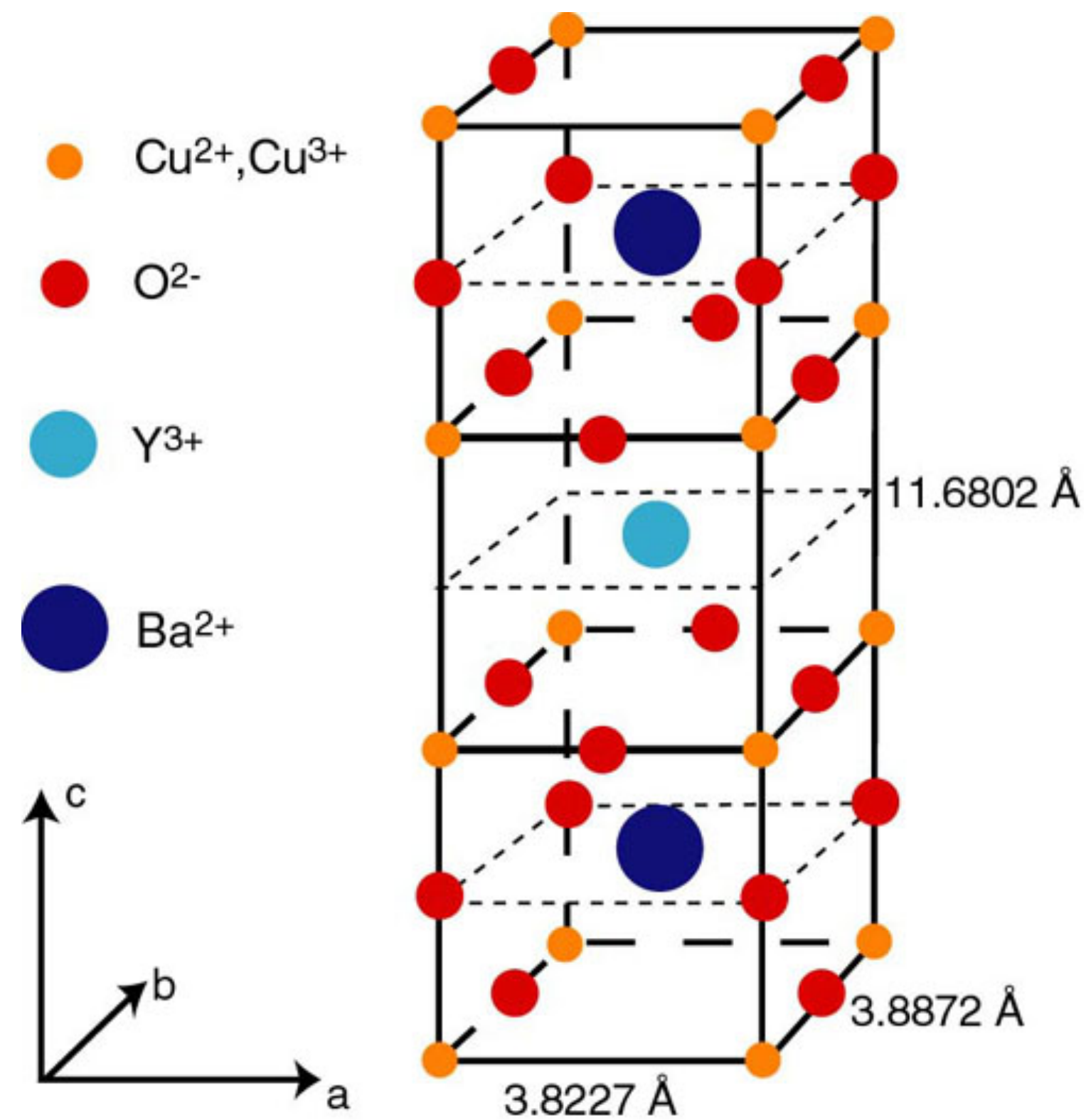
$$|G\rangle = \sum_{\mathcal{D}} c_{\mathcal{D}} |\mathcal{D}\rangle$$

$\mathcal{D} \rightarrow$ dimer covering
 of lattice



$$= \frac{1}{\sqrt{2}} (|\uparrow\downarrow\rangle - |\downarrow\uparrow\rangle)$$

P.W.Anderson and G. Baskaran (1988): The key to high temperature superconductivity
 is the formation of a “resonating valence bond state”
 (a type of **quantum spin liquid**) which entangles the electrons on Cu



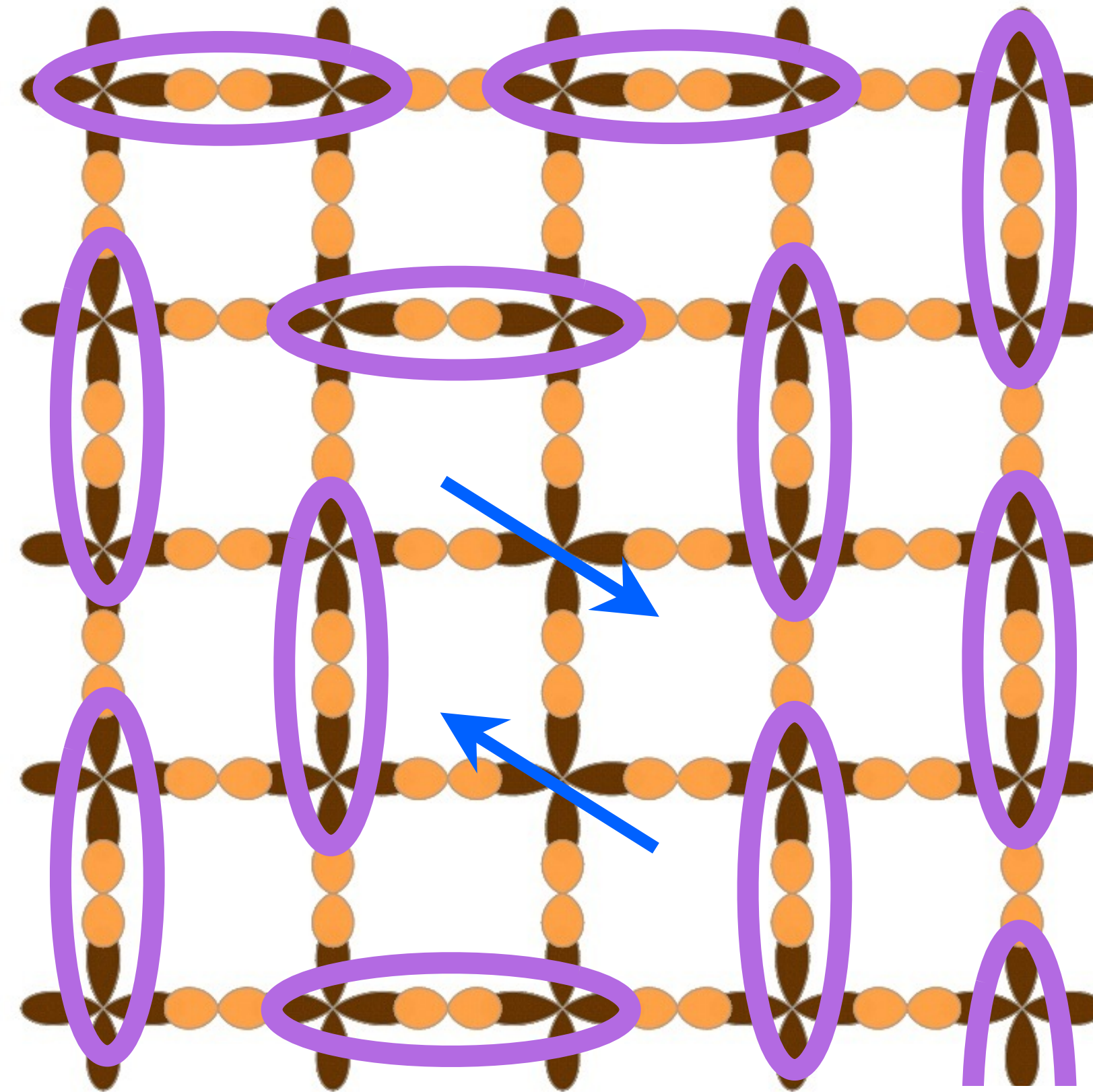
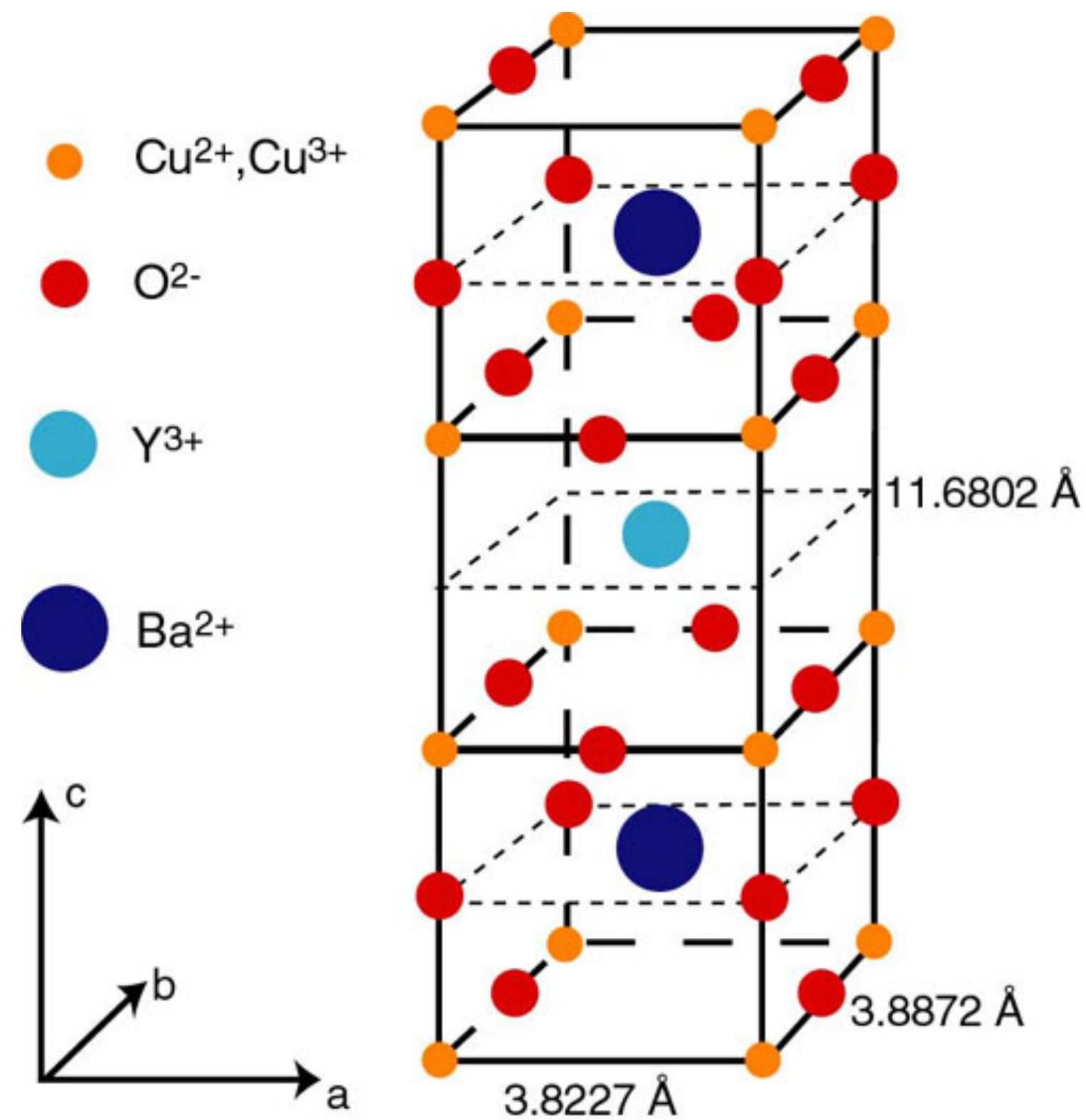
$$|G\rangle = \sum_{\mathcal{D}} c_{\mathcal{D}} |\mathcal{D}\rangle$$

$\mathcal{D} \rightarrow$ dimer covering
 of lattice

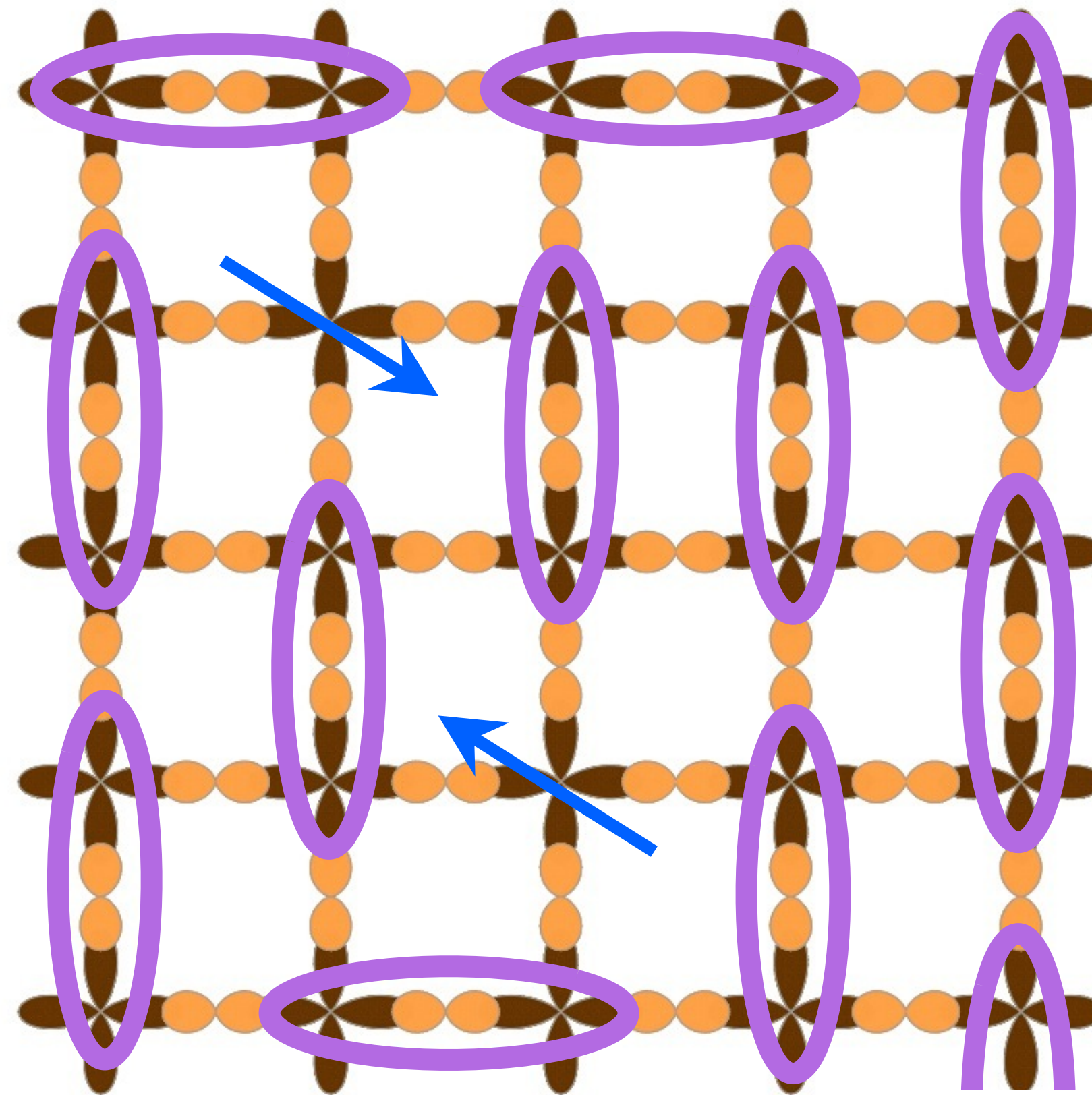
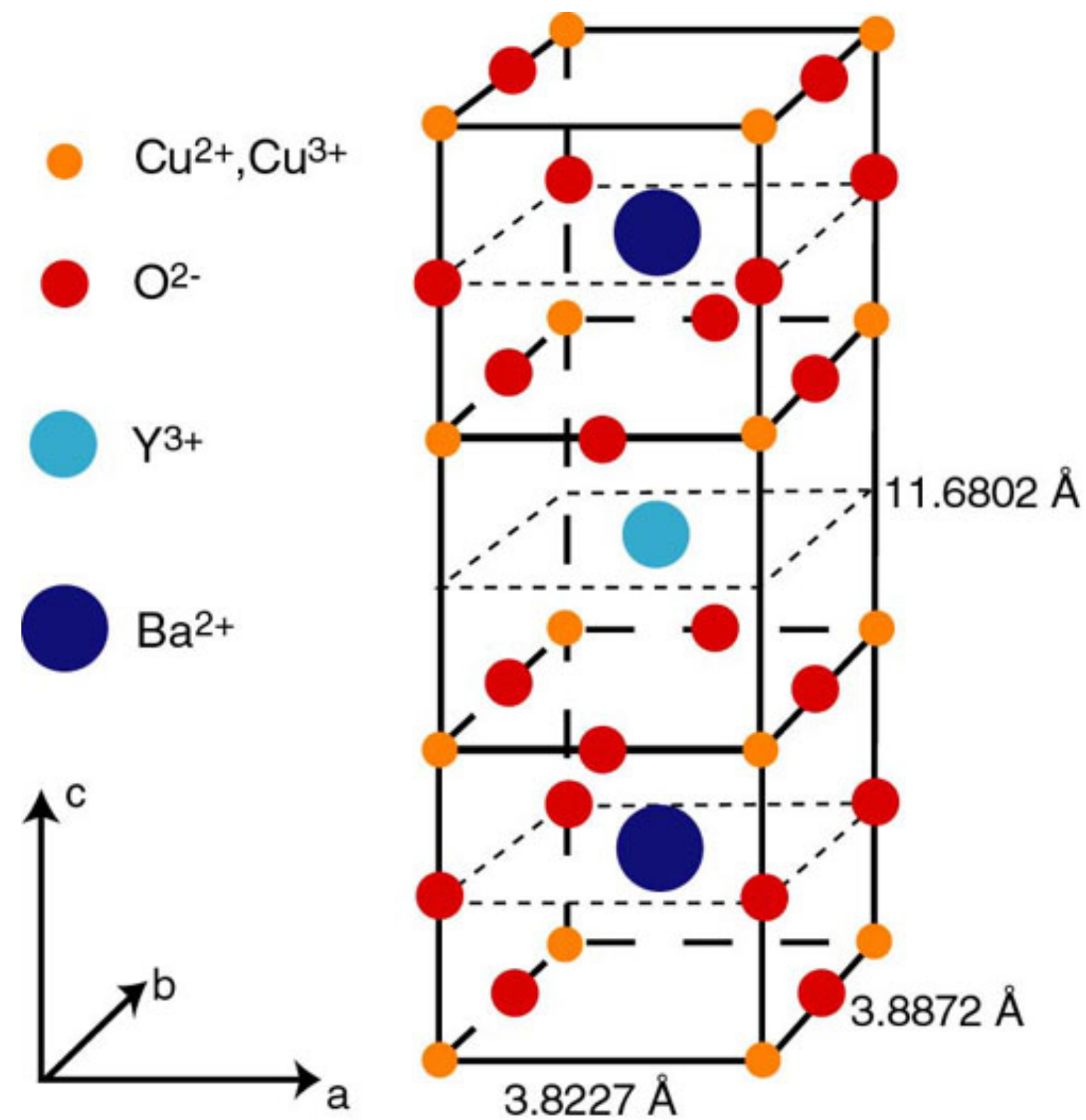


$$= \frac{1}{\sqrt{2}} (|\uparrow\downarrow\rangle - |\downarrow\uparrow\rangle)$$

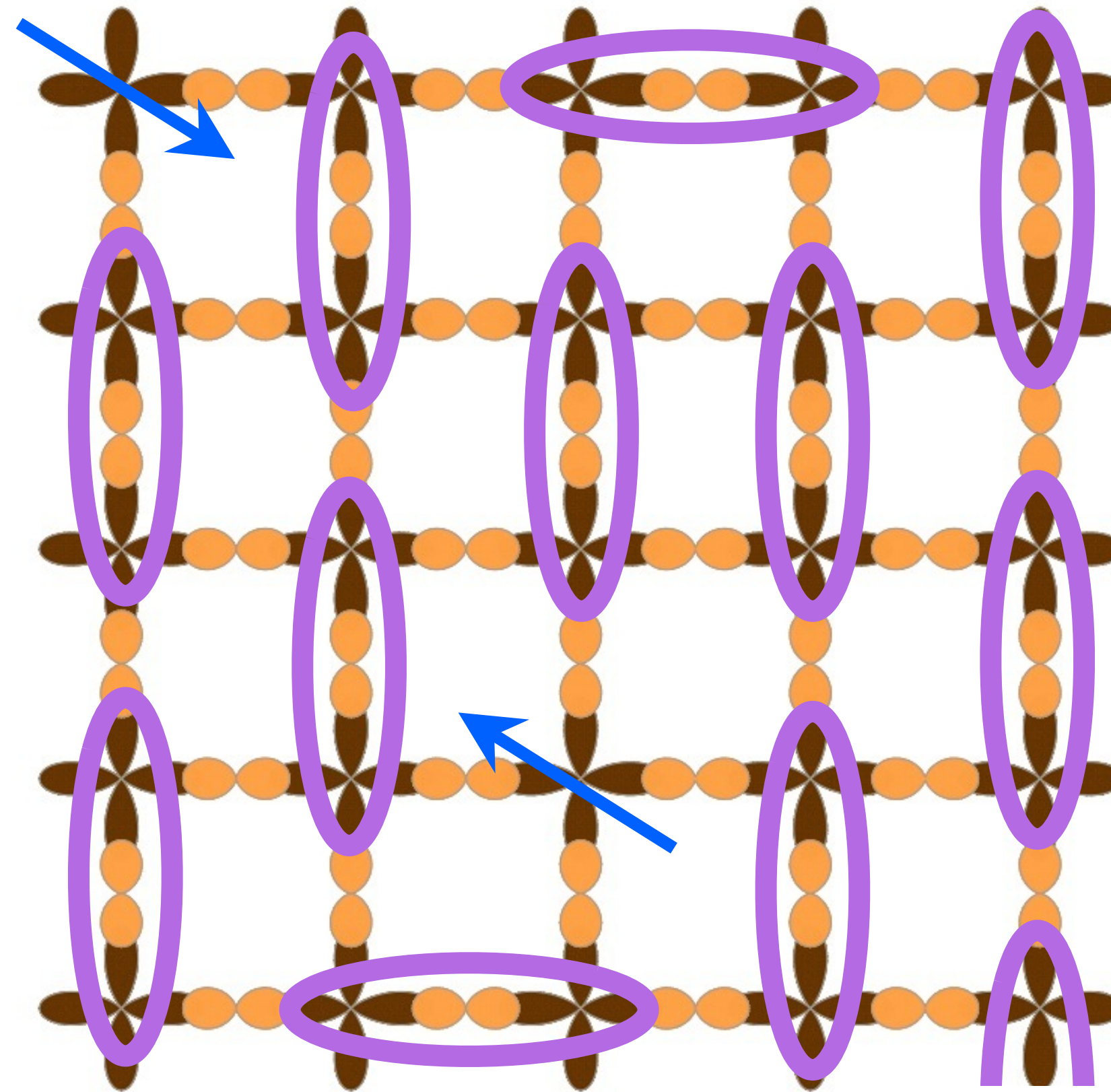
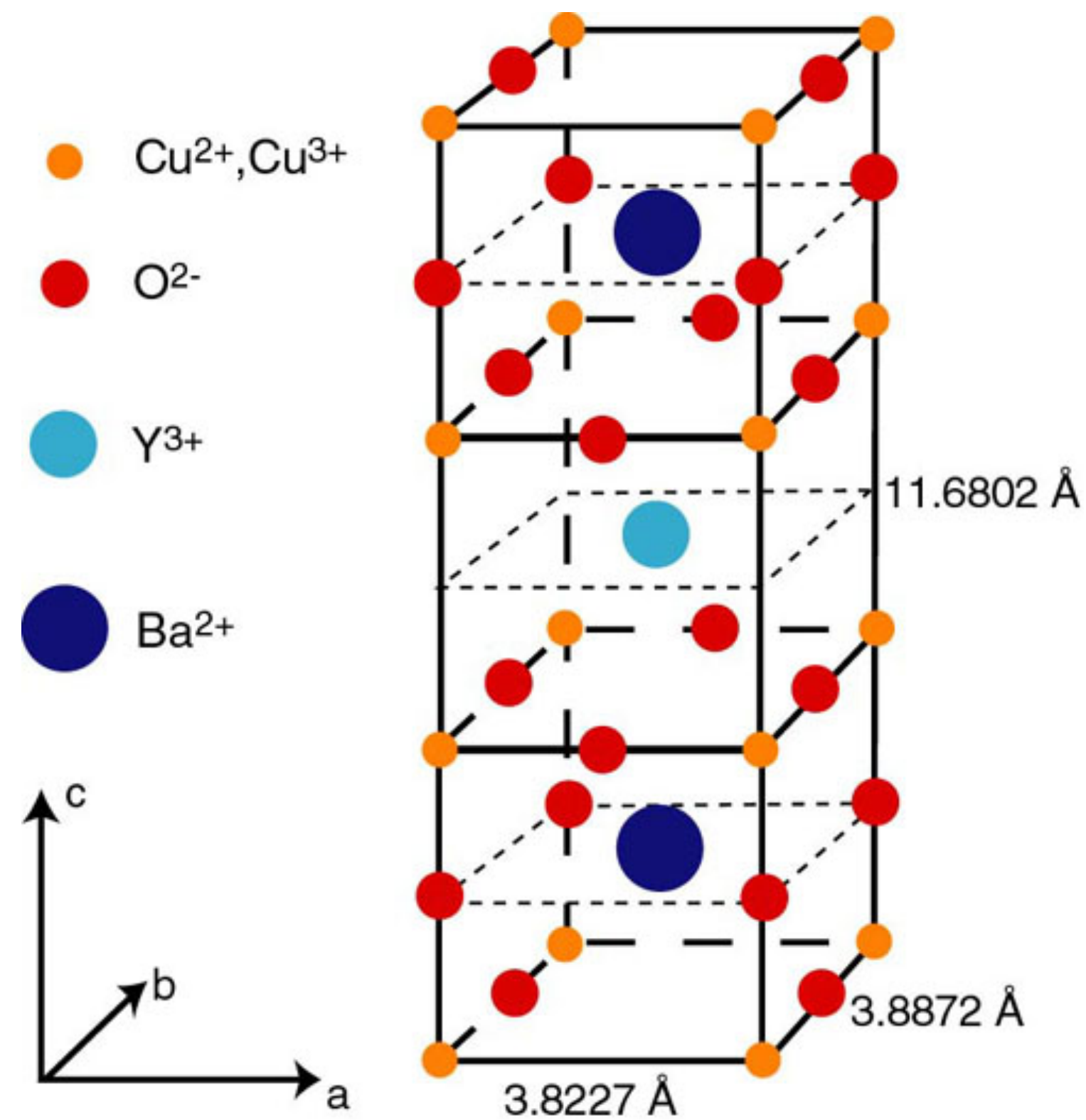
P.W.Anderson and G. Baskaran (1988): The key to high temperature superconductivity
 is the formation of a “resonating valence bond state”
 (a type of **quantum spin liquid**) which entangles the electrons on Cu



Key feature: fractionalization. Excitations are particle-like, but cannot be created by local operators: they are classified under distinct superselection/anyon sectors.

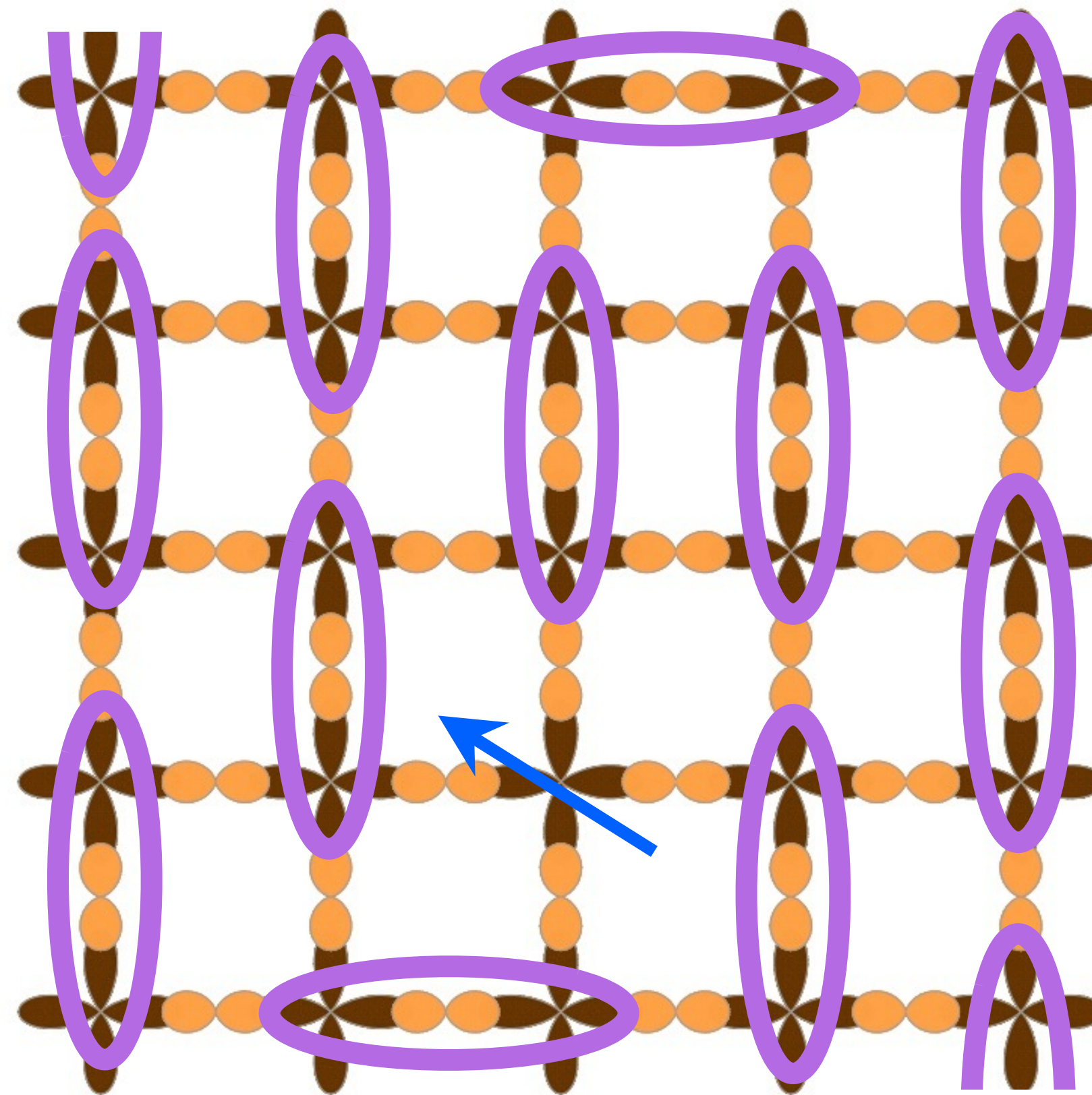
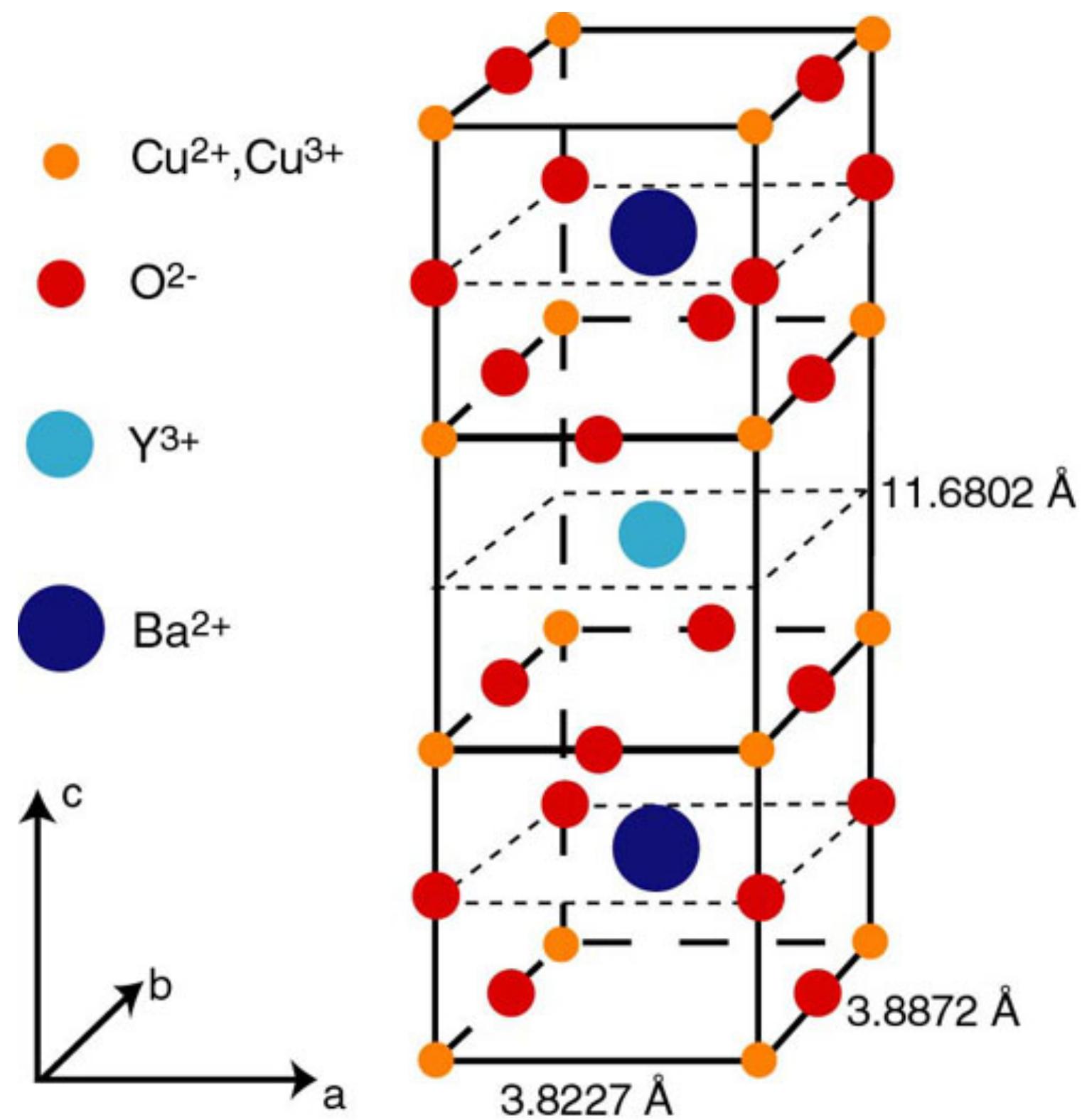


Key feature: fractionalization. Excitations are particle-like, but cannot be created by local operators: they are classified under distinct superselection/anyon sectors.



$$\text{Oval} = \frac{1}{\sqrt{2}} (|\uparrow\downarrow\rangle - |\downarrow\uparrow\rangle)$$

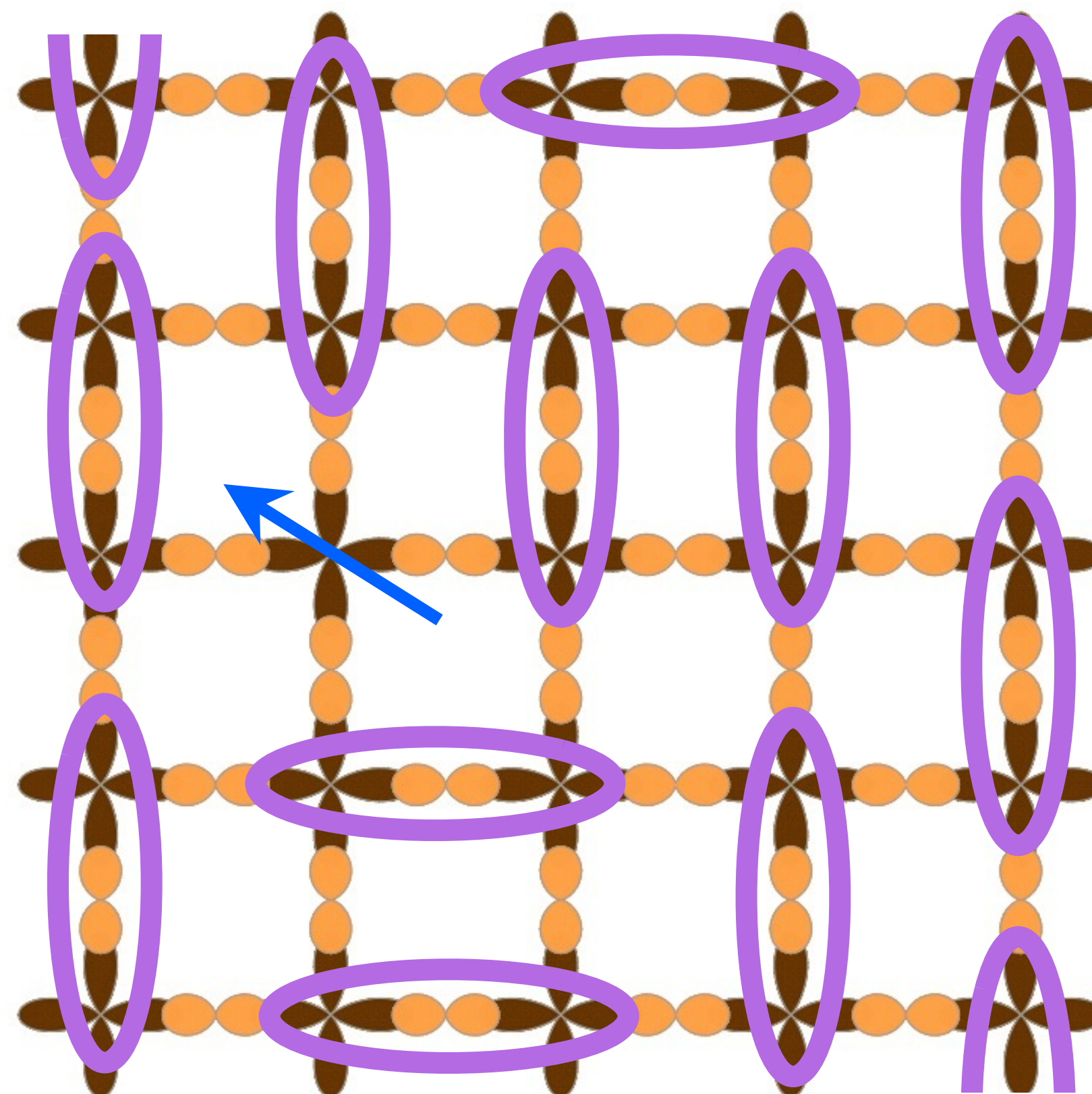
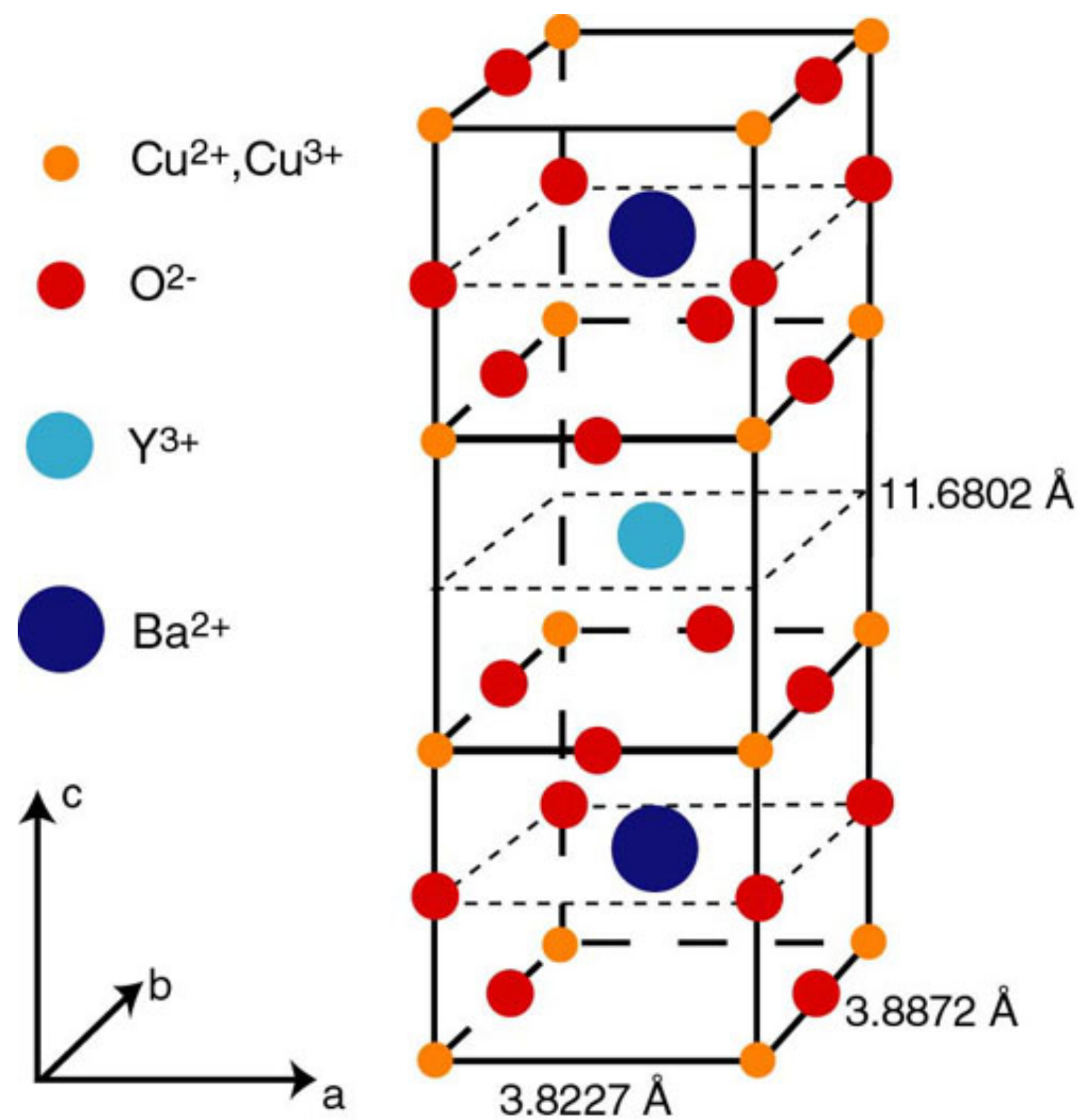
Key feature: fractionalization. Excitations are particle-like, but cannot be created by local operators: they are classified under distinct superselection/anyon sectors.



Spin $S=1/2$,
 charge
 neutral
 spinon



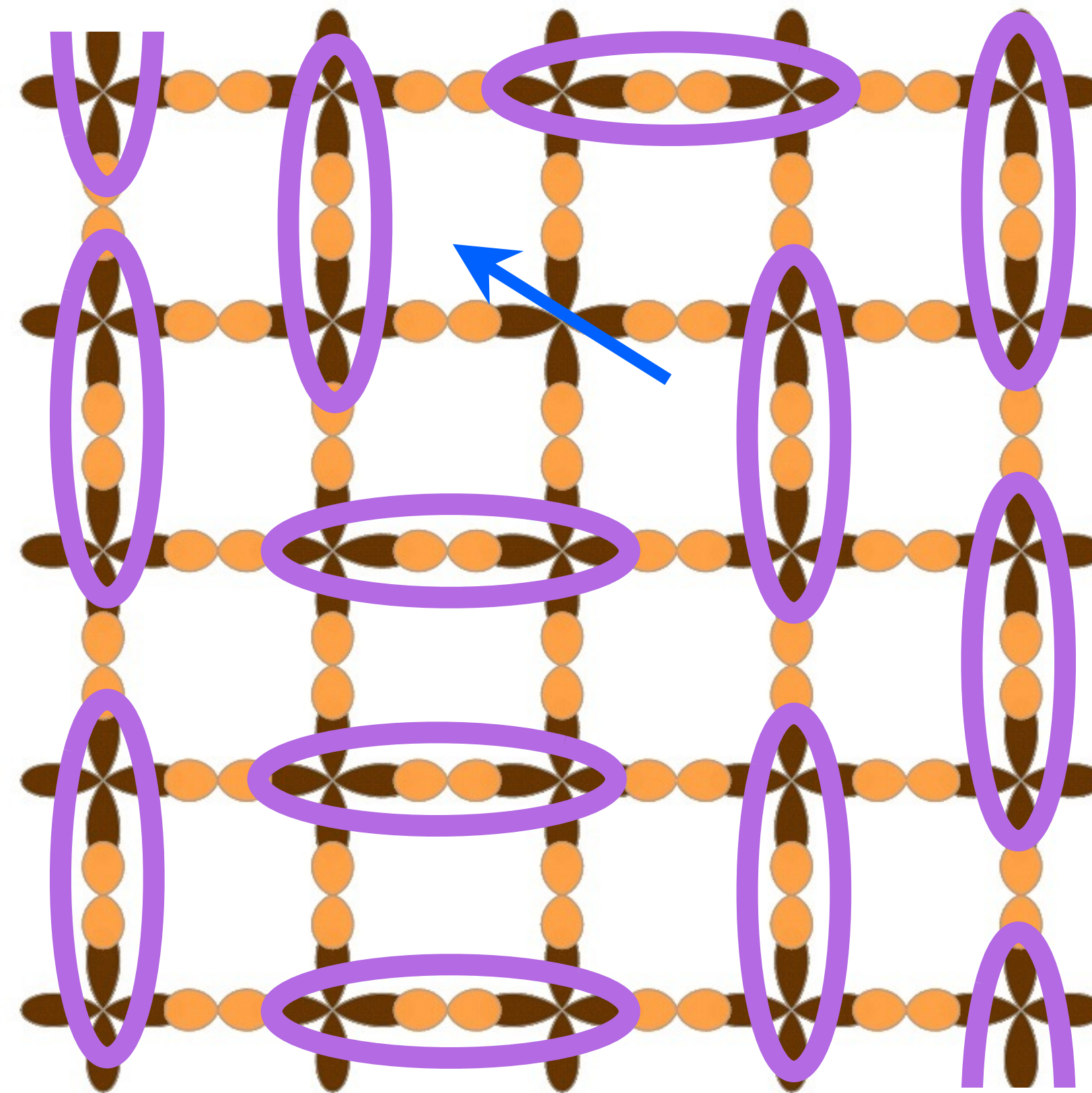
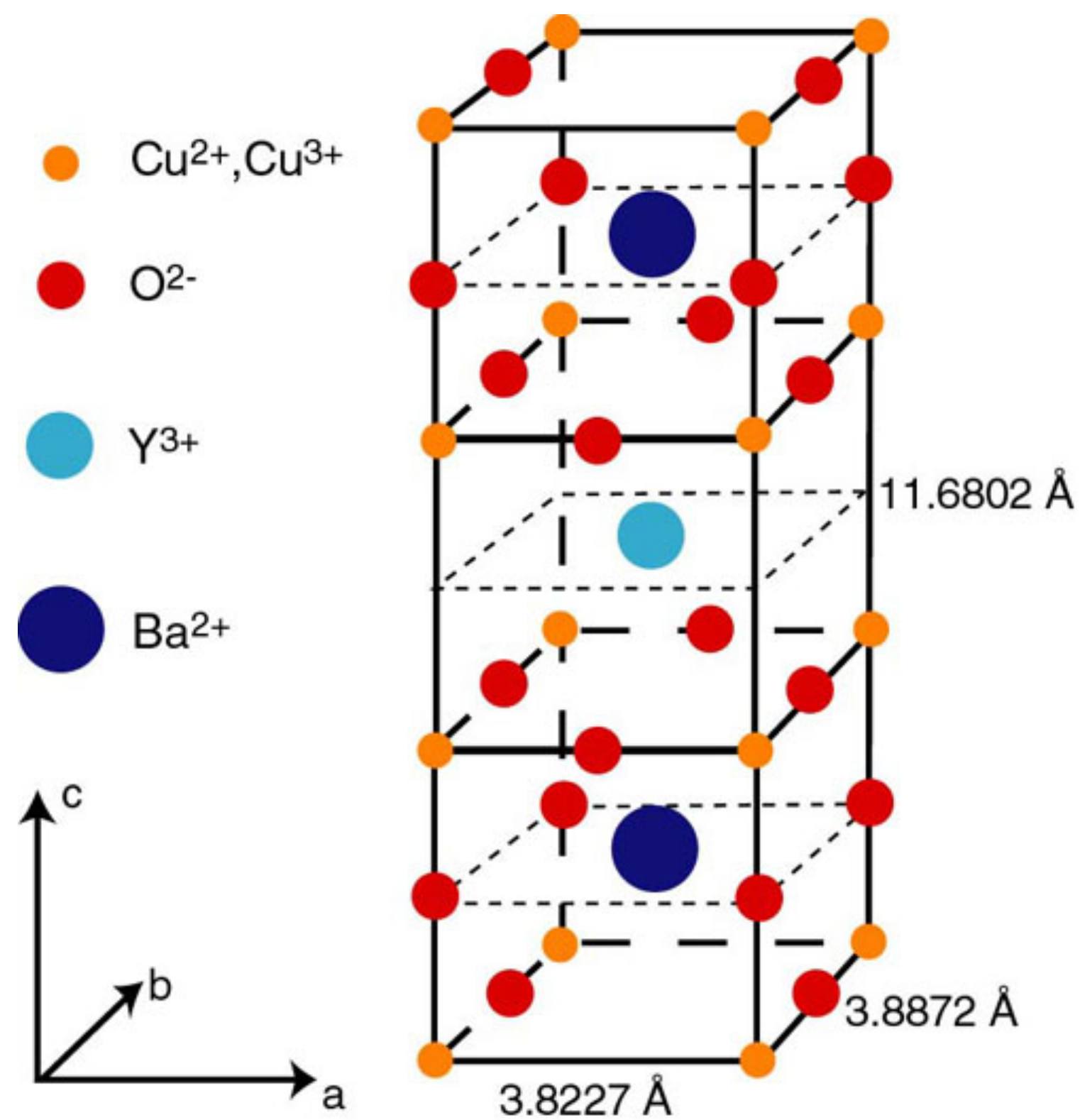
Key feature: fractionalization. Excitations are particle-like, but cannot be created by local operators: they are classified under distinct superselection/anyon sectors.



Spin $S=1/2$,
 charge
 neutral
 spinon



Key feature: fractionalization. Excitations are particle-like, but cannot be created by local operators: they are classified under distinct superselection/anyon sectors.



Spin $S=1/2$,
 charge
 neutral
 spinon

$$\text{YBa}_2\text{Cu}_3\text{O}_{6+x} \quad \text{Oval} = \frac{1}{\sqrt{2}} (|\uparrow\downarrow\rangle - |\downarrow\uparrow\rangle)$$

Key feature: fractionalization. Excitations are particle-like, but cannot be created by local operators: they are classified under distinct superselection/anyon sectors.

Quantum entanglement

in metals:

Fractionalized

Fermi liquids (FL^*)

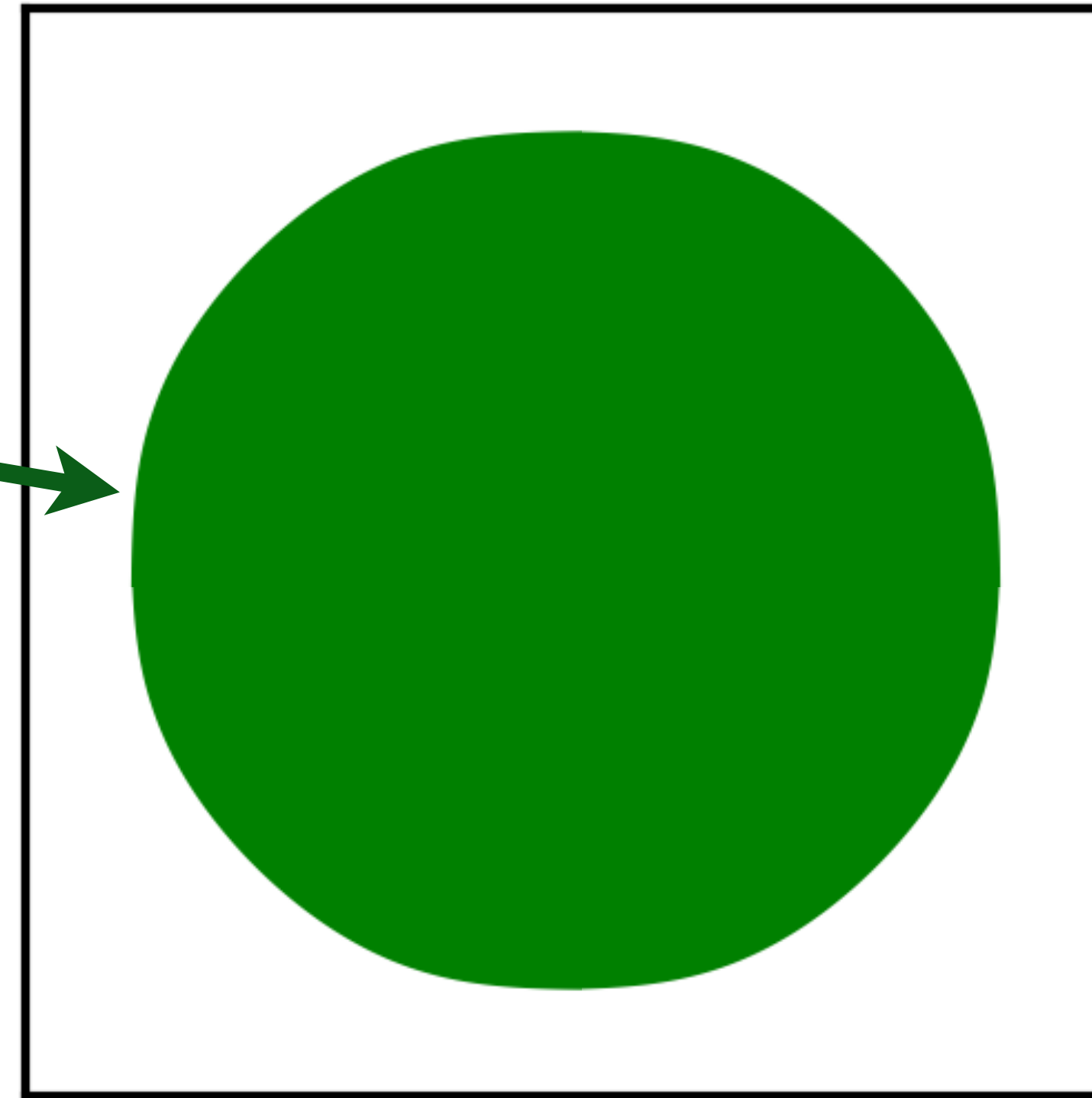
Fermi liquid

Spin-1/2 holes of density

$$\rho = 1 + p$$

Positive Hall coefficient
of carrier density ρ

Area $\rho/2$



Luttinger, 1960: Area enclosed by the Fermi surface is the same as that for free fermions *with the same symmetry*.

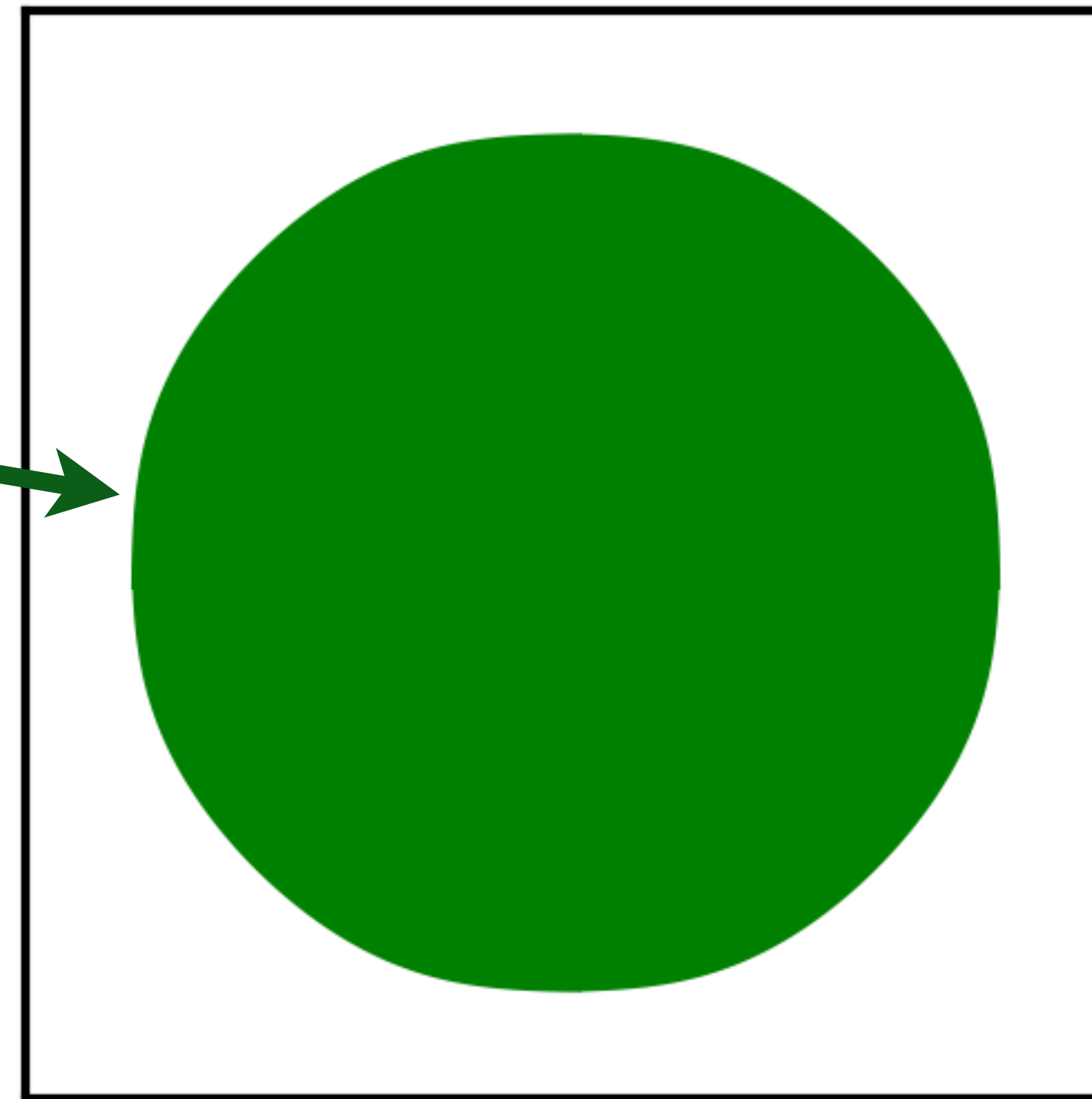
Fermi liquid

Spin-1/2 holes of density

$$\rho = 1 + p$$

Positive Hall coefficient
of carrier density ρ

Area $\rho/2$



Luttinger, 1960: Area enclosed by the Fermi surface is the same as that for free fermions *with the same symmetry*.

Oshikawa, 2000: Area constrained by a 't Hooft anomaly of global U(1) and translations

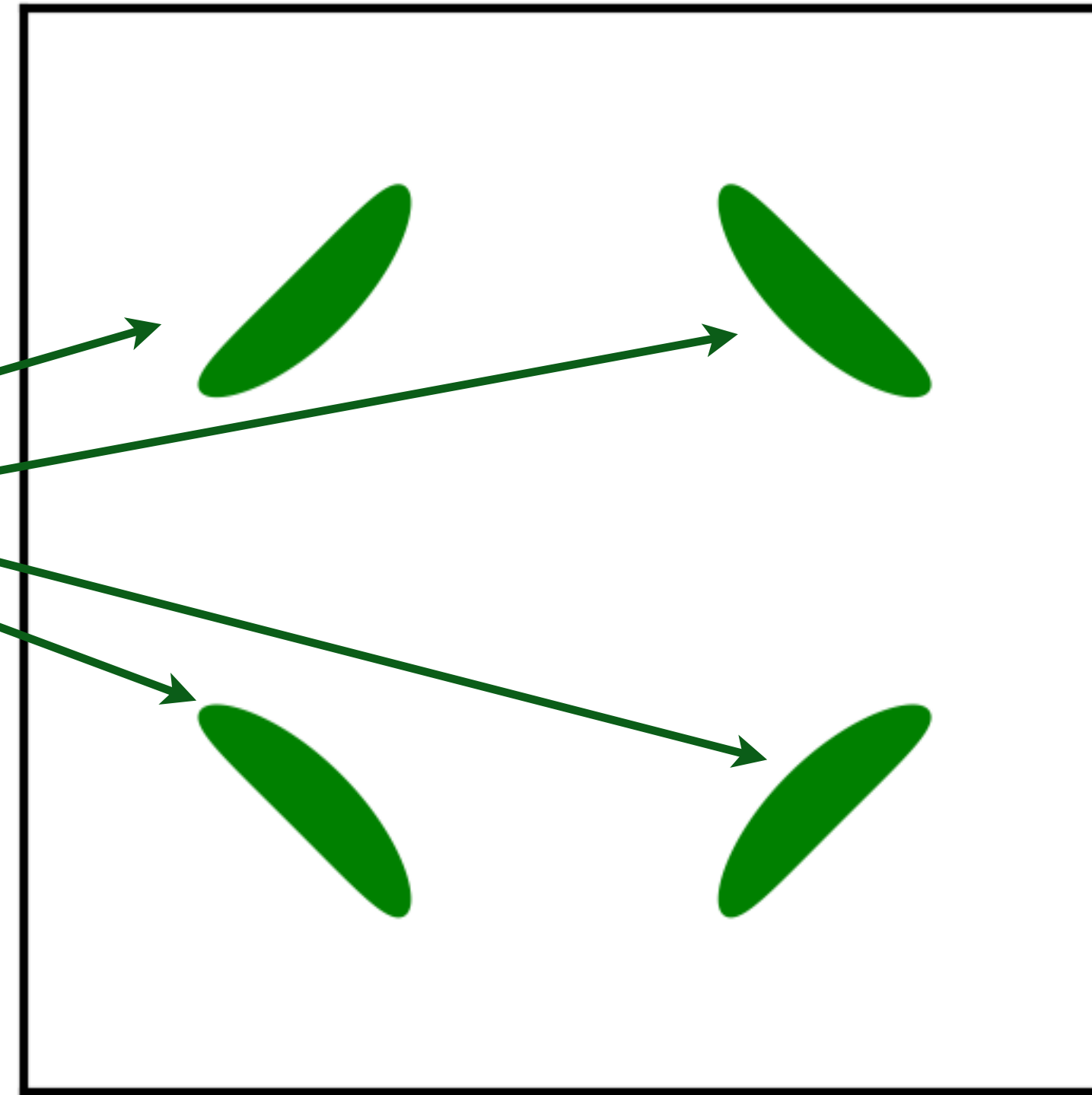
Fractionalized Fermi liquid (FL*)

Spin-1/2 holes of density

$$\rho = 1 + p$$

Positive Hall coefficient
of carrier density $\rho - 1$

Total area
 $(\rho - 1)/2$



Oshikawa anomaly is satisfied by the sum of
spin liquid (1) and
Fermi surface anomalies $(\rho - 1)$

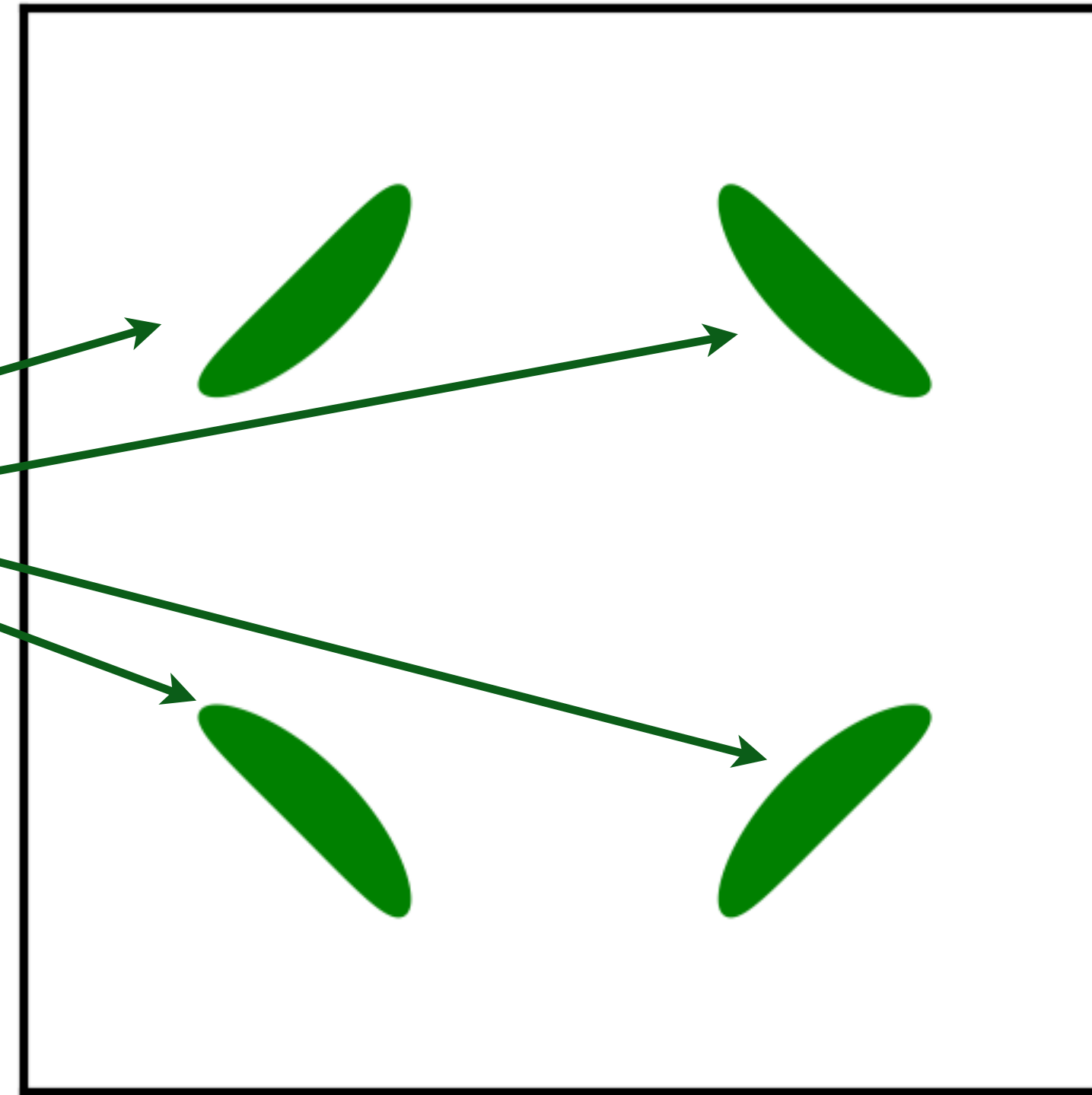
Fractionalized Fermi liquid (FL*)

Spin-1/2 holes of density

$$\rho = 1 + p$$

Positive Hall coefficient
of carrier density $\rho - 1$

Total area
 $(\rho - 1)/2$



Area of
each
hole pocket
 $= p/8$

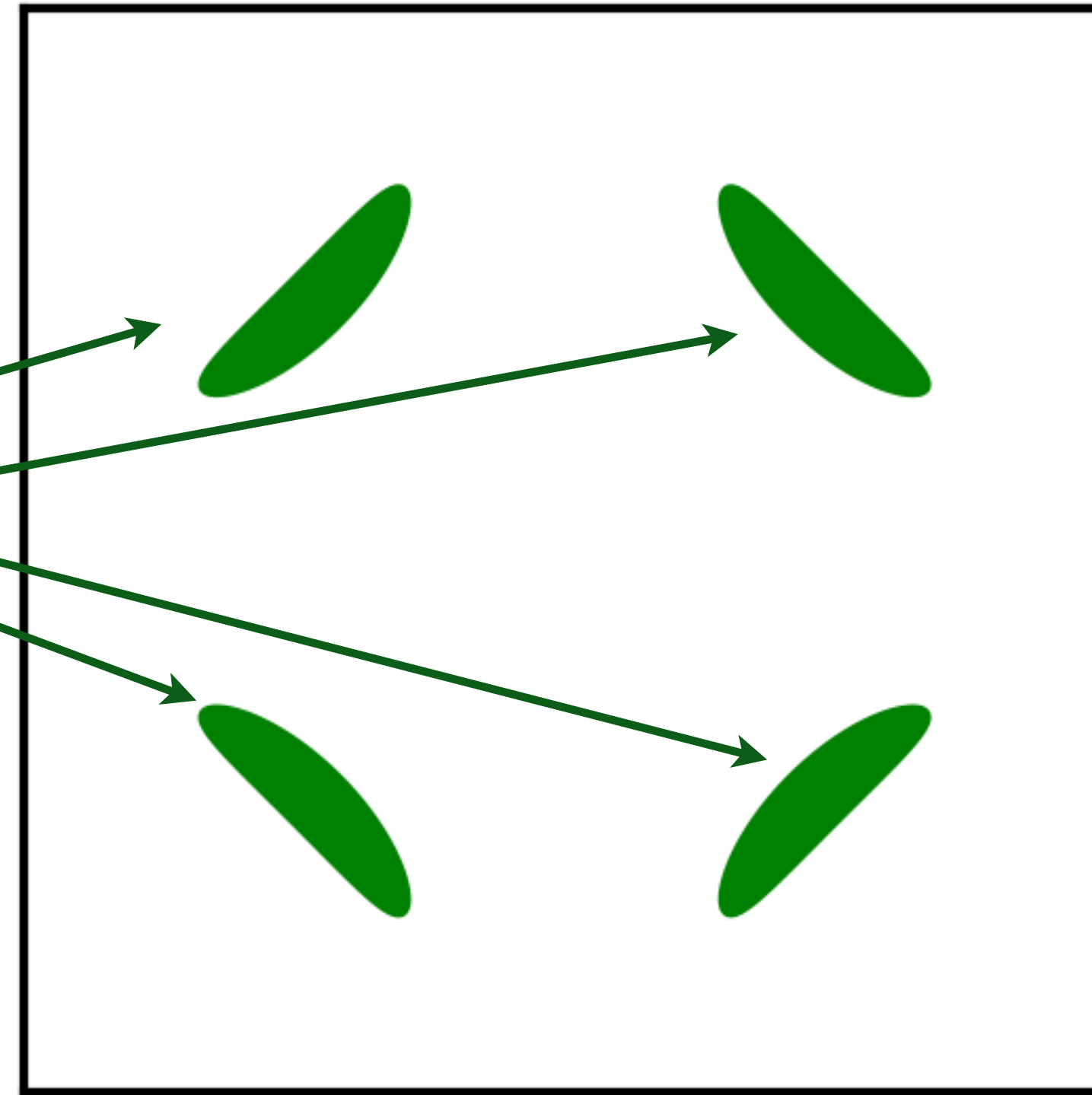
Oshikawa anomaly is satisfied by the sum of
spin liquid (1) and
Fermi surface anomalies $(\rho - 1)$

Fractionalized Fermi liquid (FL*)

Spin-1/2 holes of density
 $\rho = 1 + p$

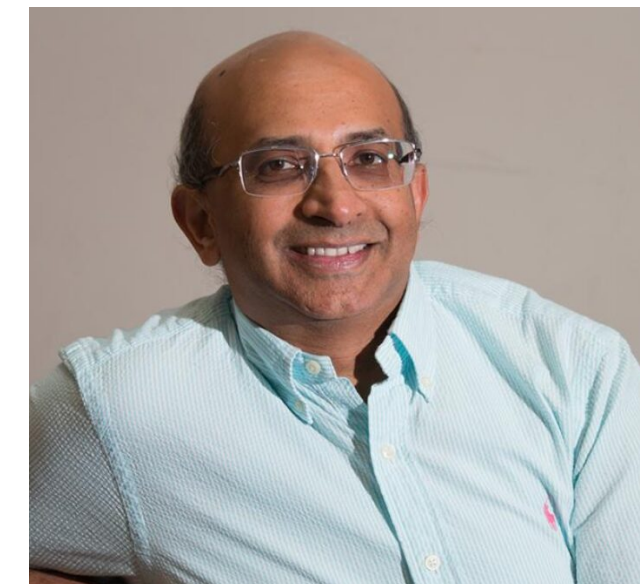
Positive Hall coefficient
of carrier density $\rho - 1$

Total area
 $(\rho - 1)/2$

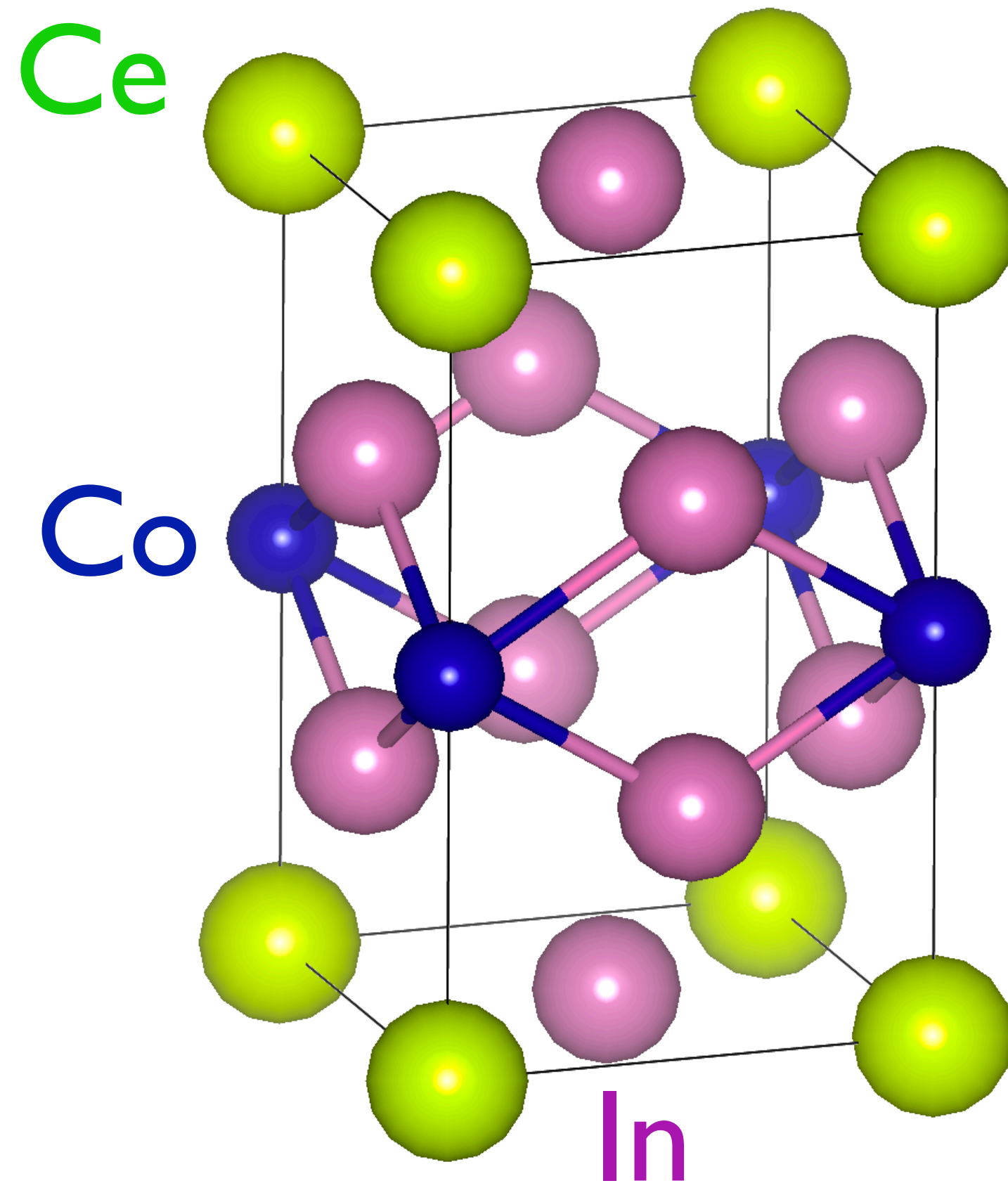


Measuring
non-Luttinger
Fermi surface
area is direct
evidence for
spin liquid
quantum
entanglement.

Oshikawa anomaly is satisfied by the sum of
spin liquid (1) and
Fermi surface anomalies $(\rho - 1)$



FL^* in $CeCoIn_5$



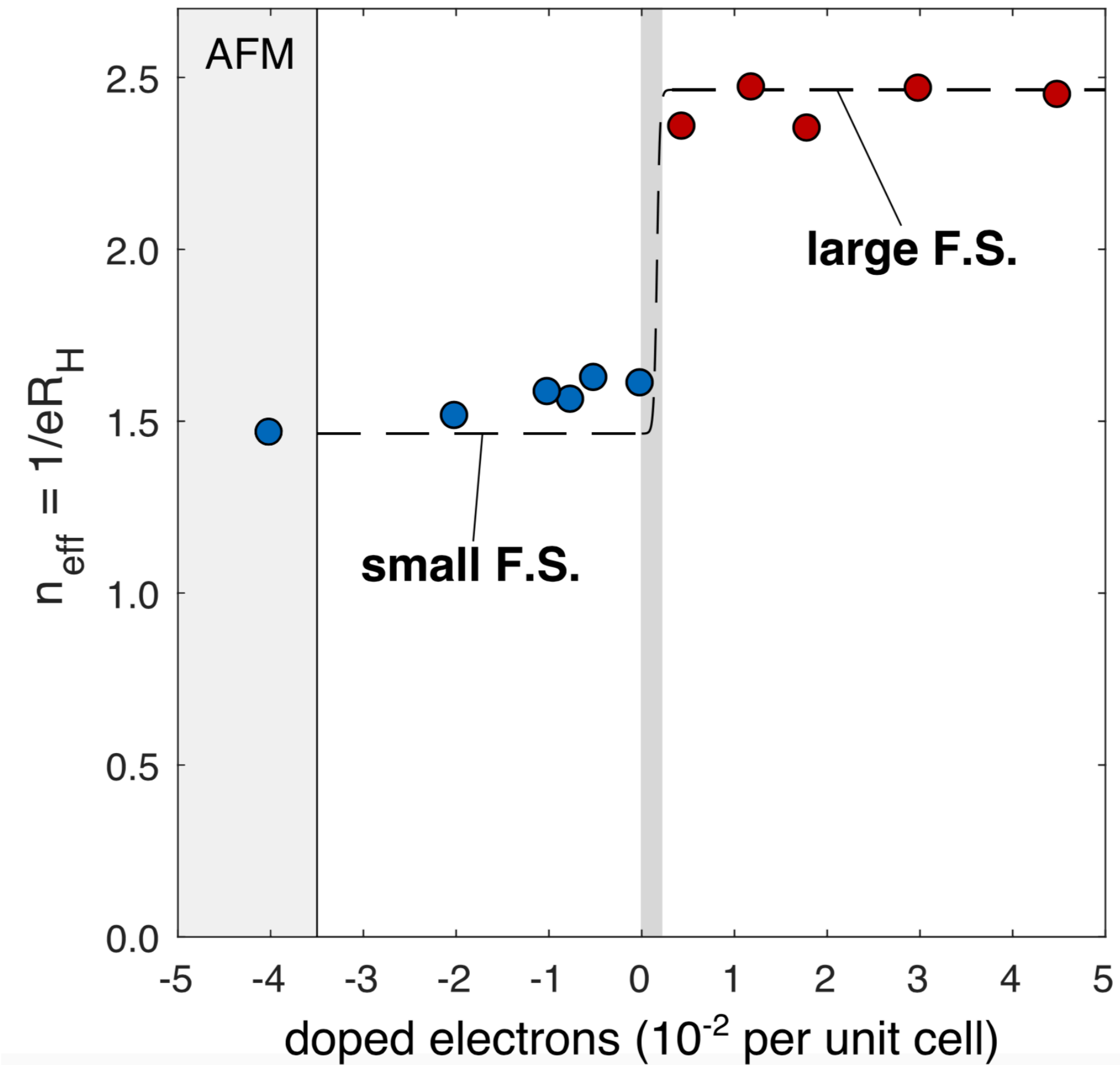
Strong on-site
repulsion U
only on Ce
sites



Evidence for a delocalization quantum phase transition without symmetry breaking in CeCoIn₅

N. Maksimovic, D.H. Eilbott, T. Cookmeyer, Fanghui Wan, J. Ruzs. V. Nagarajan, S.C. Haley, E. Maniv. Amanda Gong. S. Faubel, I.M. Hayes, A. Bangura. J. Singleton. J. C. Palmstrom, L. Winter, R. McDonald, Sooyoung Jang. Ping Ai. Yi Lin, S. Ciocys, J. Gobbo, Y. Werman, P.M. Oppeneer, E. Altman, A. Lanzara, J. G. Analytis

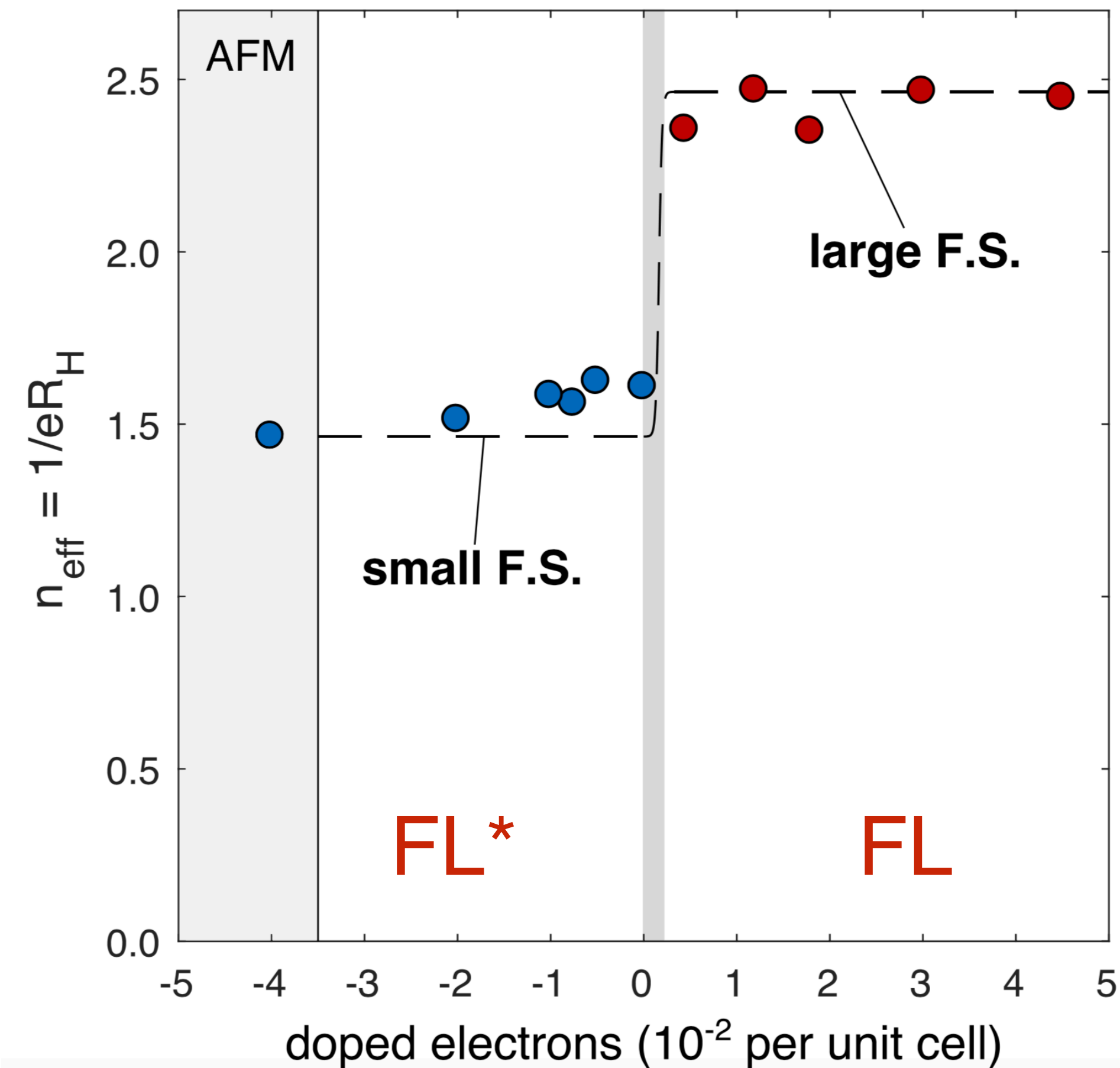
Science **375**, 76 (2021)



Evidence for a delocalization quantum phase transition without symmetry breaking in CeCoIn₅

N. Maksimovic, D.H. Eilbott, T. Cookmeyer, Fanghui Wan, J. Ruzs. V. Nagarajan, S.C. Haley, E. Maniv. Amanda Gong. S. Faubel, I.M. Hayes, A. Bangura. J. Singleton. J. C. Palmstrom, L. Winter, R. McDonald, Sooyoung Jang. Ping Ai. Yi Lin, S. Ciocys, J. Gobbo, Y. Werman, P.M. Oppeneer, E. Altman, A. Lanzara, J. G. Analytis

Science **375**, 76 (2021)

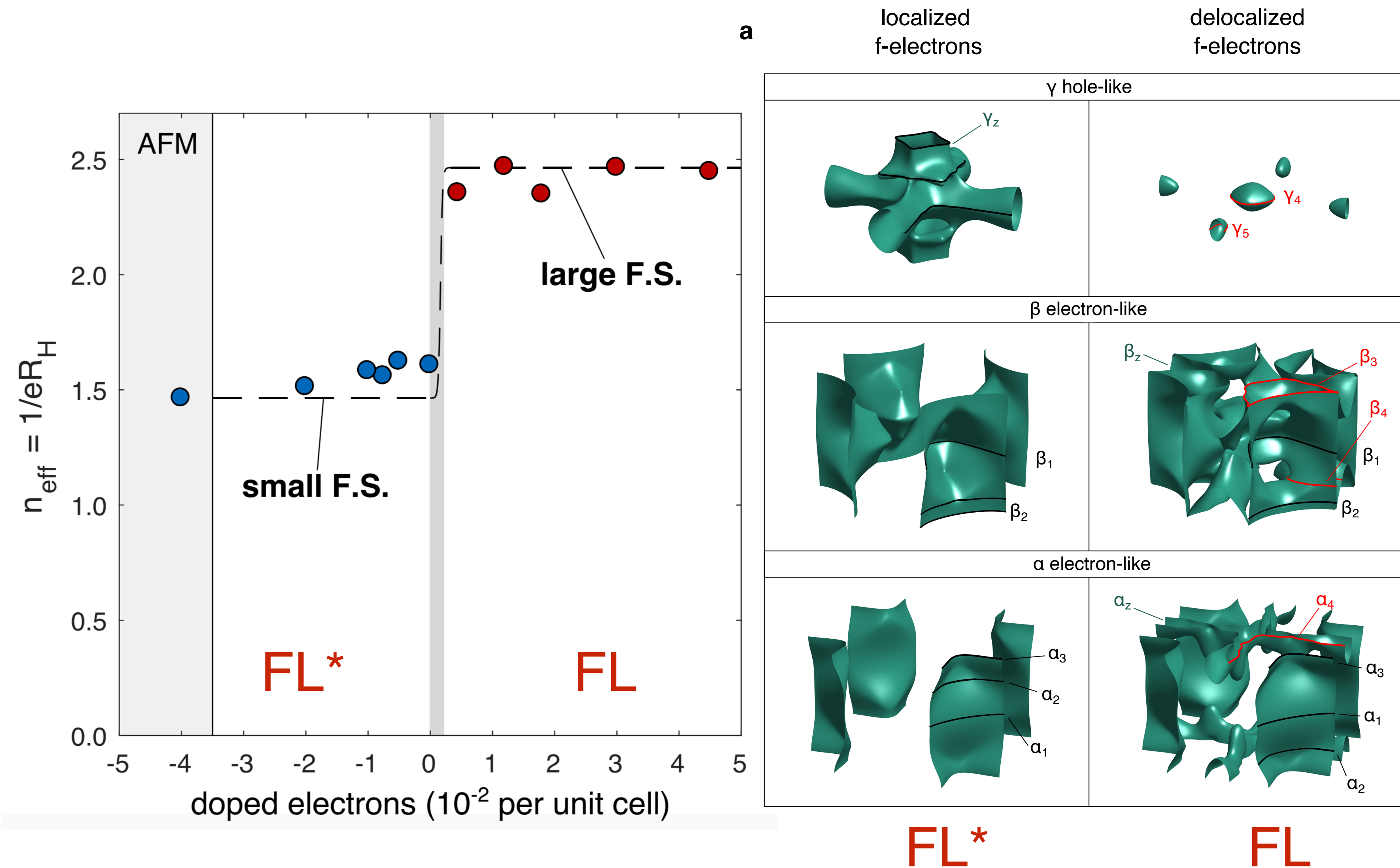


- FL \Rightarrow One electron per Ce site is included in volume enclosed by Fermi surface.
- FL* \Rightarrow One electron per Ce site forms a spin liquid, and is not part of the Fermi surface.

Evidence for a delocalization quantum phase transition without symmetry breaking in CeCoIn₅

N. Maksimovic, D.H. Eilbott, T. Cookmeyer, Fanghui Wan, J. Ruzs. V. Nagarajan, S.C. Haley, E. Maniv. Amanda Gong. S. Faubel, I.M. Hayes, A. Bangura. J. Singleton. J. C. Palmstrom, L. Winter, R. McDonald, Sooyoung Jang. Ping Ai. Yi Lin, S. Ciocys, J. Gobbo, Y. Werman, P.M. Oppeneer, E. Altman, A. Lanzara, J. G. Analytis

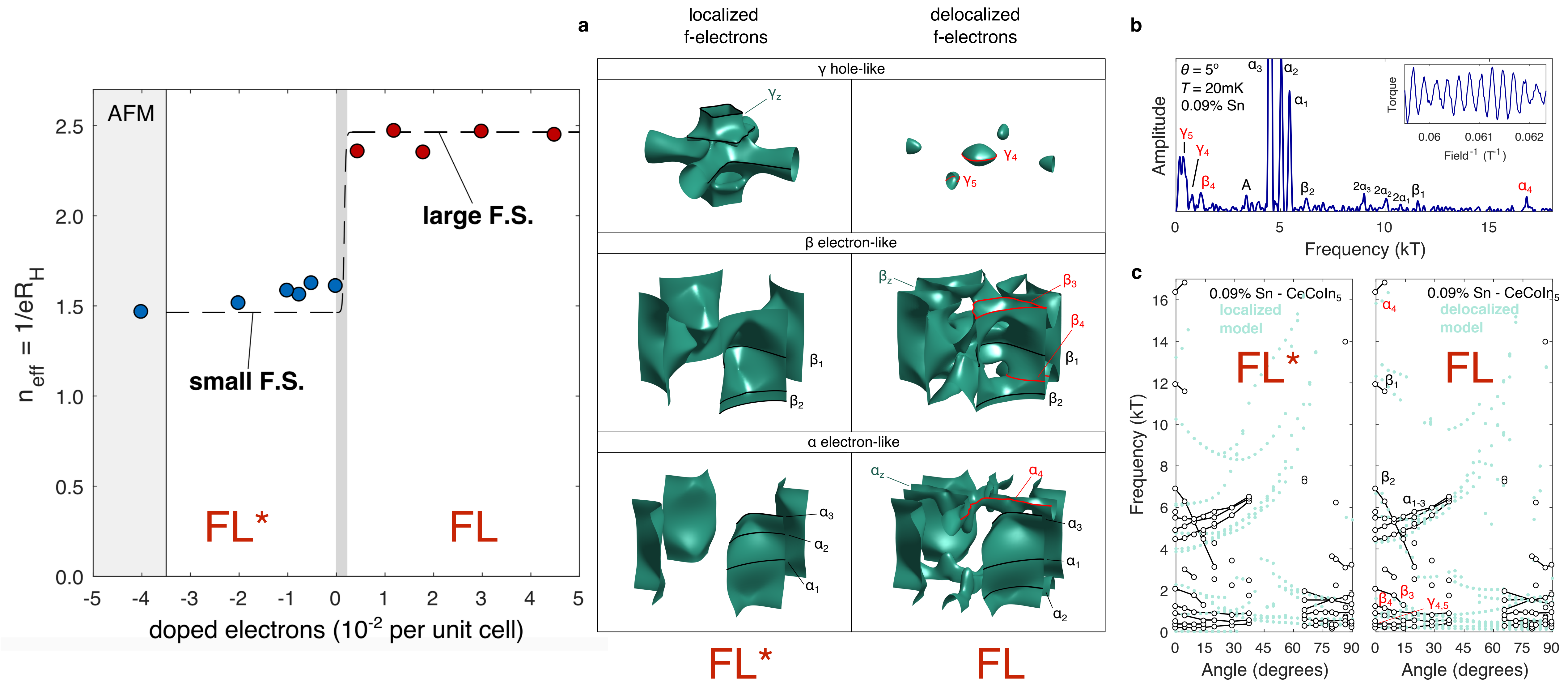
Science **375**, 76 (2021)



Evidence for a delocalization quantum phase transition without symmetry breaking in CeCoIn₅

N. Maksimovic, D.H. Eilbott, T. Cookmeyer, Fanghui Wan, J. Ruz. V. Nagarajan, S.C. Haley, E. Maniv. Amanda Gong. S. Faubel, I.M. Hayes, A. Bangura. J. Singleton. J. C. Palmstrom, L. Winter, R. McDonald, Sooyoung Jang. Ping Ai. Yi Lin, S. Ciocys, J. Gobbo, Y. Werman, P.M. Oppeneer, E. Altman, A. Lanzara, J. G. Analytis

Science **375**, 76 (2021)



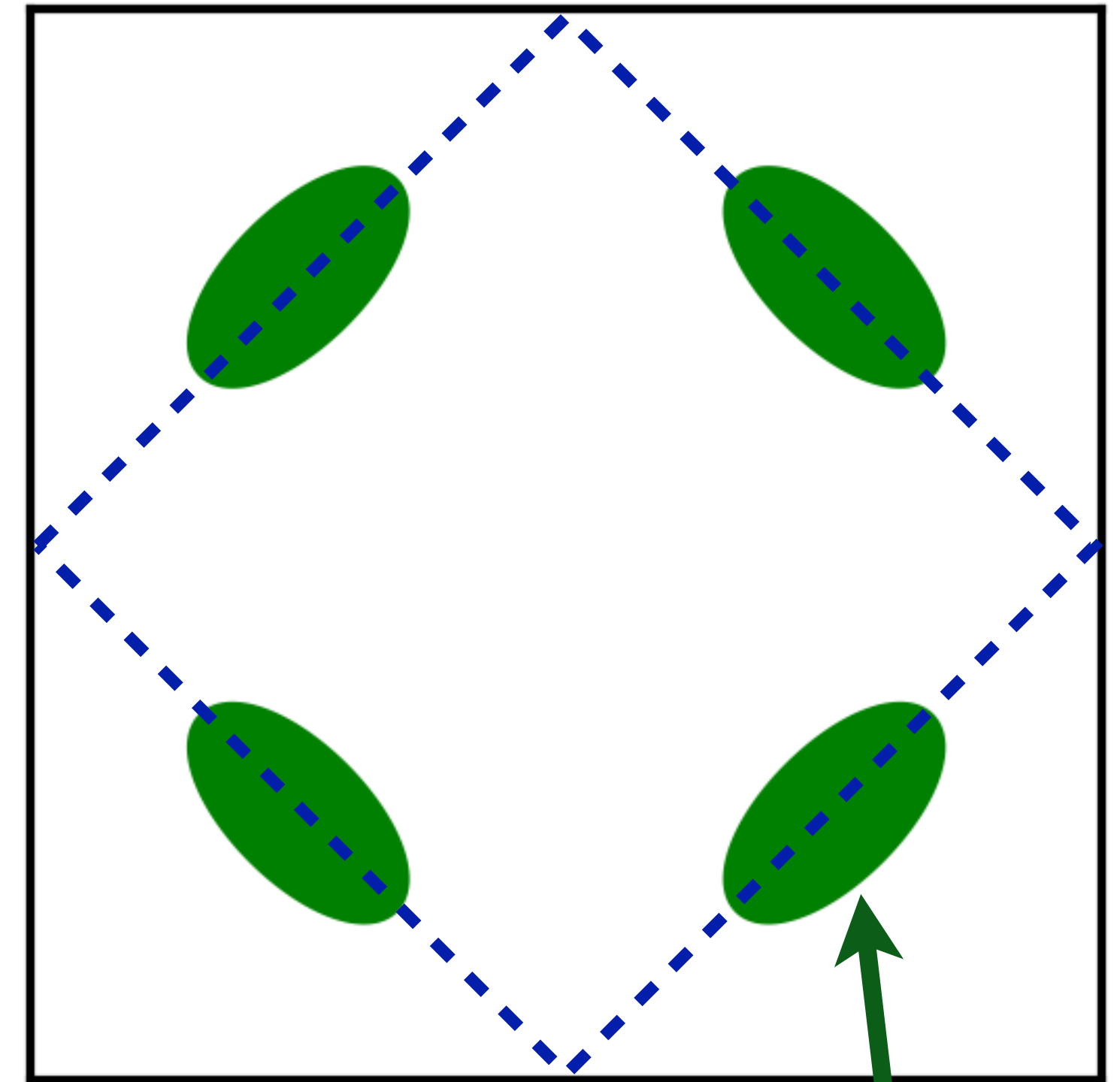
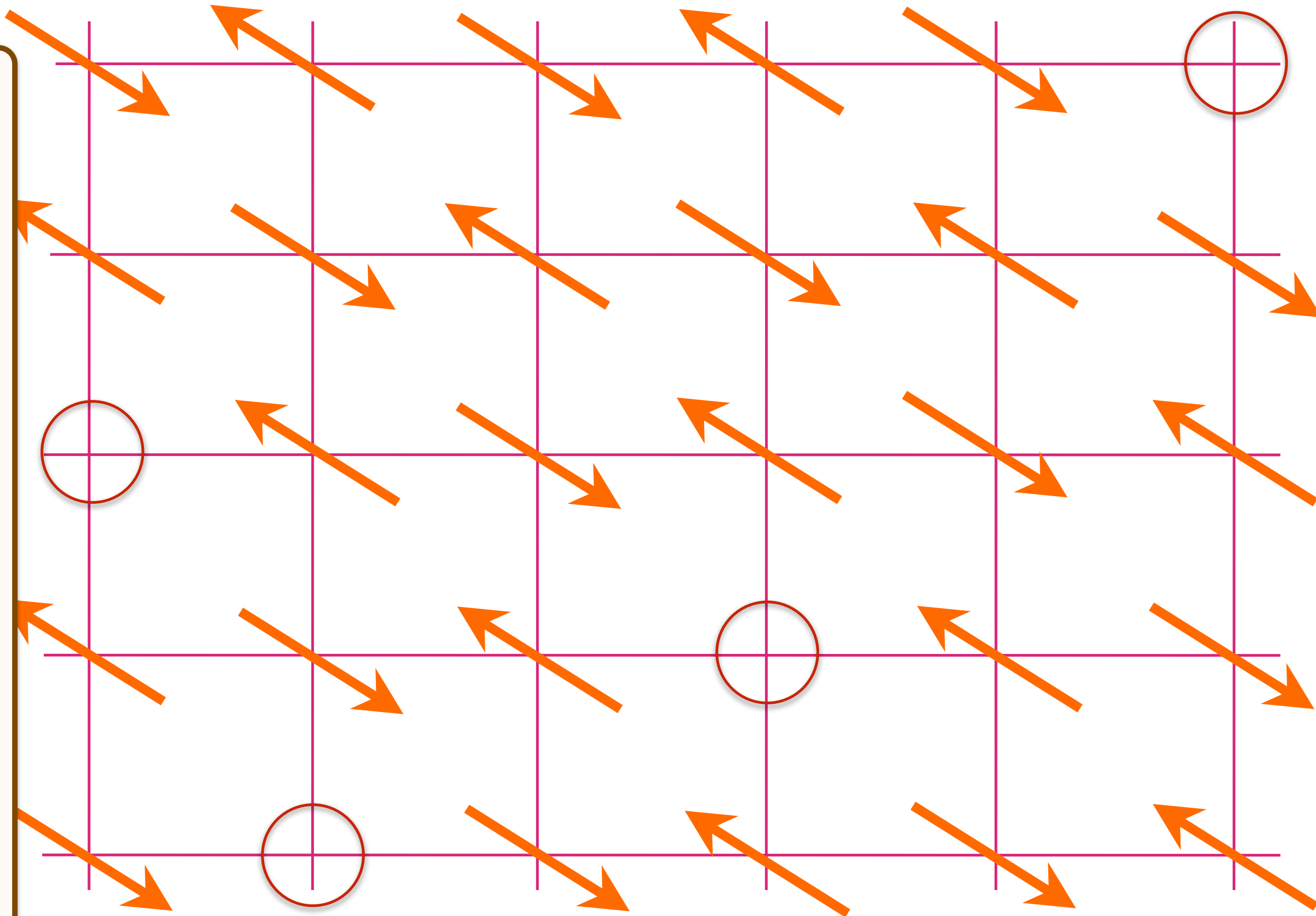
FL^* on the square lattice

Doping an insulating antiferromagnet with holes of density p

AF metal

Luttinger area.
Broken symmetry

Fermi liquid with density p of spin $1/2$, charge $+e$ holes. Yamaji effect requires inter-layer spin correlations (not present in Hg-1201).



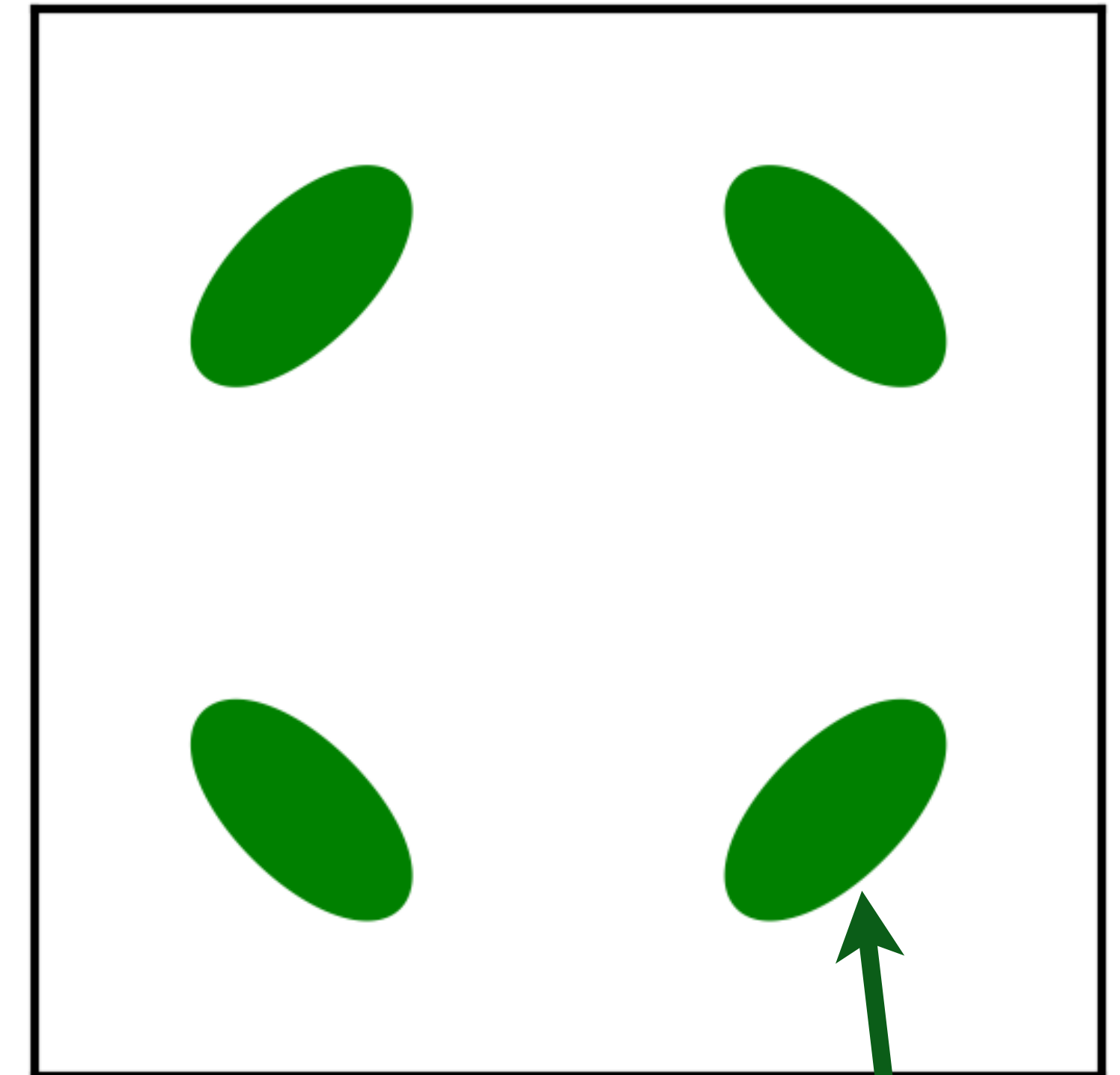
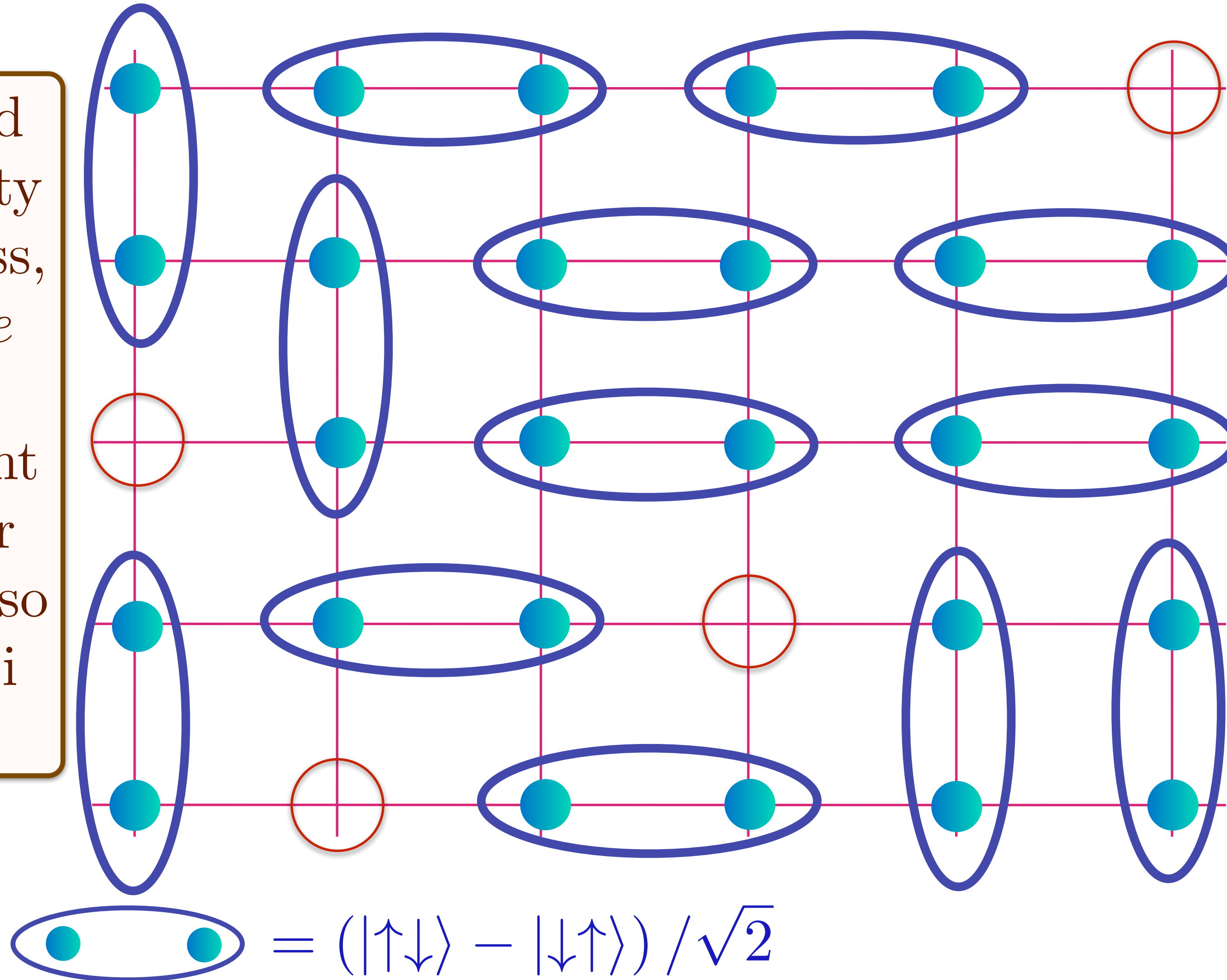
Area $p/4$

Doping an insulating antiferromagnet with holes of density p

Holon metal

Oshikawa anomaly is satisfied by sum of spin liquid (1) and Fermi surface anomalies (p)

Spin liquid with density p of spinless, charge $+e$ holons.
No coherent inter-layer transport, so no Yamaji effect.



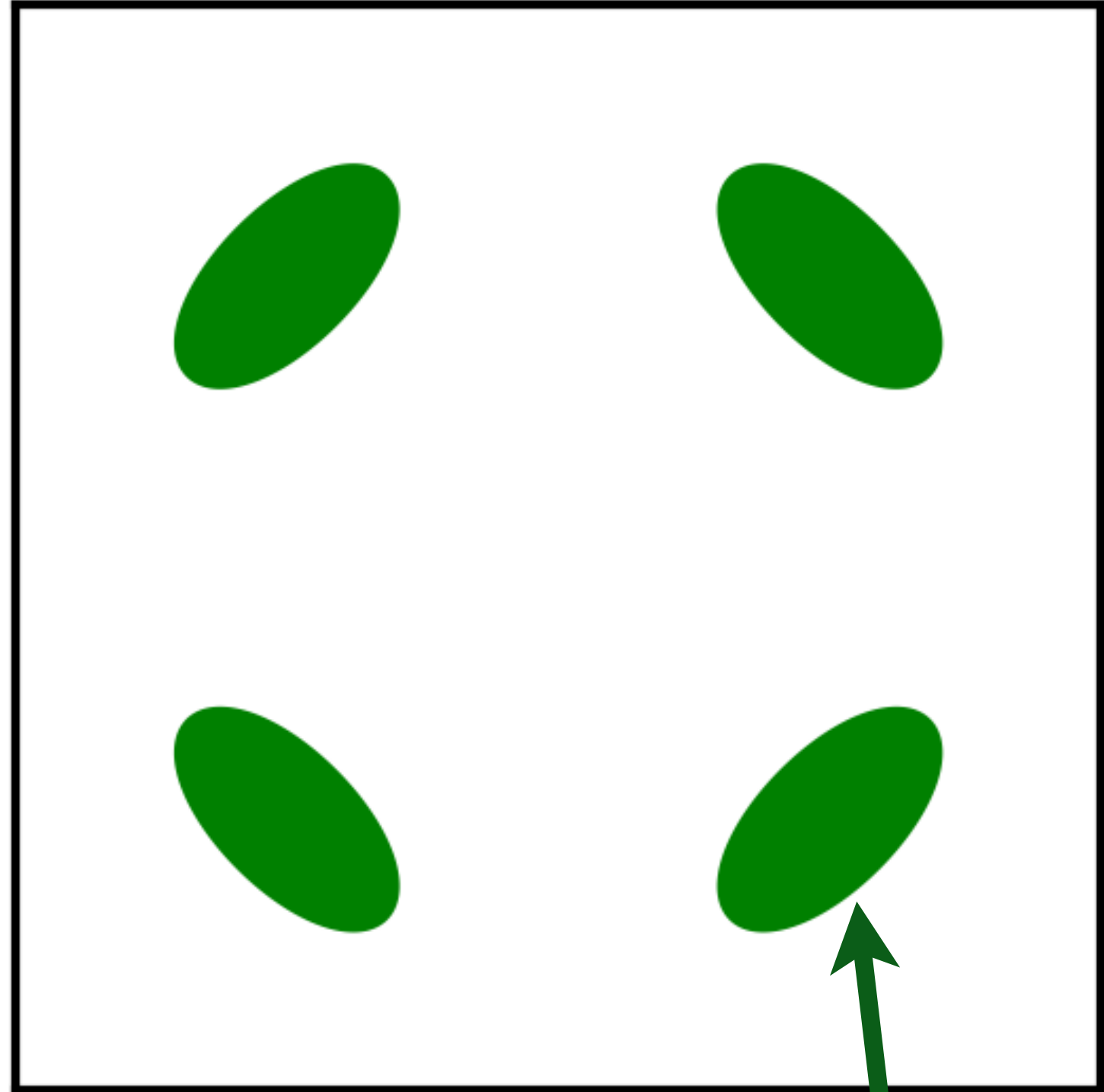
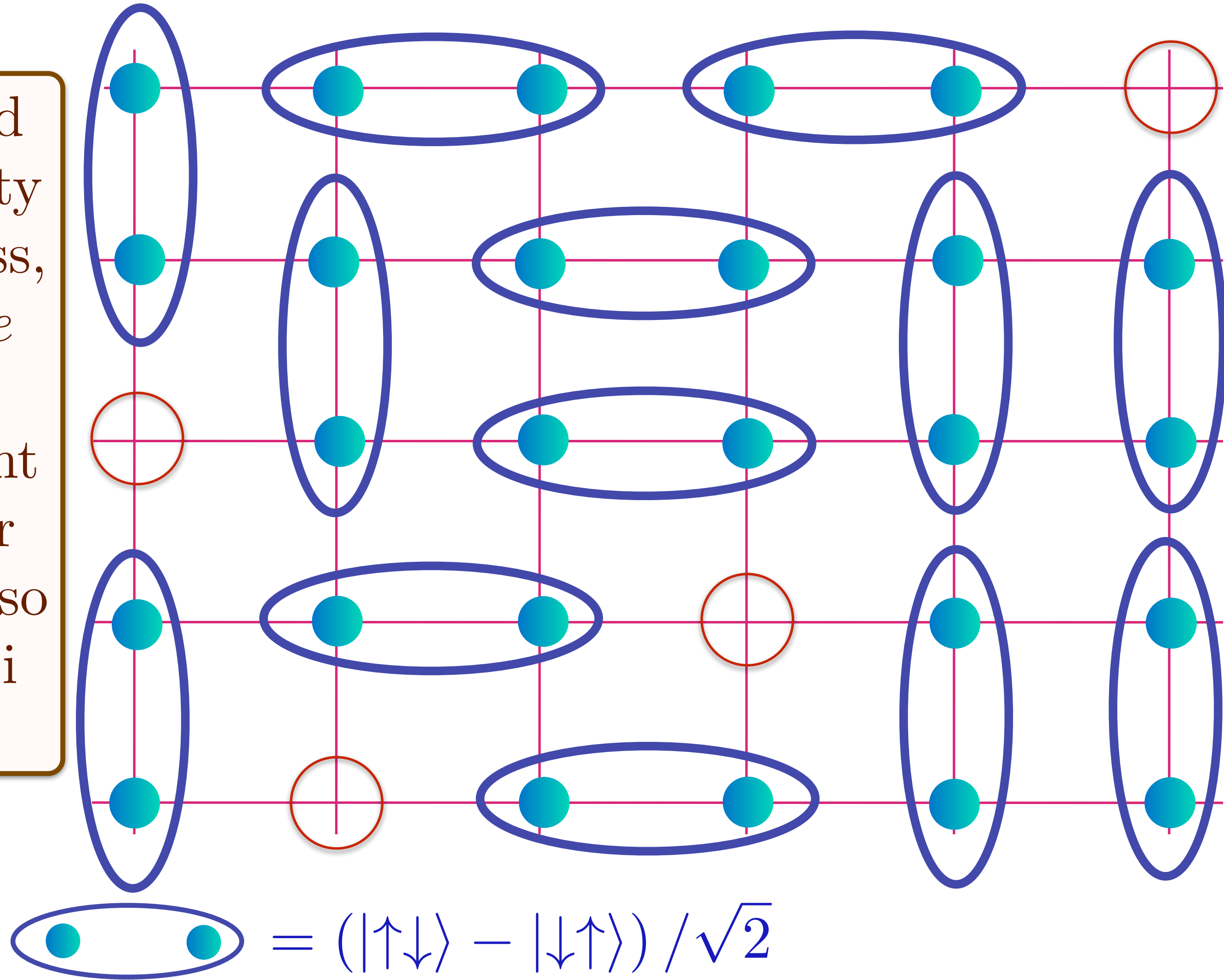
Area $p/4$

Doping an insulating antiferromagnet with holes of density p

Holon metal

Oshikawa anomaly is satisfied by sum of spin liquid (1) and Fermi surface anomalies (p)

Spin liquid with density p of spinless, charge $+e$ holons.
No coherent inter-layer transport, so no Yamaji effect.



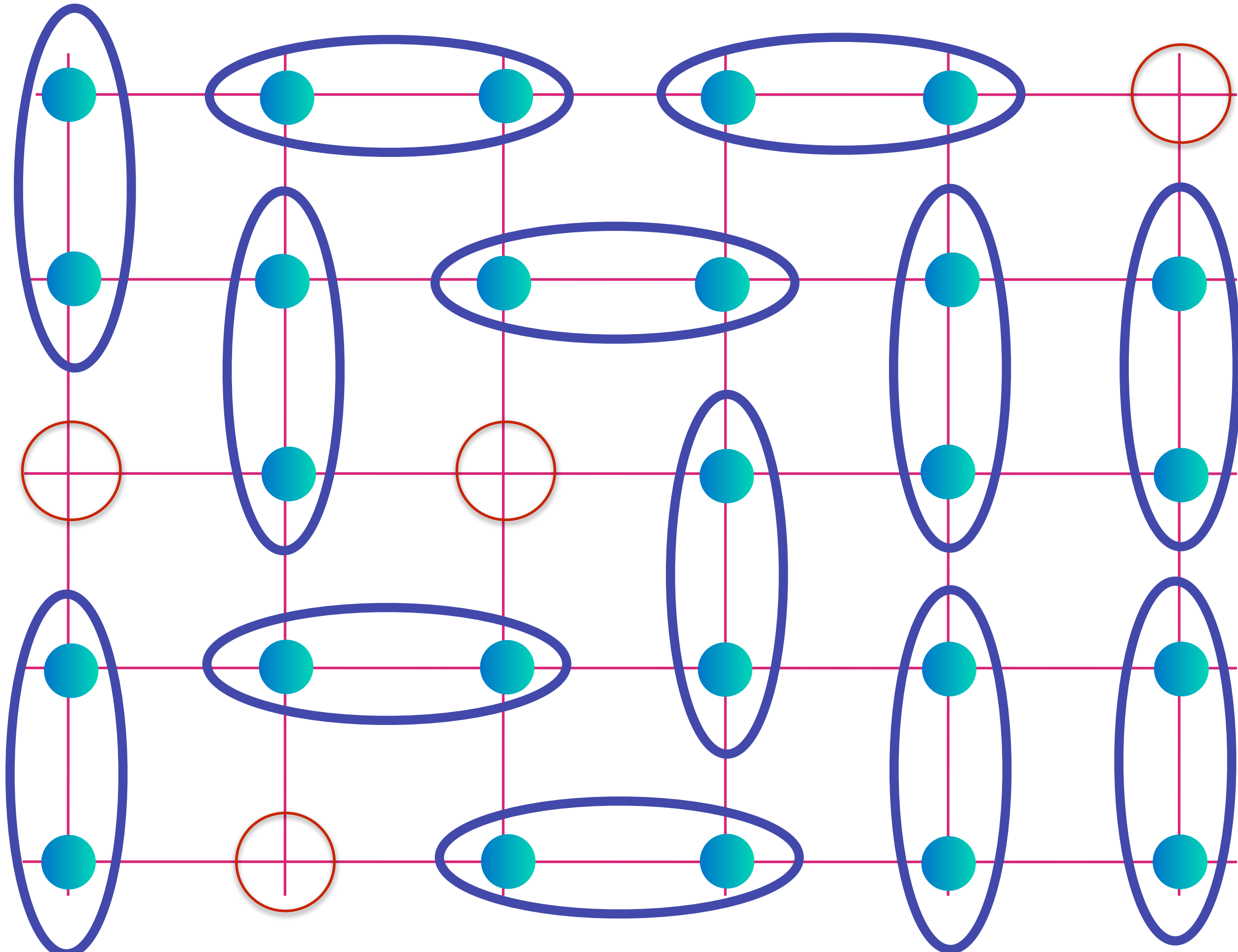
Area $p/4$

Doping an insulating antiferromagnet with holes of density p

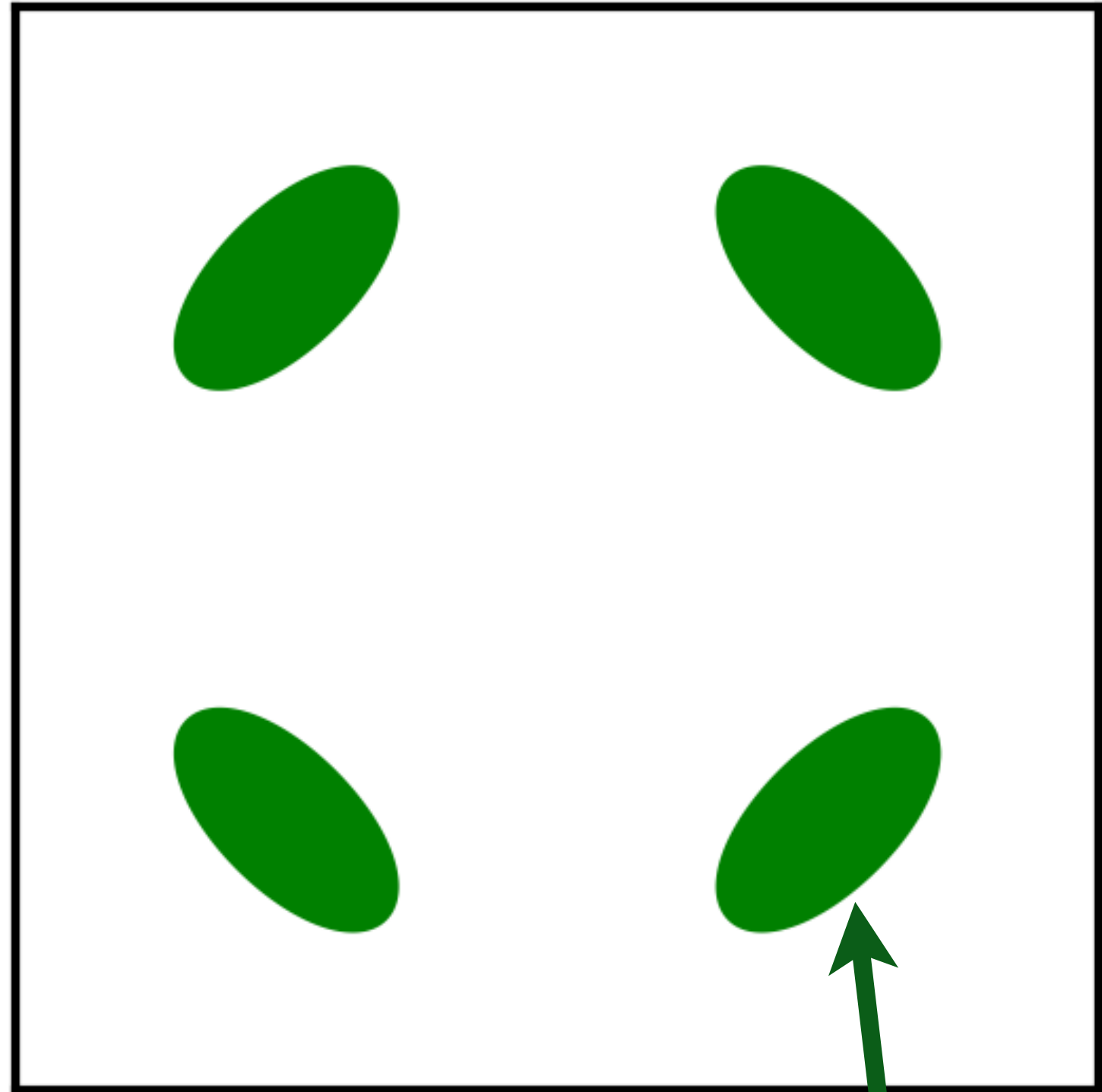
Holon metal

Oshikawa anomaly is satisfied by sum of spin liquid (1) and Fermi surface anomalies (p)

Spin liquid with density p of spinless, charge $+e$ holons.
No coherent inter-layer transport, so no Yamaji effect.



$$\text{[Diagram of a pair of cyan dots in a blue oval]} = (|\uparrow\downarrow\rangle - |\downarrow\uparrow\rangle) / \sqrt{2}$$



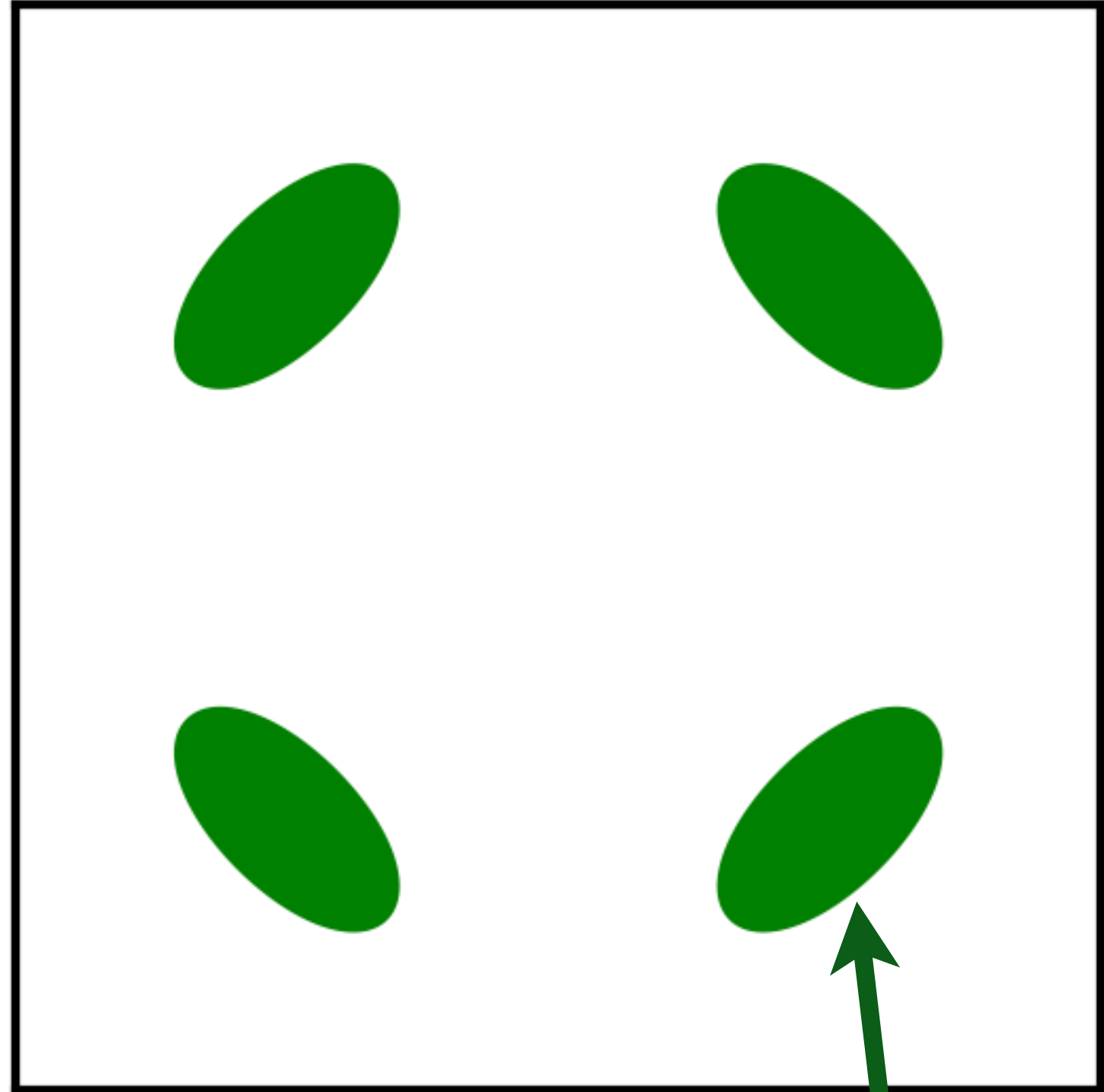
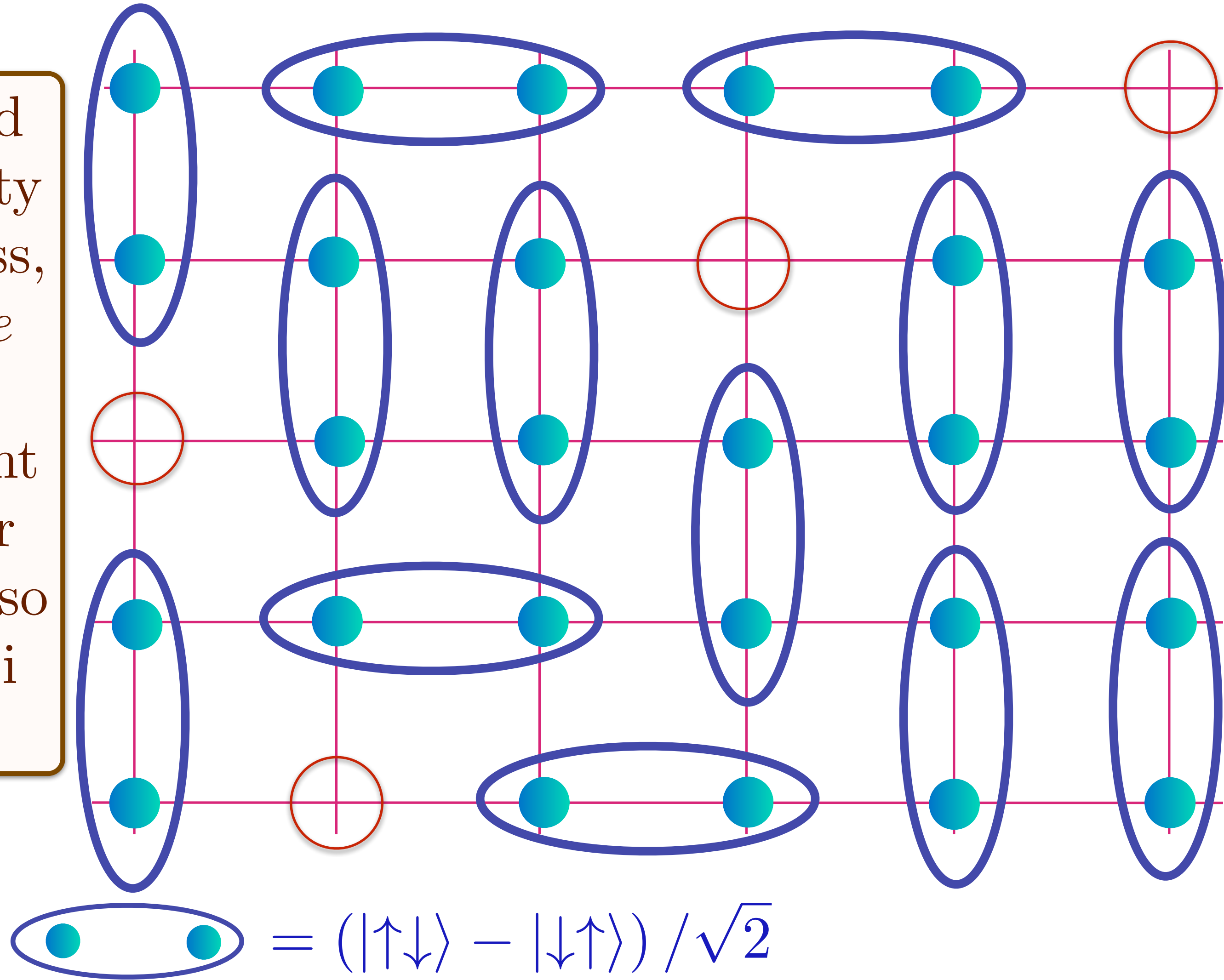
Area $p/4$

Doping an insulating antiferromagnet with holes of density p

Holon metal

Oshikawa anomaly is satisfied by sum of spin liquid (1) and Fermi surface anomalies (p)

Spin liquid with density p of spinless, charge $+e$ holons.
No coherent inter-layer transport, so no Yamaji effect.



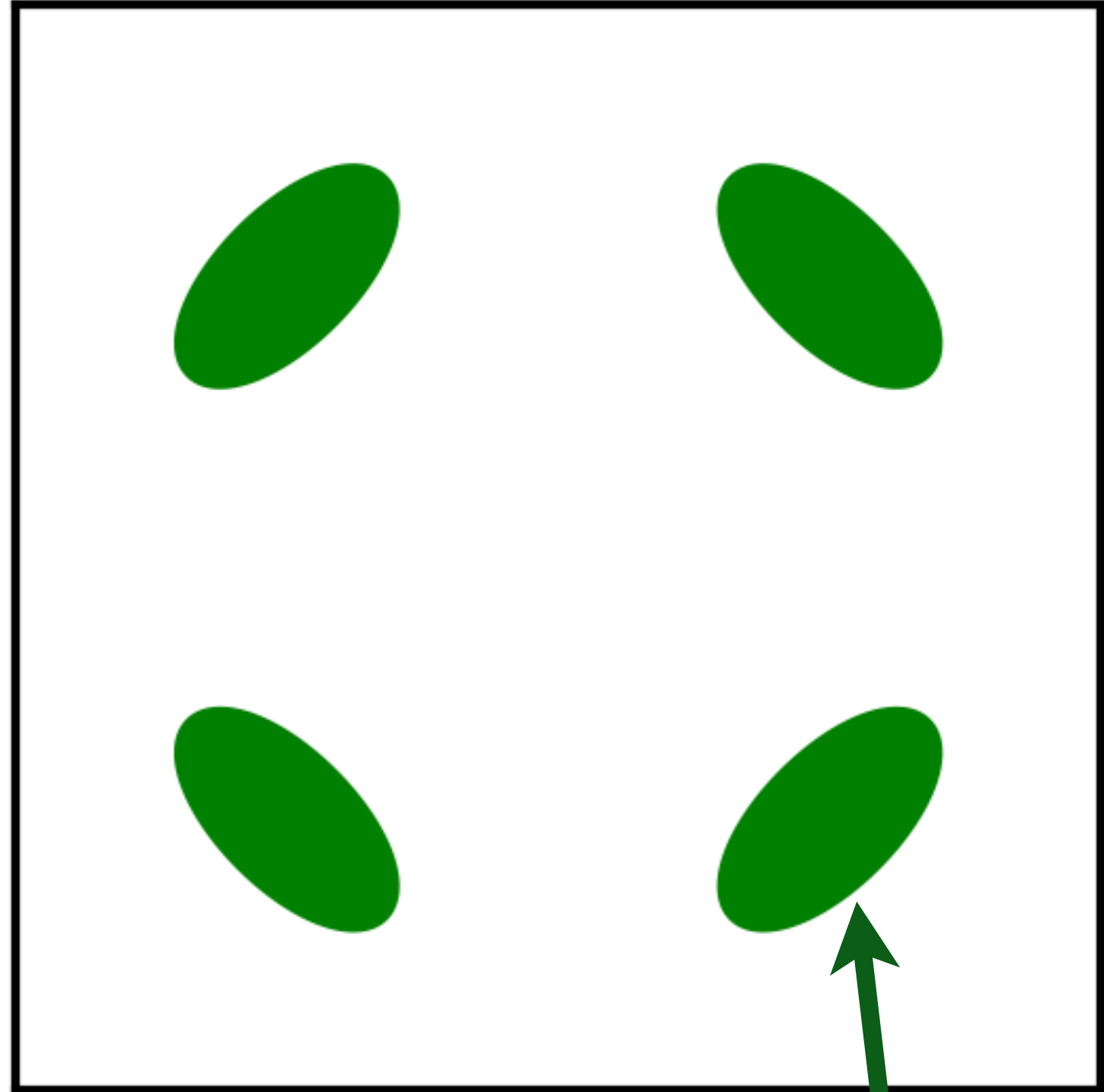
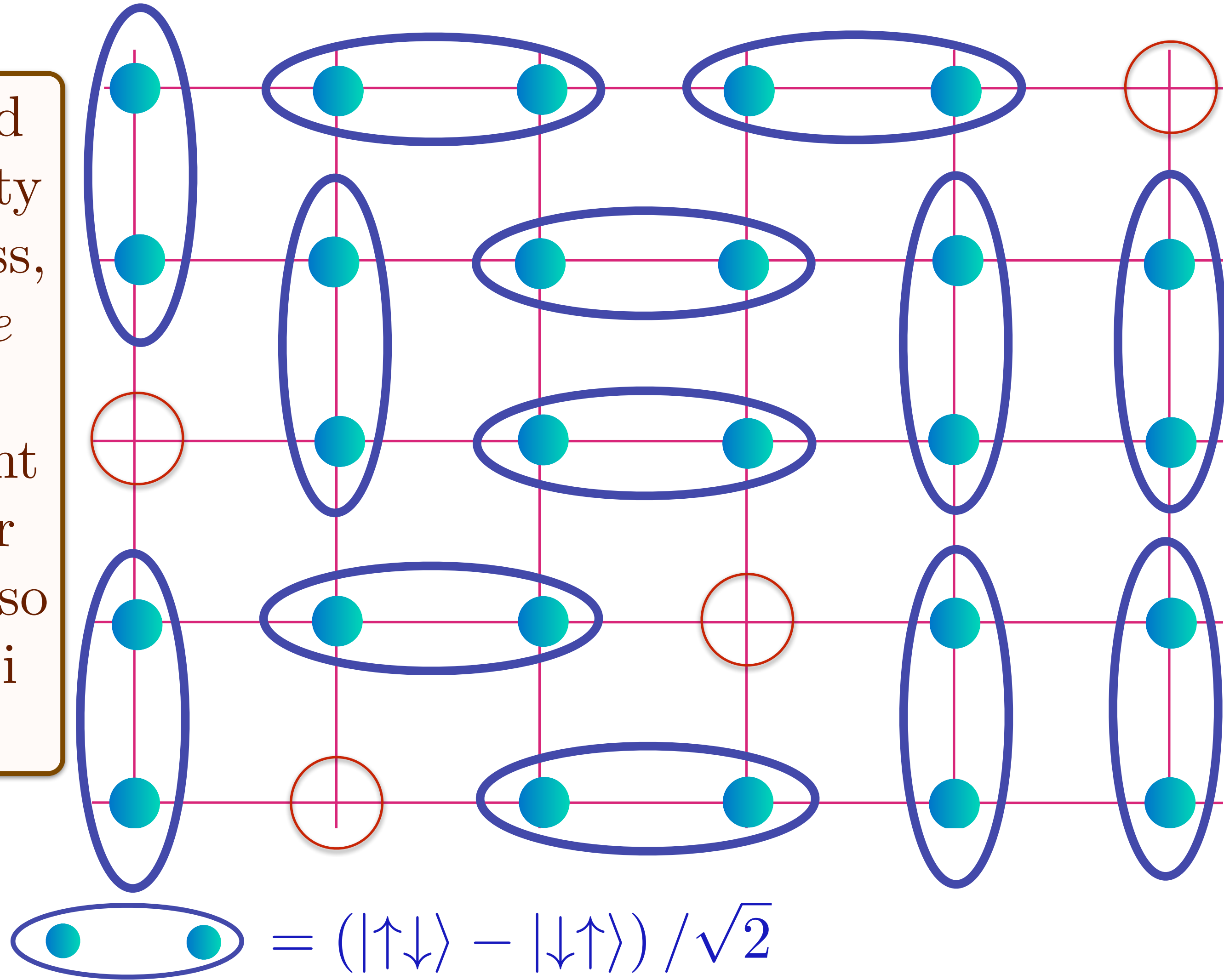
Area $p/4$

Doping an insulating antiferromagnet with holes of density p

Holon metal

Oshikawa anomaly is satisfied by sum of spin liquid (1) and Fermi surface anomalies (p)

Spin liquid with density p of spinless, charge $+e$ holons.
No coherent inter-layer transport, so no Yamaji effect.

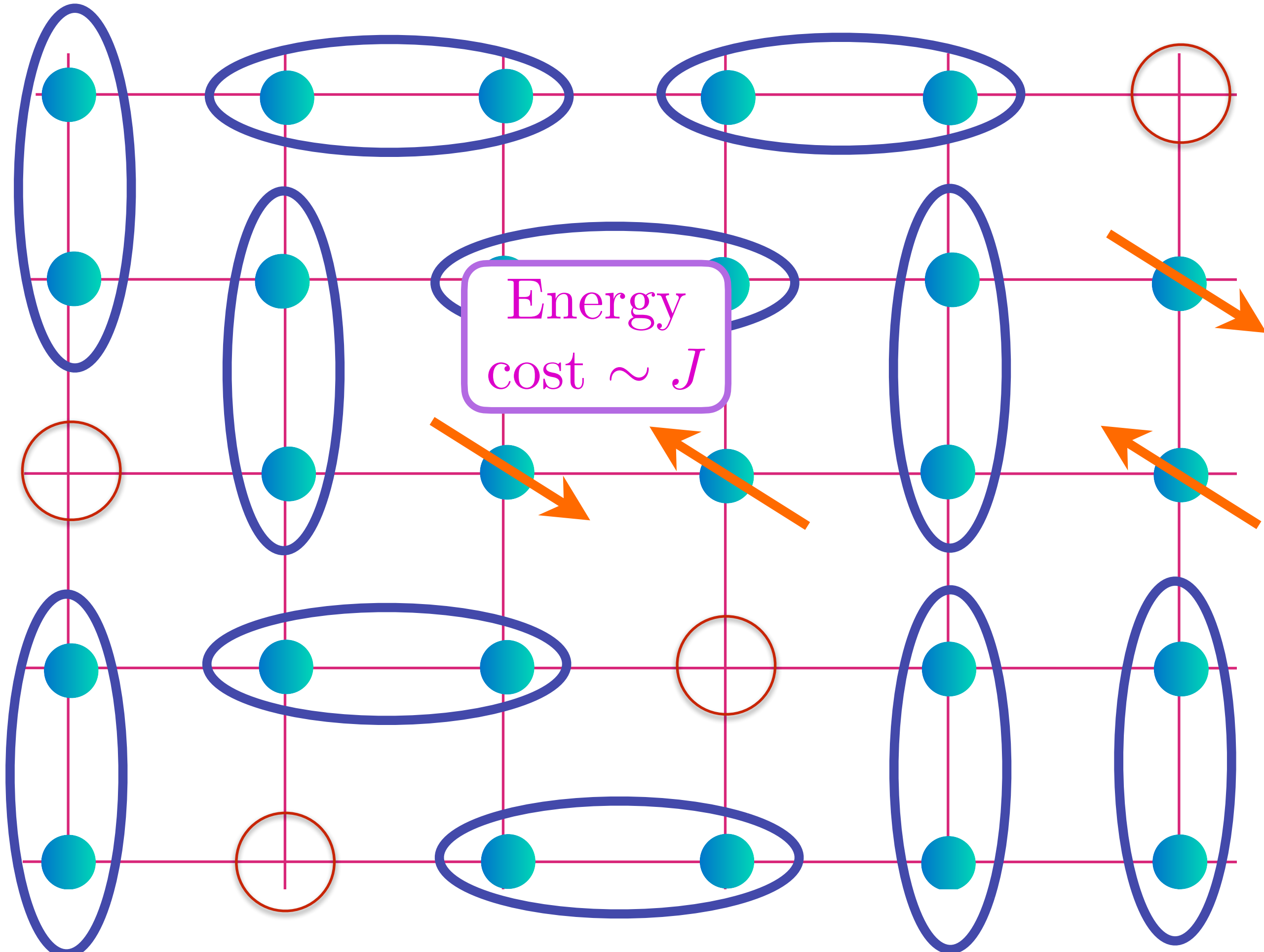


Area $p/4$

Doping an insulating antiferromagnet with holes of density p

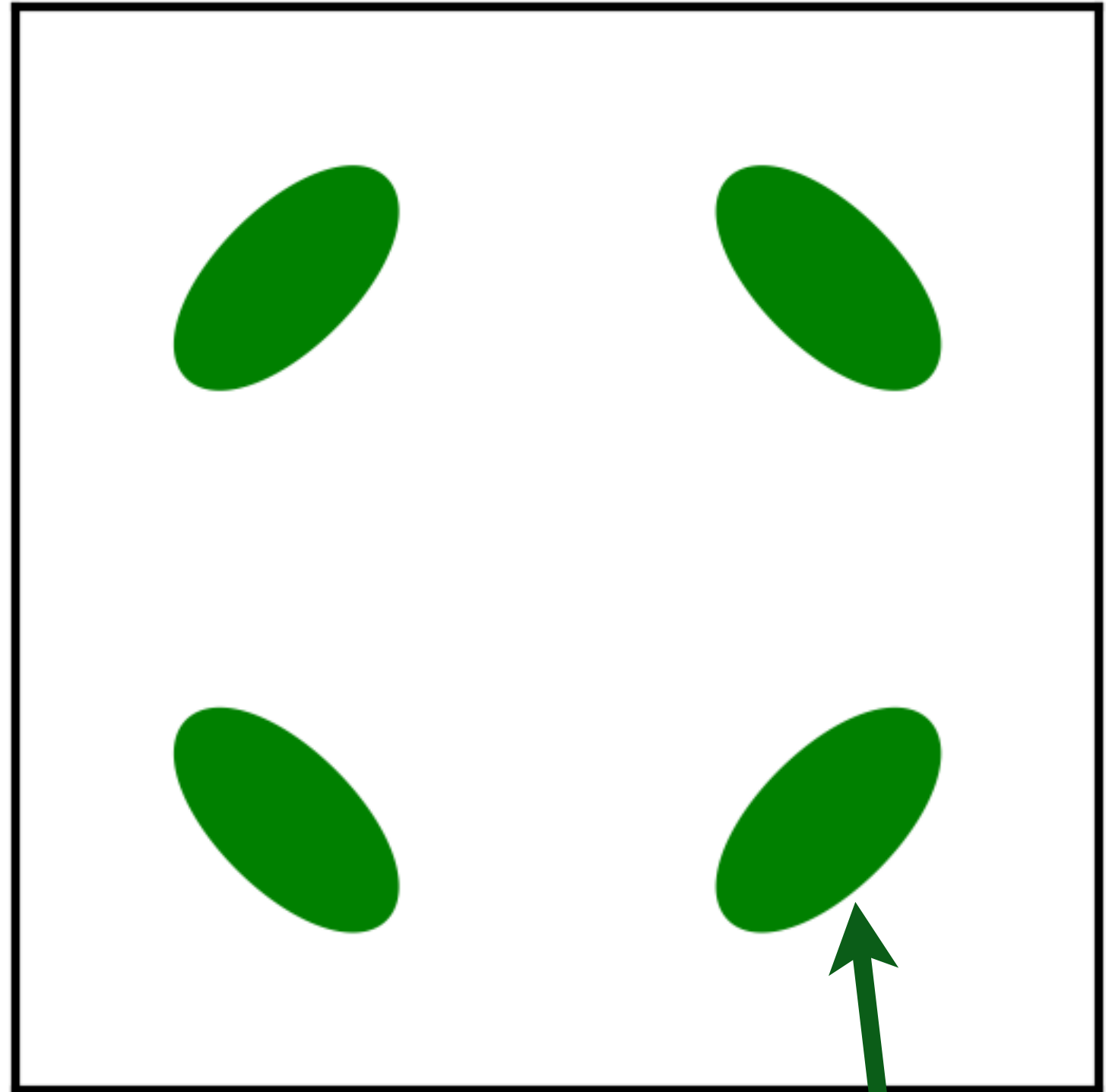
Holon metal excited states

Oshikawa anomaly is satisfied by sum of spin liquid (1) and Fermi surface anomalies (p)



Charge 0,
spin-1/2
spinons

$$\text{[Pair of electrons]} = (|\uparrow\downarrow\rangle - |\downarrow\uparrow\rangle) / \sqrt{2}$$



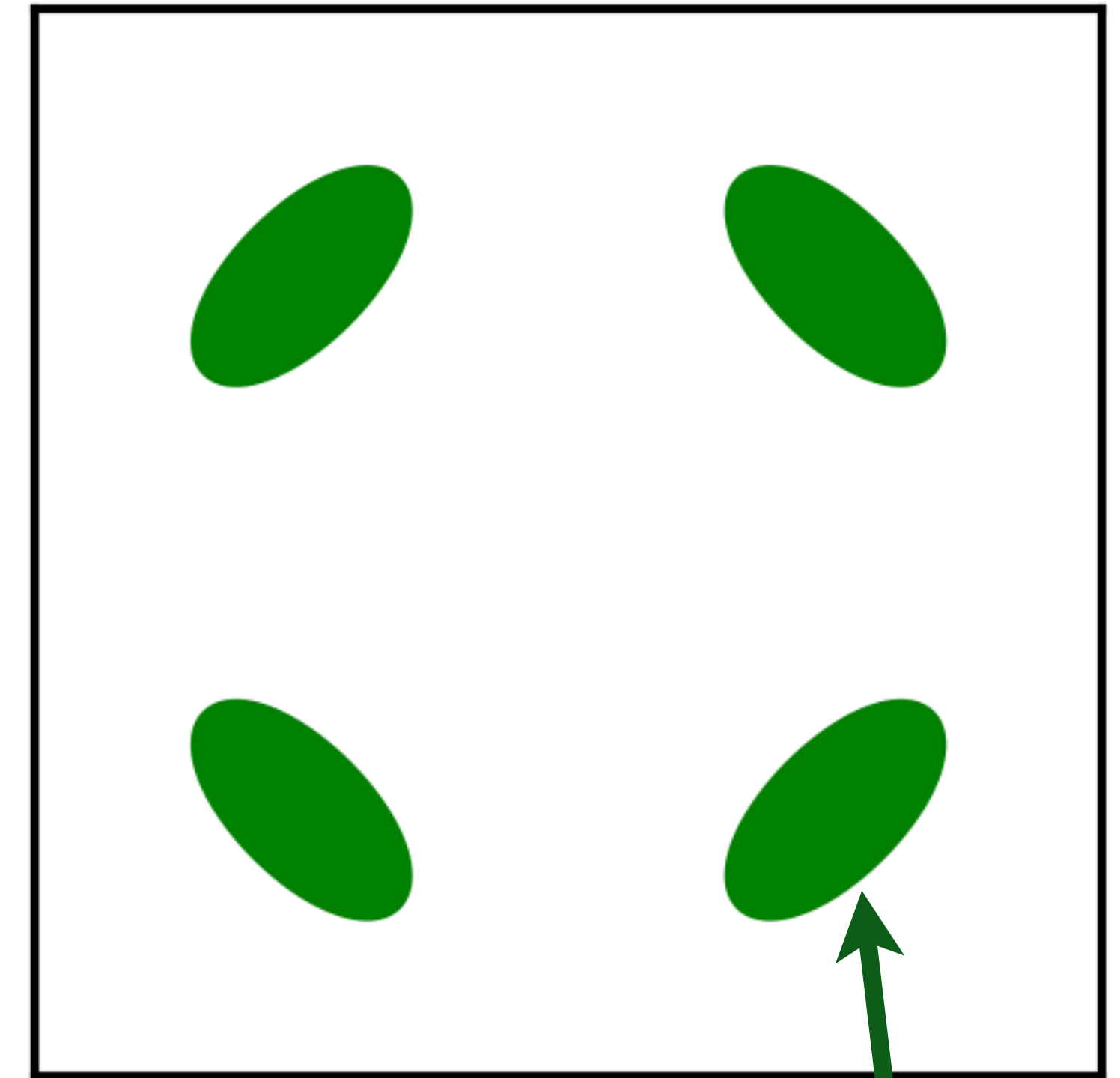
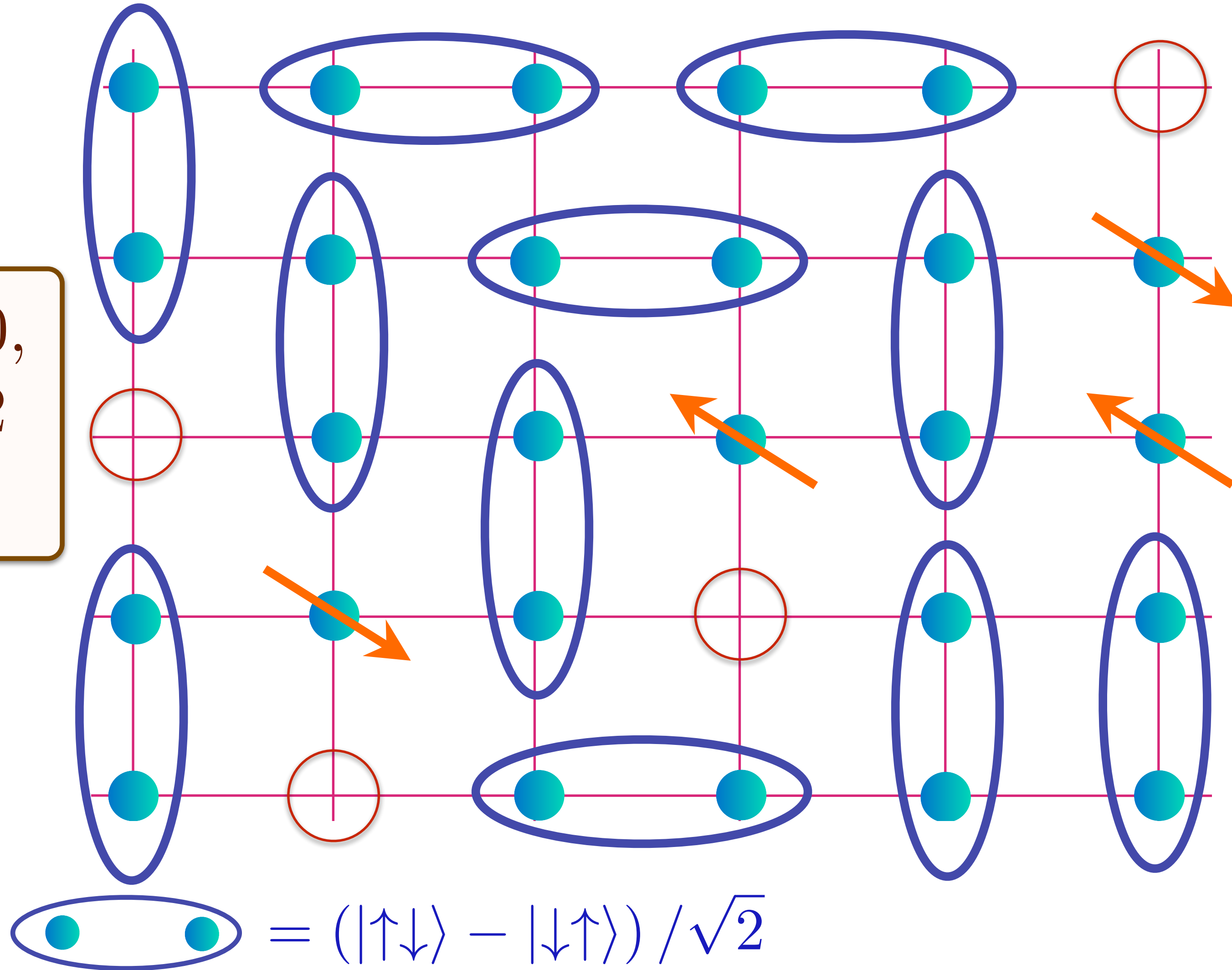
Area $p/4$

Doping an insulating antiferromagnet with holes of density p

Holon metal excited states

Oshikawa anomaly is satisfied by sum of spin liquid (1) and Fermi surface anomalies (p)

Charge 0,
spin-1/2
spinons



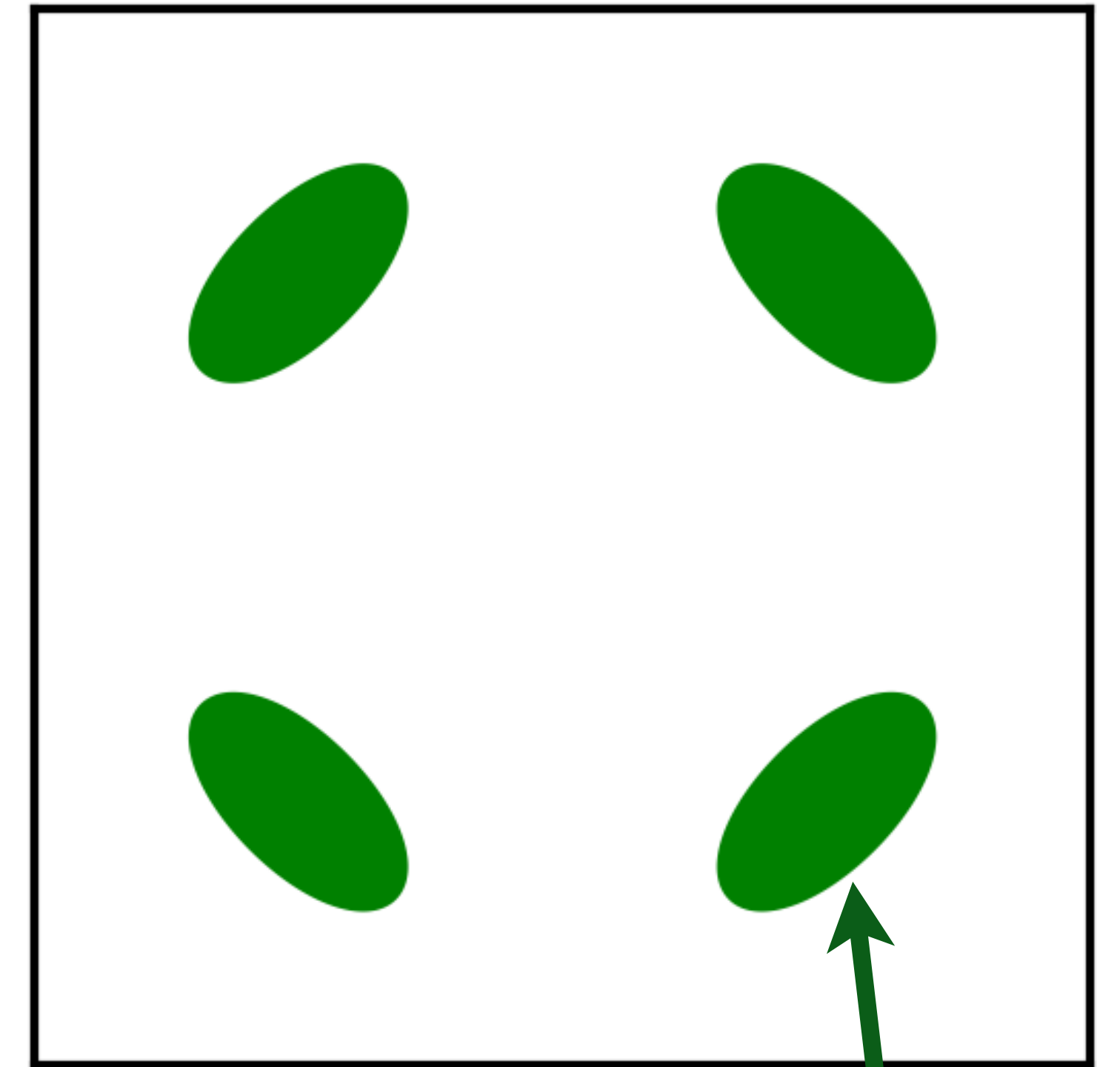
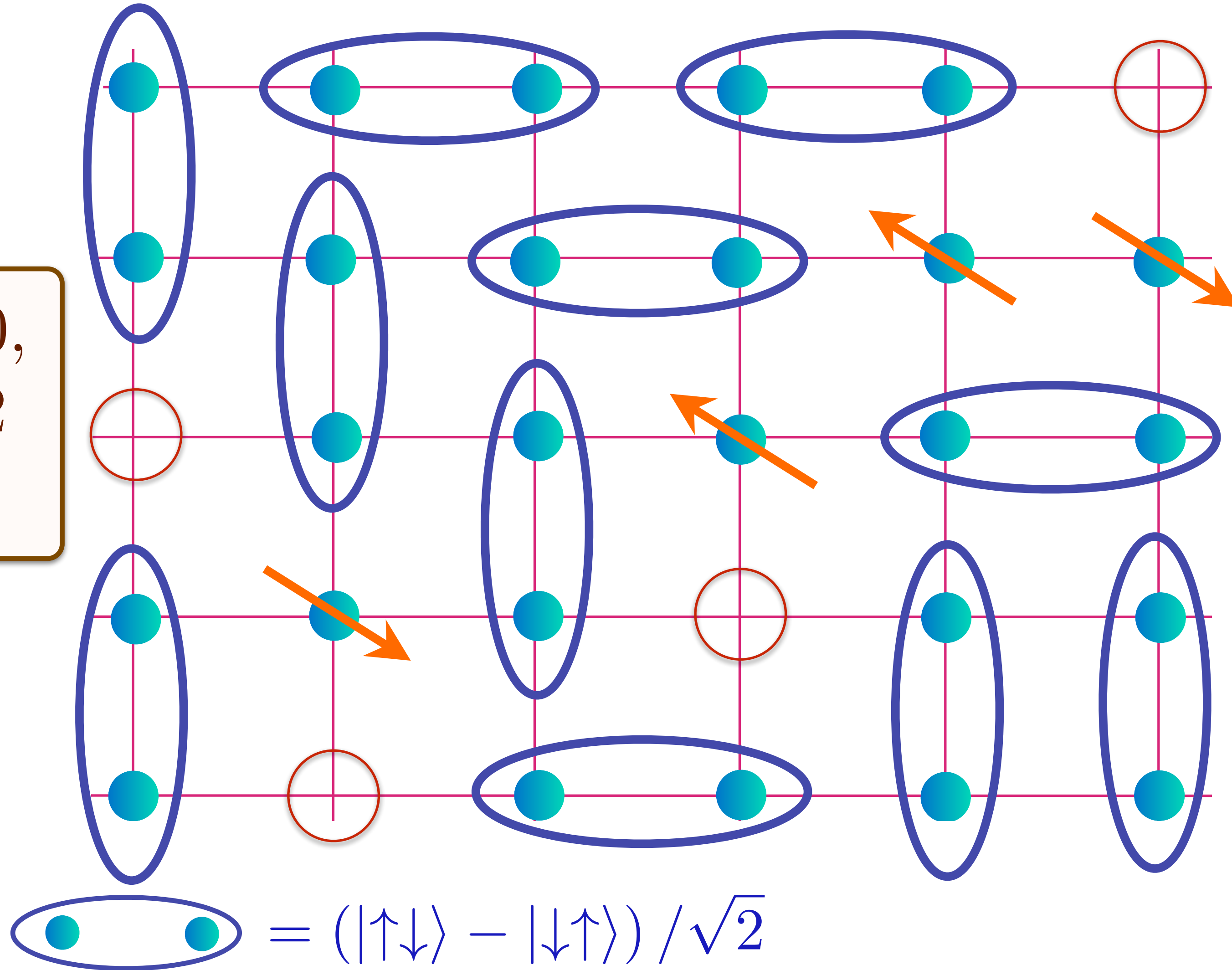
Area $p/4$

Doping an insulating antiferromagnet with holes of density p

Holon metal excited states

Oshikawa anomaly is satisfied by sum of spin liquid (1) and Fermi surface anomalies (p)

Charge 0,
spin-1/2
spinons



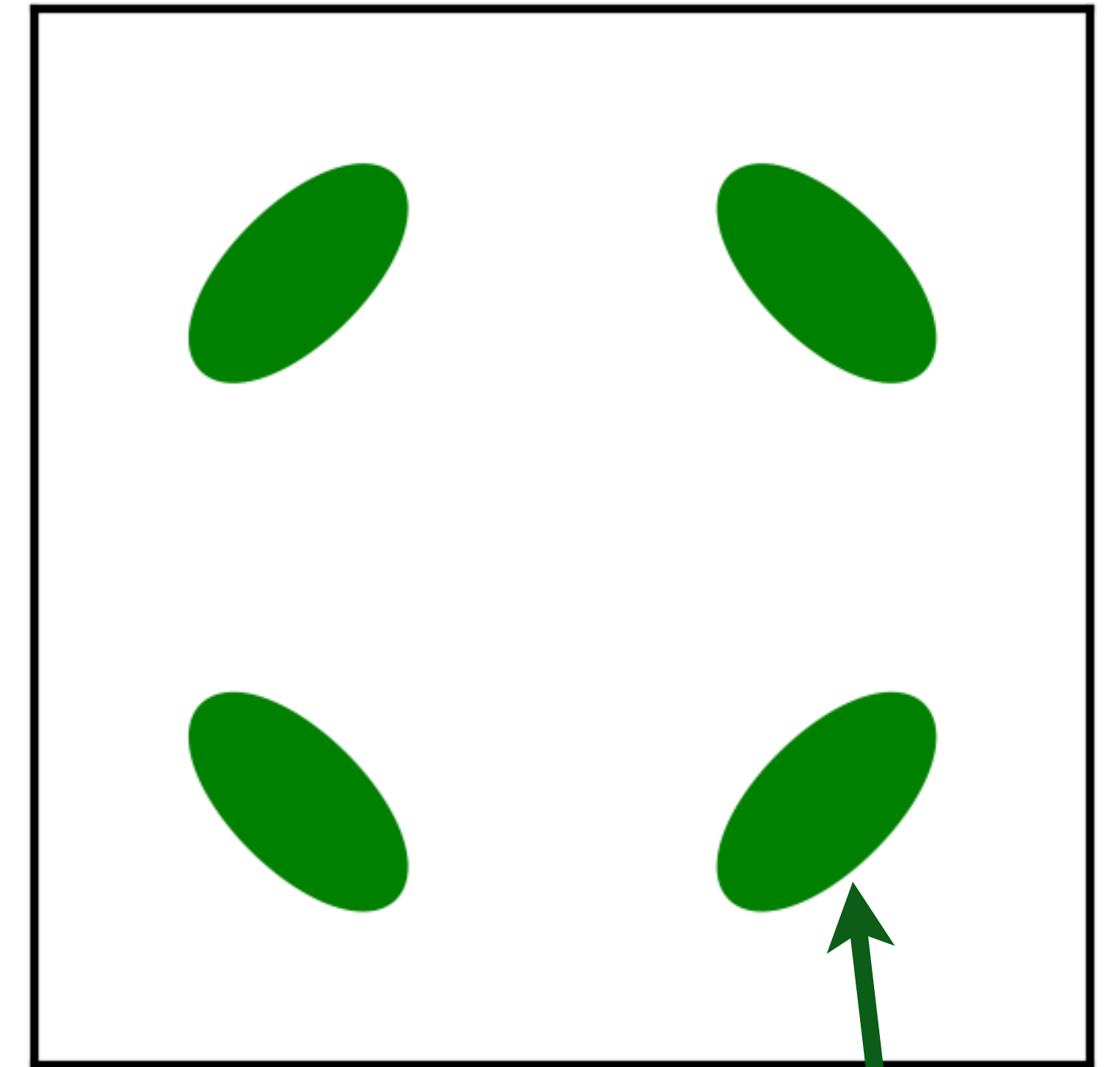
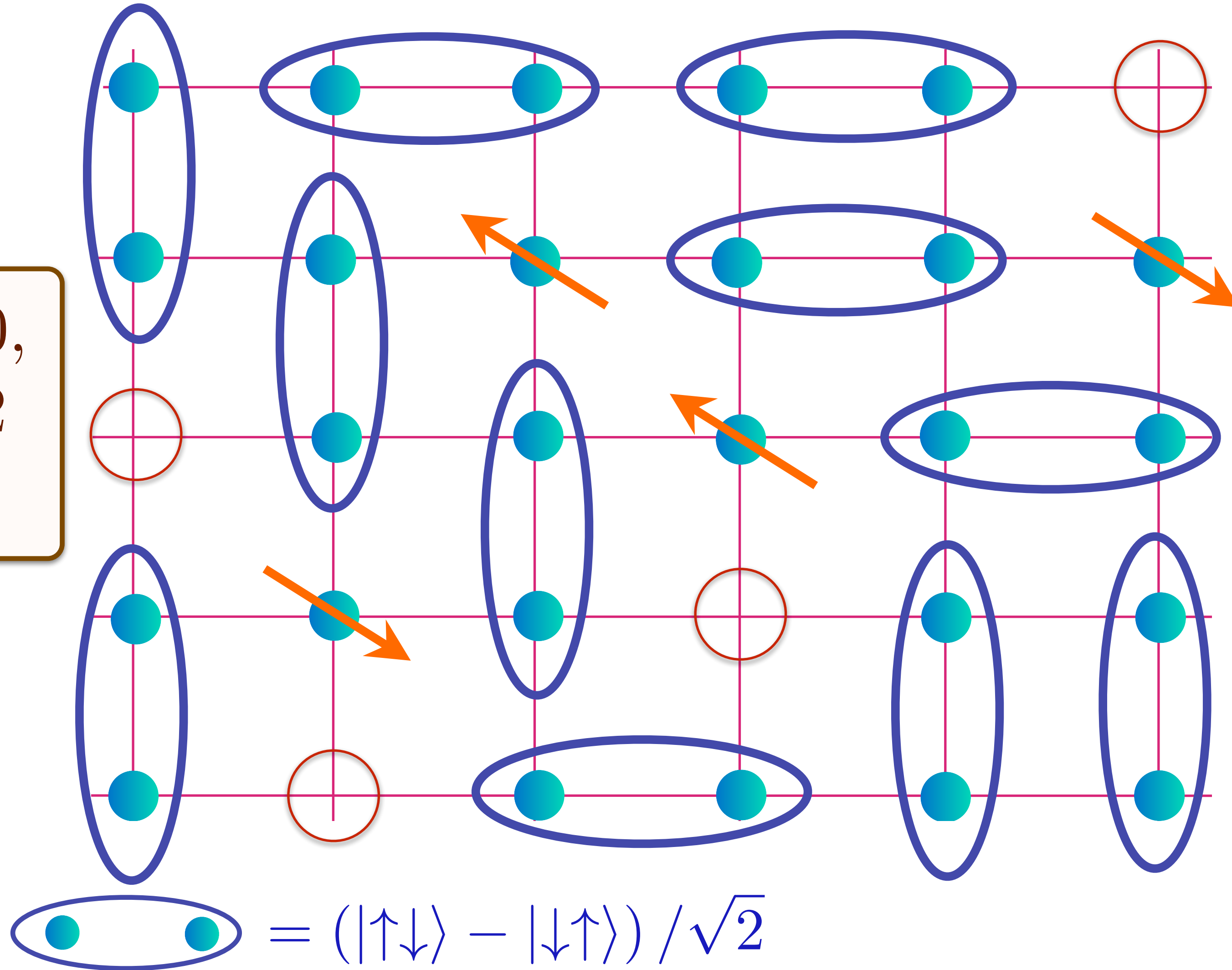
Area $p/4$

Doping an insulating antiferromagnet with holes of density p

Holon metal excited states

Oshikawa anomaly is satisfied by sum of spin liquid (1) and Fermi surface anomalies (p)

Charge 0,
spin-1/2
spinons



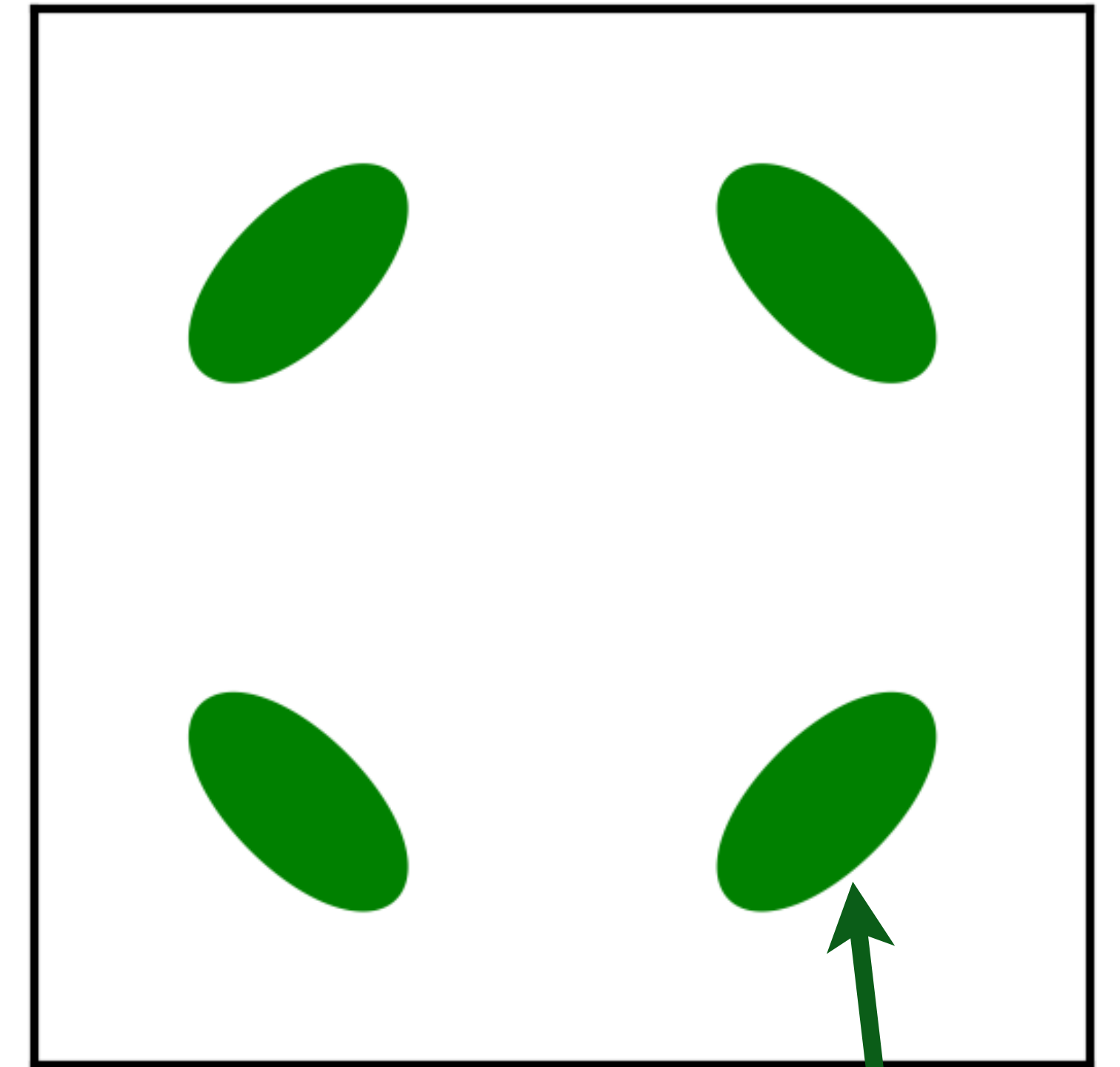
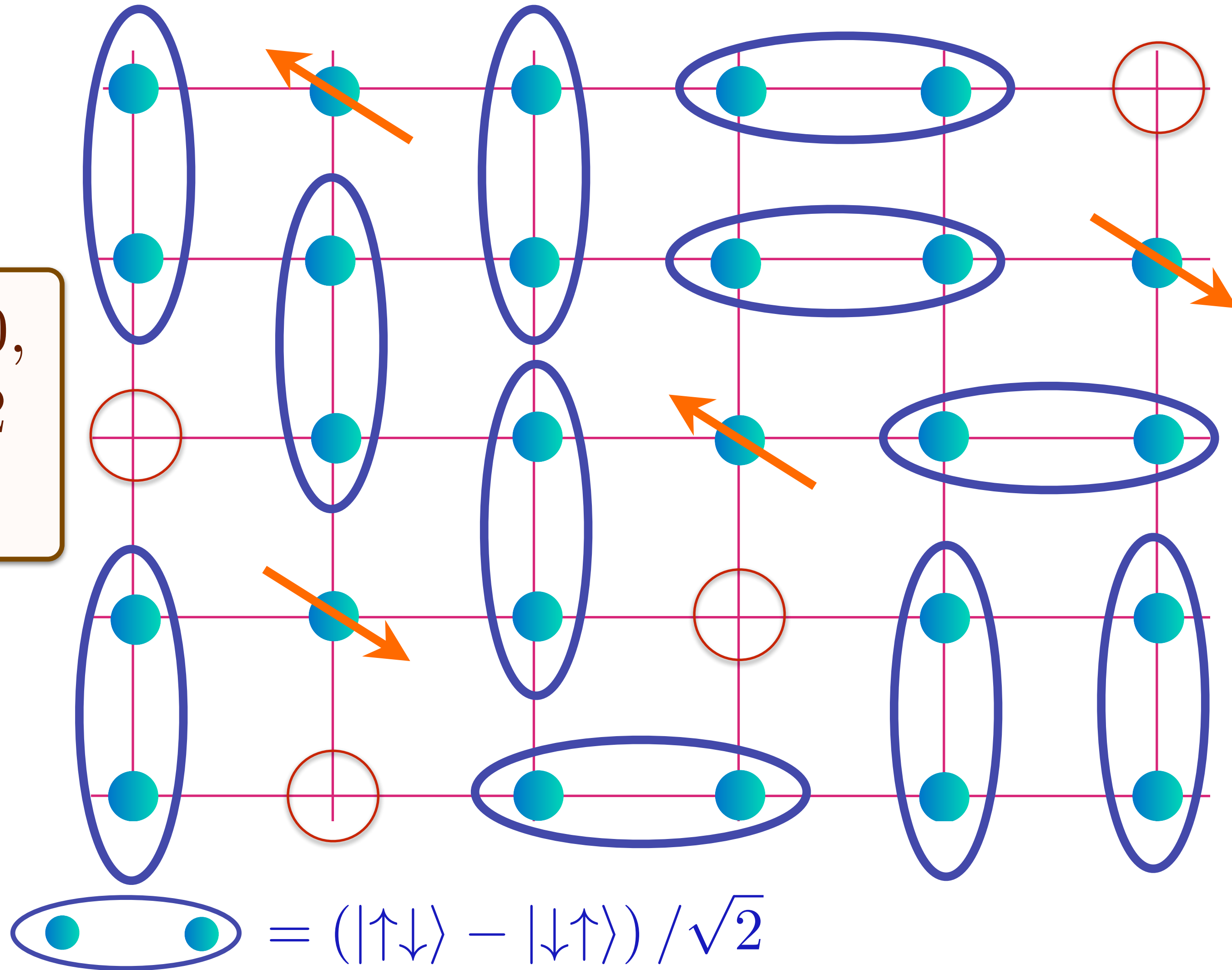
Area $p/4$

Doping an insulating antiferromagnet with holes of density p

Holon metal excited states

Oshikawa anomaly is satisfied by sum of spin liquid (1) and Fermi surface anomalies (p)

Charge 0,
spin-1/2
spinons



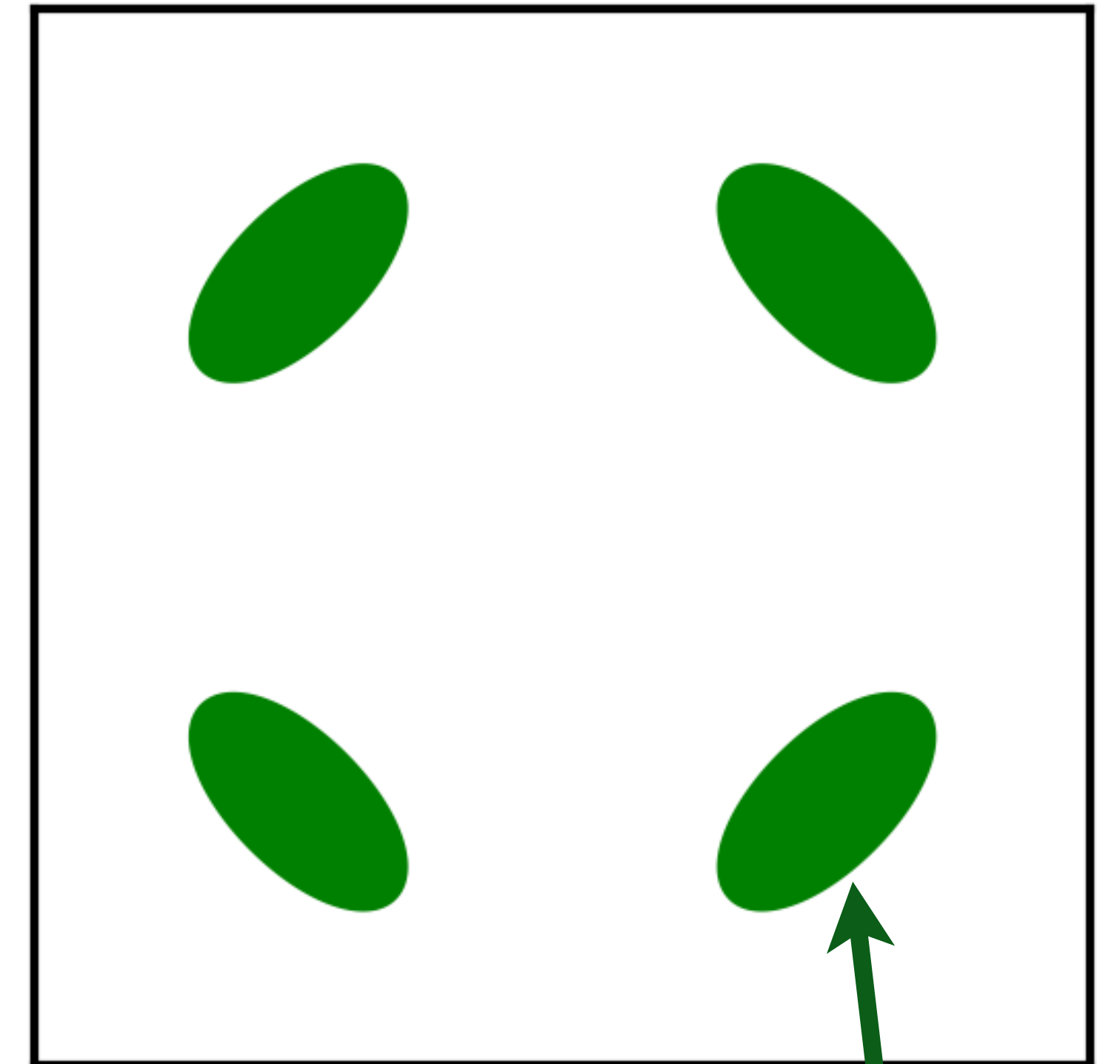
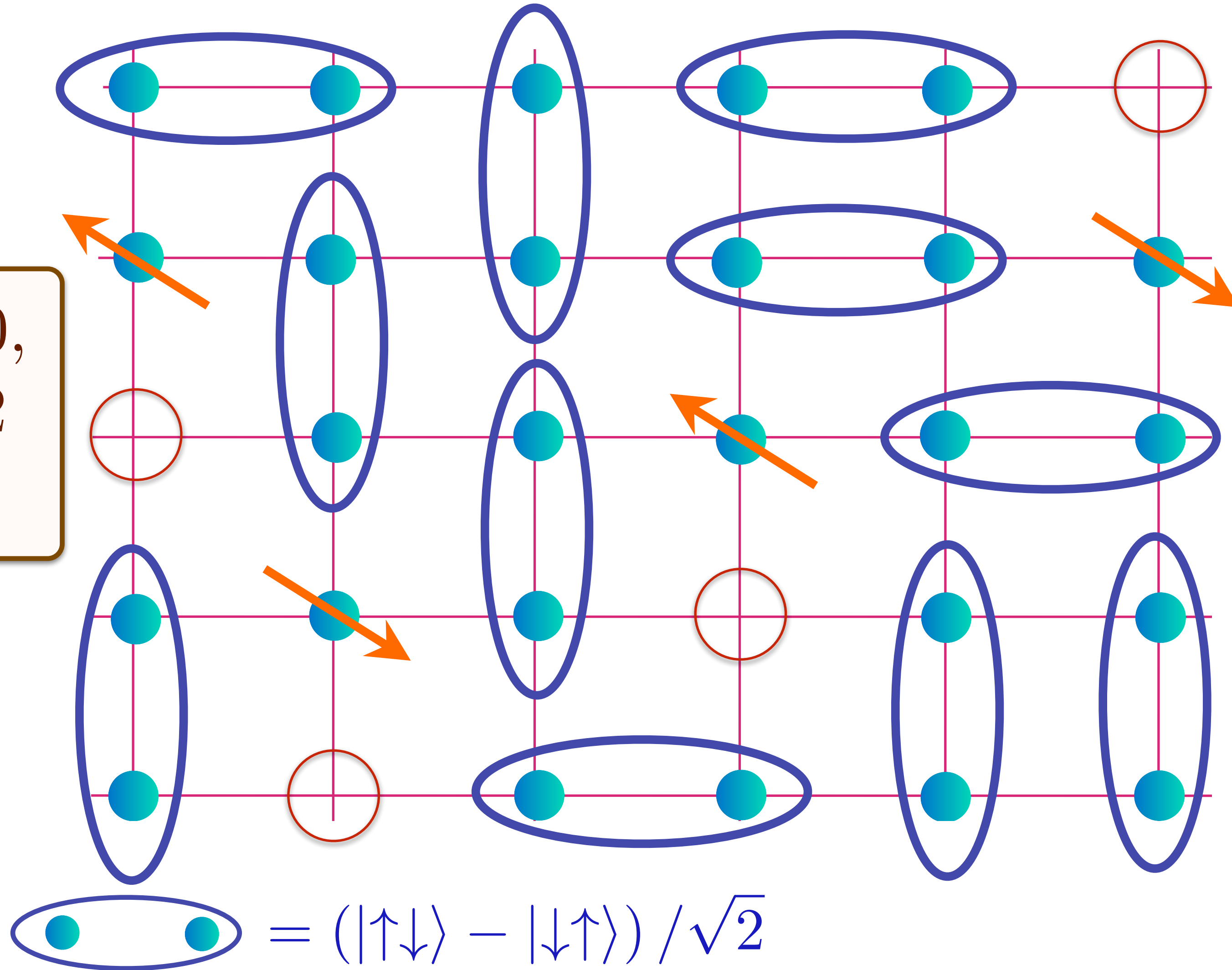
Area $p/4$

Doping an insulating antiferromagnet with holes of density p

Holon metal excited states

Oshikawa anomaly is satisfied by sum of spin liquid (1) and Fermi surface anomalies (p)

Charge 0,
spin-1/2
spinons



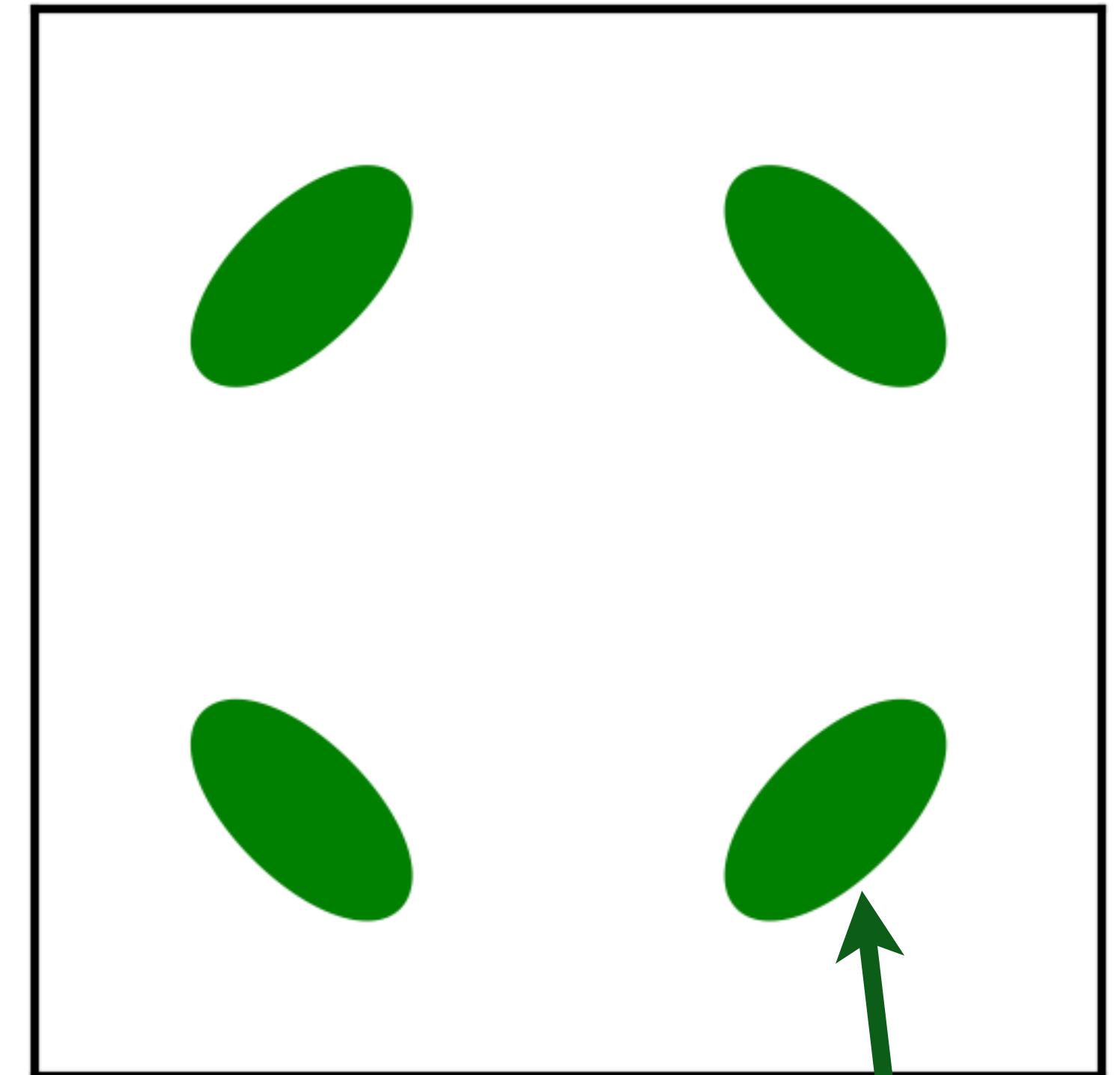
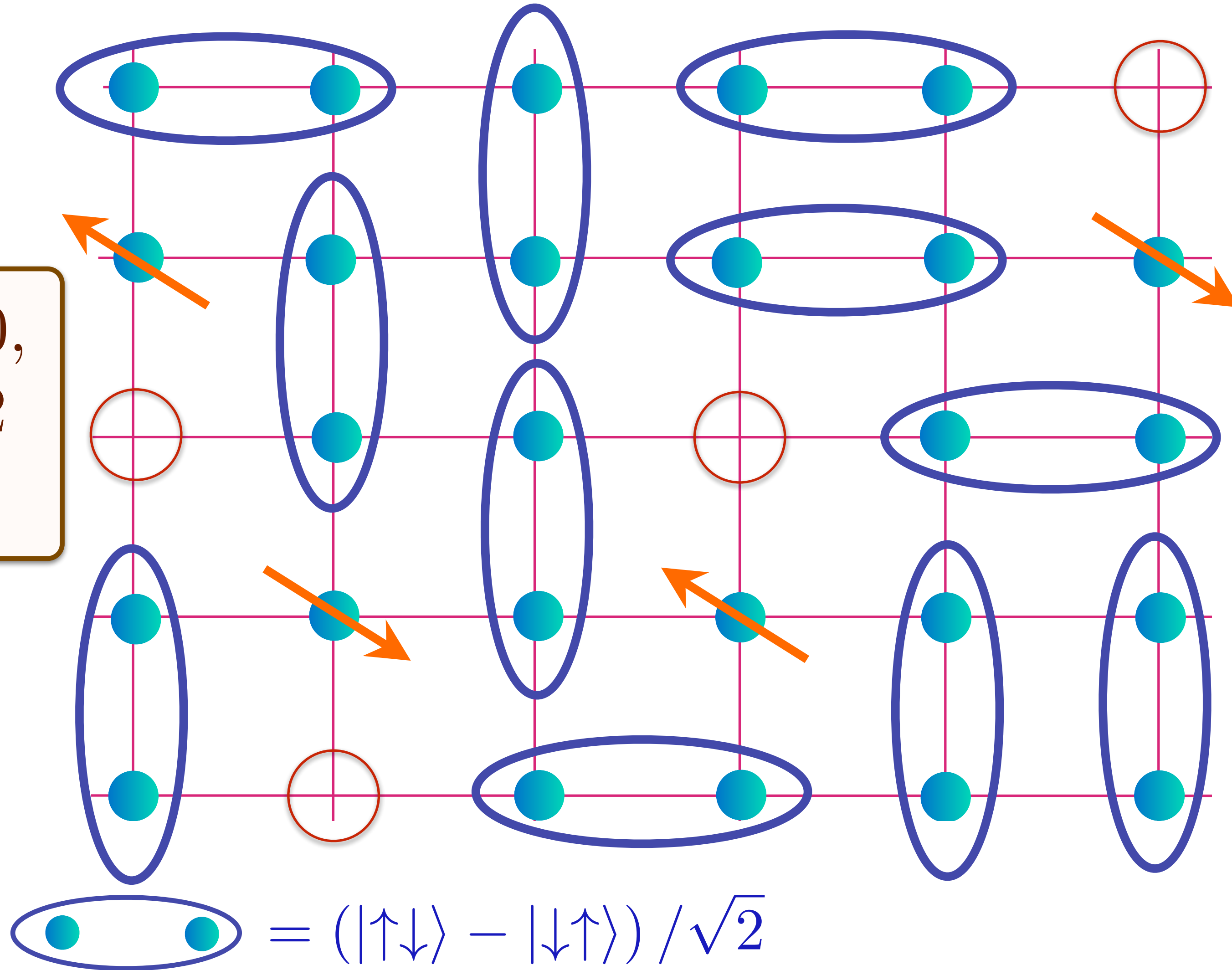
Area $p/4$

Doping an insulating antiferromagnet with holes of density p

Holon metal excited states

Oshikawa anomaly is satisfied by sum of spin liquid (1) and Fermi surface anomalies (p)

Charge 0,
spin-1/2
spinons



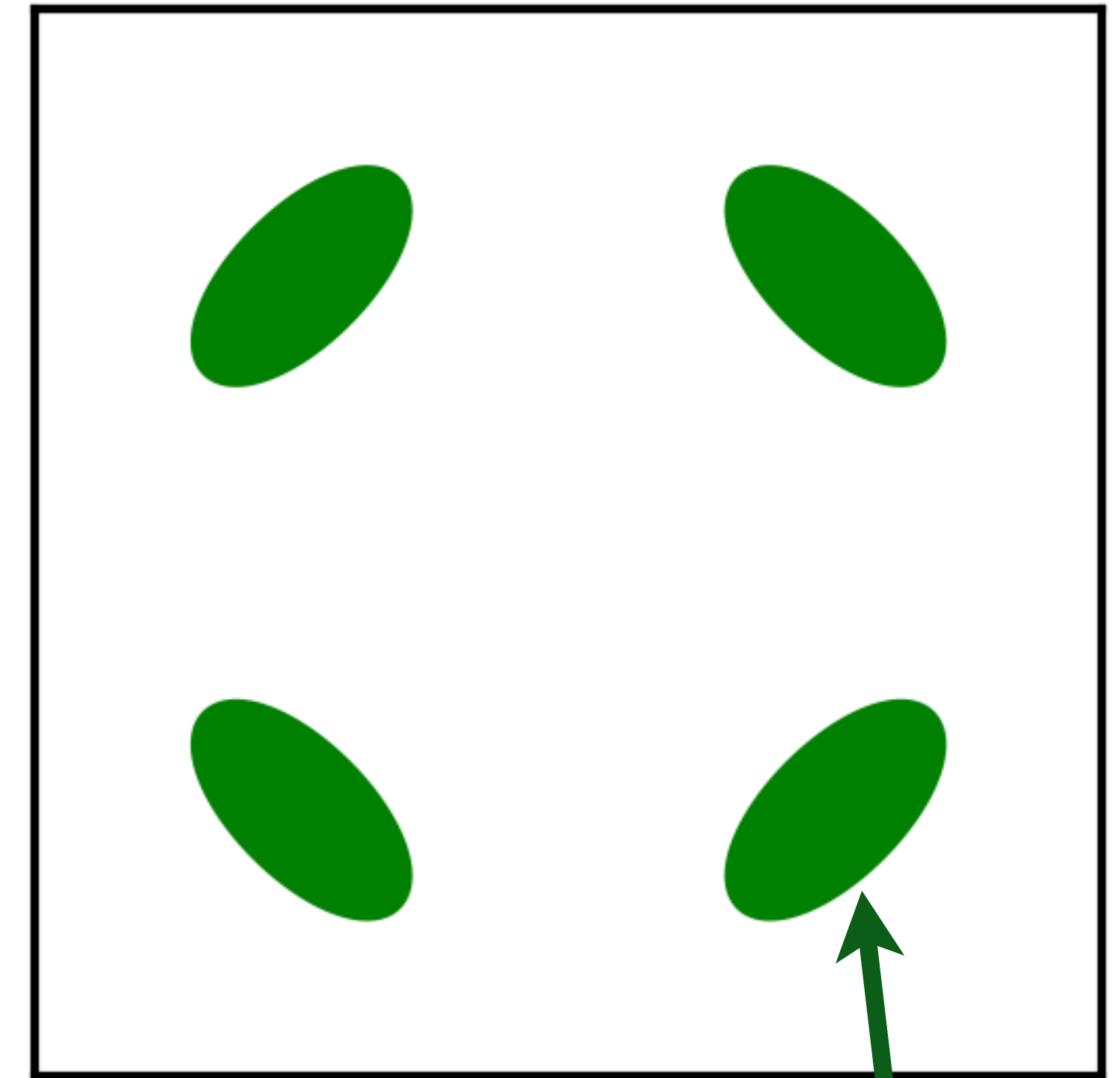
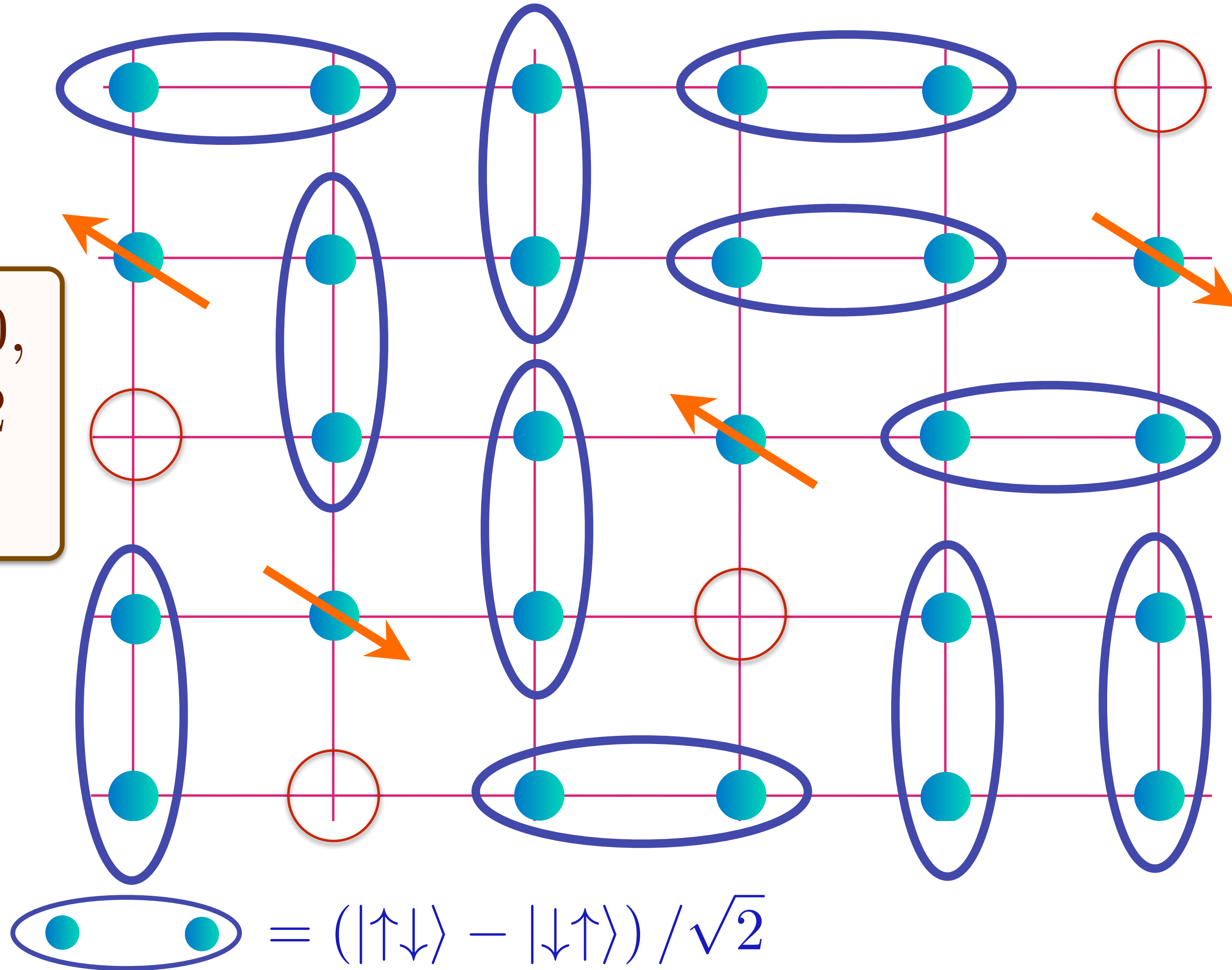
Area $p/4$

Doping an insulating antiferromagnet with holes of density p

Holon metal excited states

Oshikawa anomaly is satisfied by sum of spin liquid (1) and Fermi surface anomalies (p)

Charge 0,
spin-1/2
spinons



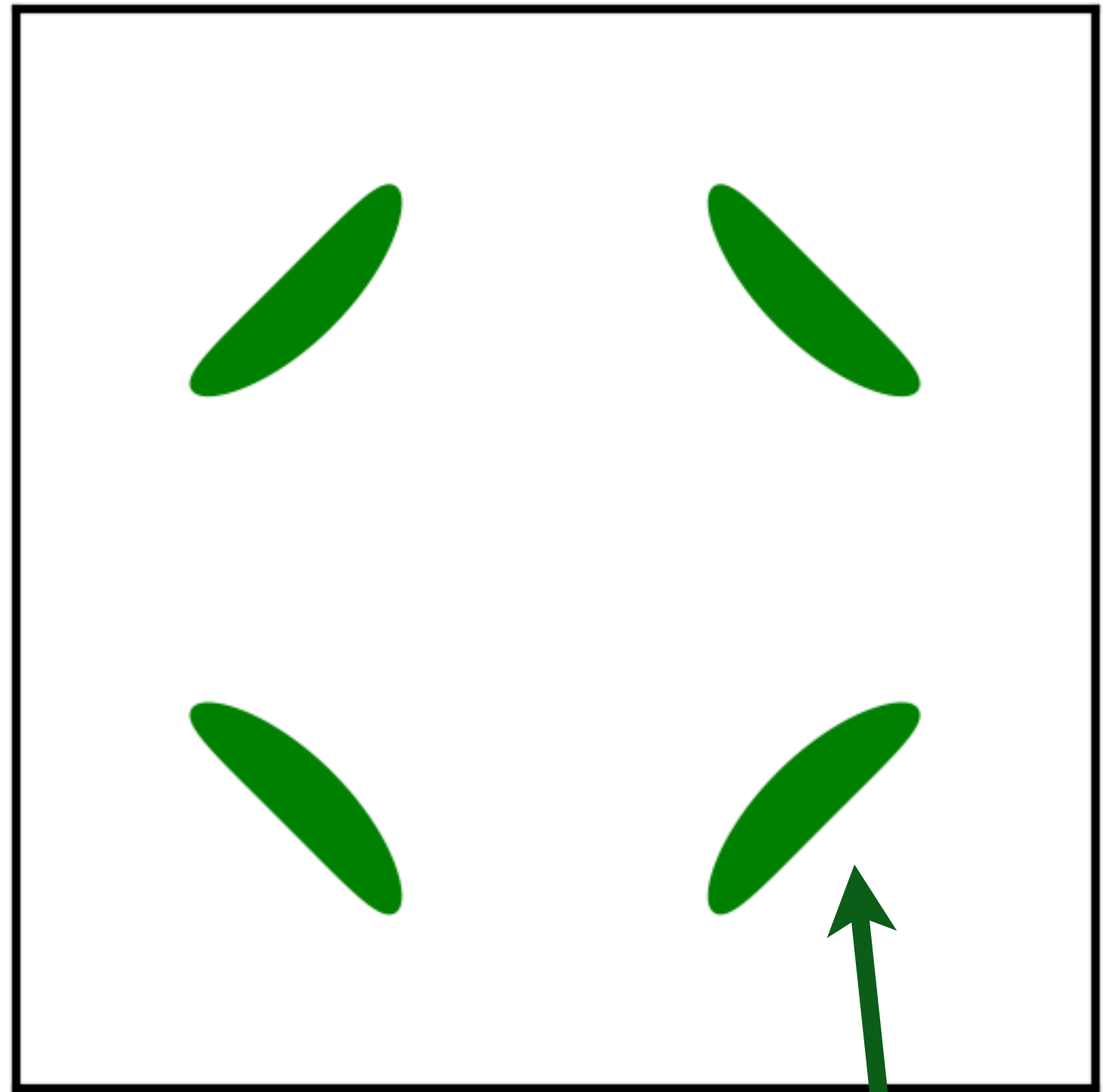
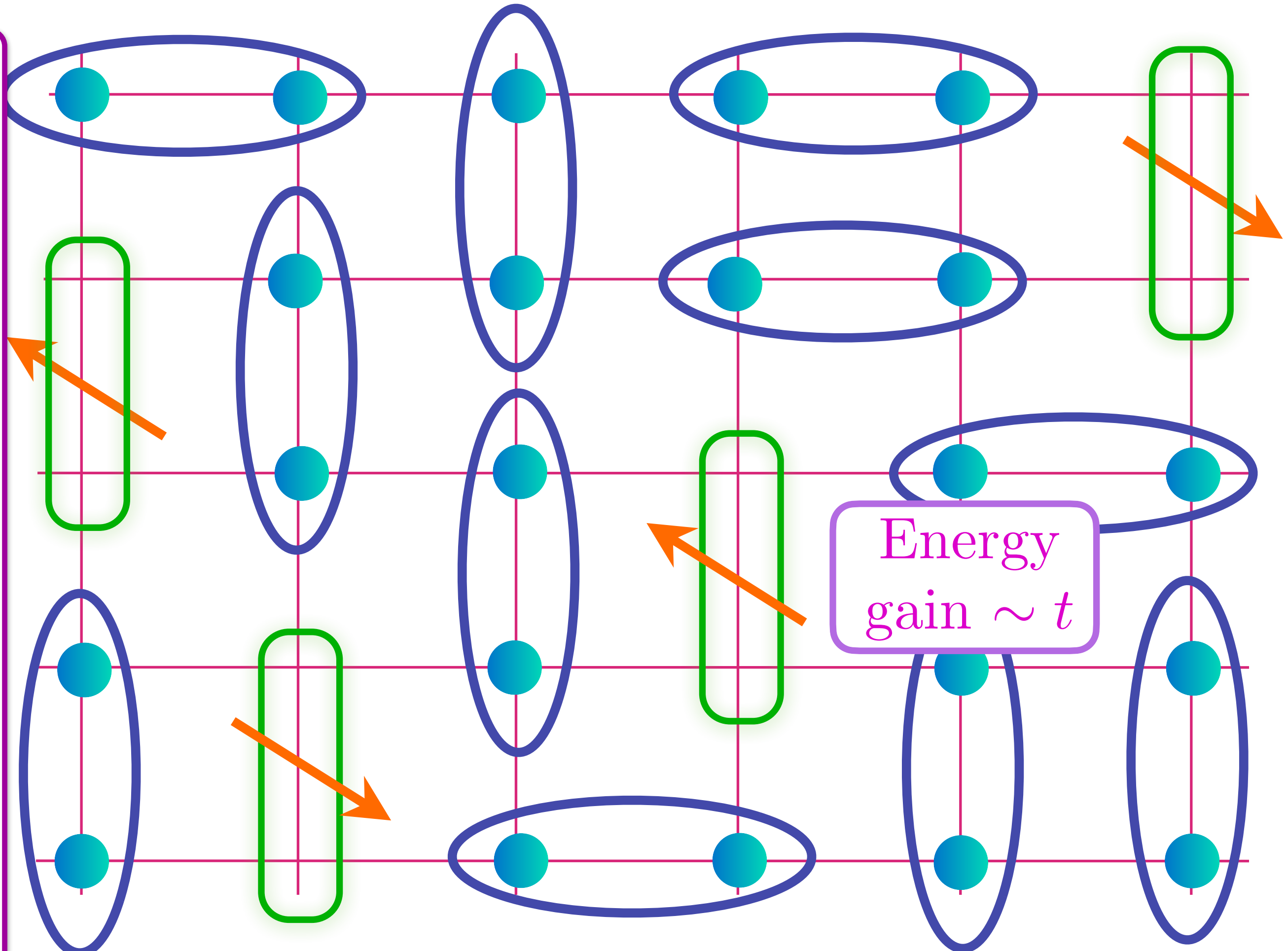
Area $p/4$

Doping an insulating antiferromagnet with holes of density p

FL*

Oshikawa anomaly is satisfied by sum of spin liquid (1) and Fermi surface anomalies (p)

Metal with density p of spin-1/2, charge $+e$ 'holes' (or 'magnetic polarons') with coherent inter-layer transport for Yamaji effect.



$$= (|\uparrow\downarrow\rangle - |\downarrow\uparrow\rangle) / \sqrt{2} \quad \text{Green oval} = (|\uparrow\circ\rangle + |\circ\uparrow\rangle) / \sqrt{2}$$

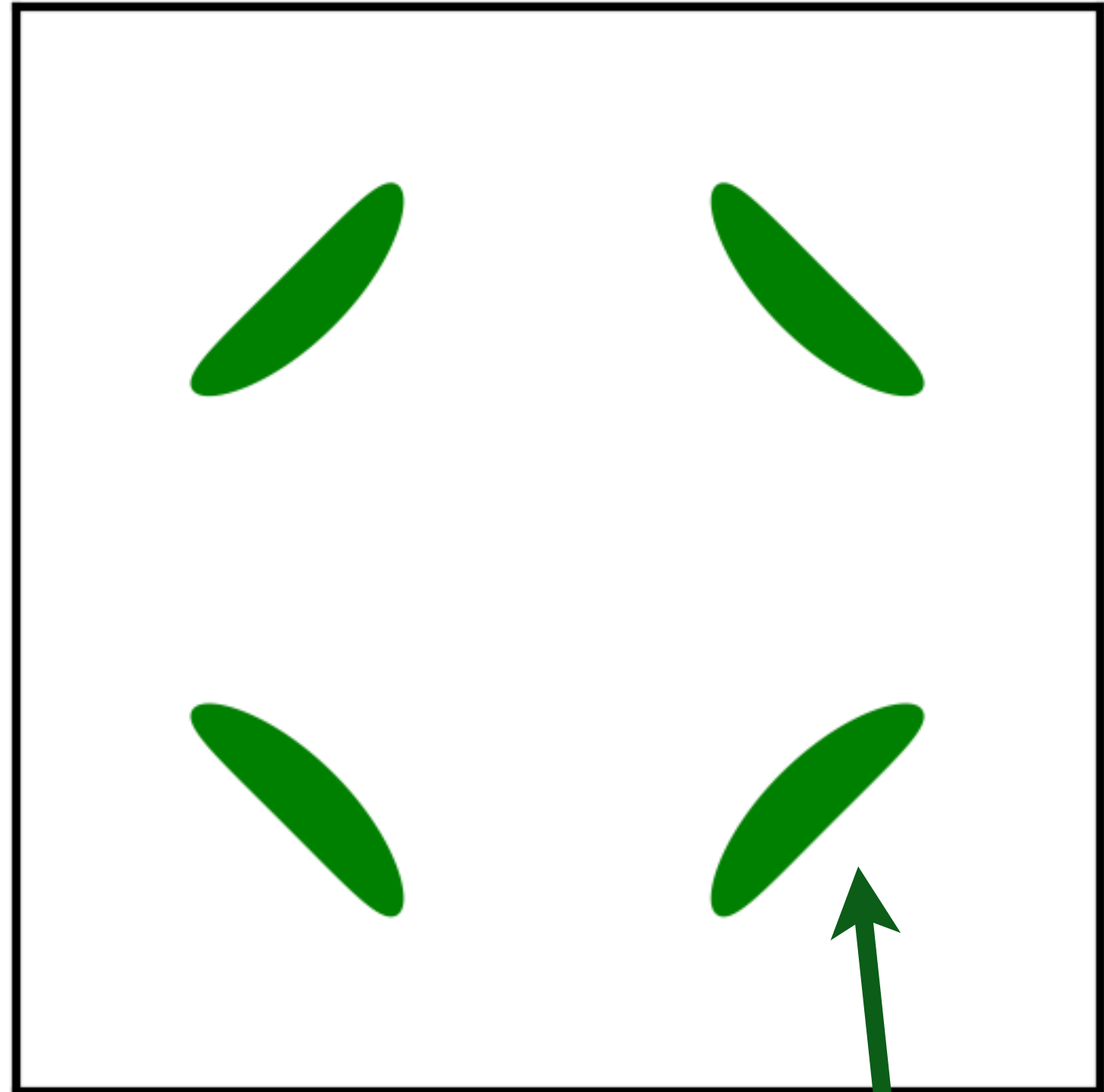
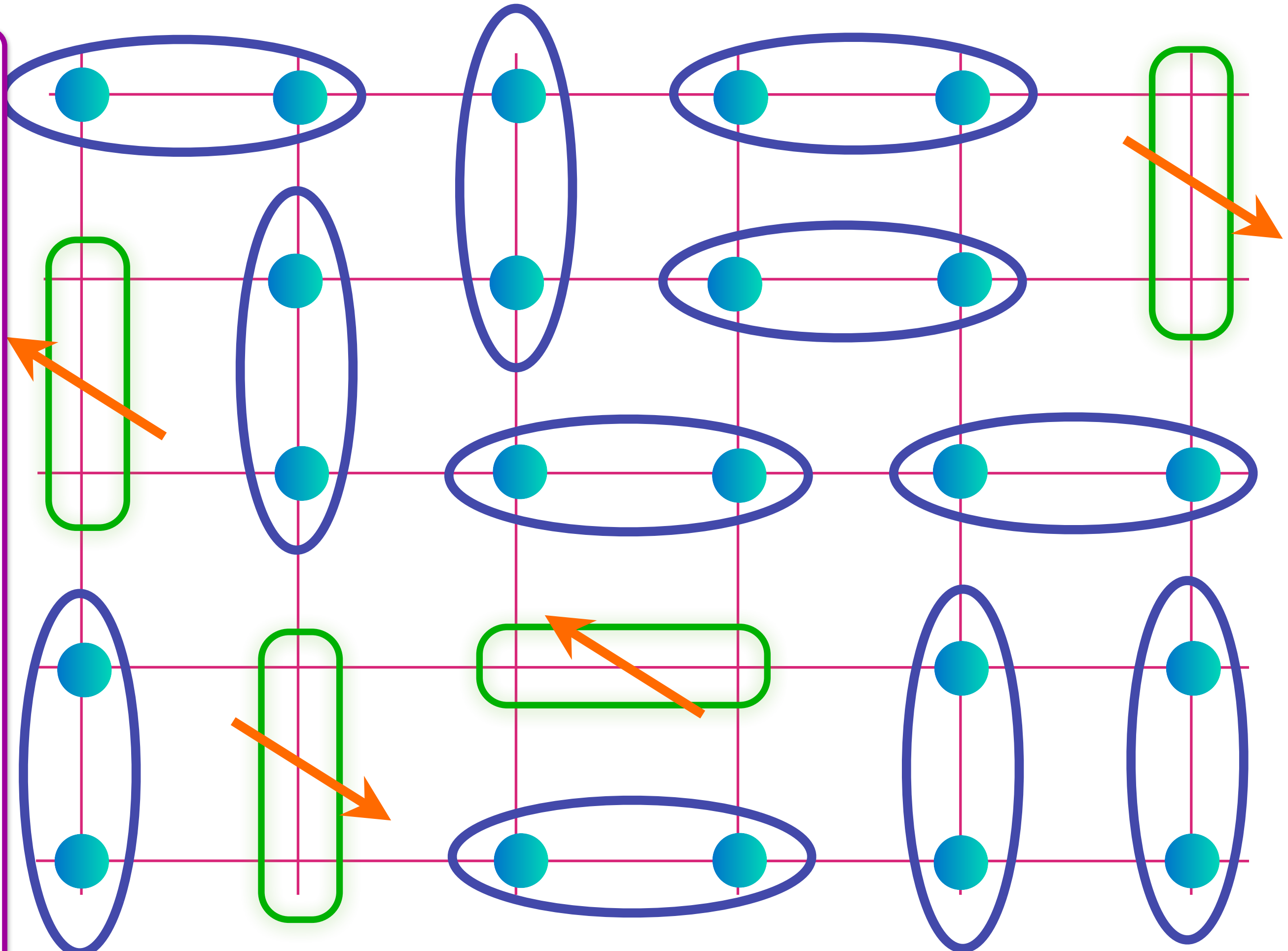
Area $p/8$

Doping an insulating antiferromagnet with holes of density p

FL*

Oshikawa anomaly is satisfied by sum of spin liquid (1) and Fermi surface anomalies (p)

Metal with density p of spin-1/2, charge $+e$ 'holes' (or 'magnetic polarons') with coherent inter-layer transport for Yamaji effect.



$$= (|\uparrow\downarrow\rangle - |\downarrow\uparrow\rangle) / \sqrt{2} \quad \text{Green oval with arrow} = (|\uparrow\circ\rangle + |\circ\uparrow\rangle) / \sqrt{2}$$

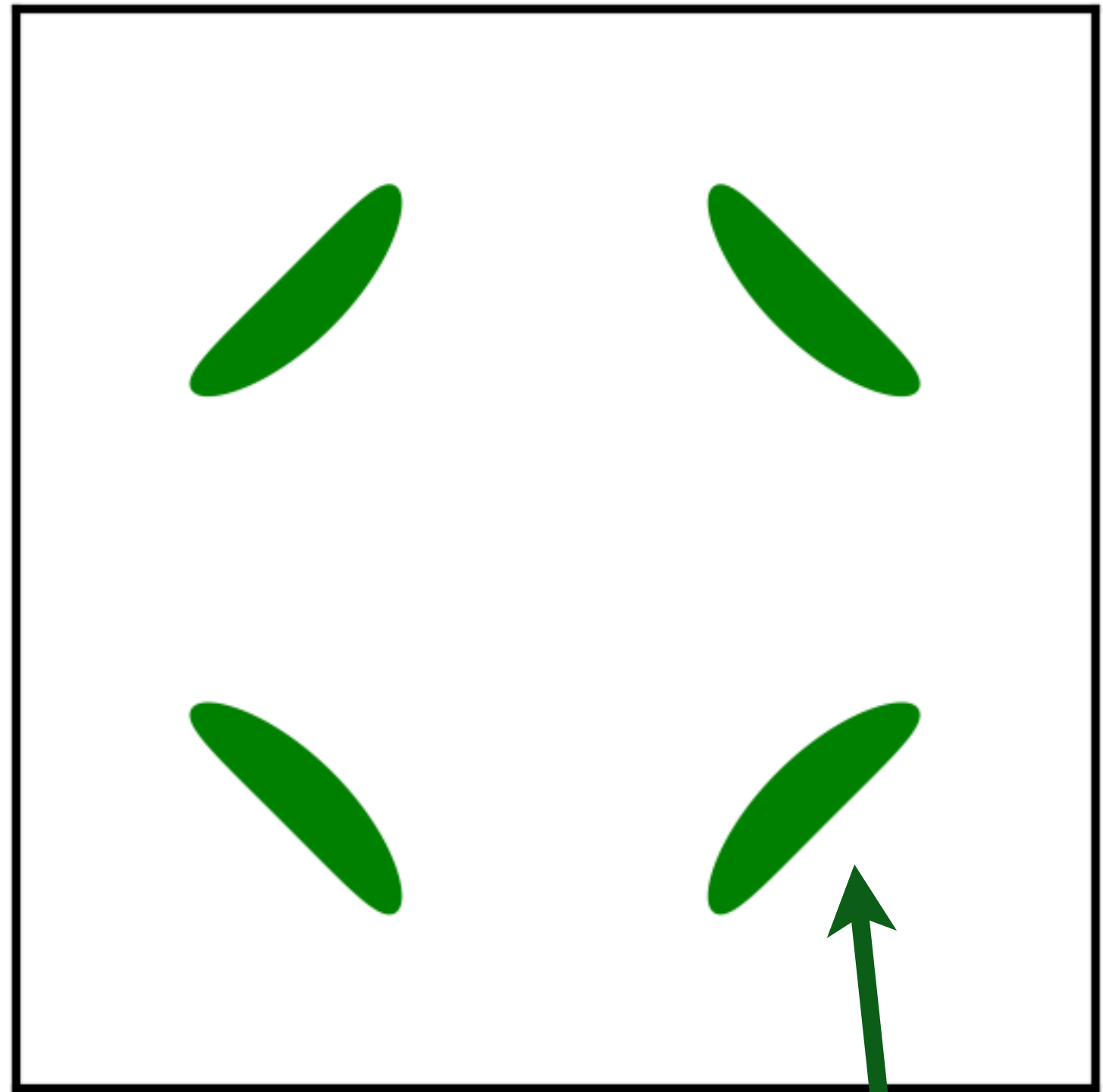
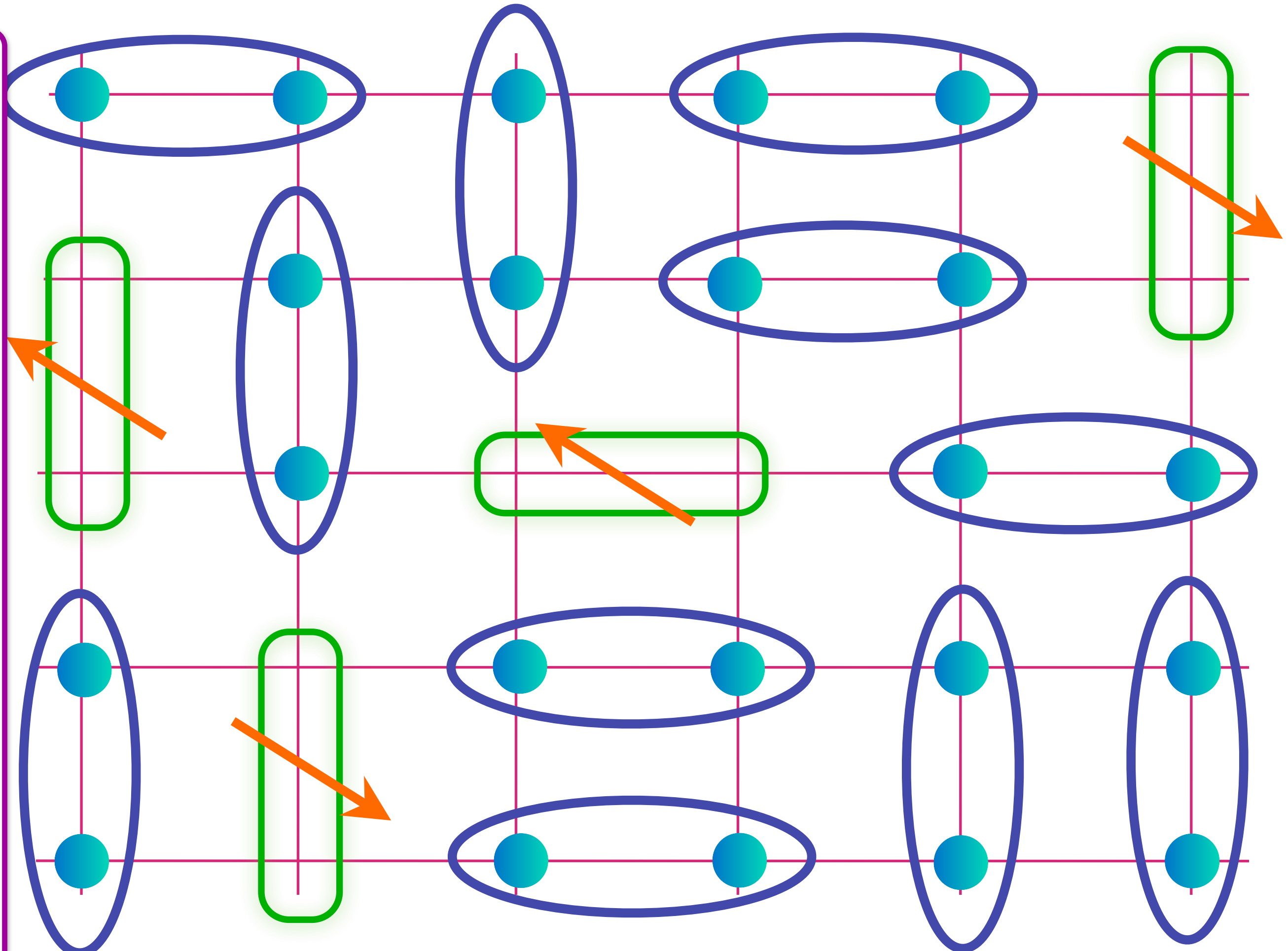
Area $p/8$

Doping an insulating antiferromagnet with holes of density p

FL*

Oshikawa anomaly is satisfied by sum of spin liquid (1) and Fermi surface anomalies (p)

Metal with density p of spin-1/2, charge $+e$ 'holes' (or 'magnetic polarons') with coherent inter-layer transport for Yamaji effect.



$$= (|\uparrow\downarrow\rangle - |\downarrow\uparrow\rangle) / \sqrt{2} \quad \text{Green box with arrow} = (|\uparrow\circ\rangle + |\circ\uparrow\rangle) / \sqrt{2}$$

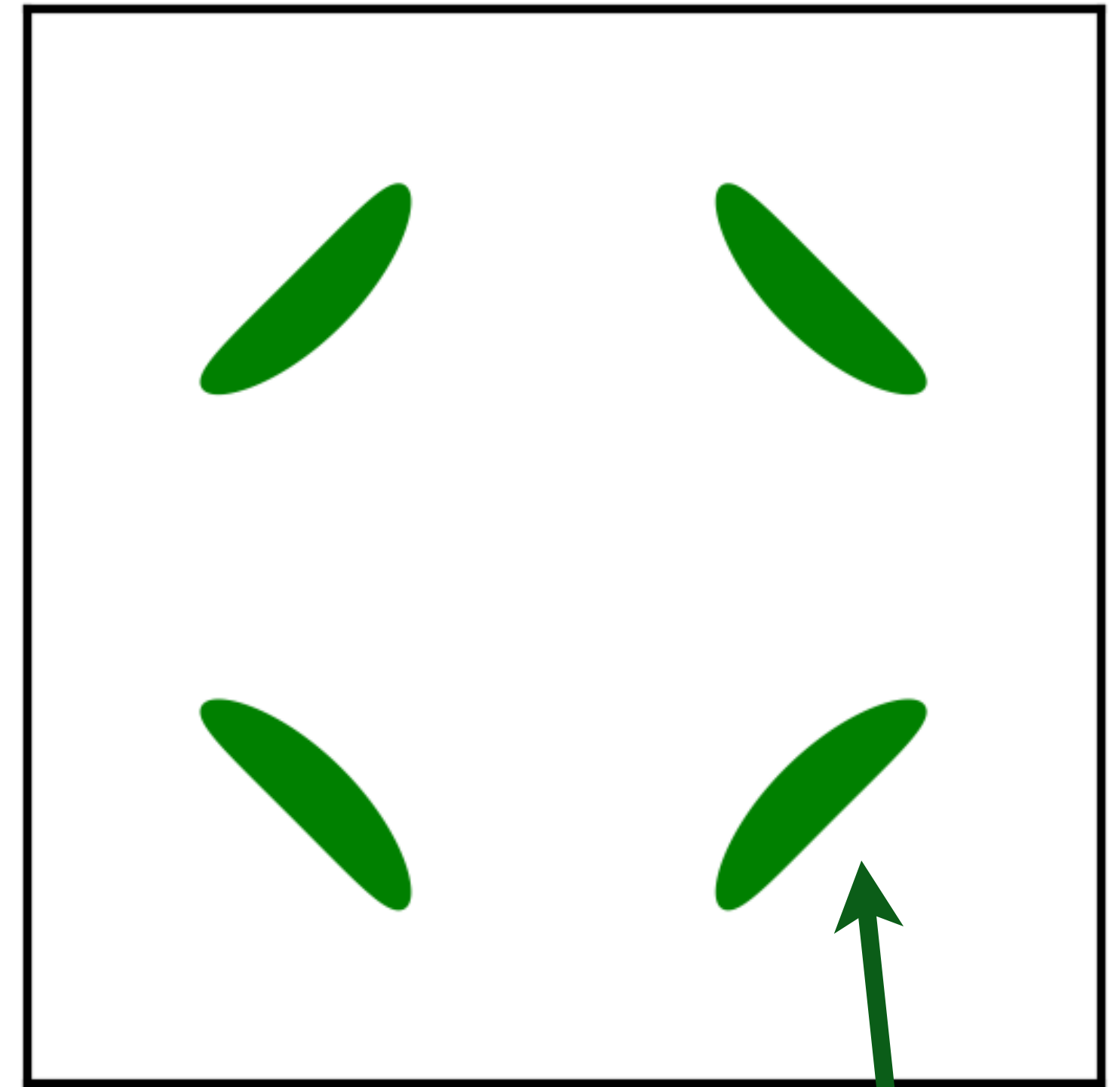
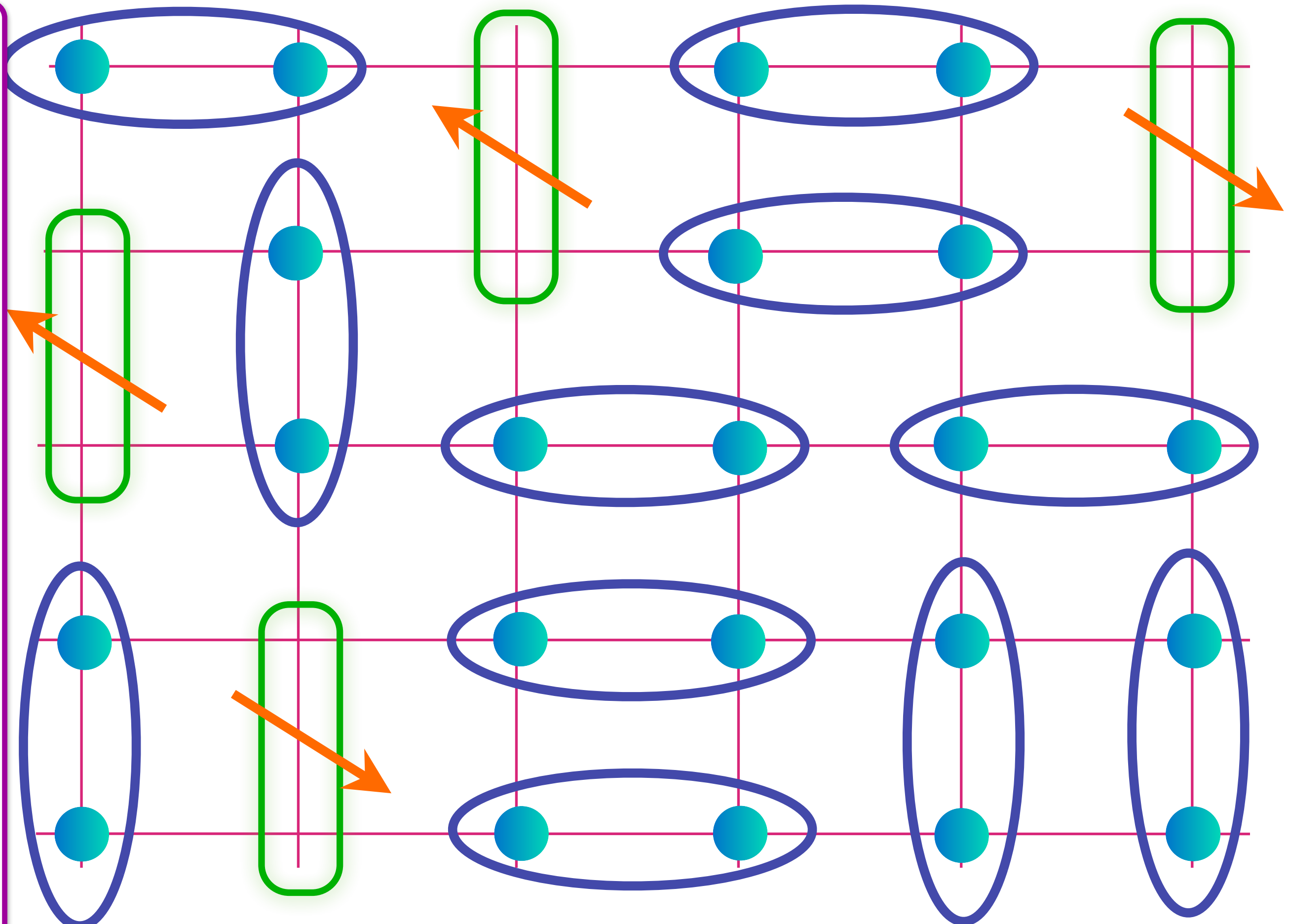
Area $p/8$

Doping an insulating antiferromagnet with holes of density p

FL*

Oshikawa anomaly is satisfied by sum of spin liquid (1) and Fermi surface anomalies (p)

Metal with density p of spin-1/2, charge $+e$ 'holes' (or 'magnetic polarons') with coherent inter-layer transport for Yamaji effect.



$$= (|\uparrow\downarrow\rangle - |\downarrow\uparrow\rangle) / \sqrt{2} \quad \text{Green bar with arrow} = (|\uparrow\circ\rangle + |\circ\uparrow\rangle) / \sqrt{2}$$

Area $p/8$

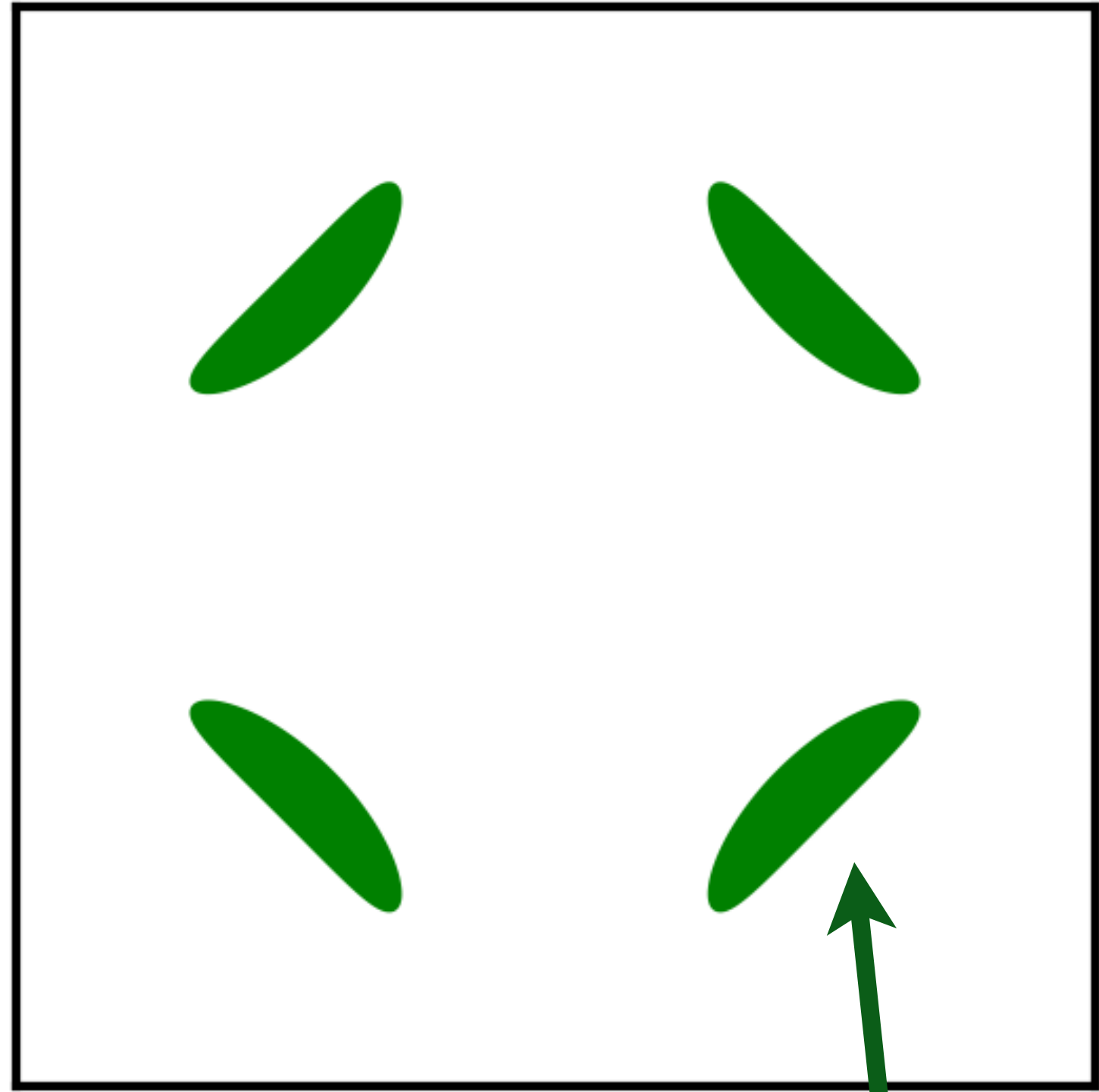
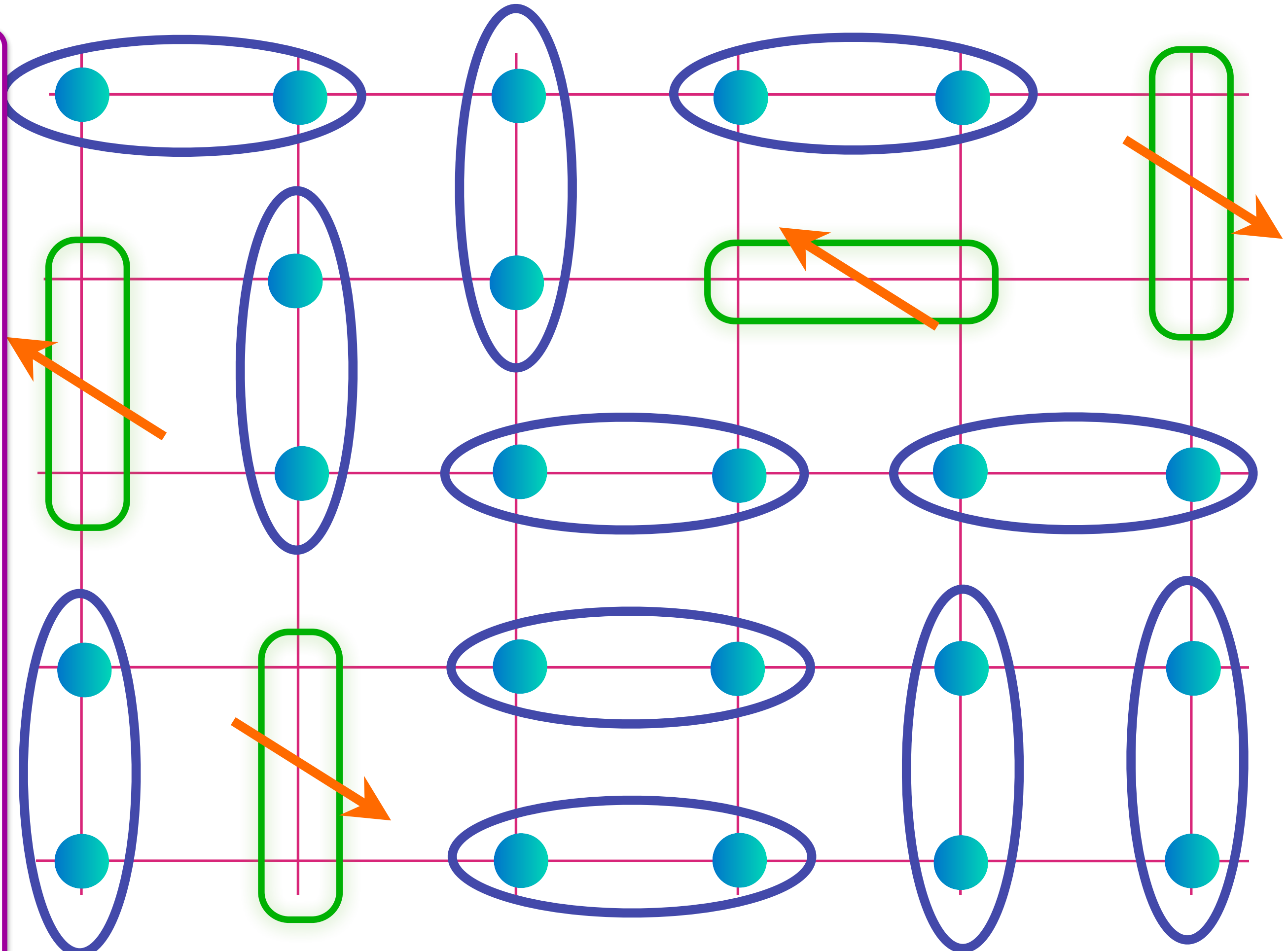
T. Senthil, S. S., M. Vojta, PRL **90**, 216403 (2003); R. K. Kaul, A. Kolezhuk, M. Levin, S.S., T. Senthil, PRB **75**, 235122 (2007)
M. Punk, A. Allais, and S. Sachdev, PNAS **112**, 9552 (2015)

Doping an insulating antiferromagnet with holes of density p

FL*

Oshikawa anomaly is satisfied by sum of spin liquid (1) and Fermi surface anomalies (p)

Metal with density p of spin-1/2, charge $+e$ 'holes' (or 'magnetic polarons') with coherent inter-layer transport for Yamaji effect.



Area $p/8$

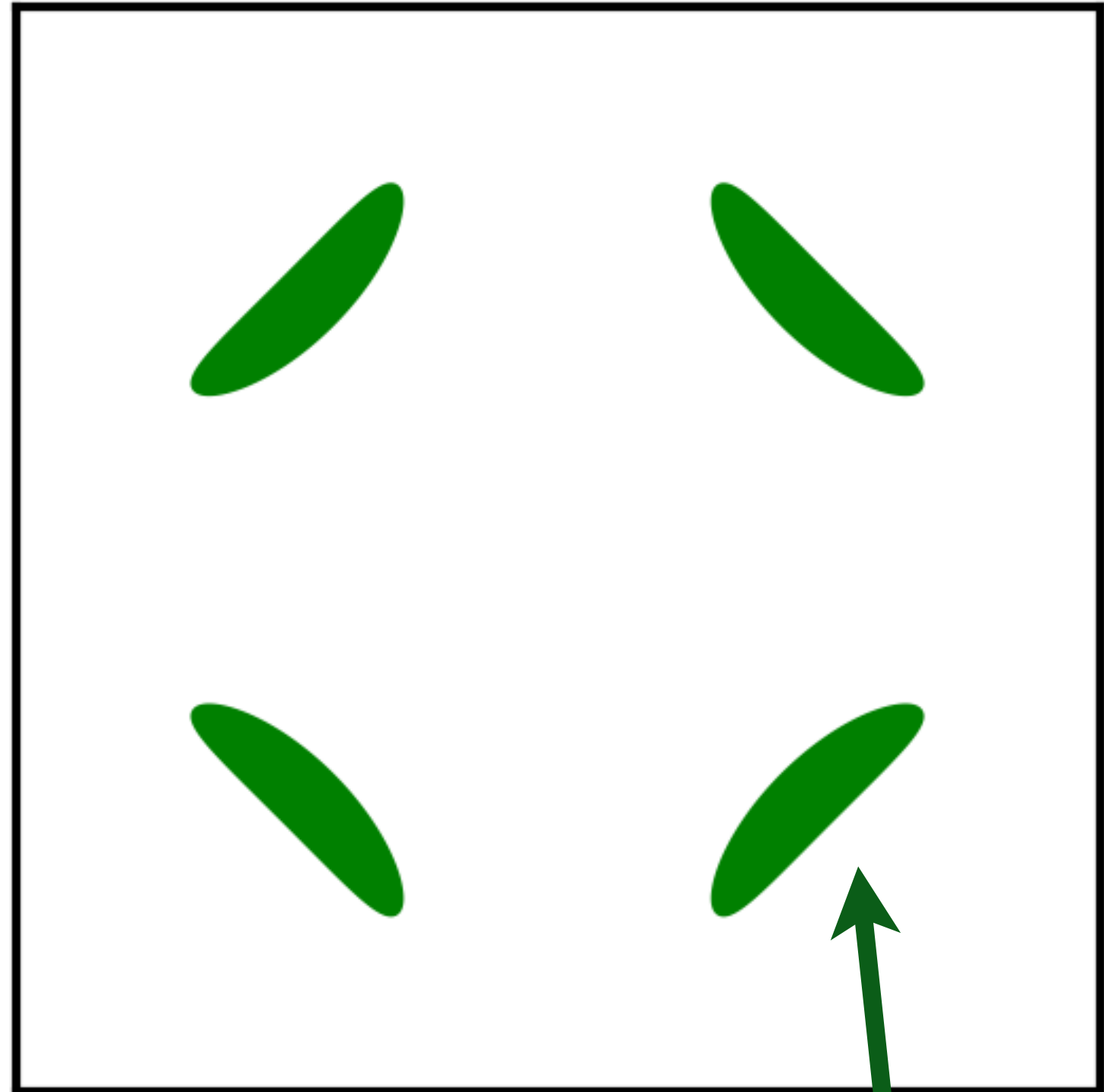
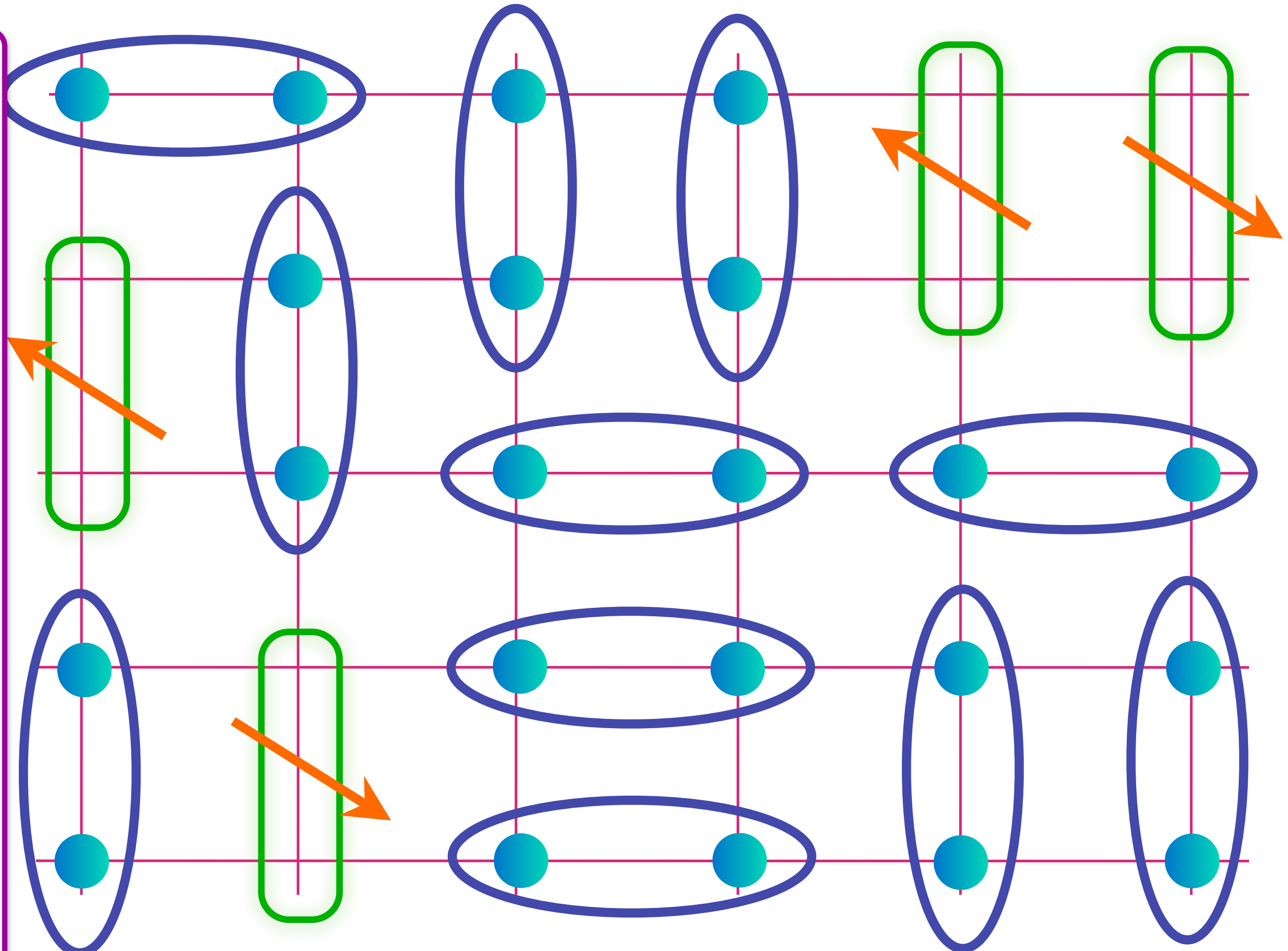
$$= (|\uparrow\downarrow\rangle - |\downarrow\uparrow\rangle) / \sqrt{2} \quad \text{Green box} = (|\uparrow\circ\rangle + |\circ\uparrow\rangle) / \sqrt{2}$$

Doping an insulating antiferromagnet with holes of density p

FL*

Oshikawa anomaly is satisfied by sum of spin liquid (1) and Fermi surface anomalies (p)

Metal with density p of spin-1/2, charge $+e$ 'holes' (or 'magnetic polarons') with coherent inter-layer transport for Yamaji effect.



$$= (|\uparrow\downarrow\rangle - |\downarrow\uparrow\rangle) / \sqrt{2} \quad \text{Green oval with arrow} = (|\uparrow\circ\rangle + |\circ\uparrow\rangle) / \sqrt{2}$$

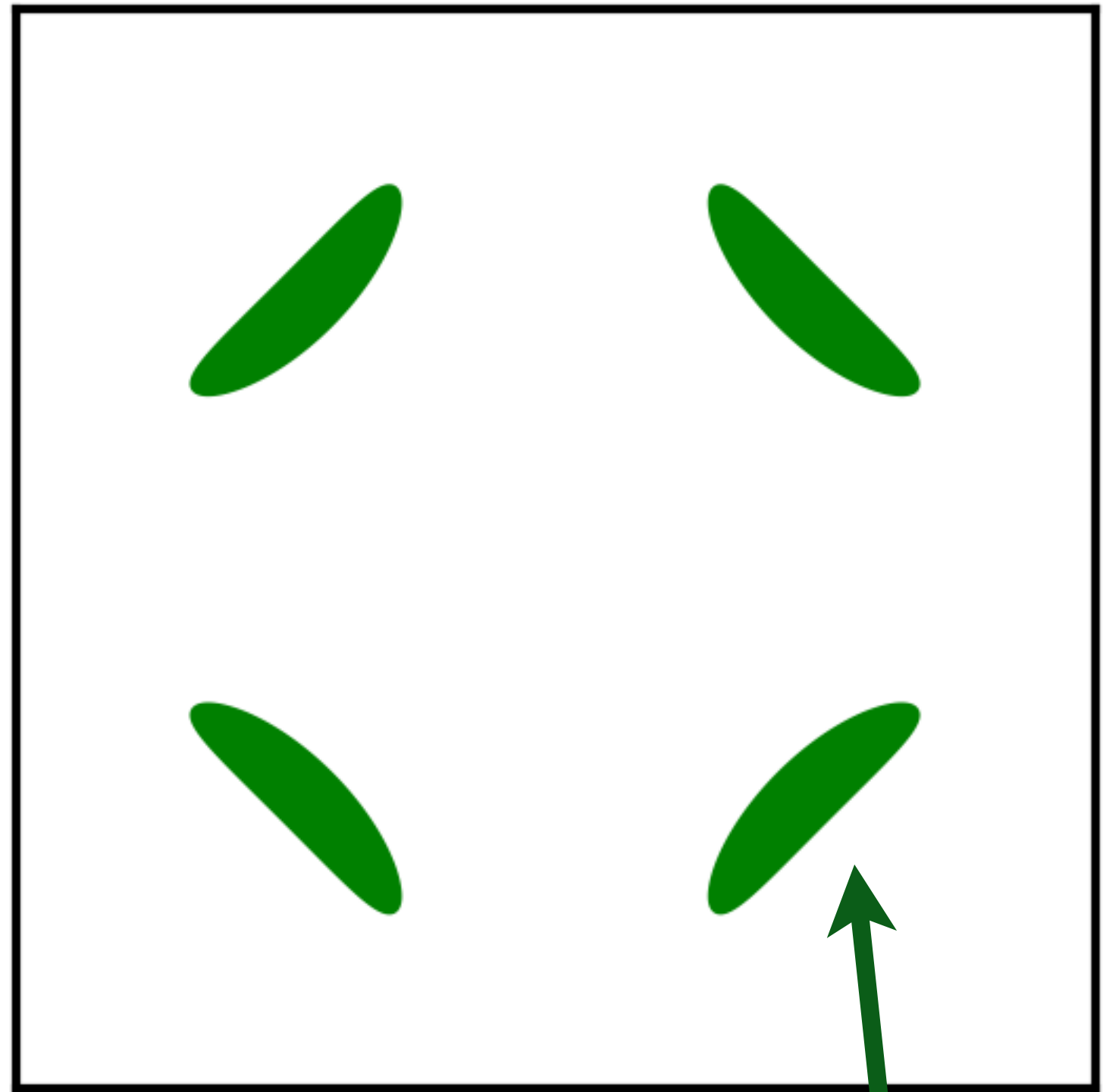
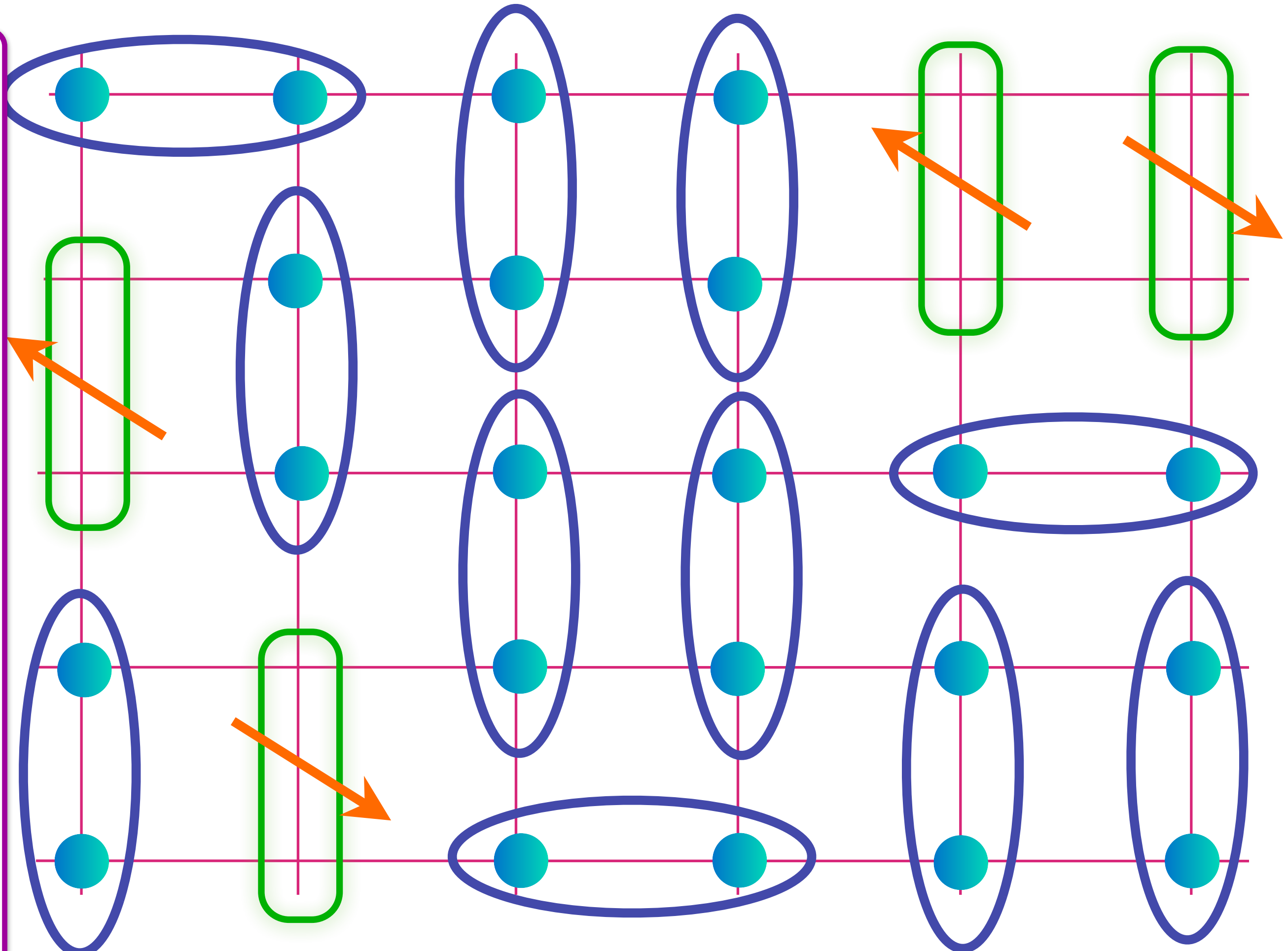
Area $p/8$

Doping an insulating antiferromagnet with holes of density p

FL*

Oshikawa anomaly is satisfied by sum of spin liquid (1) and Fermi surface anomalies (p)

Metal with density p of spin-1/2, charge $+e$ 'holes' (or 'magnetic polarons') with coherent inter-layer transport for Yamaji effect.



$$= (|\uparrow\downarrow\rangle - |\downarrow\uparrow\rangle) / \sqrt{2} \quad \text{Green oval with arrow} = (|\uparrow\circ\rangle + |\circ\uparrow\rangle) / \sqrt{2}$$

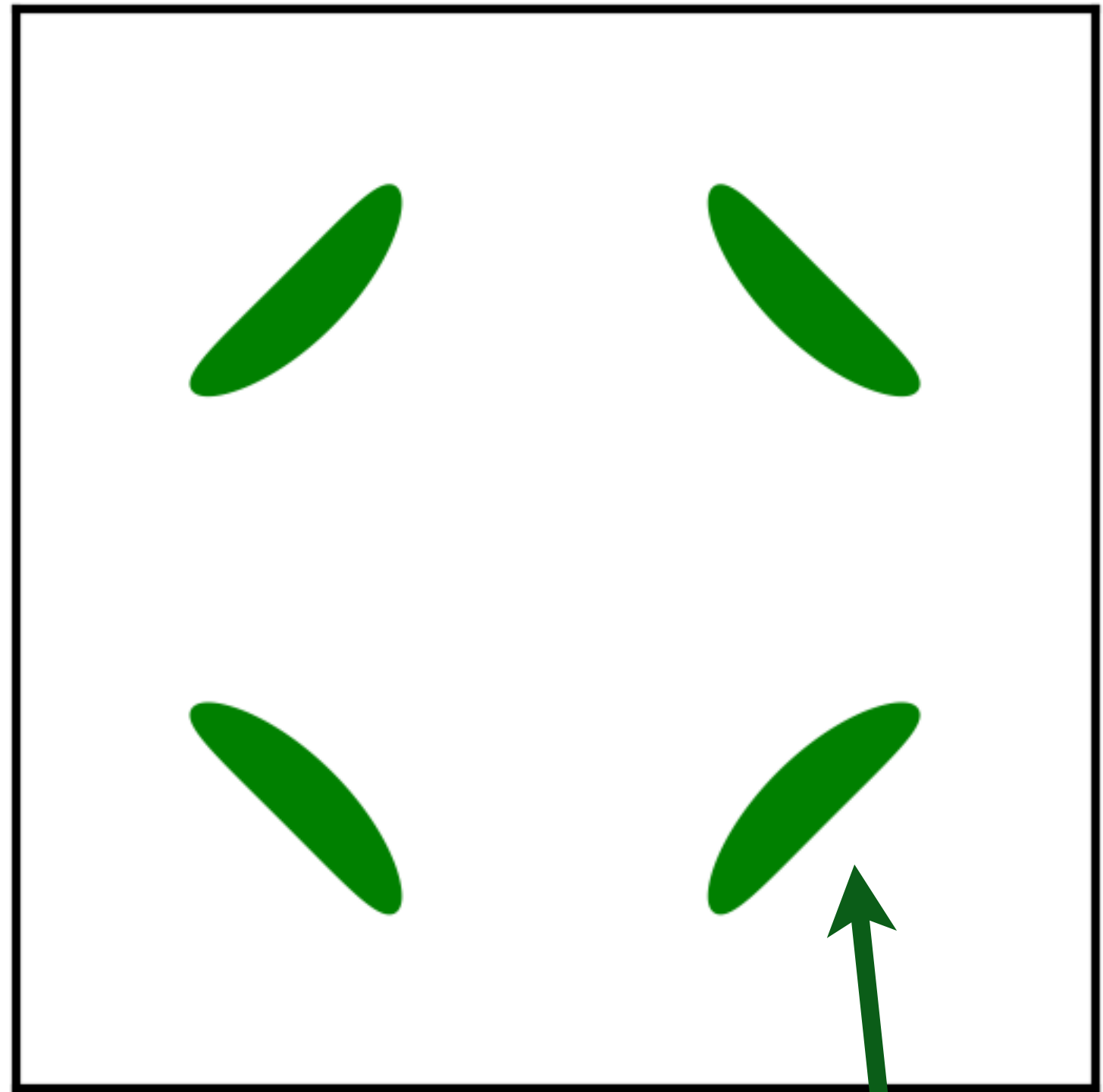
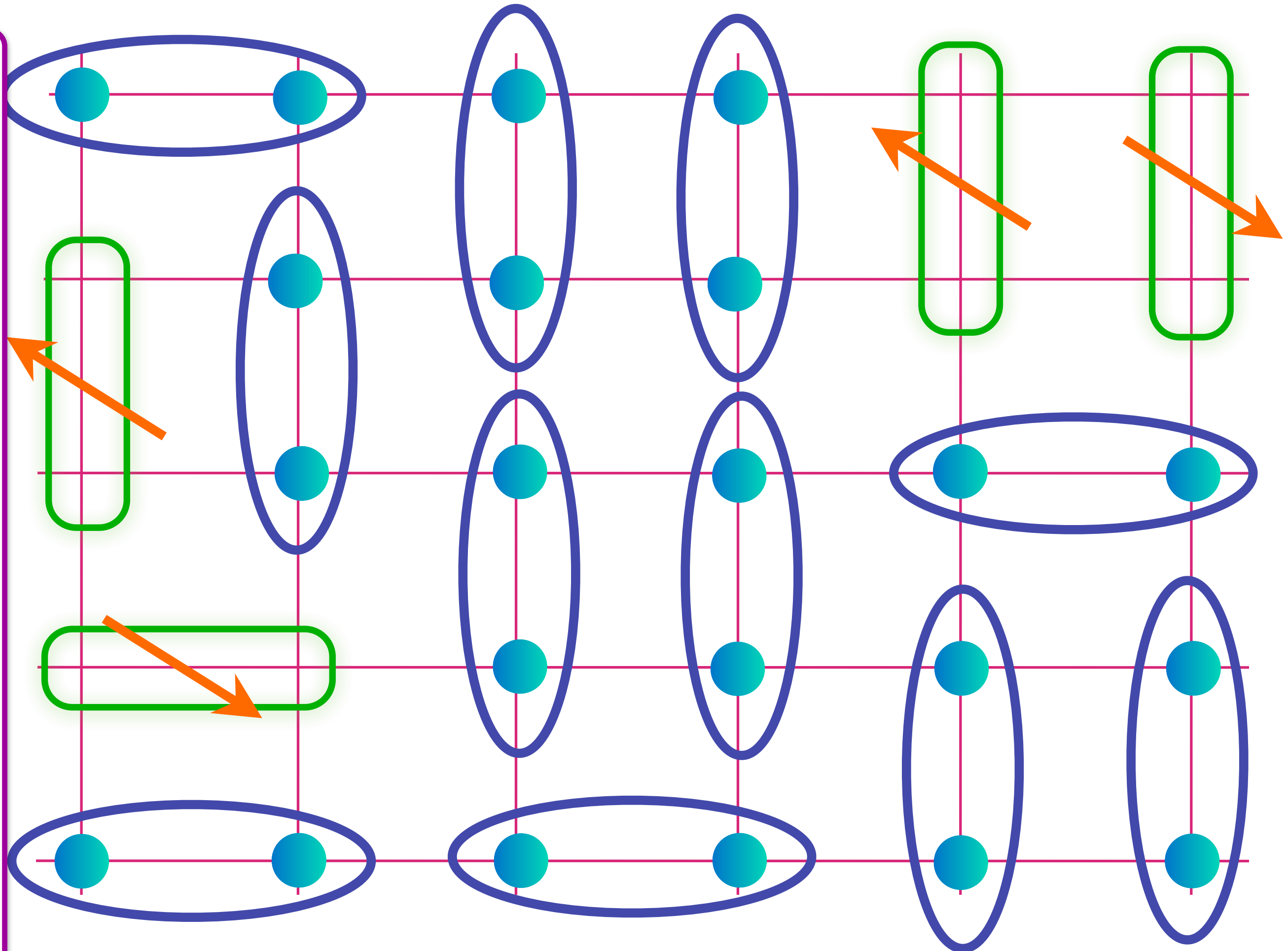
Area $p/8$

Doping an insulating antiferromagnet with holes of density p

FL*

Oshikawa anomaly is satisfied by sum of spin liquid (1) and Fermi surface anomalies (p)

Metal with density p of spin-1/2, charge $+e$ 'holes' (or 'magnetic polarons') with coherent inter-layer transport for Yamaji effect.



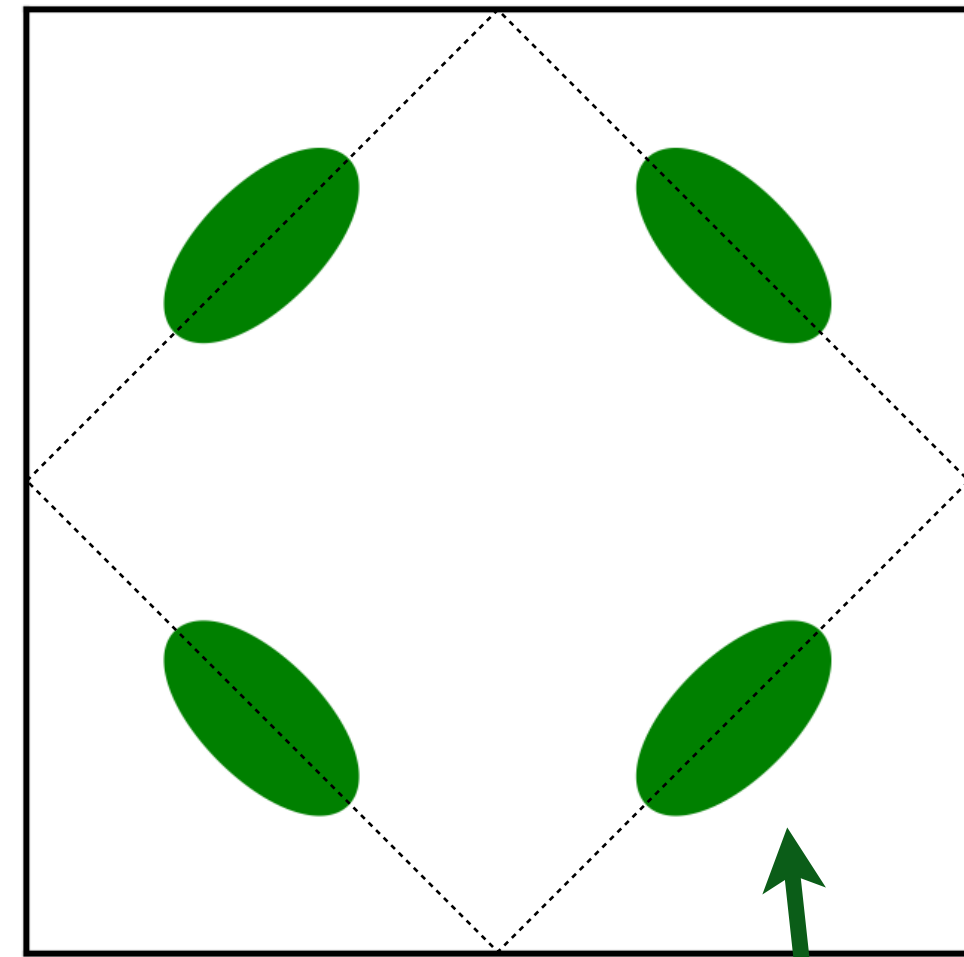
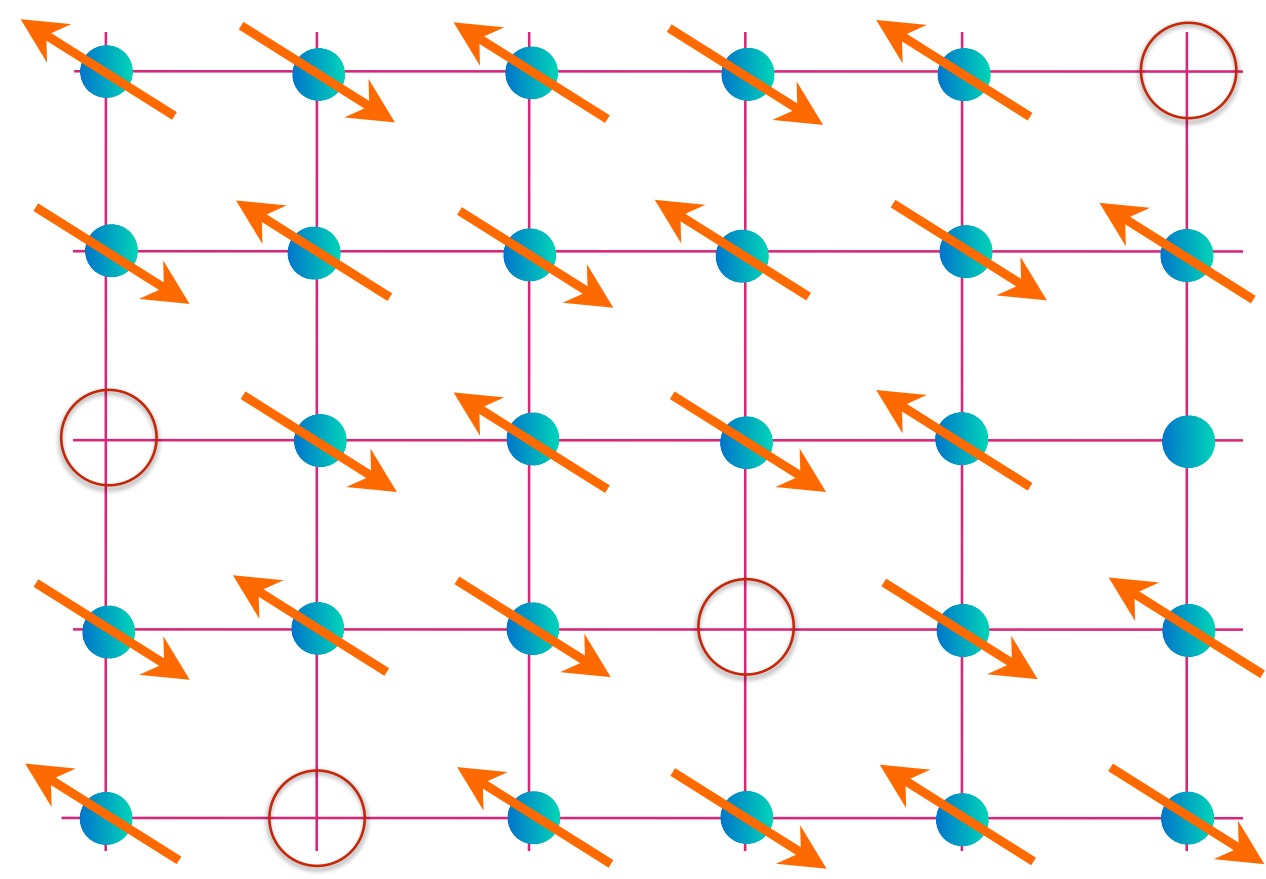
Area $p/8$

$$\text{Blue oval} = (|\uparrow\downarrow\rangle - |\downarrow\uparrow\rangle) / \sqrt{2} \quad \text{Green oval} = (|\uparrow\circ\rangle + |\circ\uparrow\rangle) / \sqrt{2}$$

T. Senthil, S. S., M. Vojta, PRL **90**, 216403 (2003); R. K. Kaul, A. Kolezhuk, M. Levin, S.S., T. Senthil, PRB **75**, 235122 (2007)

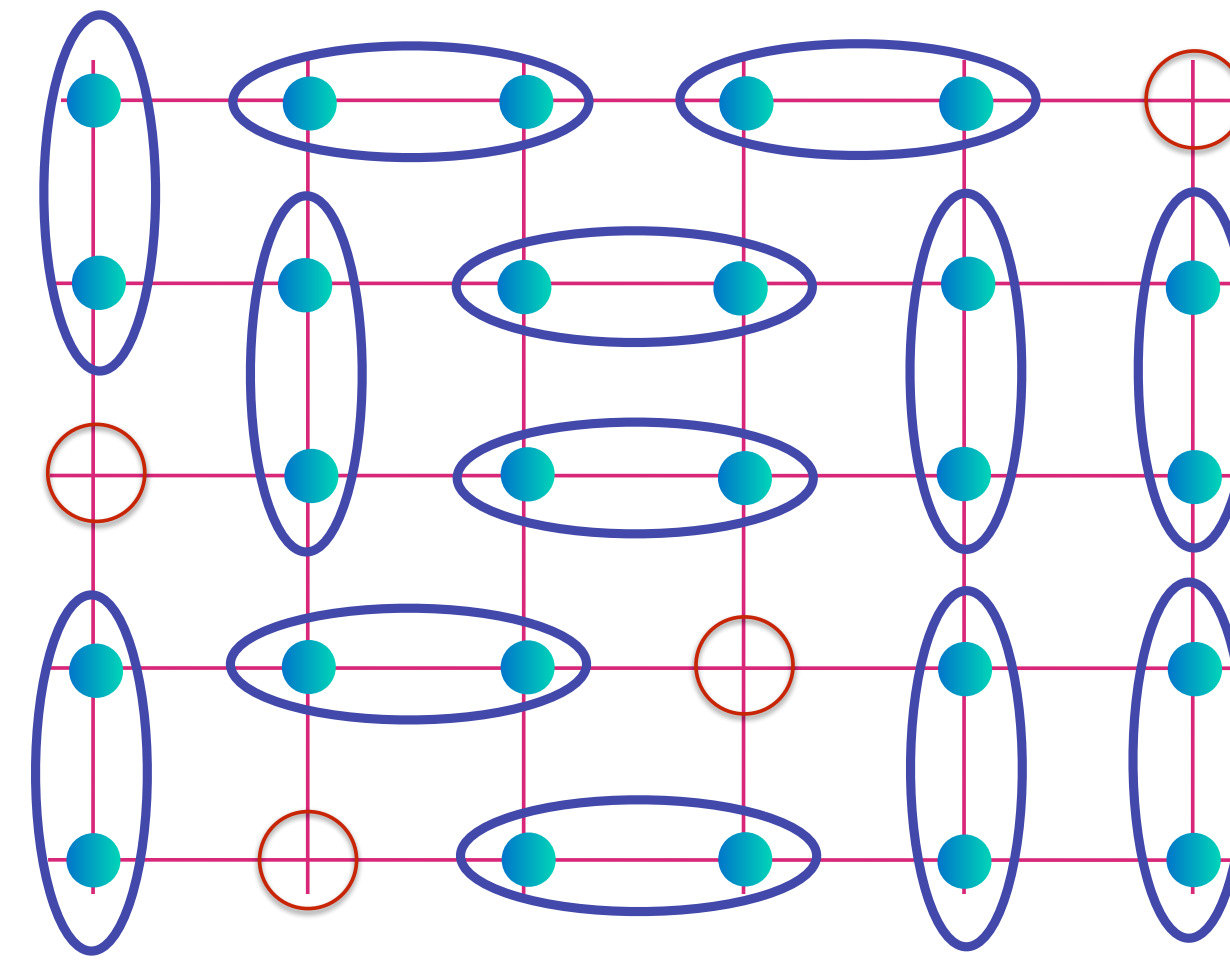
M. Punk, A. Allais, and S. Sachdev, PNAS **112**, 9552 (2015)

Doping an insulating antiferromagnet with holes of density p



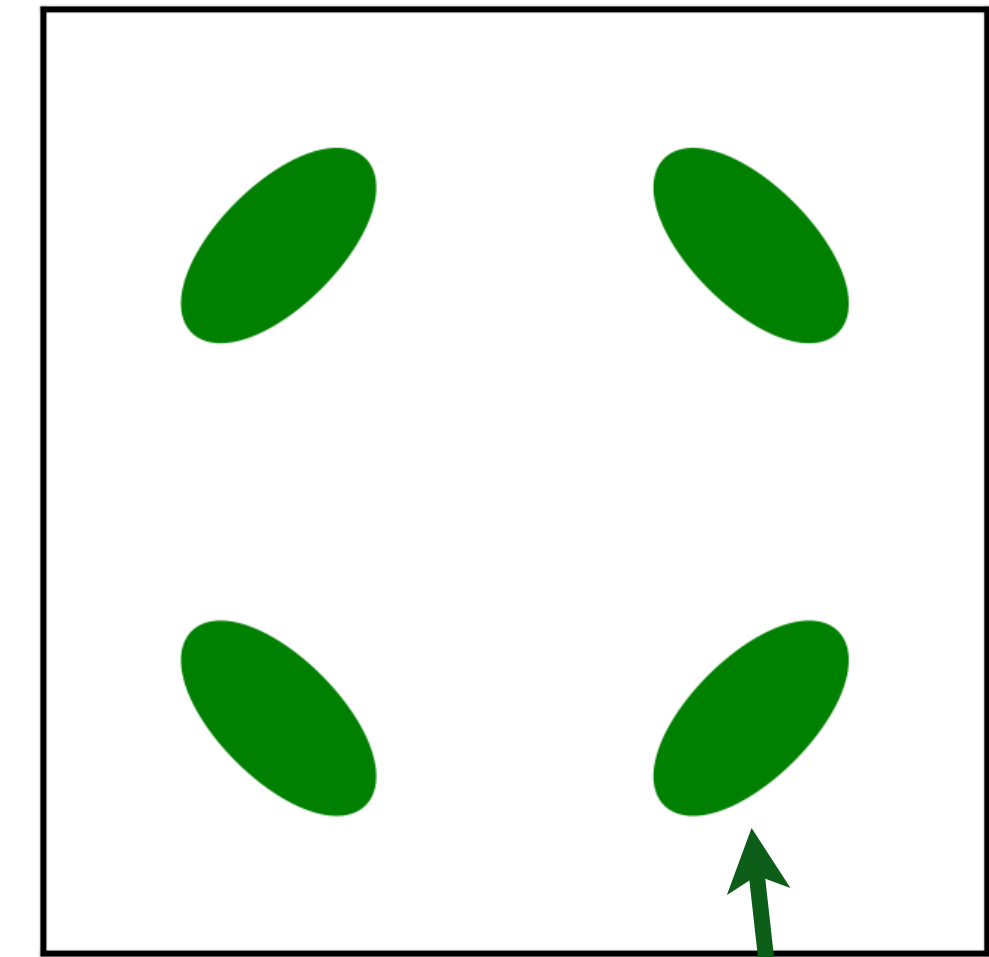
Area $p/4$

AF metal and SDW fluctuation

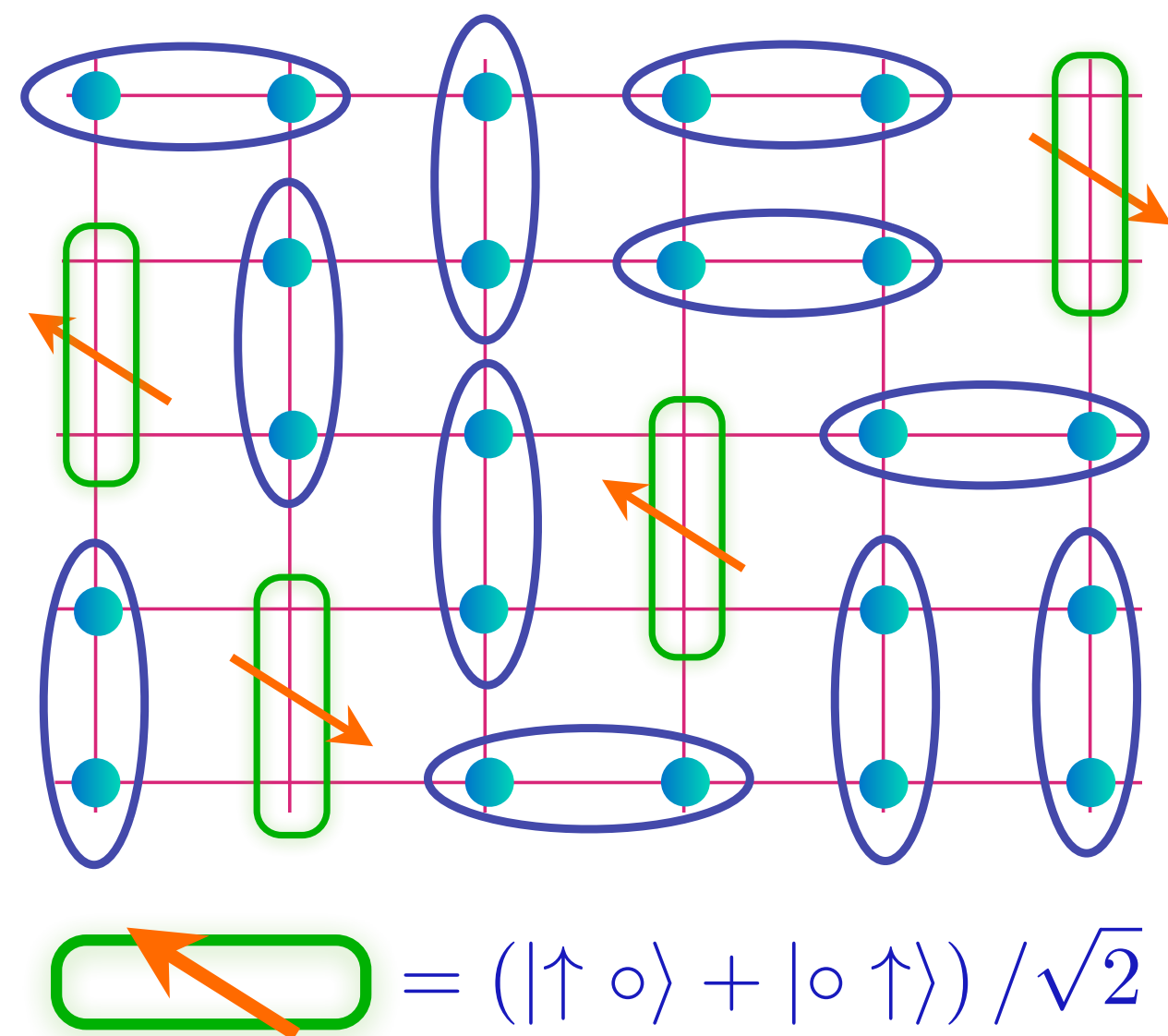


$$\text{Oval} = (|\uparrow\downarrow\rangle - |\downarrow\uparrow\rangle) / \sqrt{2}$$

Holon metal

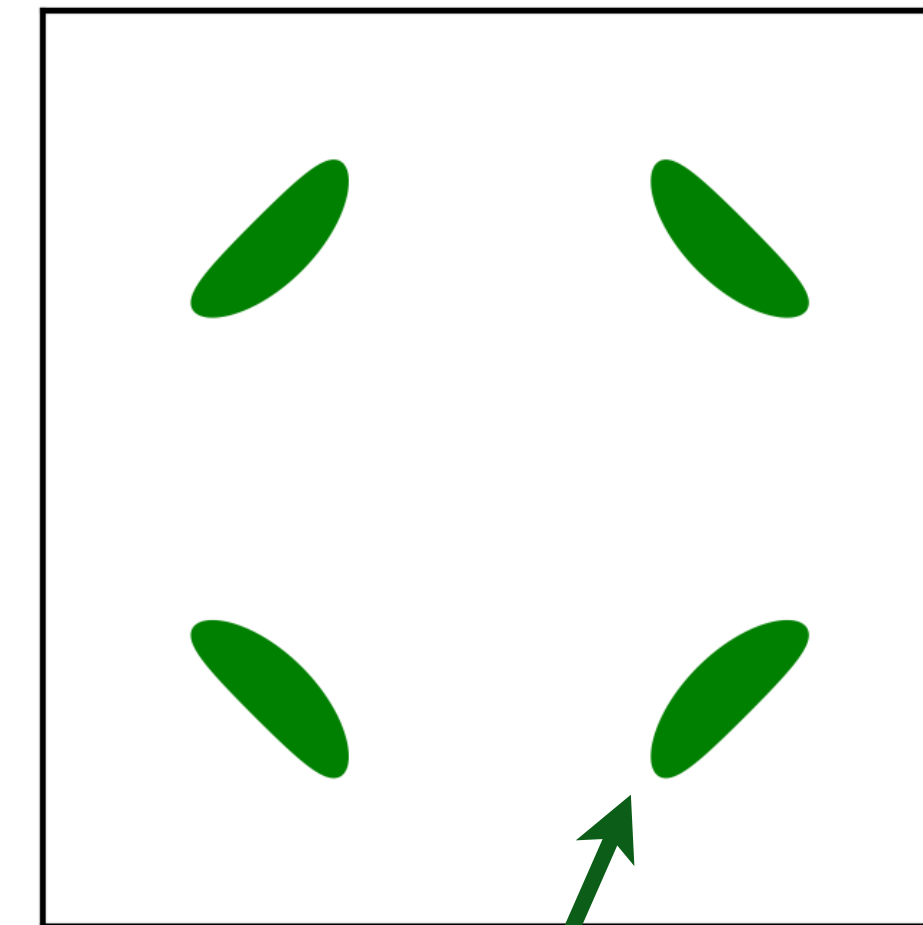


Area $p/4$



$$\text{Green Oval} = (|\uparrow\circ\rangle + |\circ\uparrow\rangle) / \sqrt{2}$$

FL*



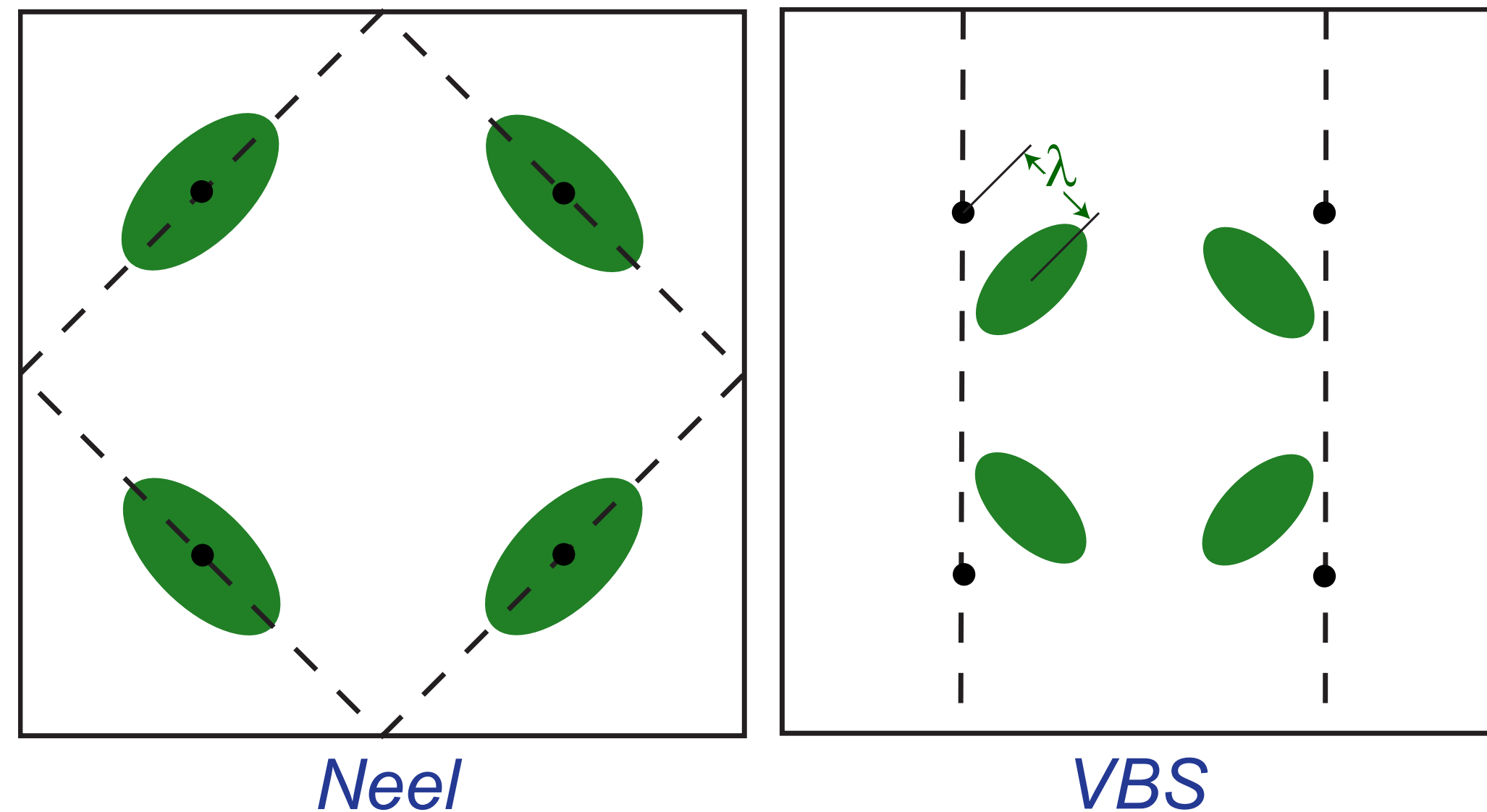
Area $p/8$

Quantization of spin liquid anomaly implies Fermi surface areas are also quantized and robust to all corrections.

T. Senthil, S. S., M. Vojta, PRL **90**, 216403 (2003);
 R. K. Kaul, A. Kolezhuk, M. Levin, S.S., T. Senthil, PRB **75**, 235122 (2007)
 M. Punk, A. Allais, and S. S., PNAS **112**, 9552 (2015)
 E. Mascot, A. Nikolaenko, M. Tikhanovskaya, Ya-Hui Zhang, D. K. Morr, S. S., PRB **105**, 075146 (2022)

Hole dynamics in an antiferromagnet across a deconfined quantum critical point

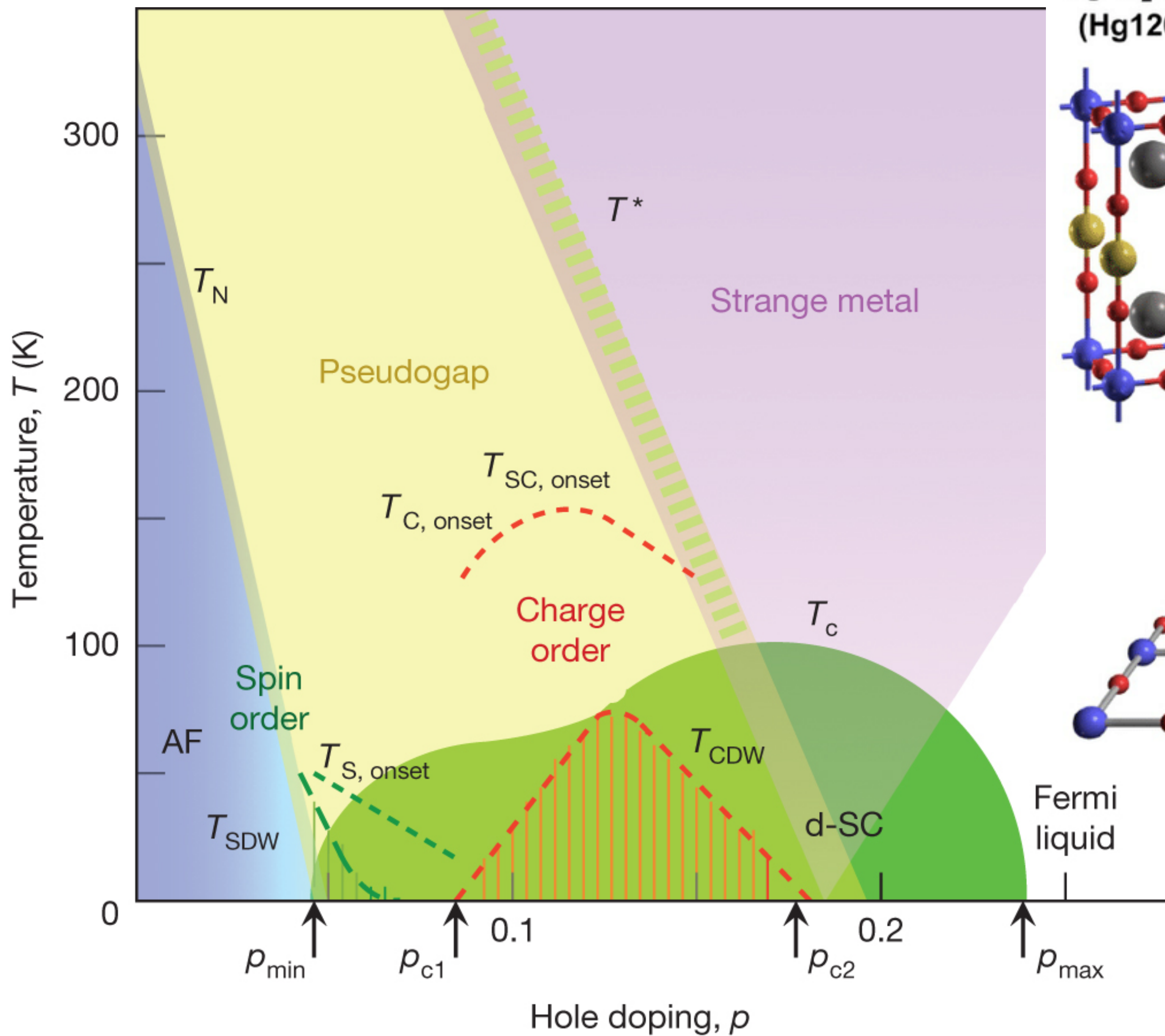
Ribhu K. Kaul,¹ Alexei Kolezhuk,^{1,2} Michael Levin,¹ Subir Sachdev,¹ and T. Senthil^{3,4}



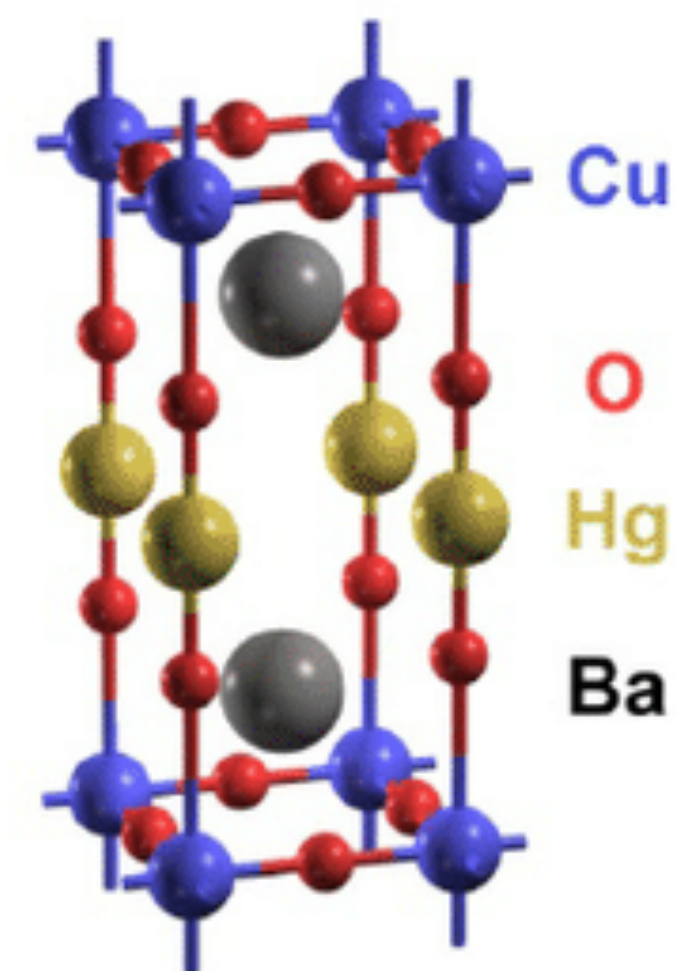
The dashed line in the Néel phase indicates the boundary of the magnetic Brillouin zone. Only the Fermi surfaces within this zone contribute to the Luttinger counting, and so the area of each ellipse is $\mathcal{A}_F = (2\pi)^2 \delta/4$. In the VBS phase, all four pockets are inequivalent, and so the area of each ellipse is $\mathcal{A}_F = (2\pi)^2 \delta/8$.

Factor of 2 between
SDW fluctuation
and FL*

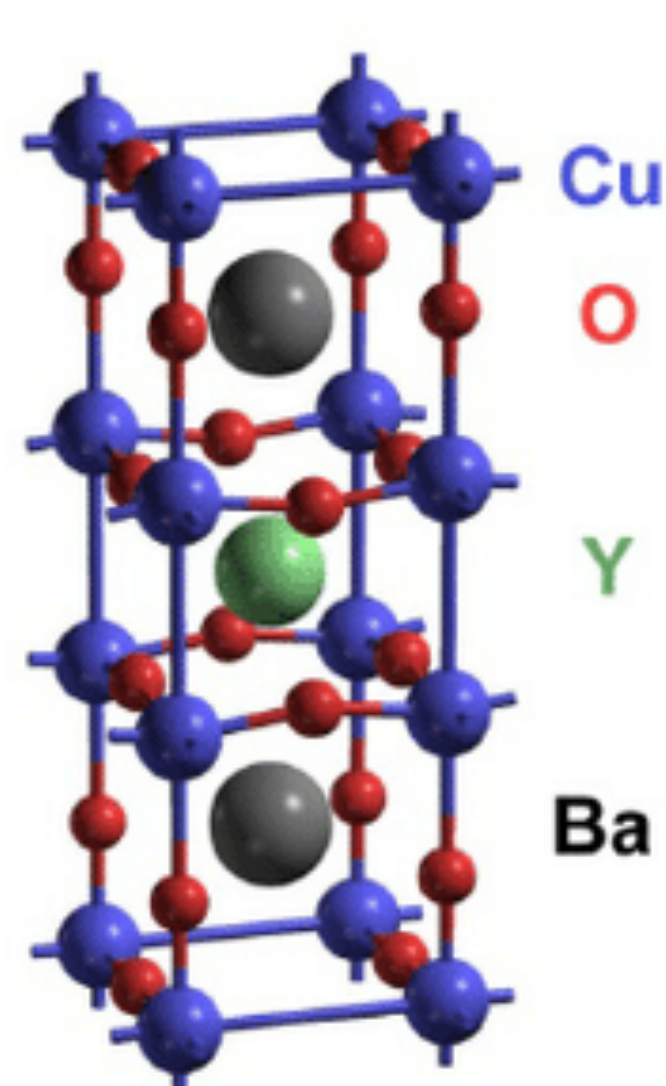
Observation of the Yamaji
effect in a cuprate



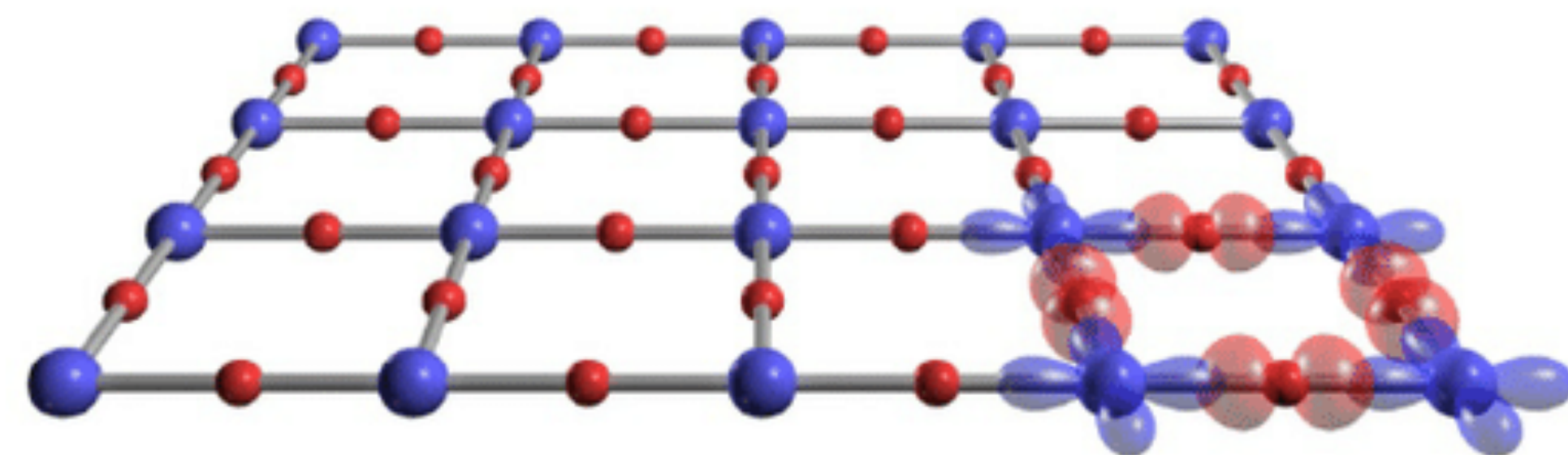
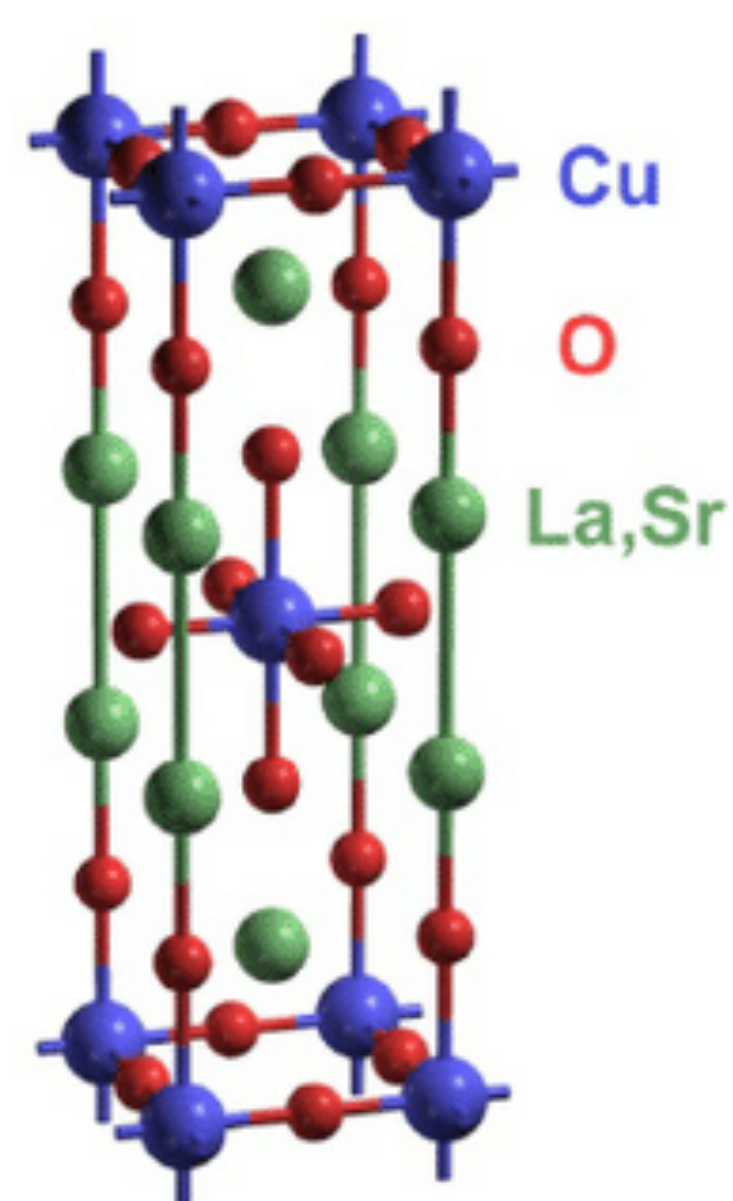
HgBa₂CuO_{4+δ}
(Hg1201)



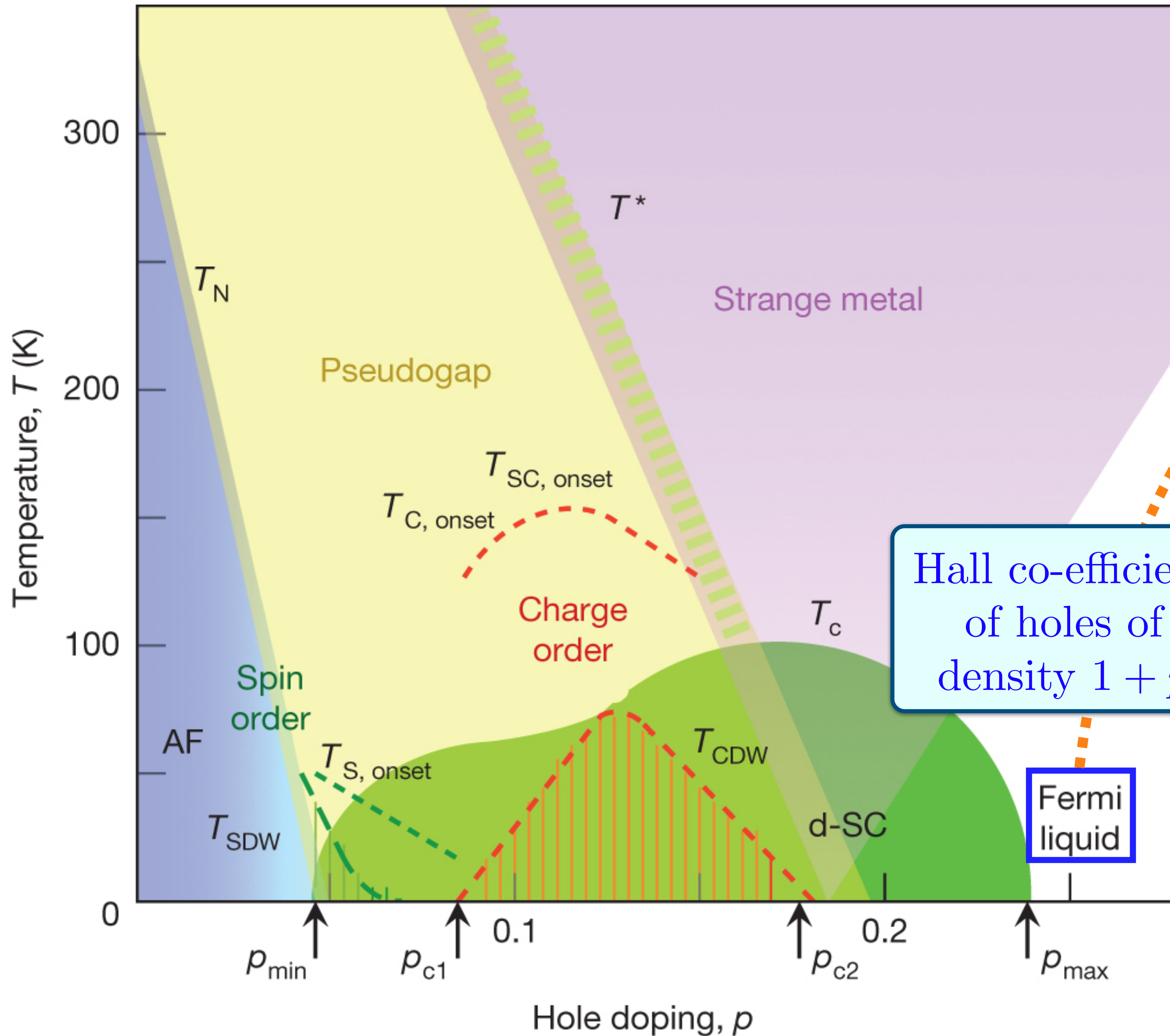
YBa₂Cu₃O_{7-δ}
(YBCO)



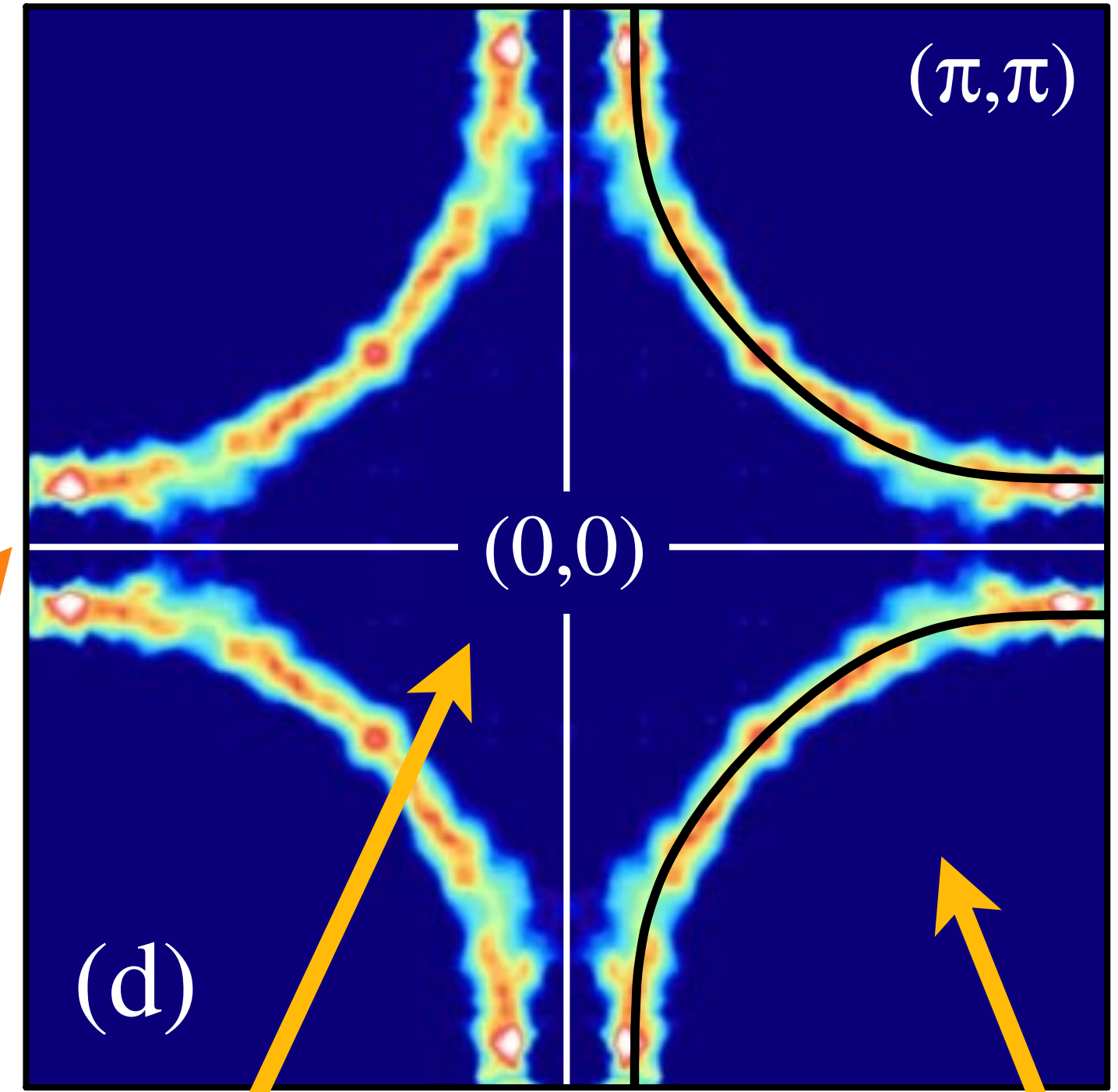
La_{2-x}Sr_xCuO₄
(LSCO)



Fermi liquid

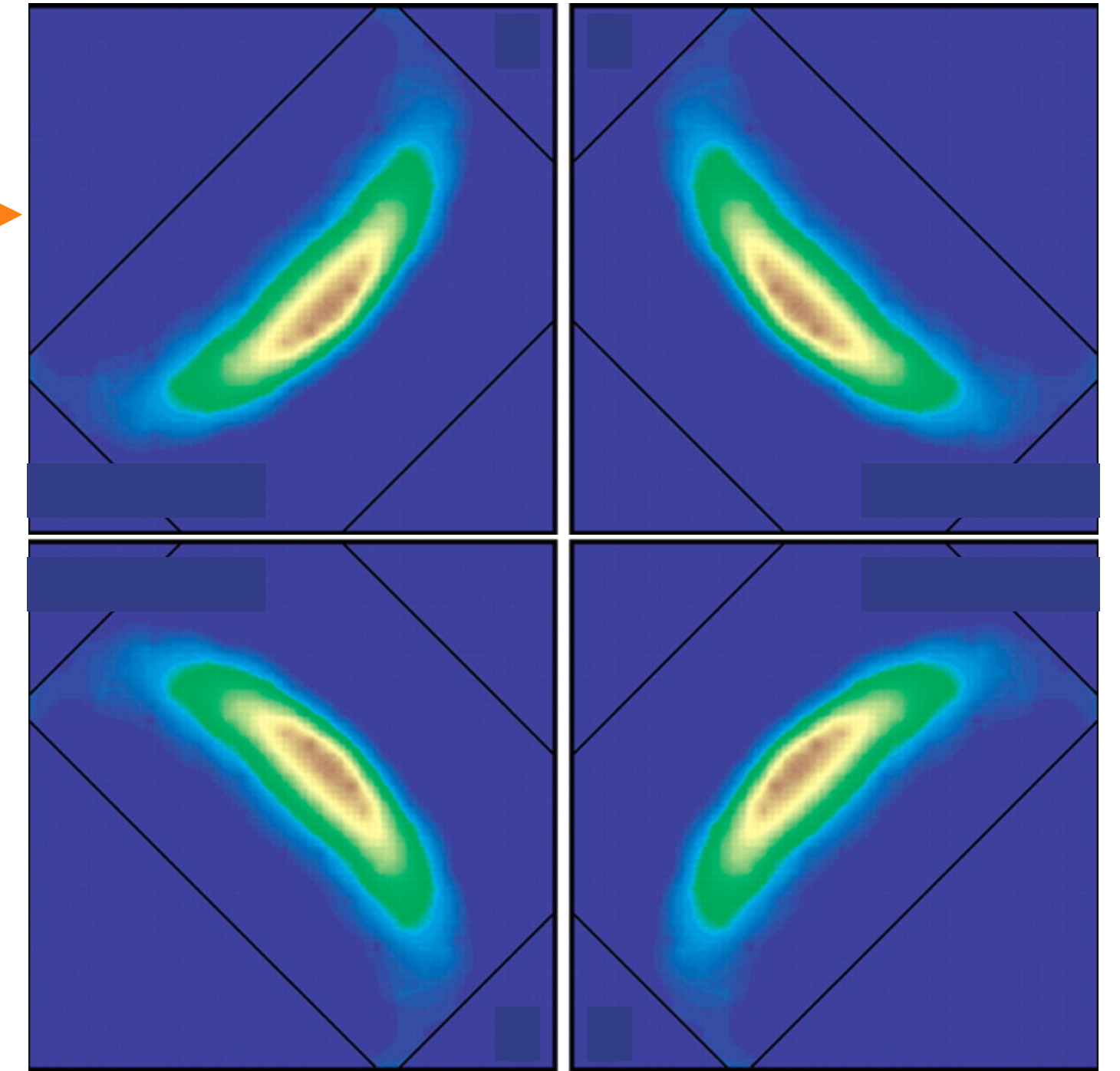
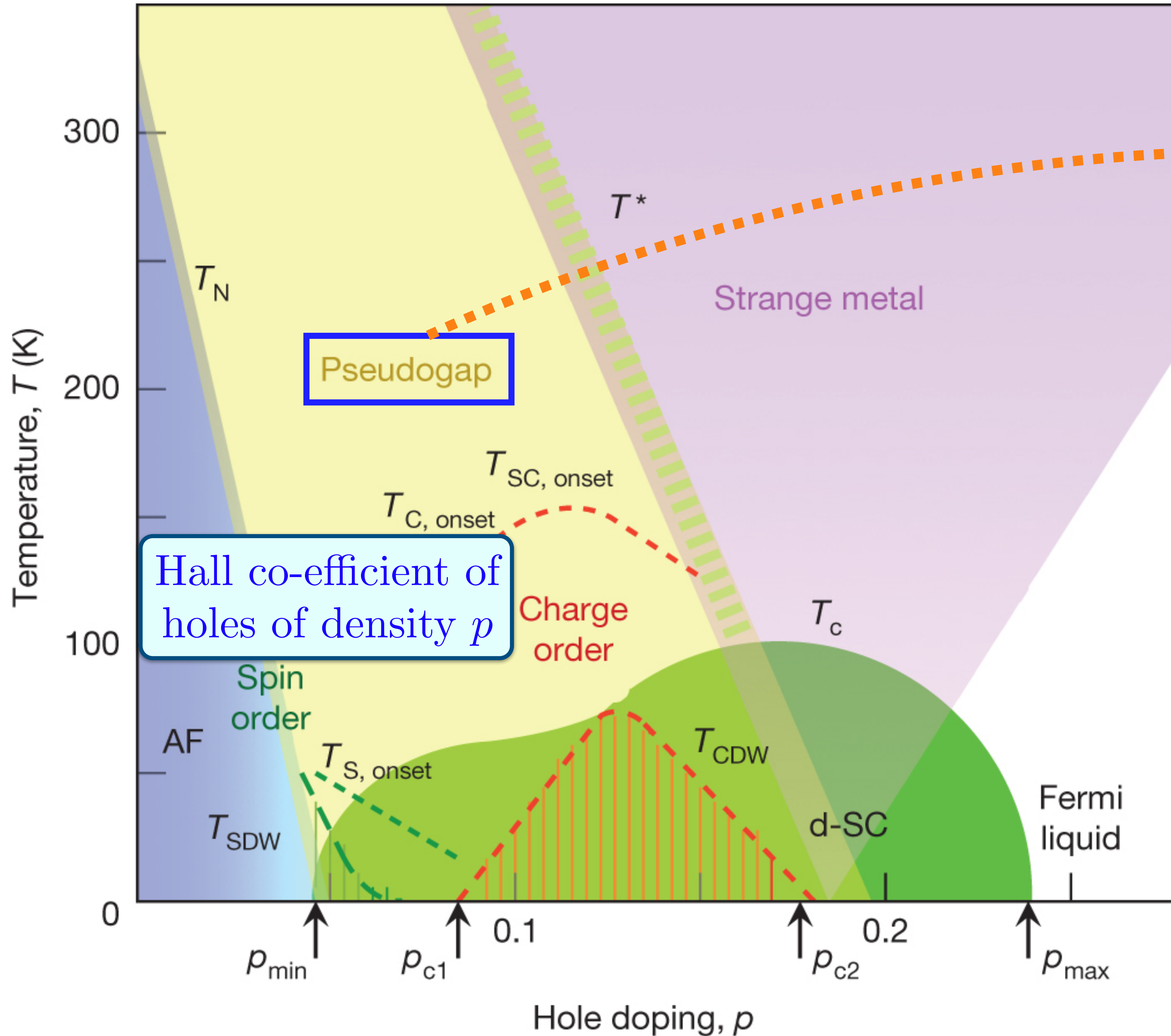


Hall co-efficient of holes of density $1 + p$



$1-p$ electrons

$1+p$ holes

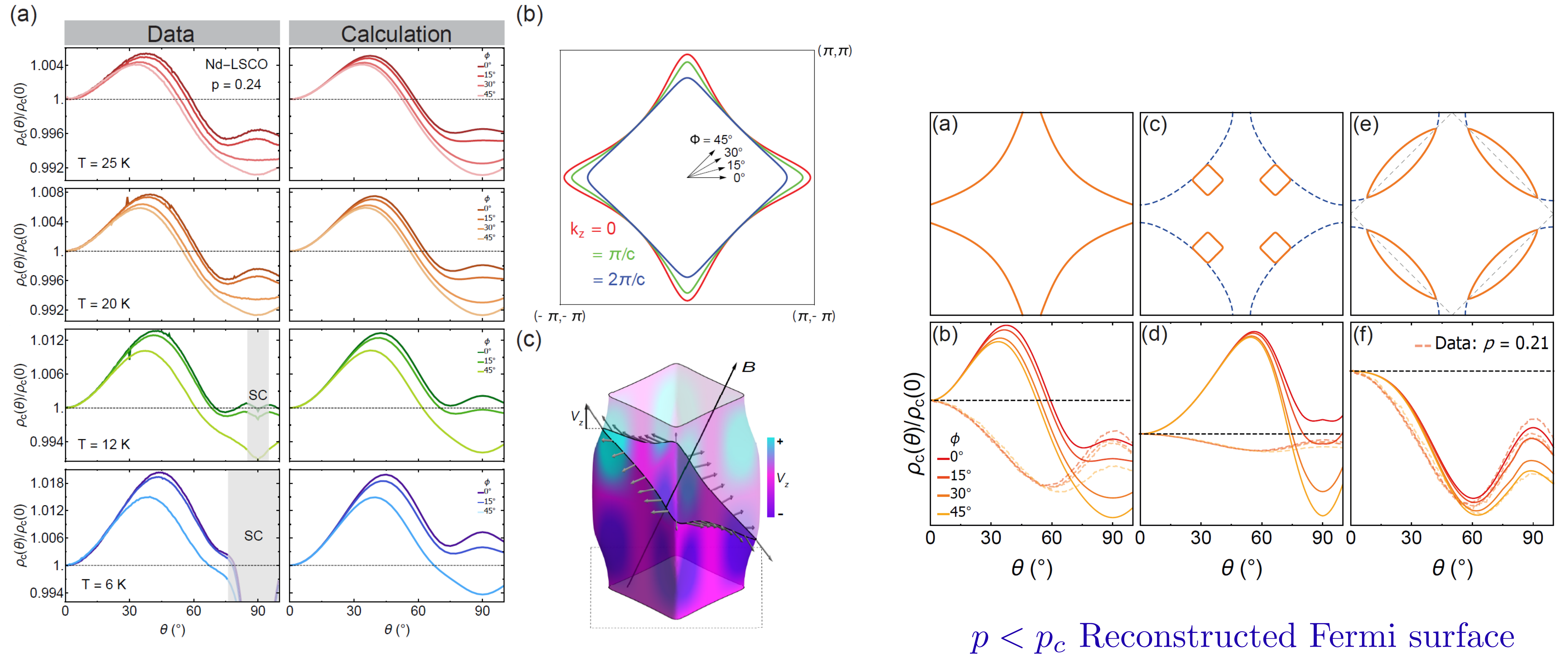


'Fermi arcs' ?

Fermi surface transformation at the pseudogap critical point of a cuprate superconductor

Yawen Fang, Gaël Grissonnanche, Anaëlle Legros, Simon Verret, Francis Laliberté, Clément Collignon, Amirreza Ataei, Maxime Dion, Jianshi Zhou, David Graf, M. J. Lawler, Paul Goddard, Louis Taillefer, and B. J. Ramshaw, *Nature Physics* **18**, 558 (2022)

Angle-dependent magnetoresistance (ADMR) of $\text{La}_{1.6-x}\text{Nd}_{0.4}\text{Sr}_x\text{CuO}_4$



$p > p_c$ Large Fermi surface

$p < p_c$ Reconstructed Fermi surface

Observation of the Yamaji effect in a cuprate superconductor

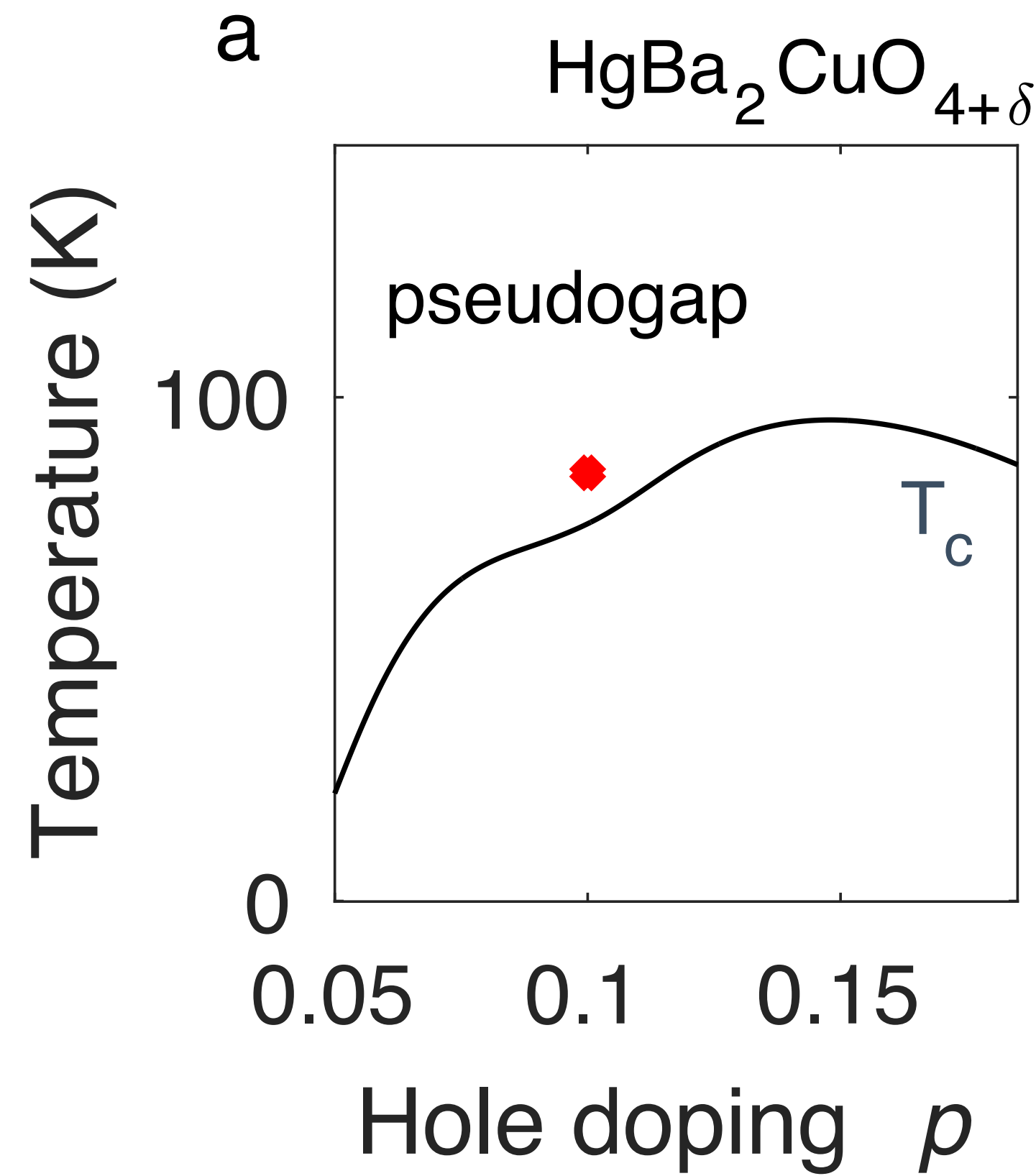
superconductor

Mun K. Chan¹✉, Katherine A. Schreiber¹, Oscar E. Ayala-Valenzuela¹,
Eric D. Bauer², Arkady Shekhter¹ & Neil Harrison¹

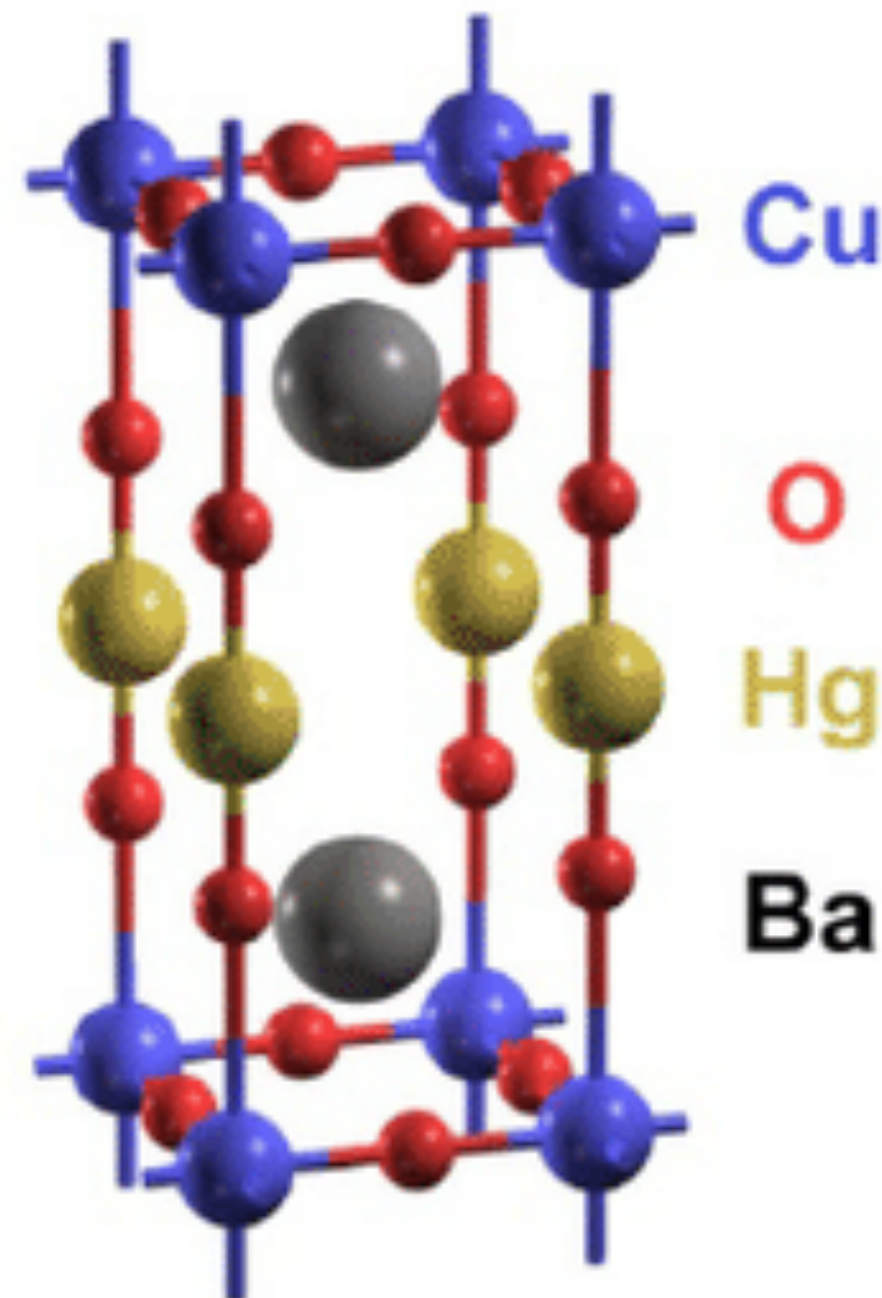
nature physics

21, 1753 (2025)

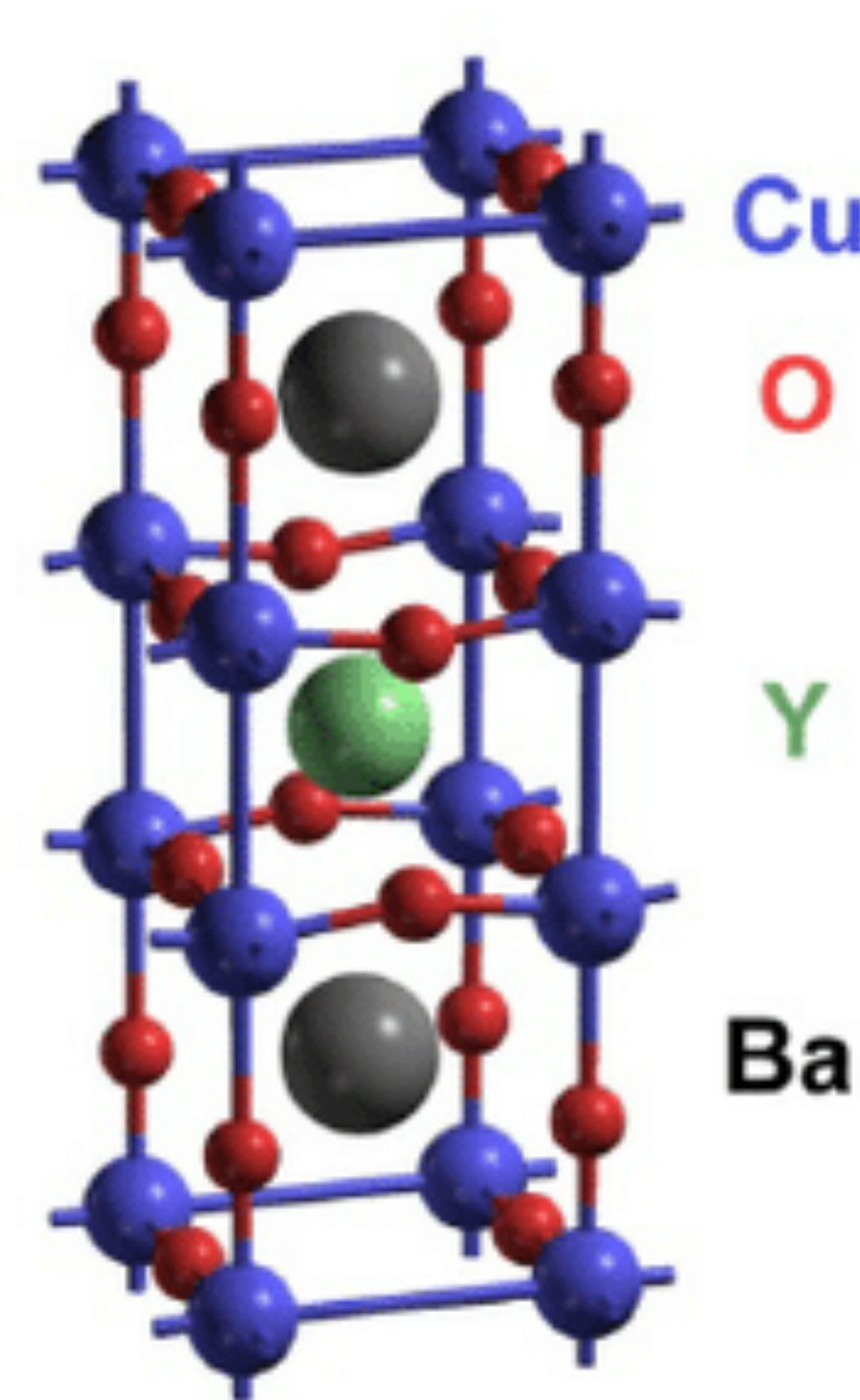
Published online: 16 September 2025



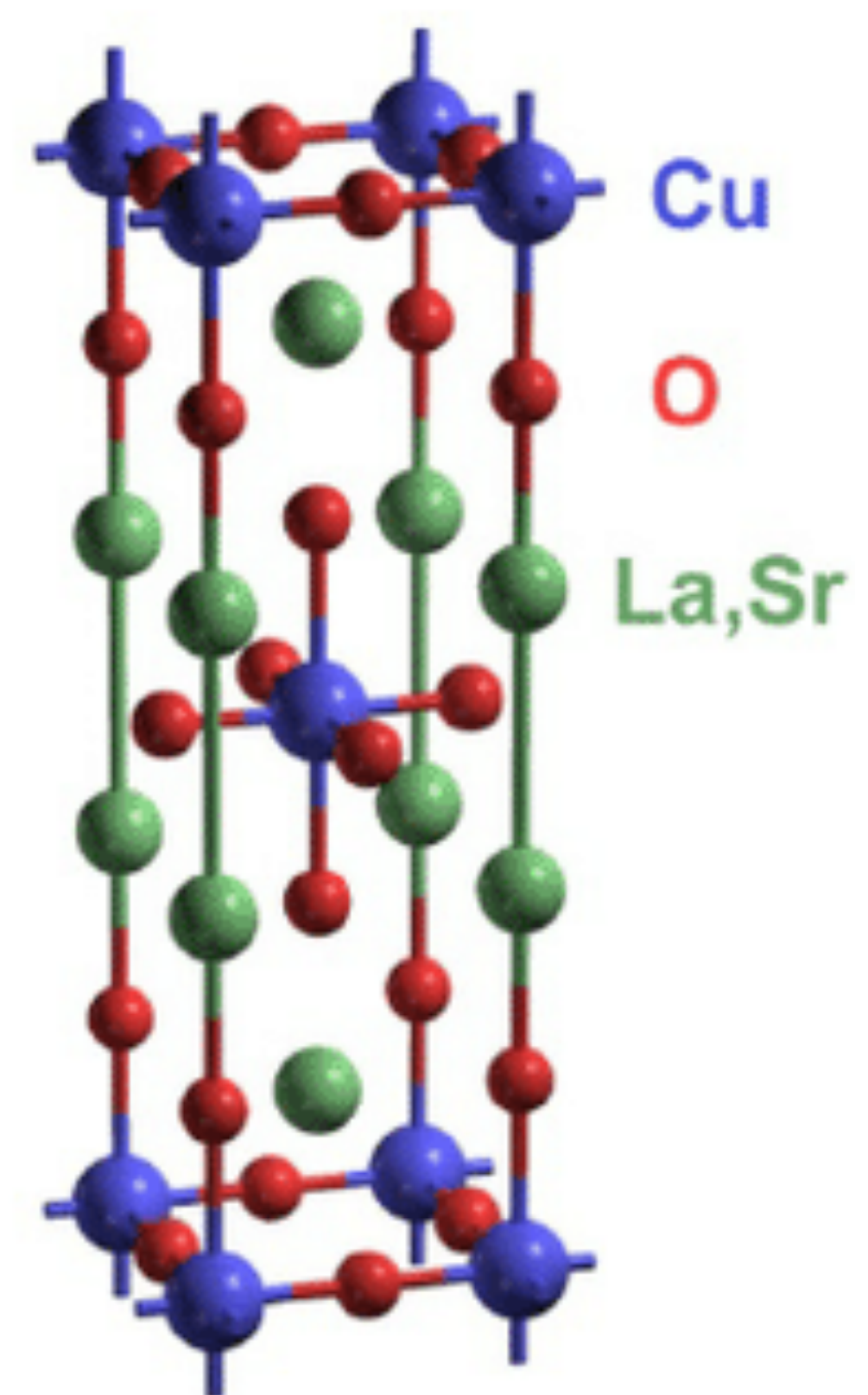
$\text{HgBa}_2\text{CuO}_{4+\delta}$
(Hg1201)



$\text{YBa}_2\text{Cu}_3\text{O}_{7-\delta}$
(YBCO)



$\text{La}_{2-x}\text{Sr}_x\text{CuO}_4$
(LSCO)



Observation of the Yamaji effect in a cuprate superconductor

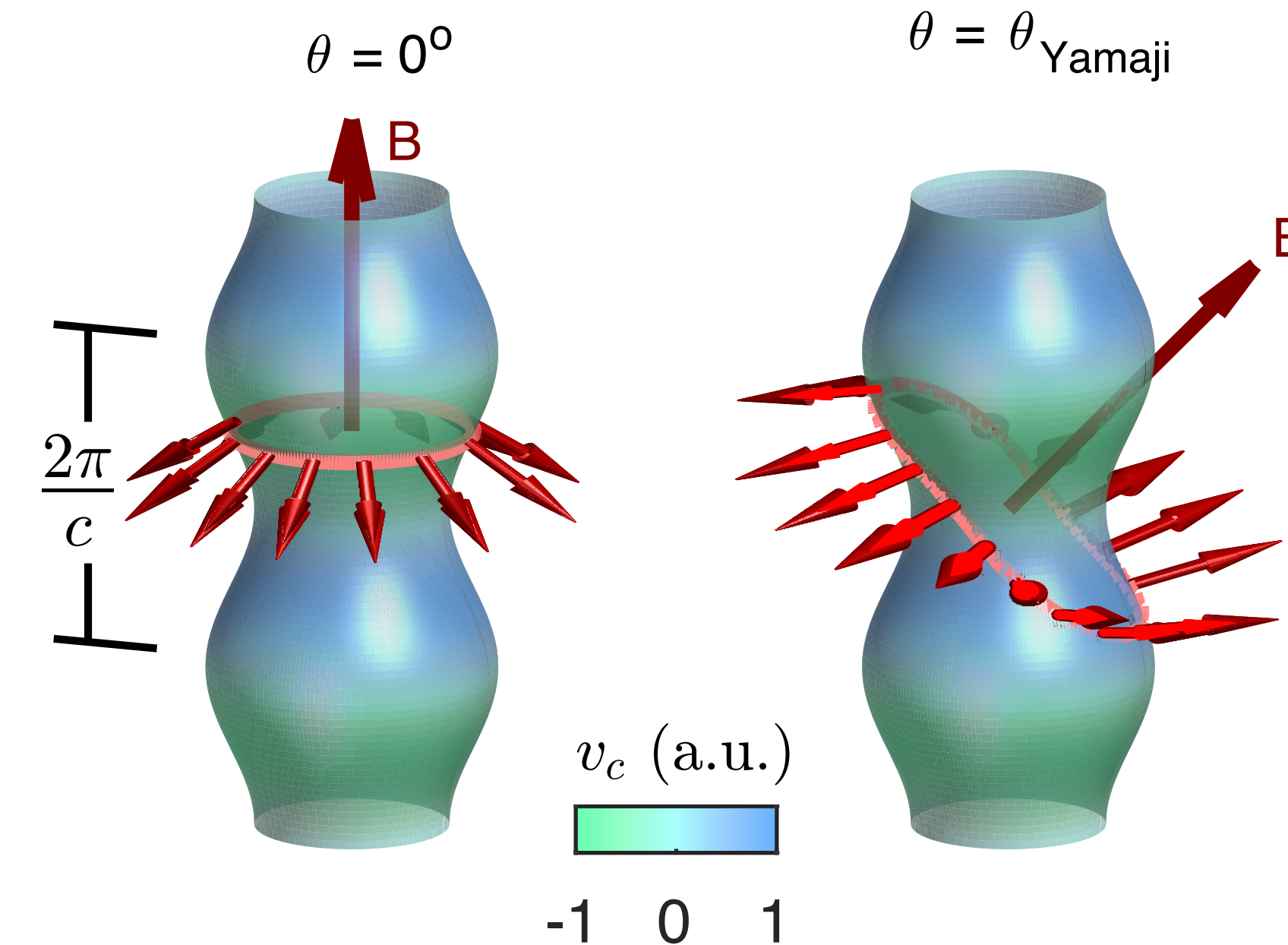
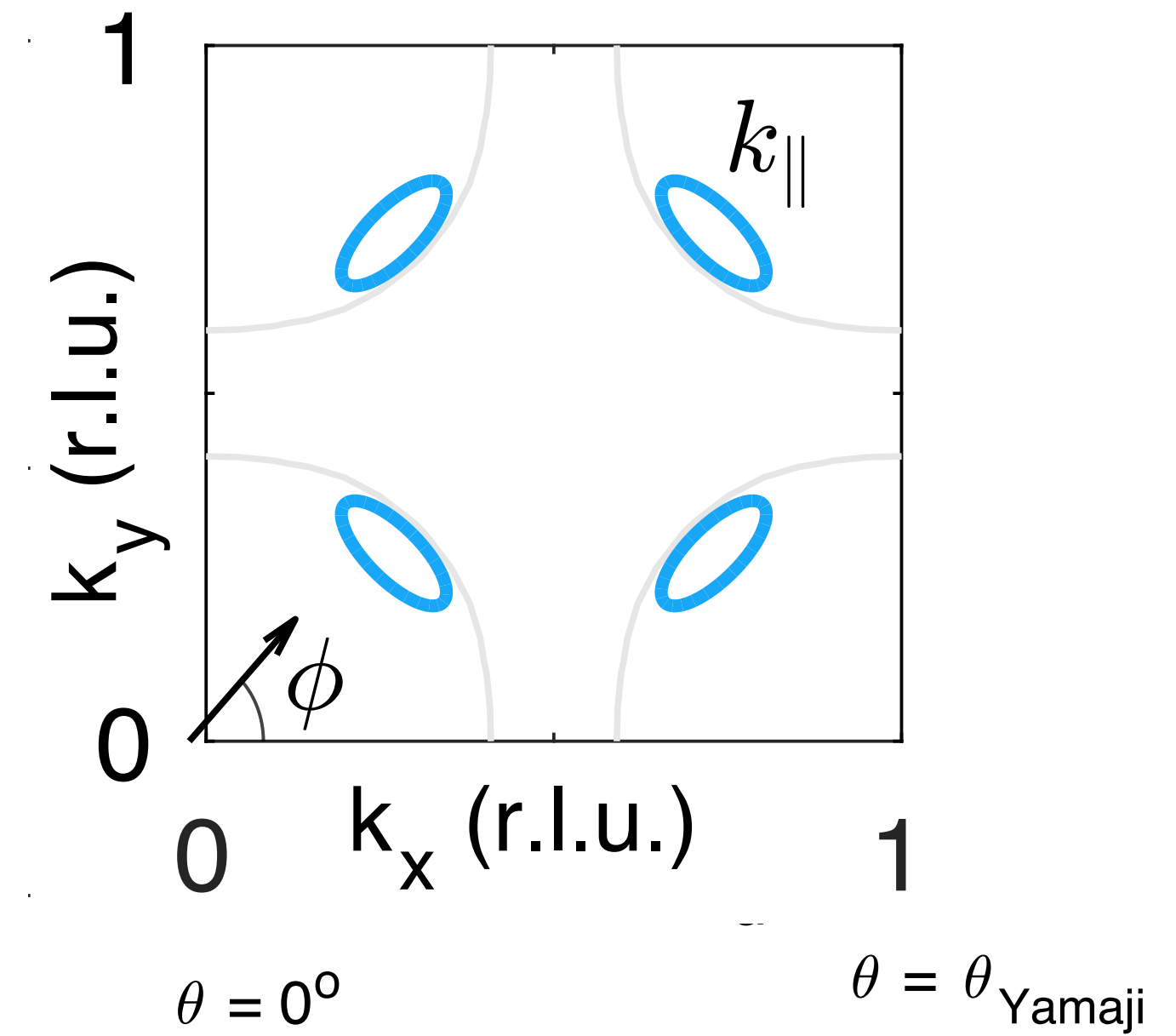
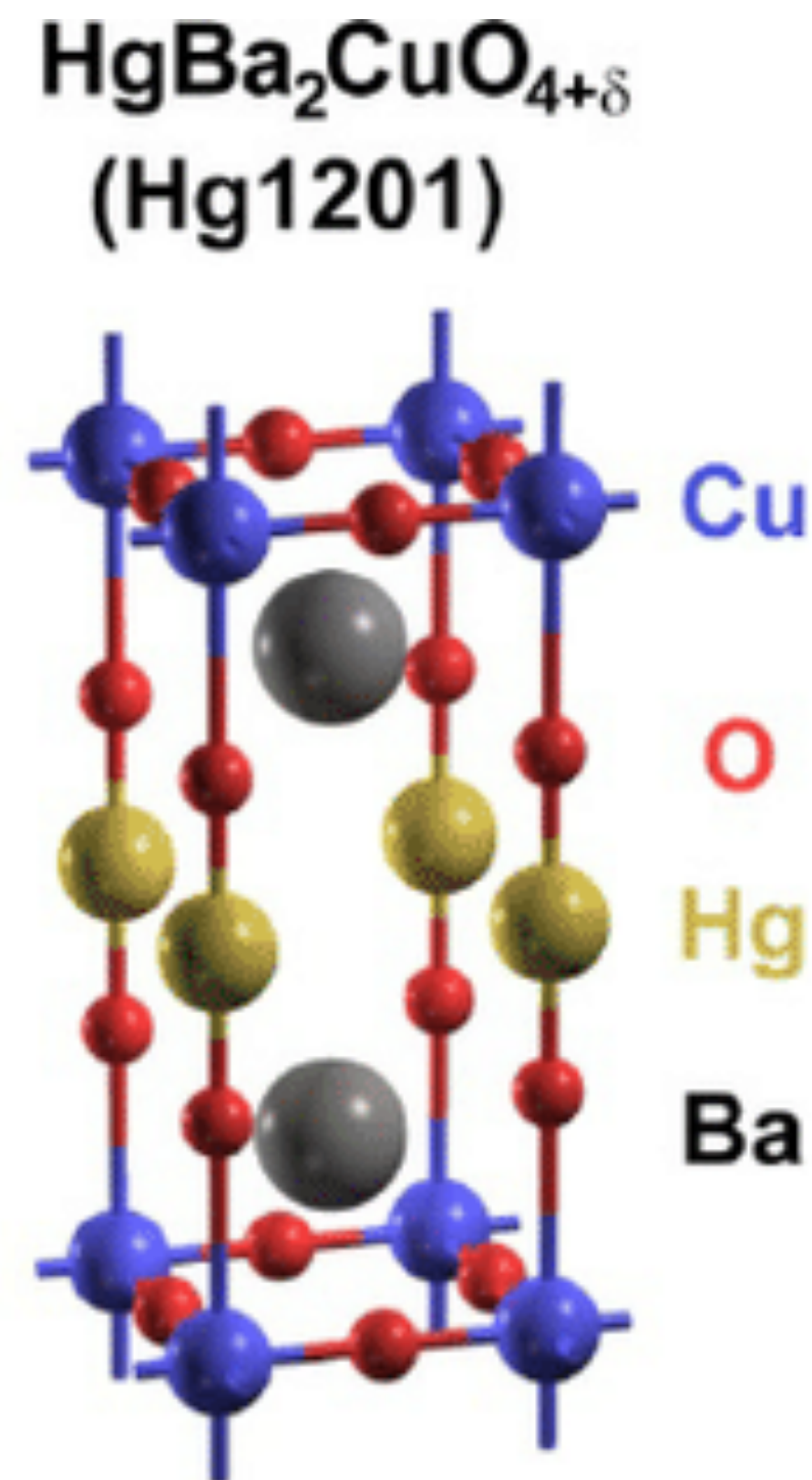
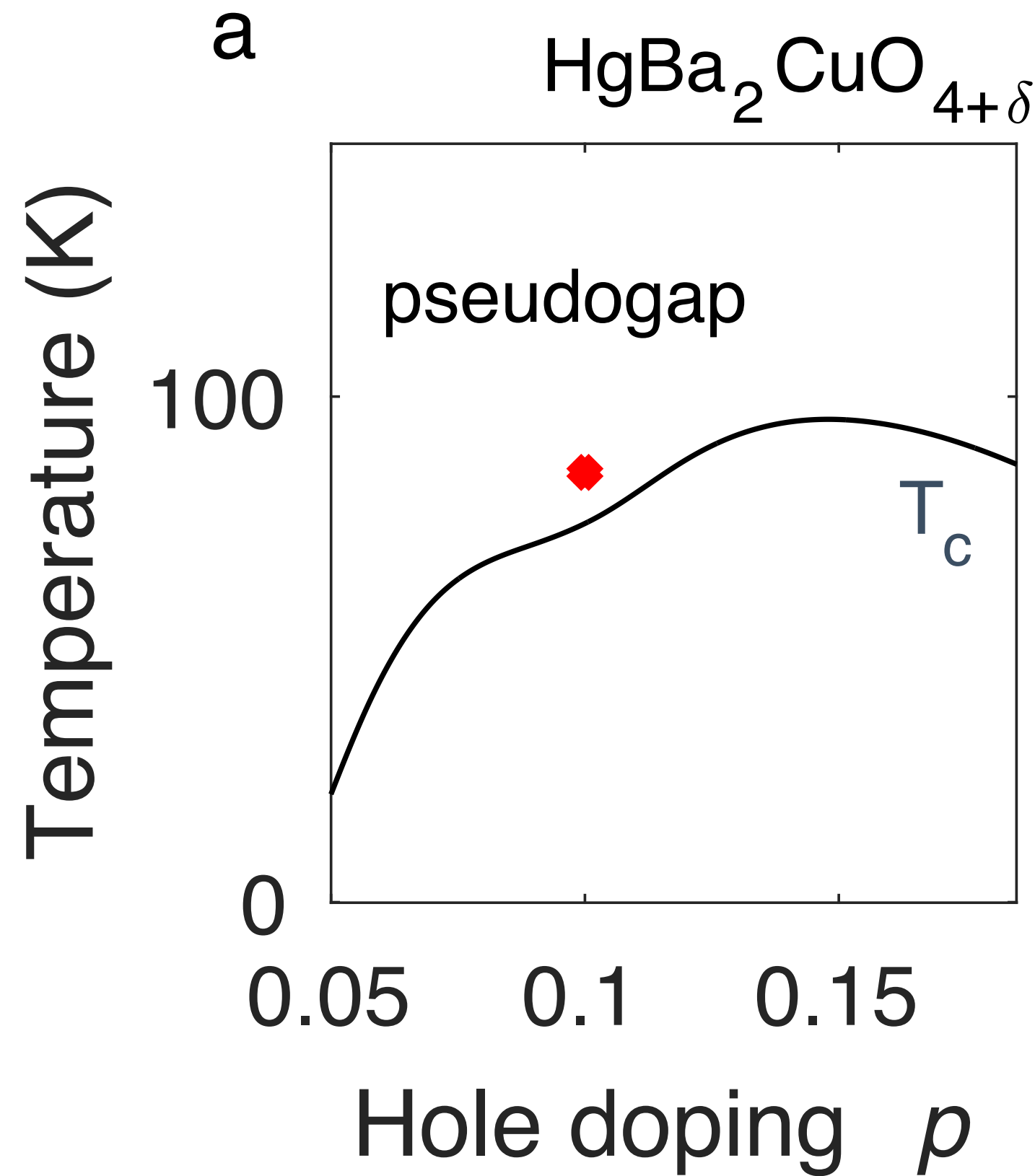
superconductor

Mun K. Chan¹✉, Katherine A. Schreiber¹, Oscar E. Ayala-Valenzuela¹,
Eric D. Bauer², Arkady Shekhter¹ & Neil Harrison¹

nature physics

21, 1753 (2025)

Published online: 16 September 2025



At the Yamaji angle, the orbits in the plane orthogonal to \mathbf{B} have an area which is independent of momentum in the c direction, to first order in the hopping along the c direction.

K. Yamaji JPSJ **58**, 1520 (1989)

Observation of the Yamaji effect in a cuprate

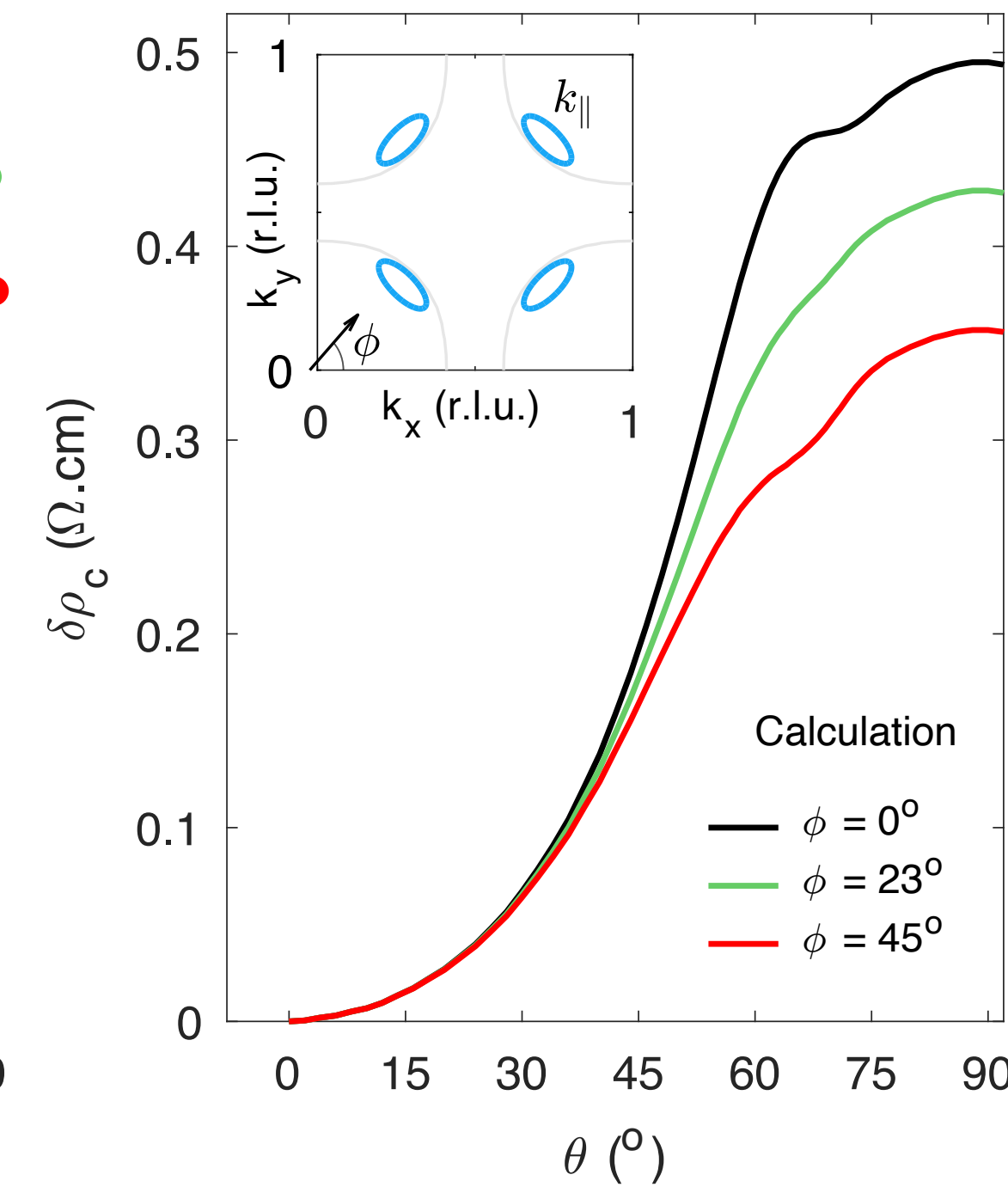
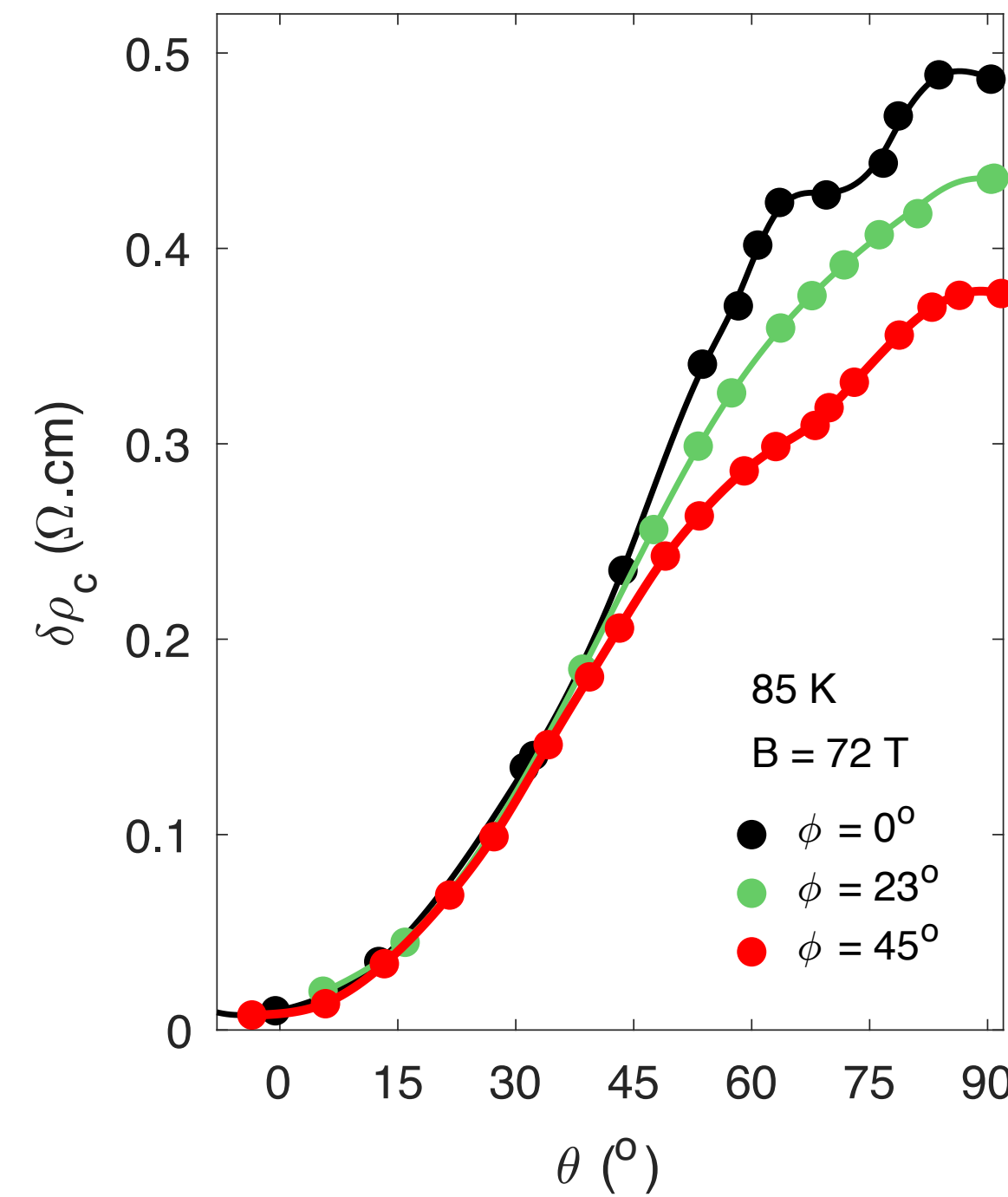
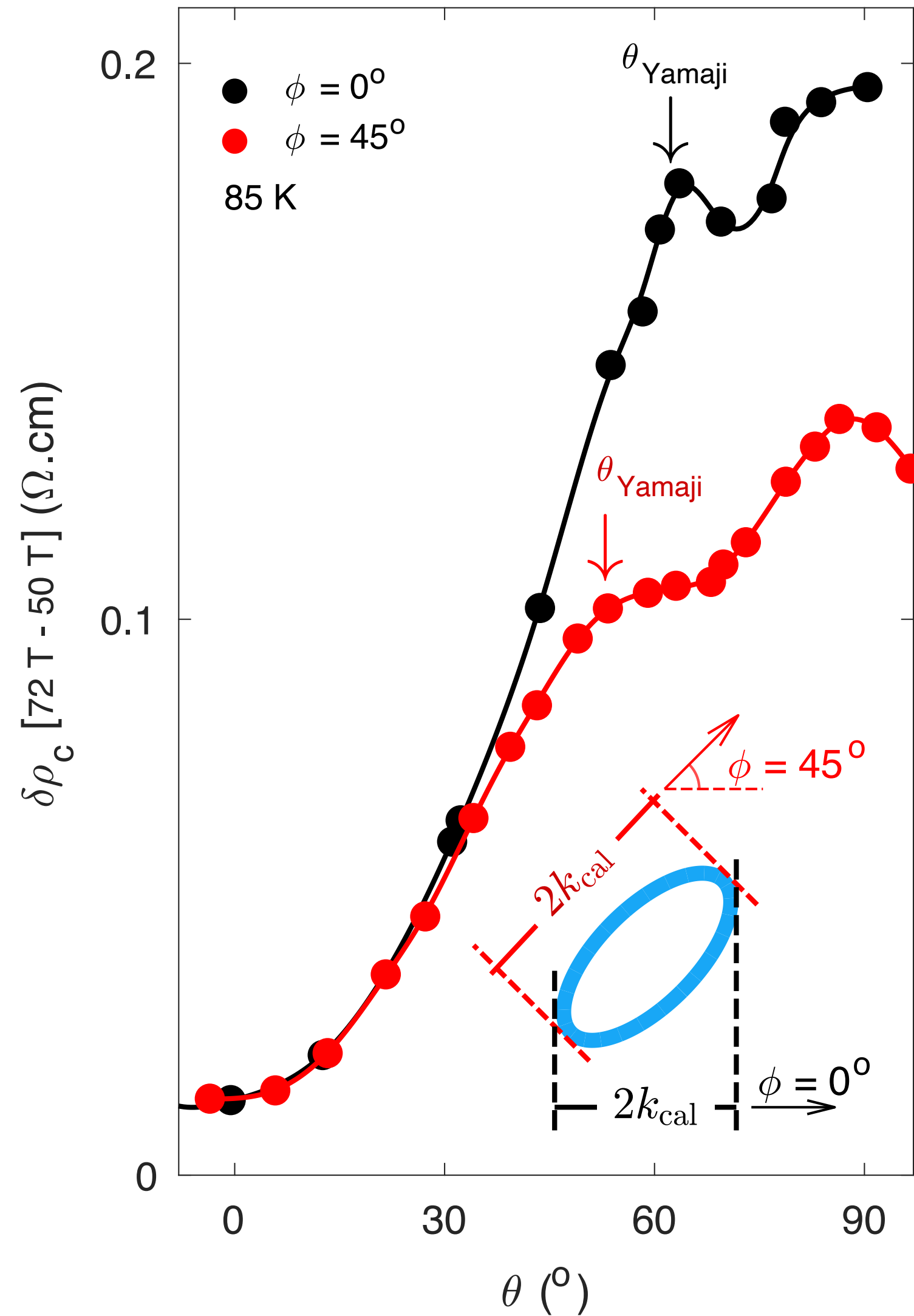
superconductor

Mun K. Chan¹✉, Katherine A. Schreiber¹, Oscar E. Ayala-Valenzuela¹,
Eric D. Bauer², Arkady Shekhter¹ & Neil Harrison¹

nature physics

21, 1753 (2025)

Published online: 16 September 2025



Doping
 $p = 0.1$

The observation of the Yamaji peak is evidence for small Fermi-surface pockets in the normal state of the pseudogap phase.

Observation of the Yamaji effect in a cuprate superconductor

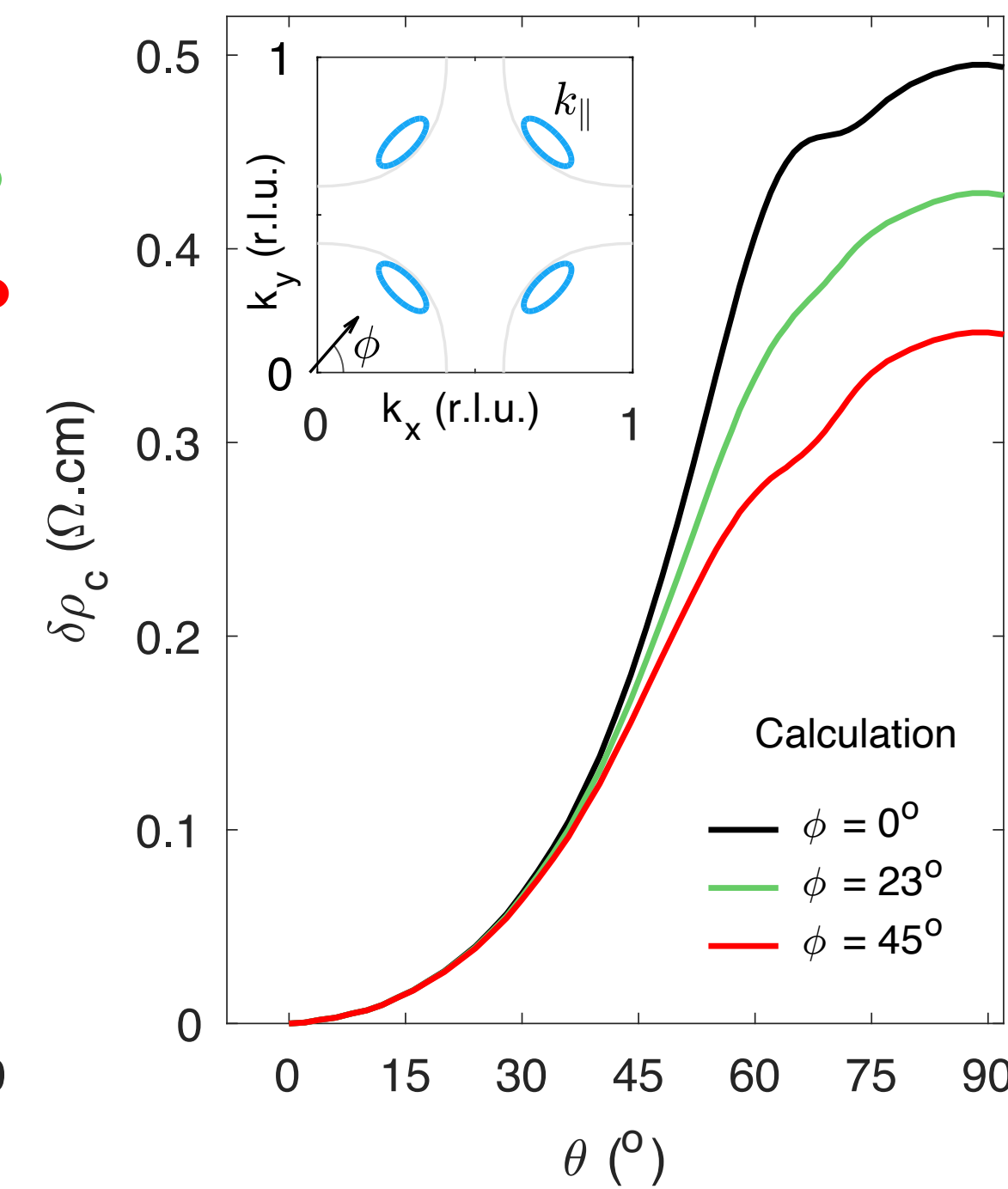
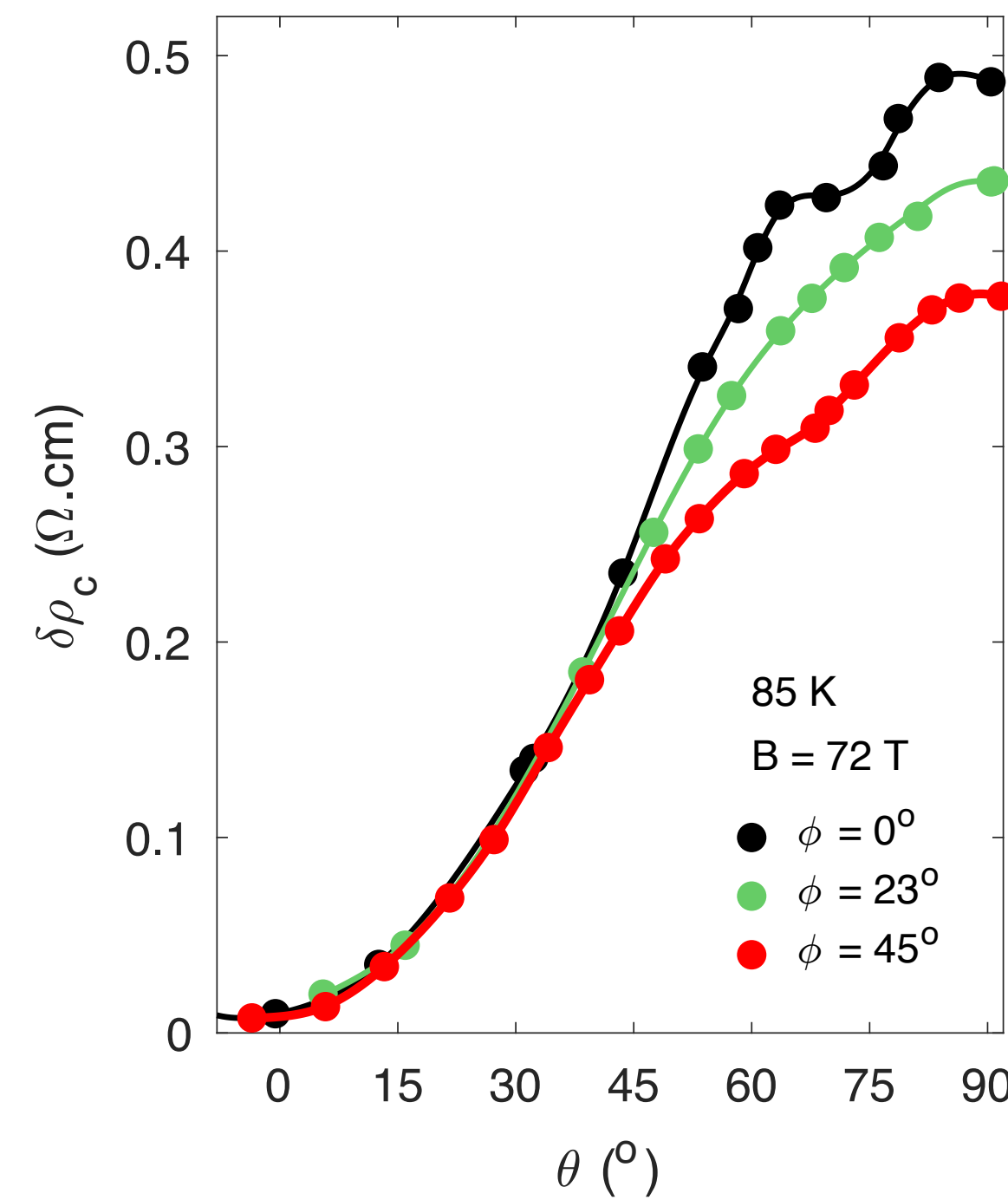
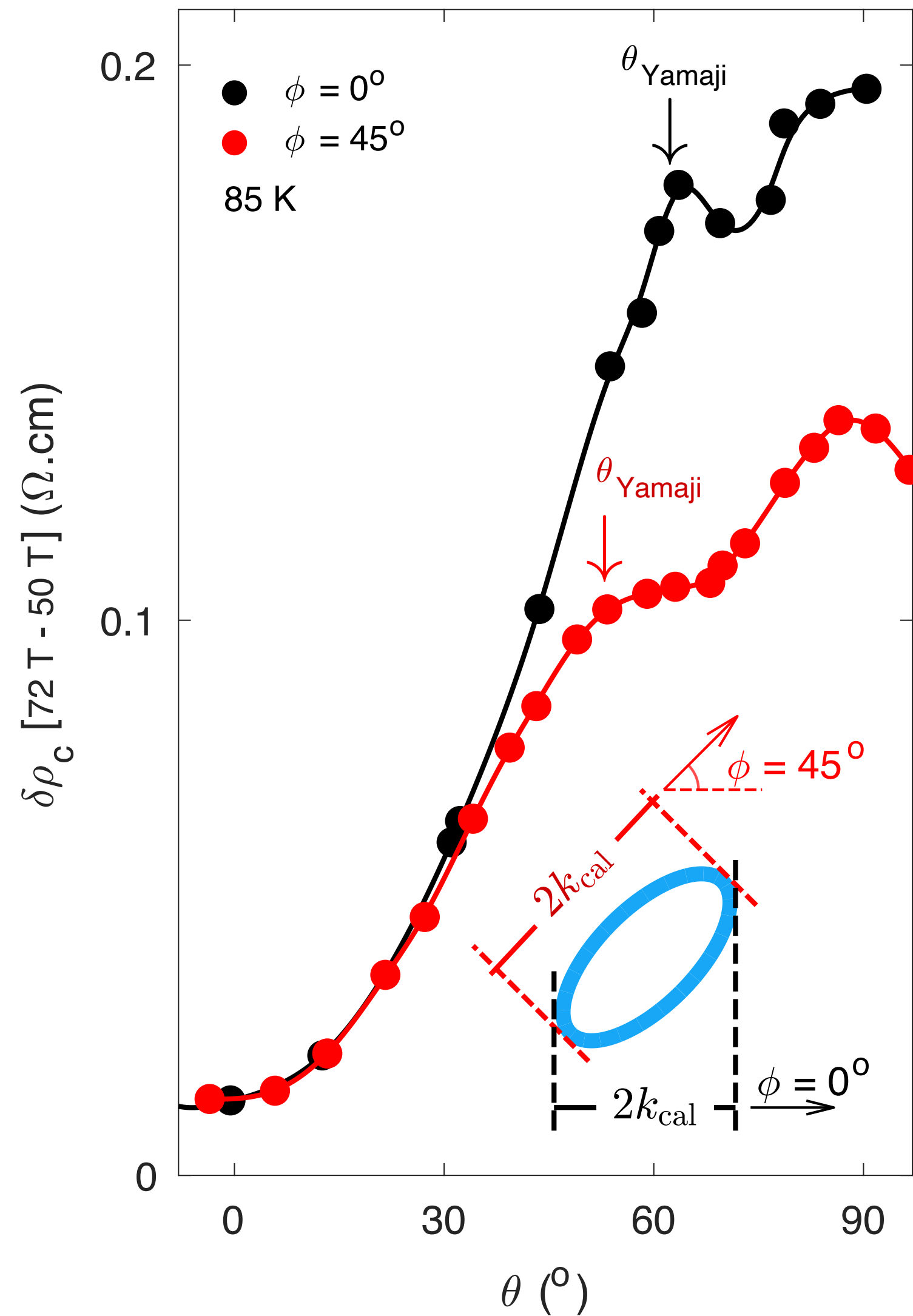
superconductor

Mun K. Chan¹✉, Katherine A. Schreiber¹, Oscar E. Ayala-Valenzuela¹,
Eric D. Bauer², Arkady Shekhter¹ & Neil Harrison¹

nature physics

21, 1753 (2025)

Published online: 16 September 2025



Doping
 $p = 0.1$

The observation of the Yamaji peak is evidence for small Fermi-surface pockets in the normal state of the pseudogap phase.

Excellent evidence for hole pockets with coherent interlayer-transport.

Observation of the Yamaji effect in a cuprate superconductor

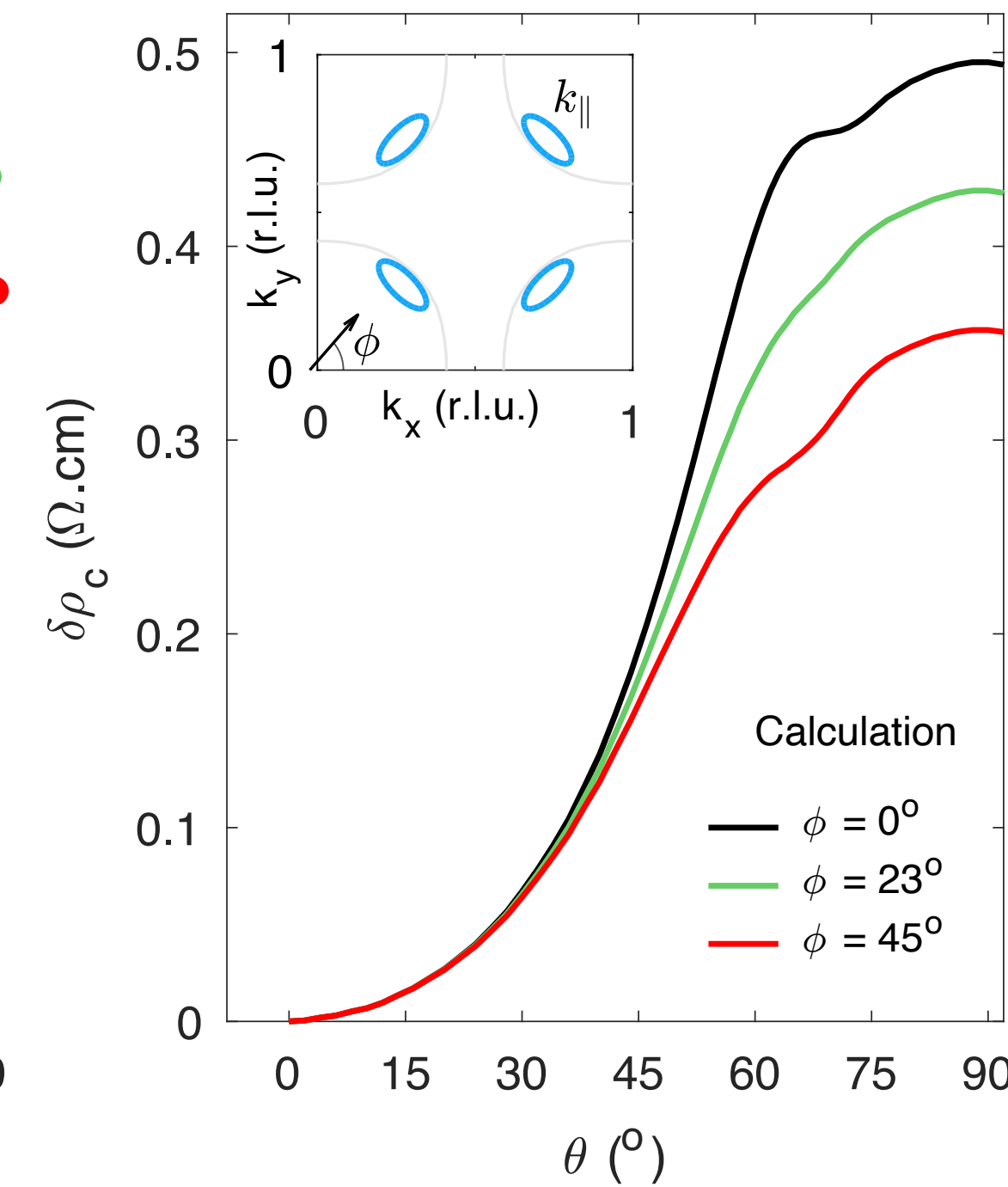
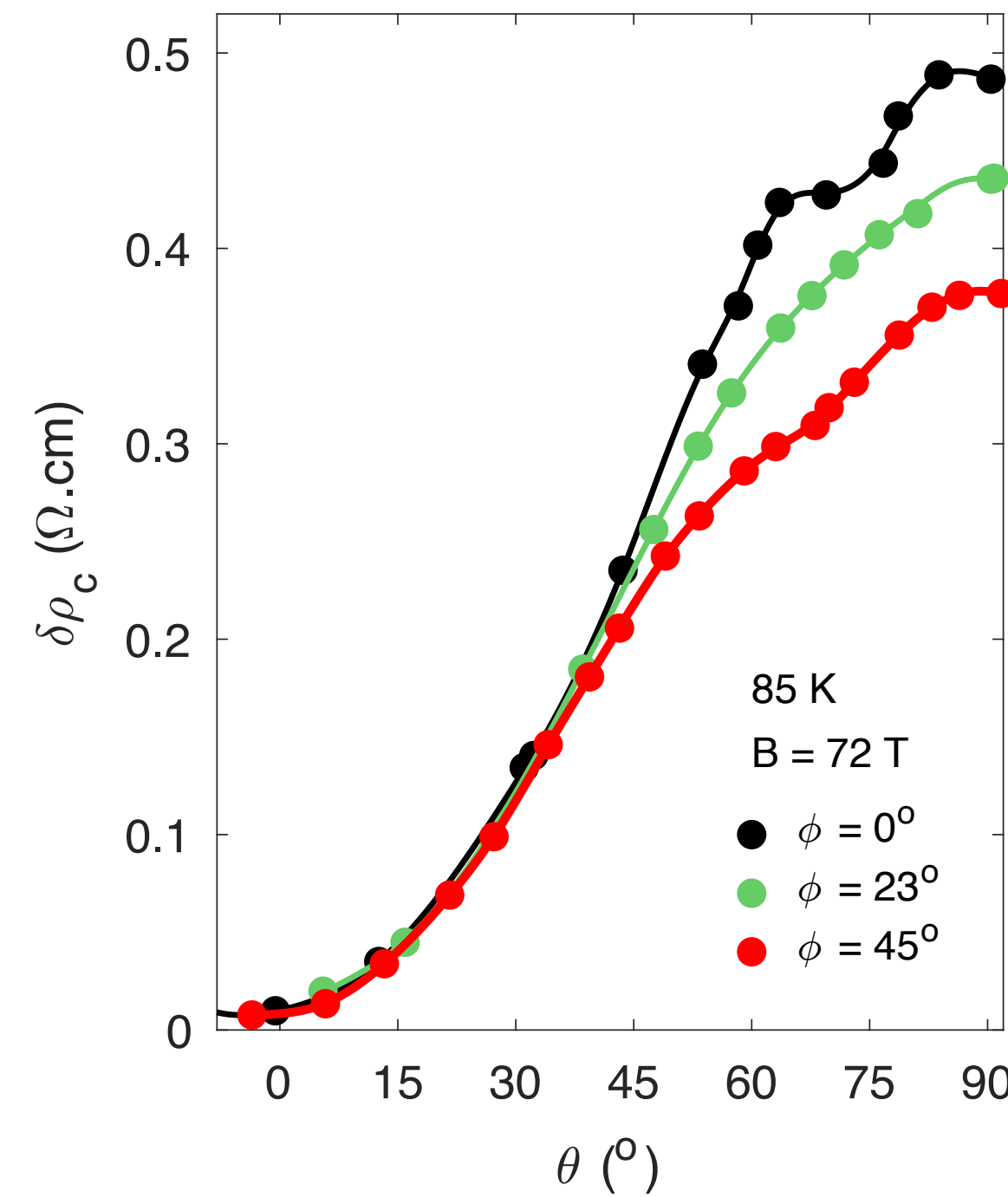
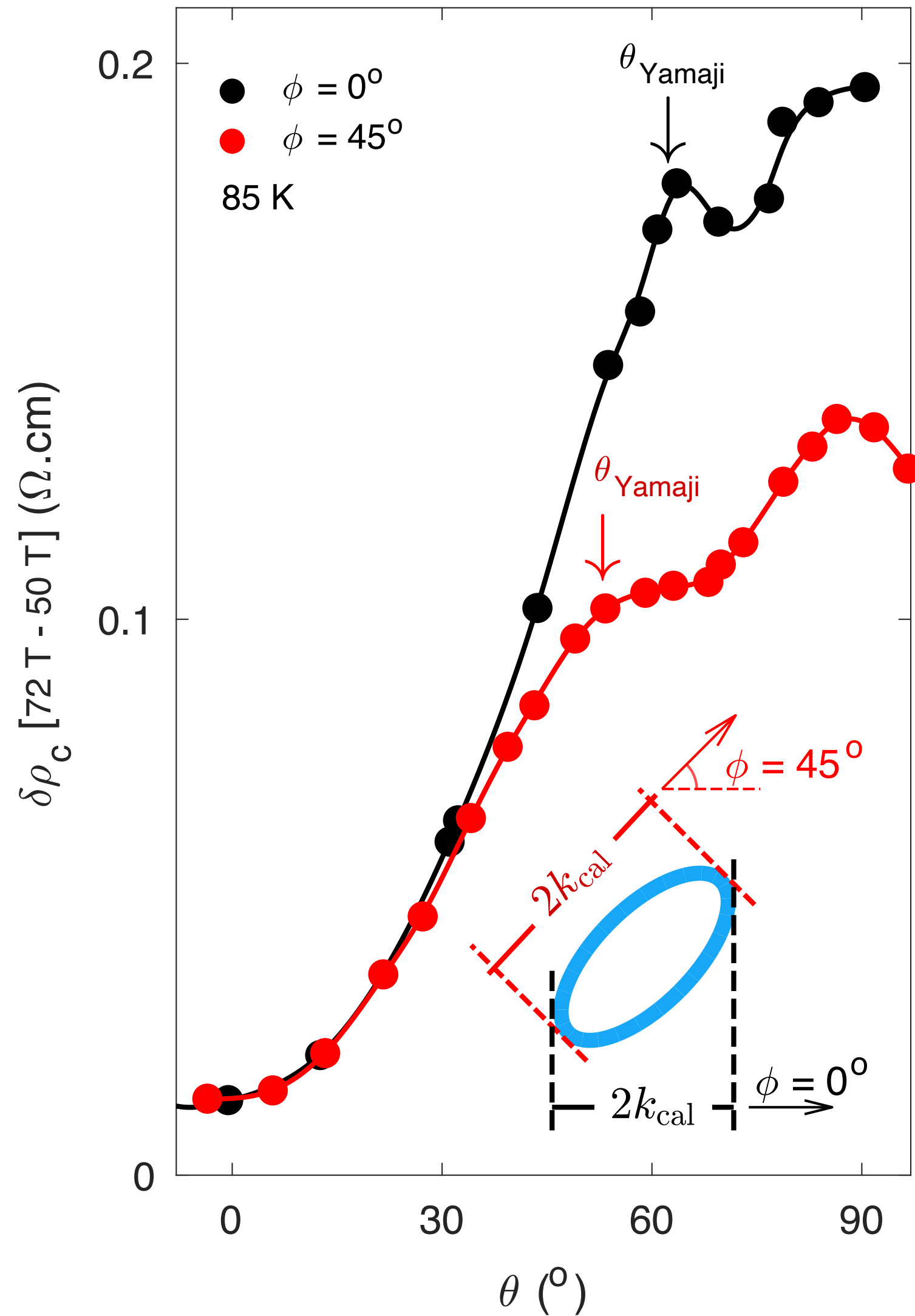
superconductor

Mun K. Chan¹✉, Katherine A. Schreiber¹, Oscar E. Ayala-Valenzuela¹,
Eric D. Bauer², Arkady Shekhter¹ & Neil Harrison¹

nature physics

21, 1753 (2025)

Published online: 16 September 2025



Doping
 $p = 0.1$

The observation of the Yamaji peak is evidence for small Fermi-surface pockets in the normal state of the pseudogap phase.

Excellent evidence for hole pockets with coherent interlayer-transport.
Rules out holon metal

Observation of the Yamaji effect in a cuprate superconductor

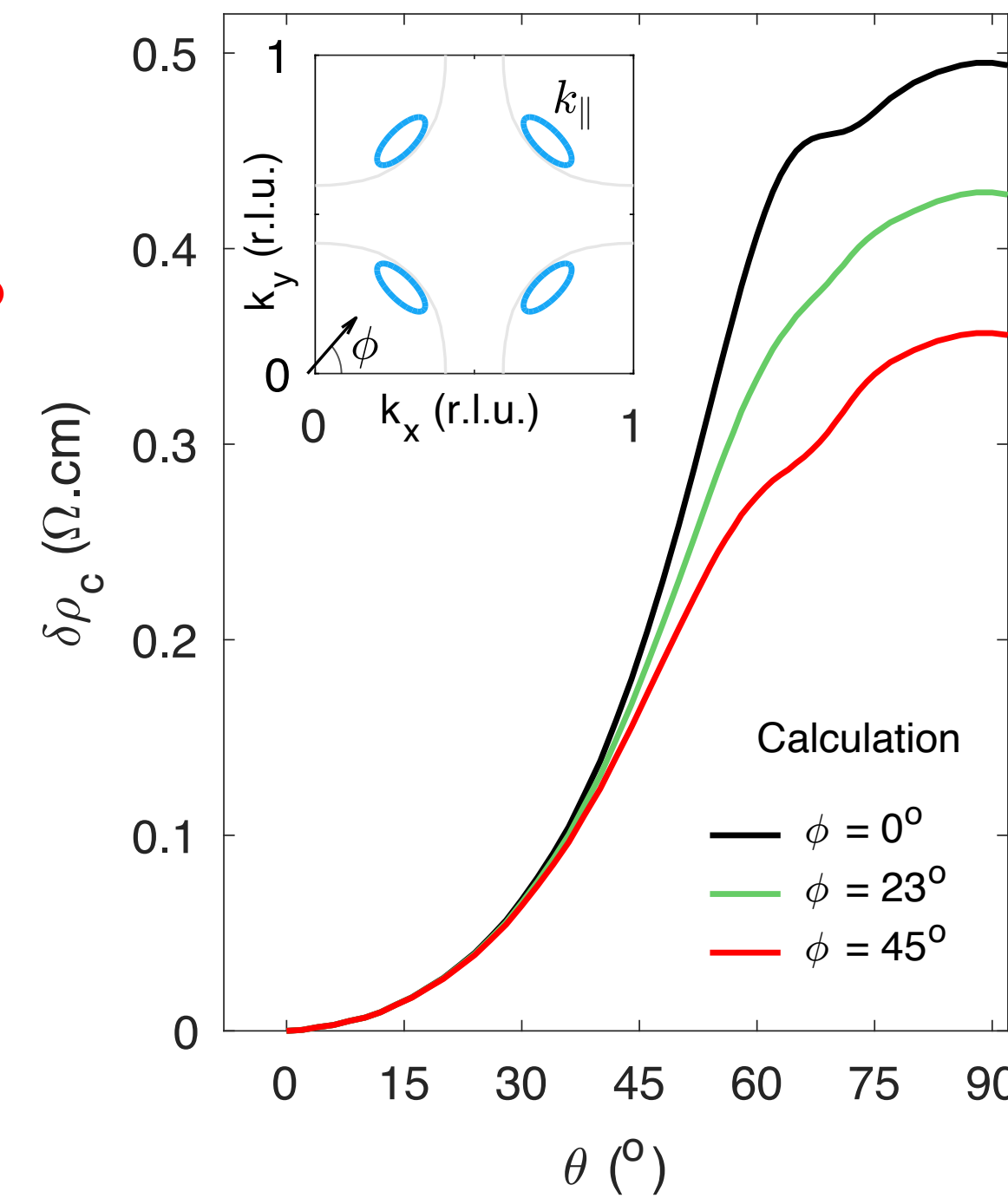
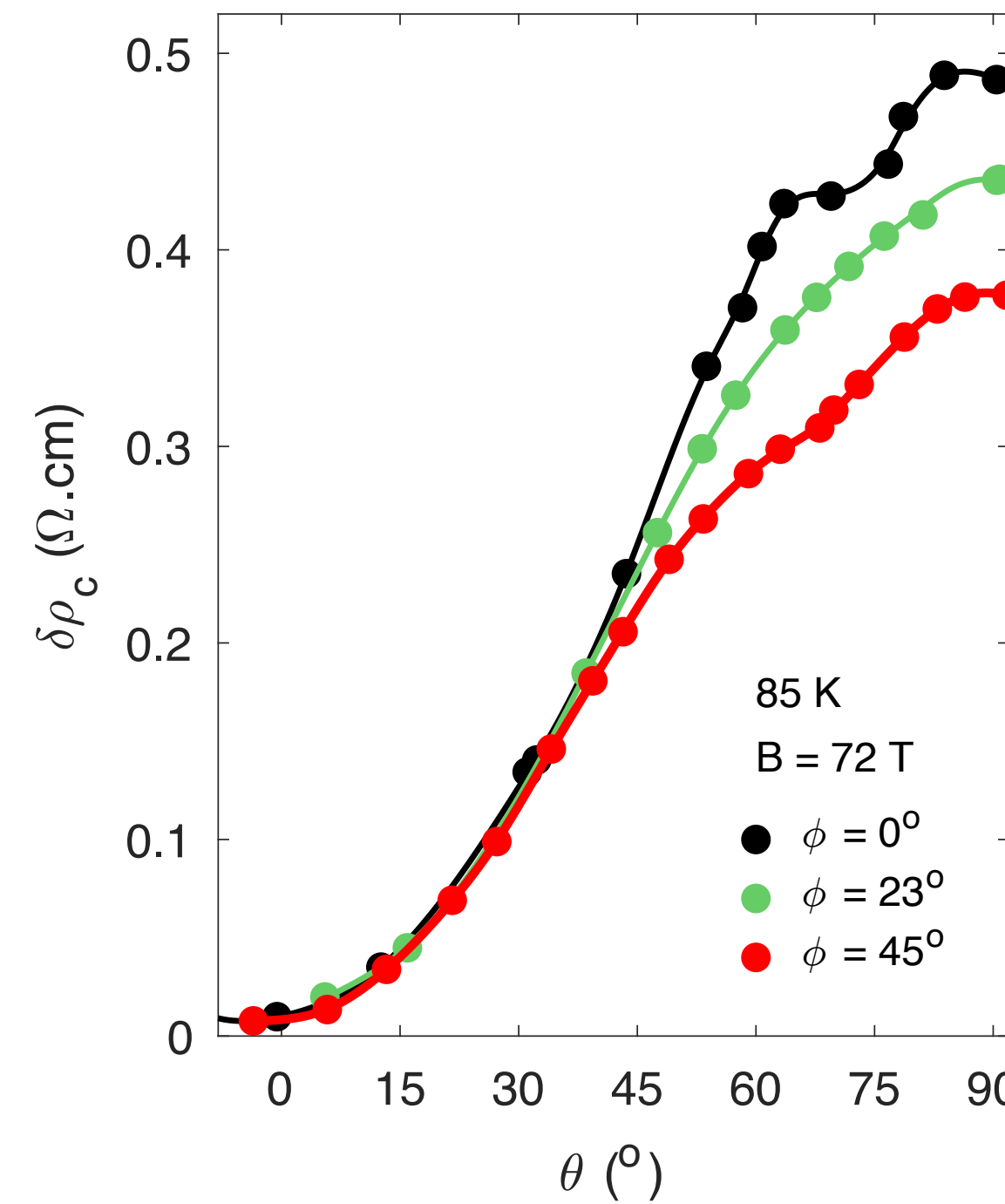
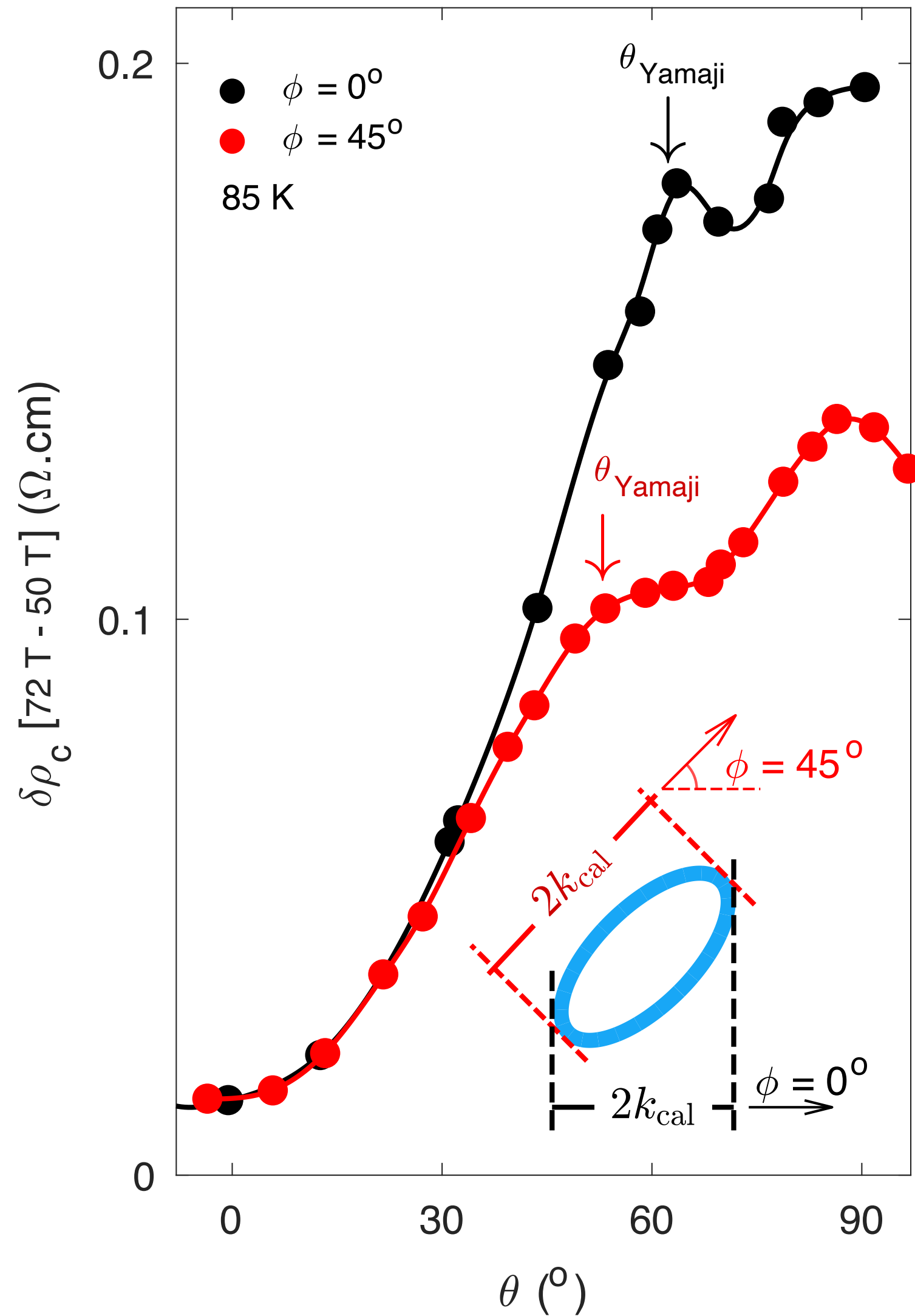
superconductor

Mun K. Chan¹✉, Katherine A. Schreiber¹, Oscar E. Ayala-Valenzuela¹,
Eric D. Bauer², Arkady Shekhter¹ & Neil Harrison¹

nature physics

21, 1753 (2025)

Published online: 16 September 2025



Doping
 $p = 0.1$

The observation of the Yamaji peak is evidence for small Fermi-surface pockets in the normal state of the pseudogap phase.

Excellent evidence for hole pockets with coherent interlayer-transport.
Rules out holon metal and possibly SDW metal

Observation of the Yamaji effect in a cuprate superconductor

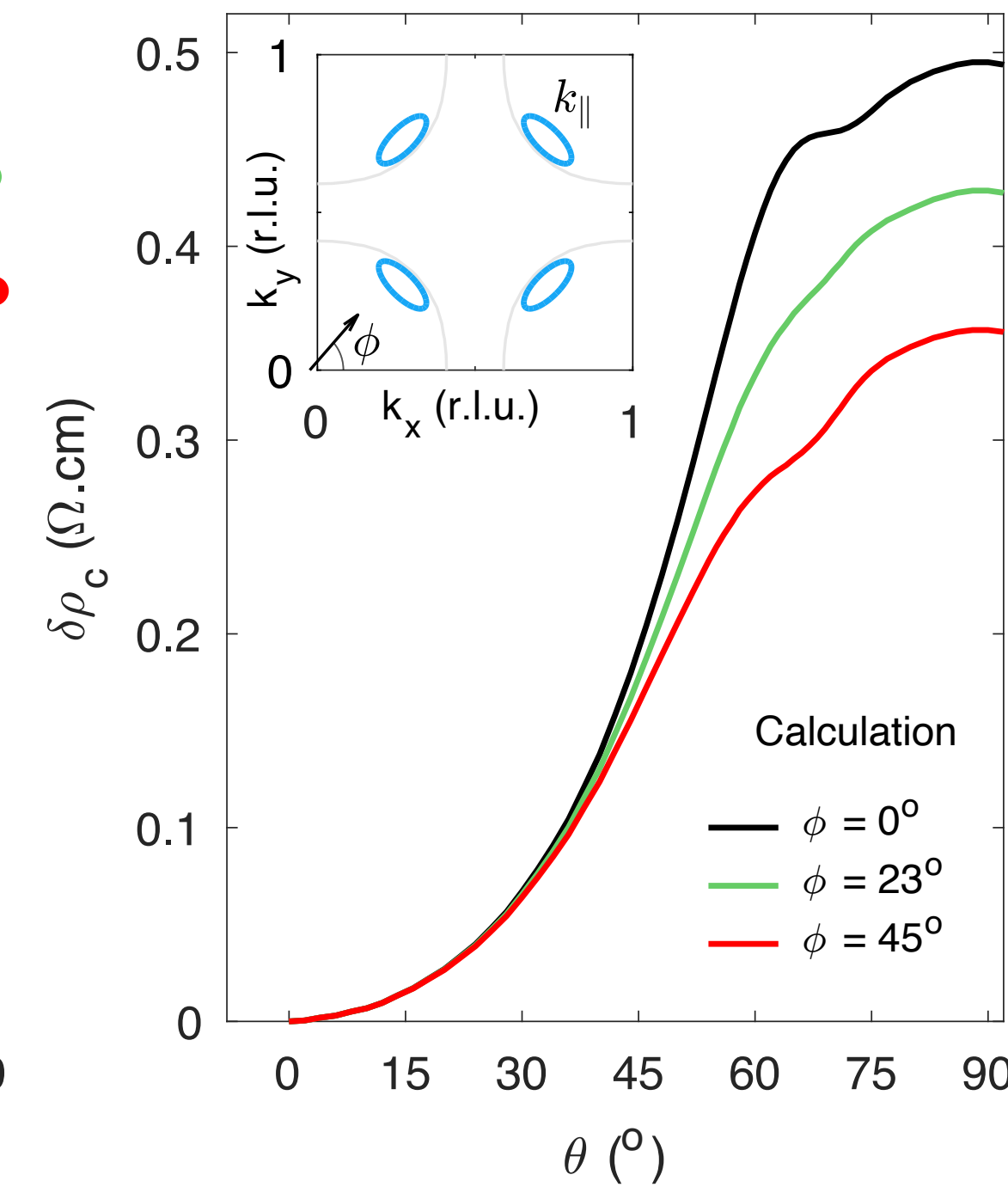
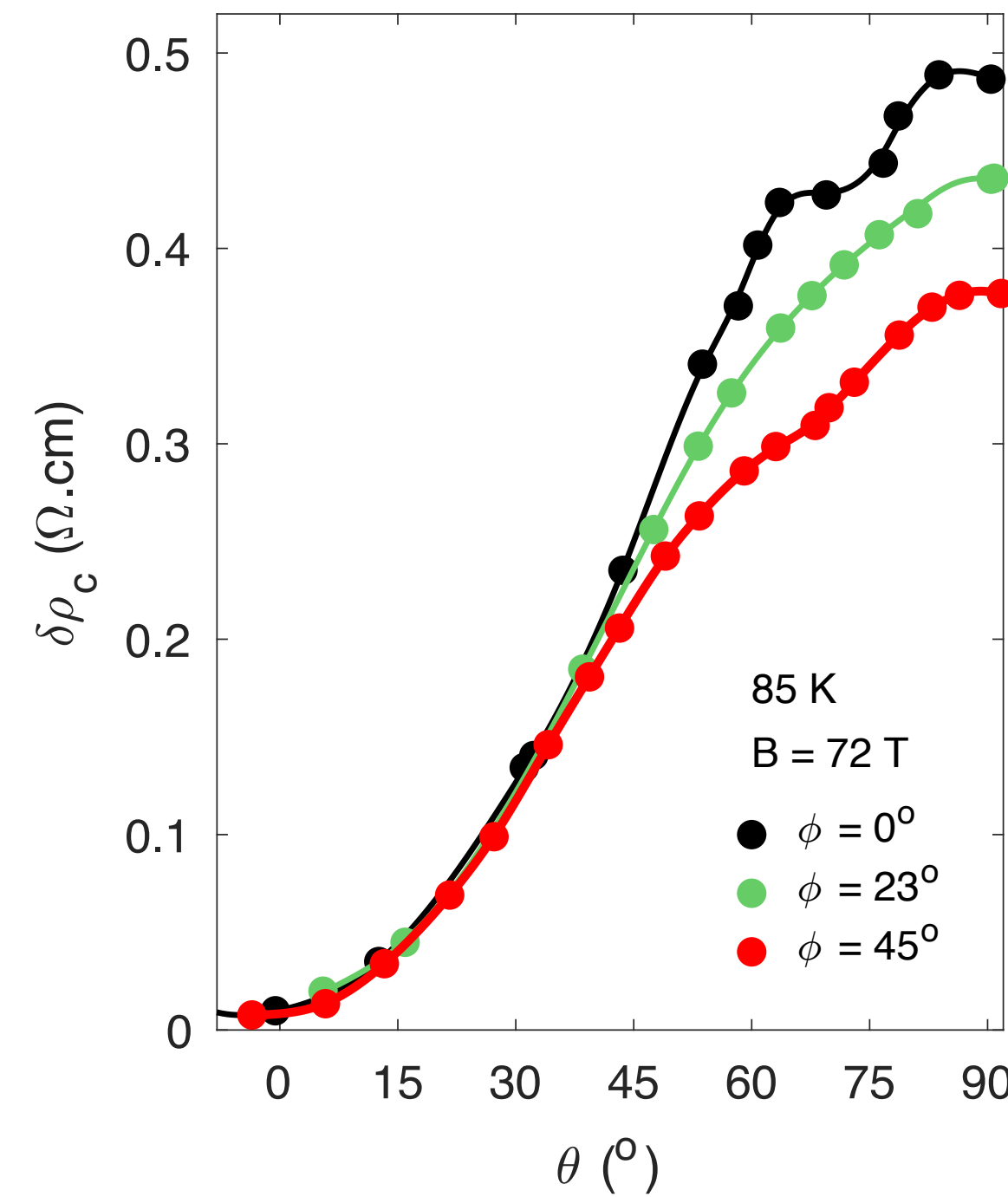
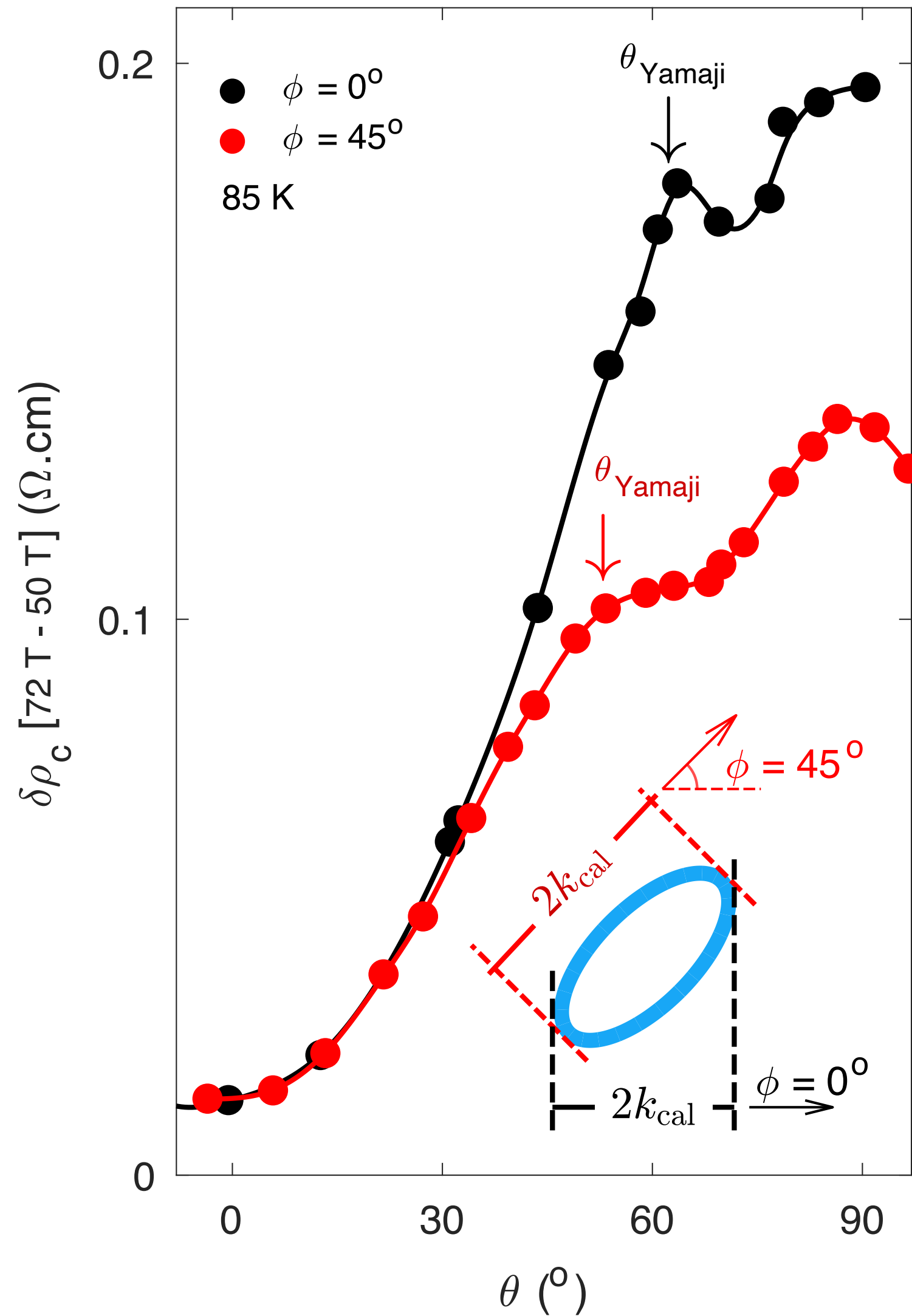
superconductor

Mun K. Chan¹✉, Katherine A. Schreiber¹, Oscar E. Ayala-Valenzuela¹,
Eric D. Bauer², Arkady Shekhter¹ & Neil Harrison¹

nature physics

21, 1753 (2025)

Published online: 16 September 2025



Doping
 $p = 0.1$

The observation of the Yamaji peak is evidence for small Fermi-surface pockets in the normal state of the pseudogap phase. The small size of the pockets, each estimated to occupy only 1.3% of the Brillouin zone area, is not expected given the absence of long-range broken translational symmetry.

Observation of the Yamaji effect in a cuprate superconductor

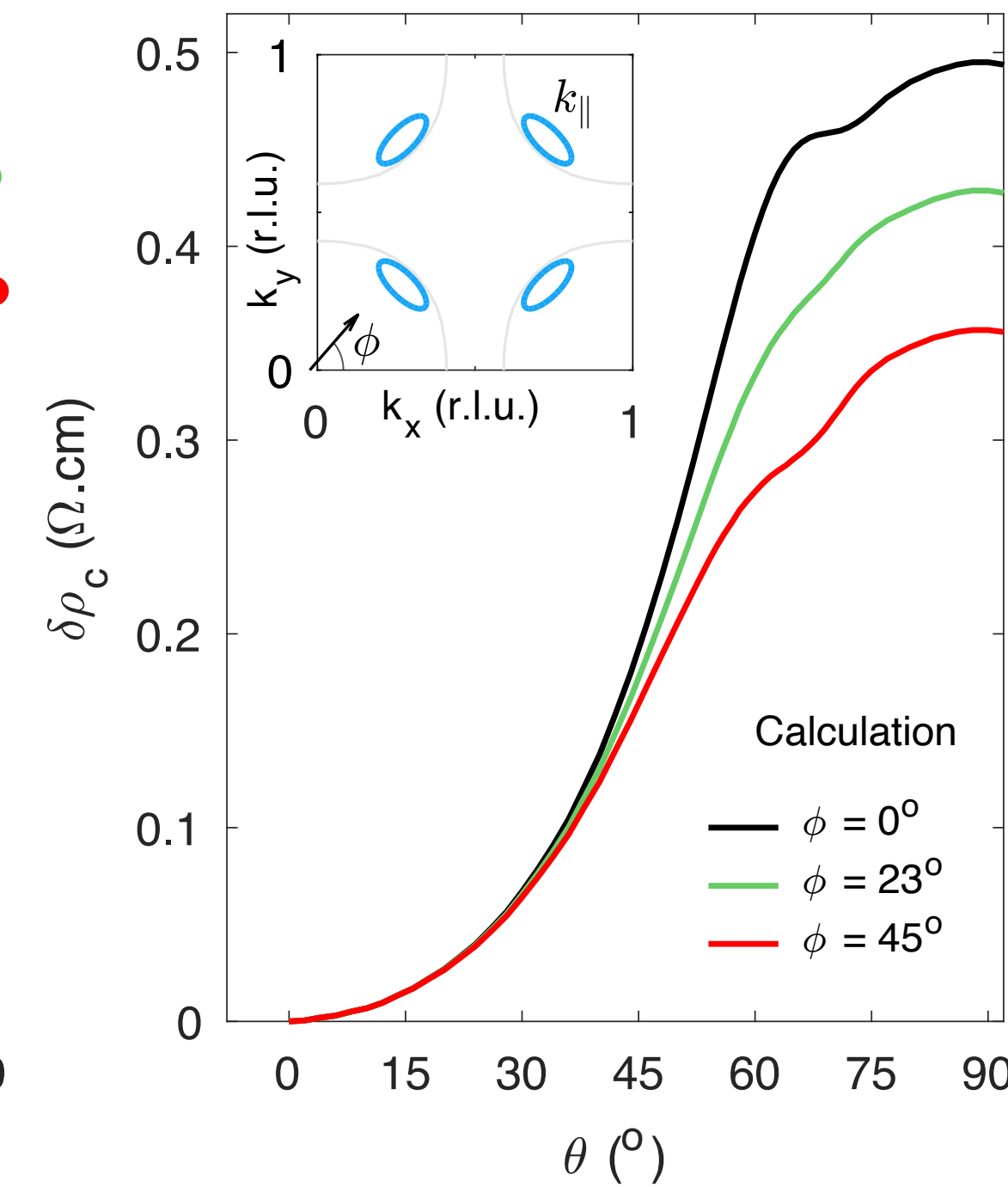
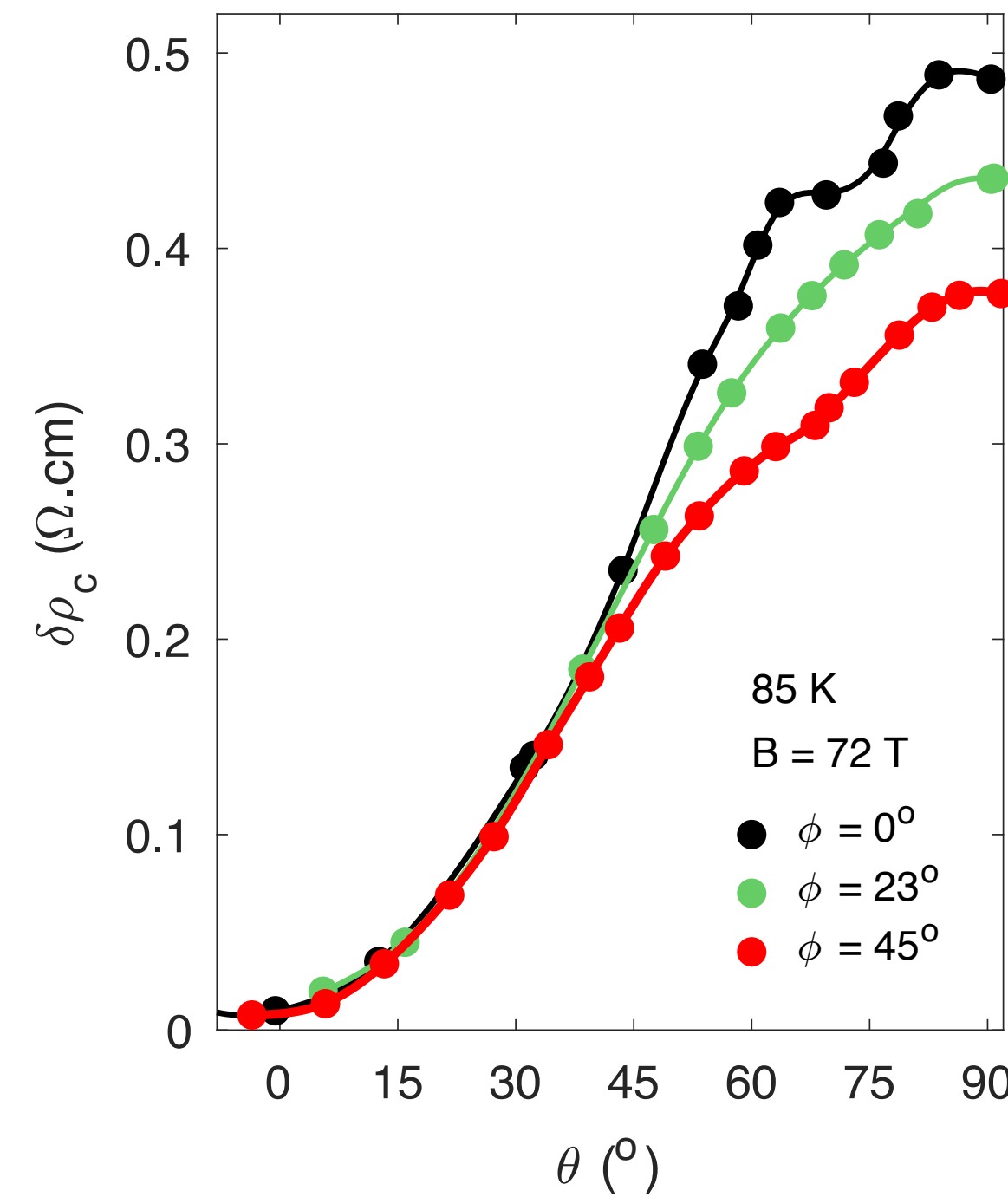
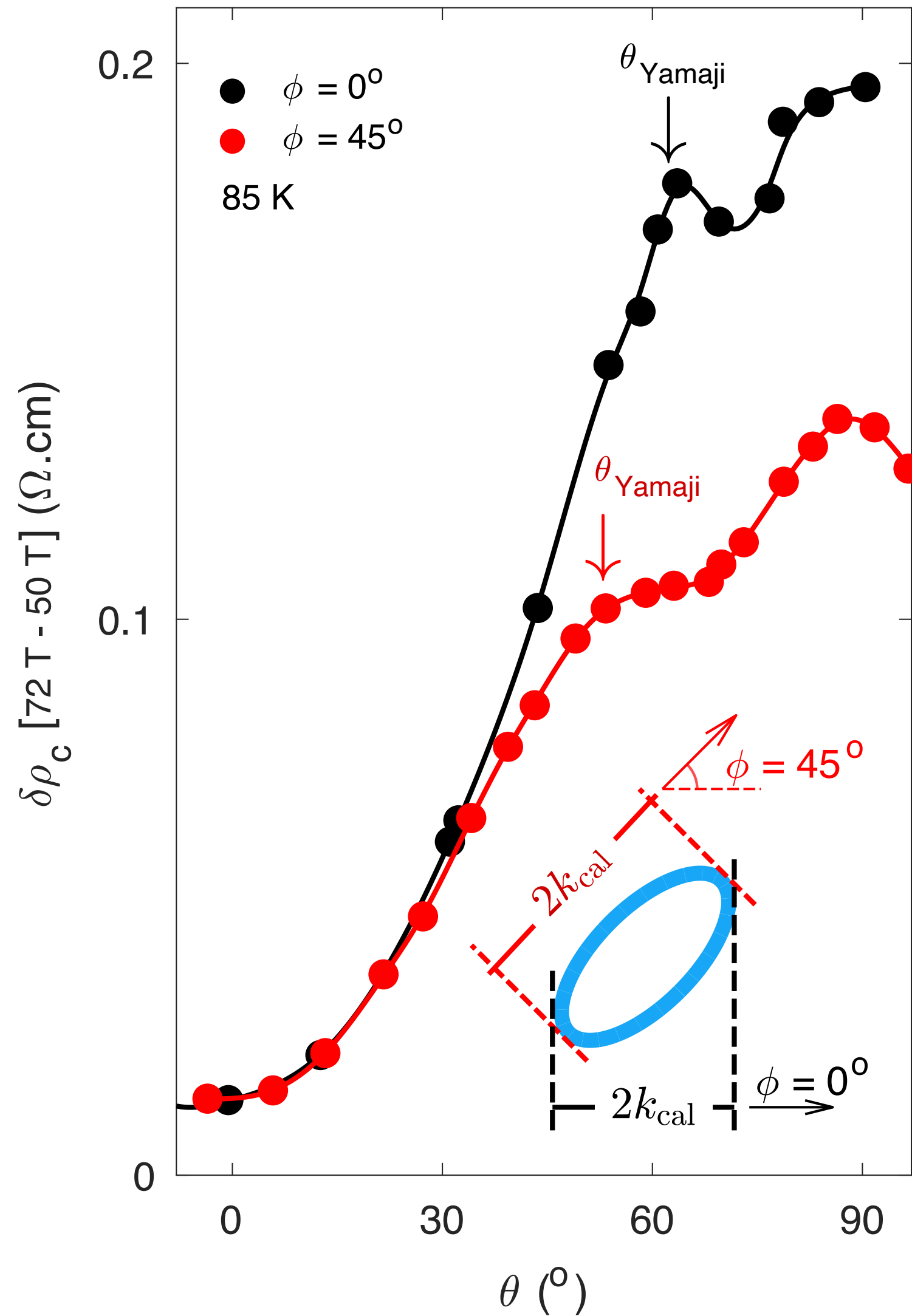
superconductor

Mun K. Chan¹✉, Katherine A. Schreiber¹, Oscar E. Ayala-Valenzuela¹,
Eric D. Bauer², Arkady Shekhter¹ & Neil Harrison¹

nature physics

21, 1753 (2025)

Published online: 16 September 2025



Doping
 $p = 0.1$

The observation of the Yamaji peak is evidence for small Fermi-surface pockets in the normal state of the pseudogap phase. The small size of the pockets, each estimated to occupy only 1.3% of the Brillouin zone area, is not expected given the absence of long-range broken translational symmetry.

Observation of the Yamaji effect in a cuprate superconductor

nature physics

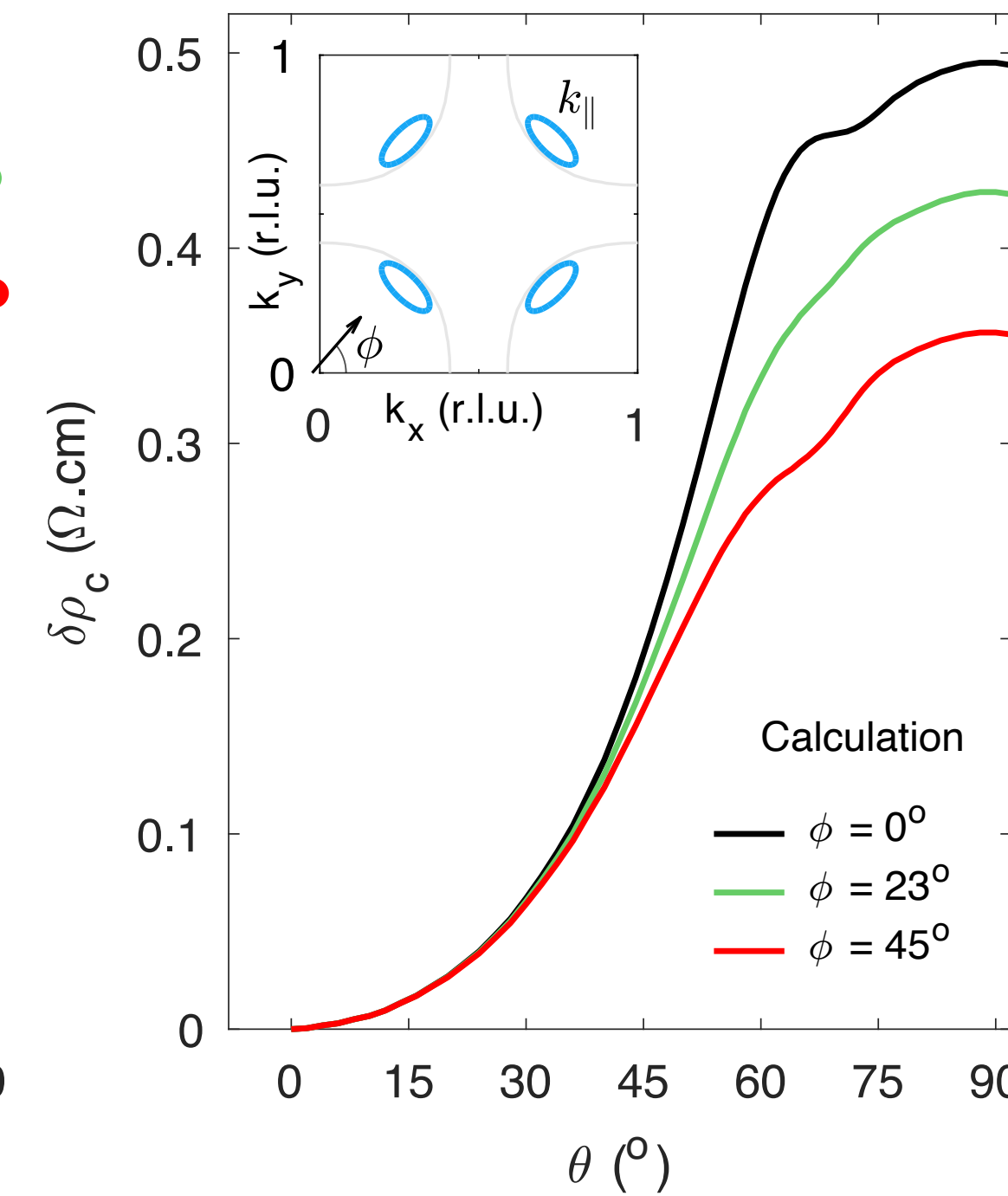
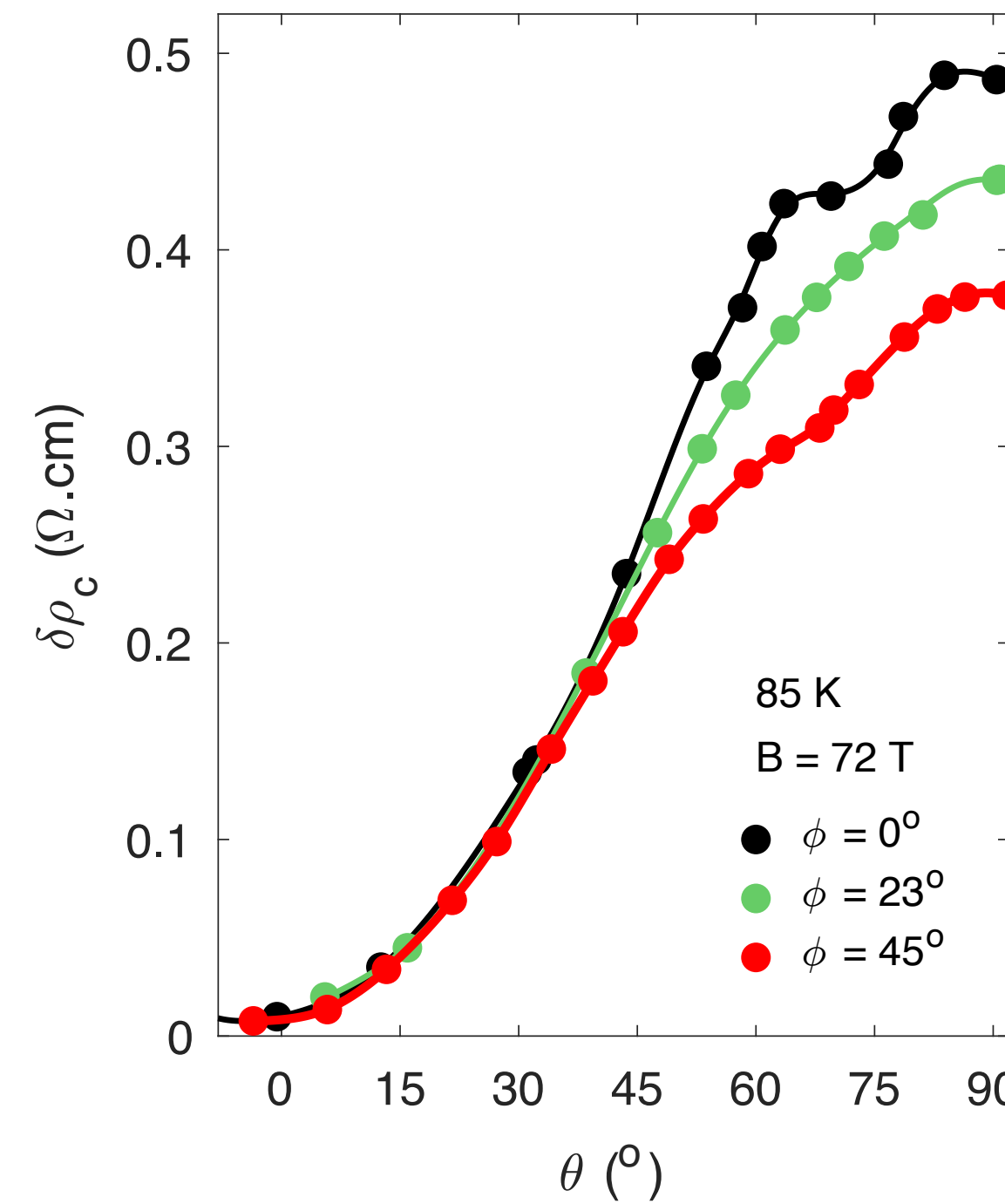
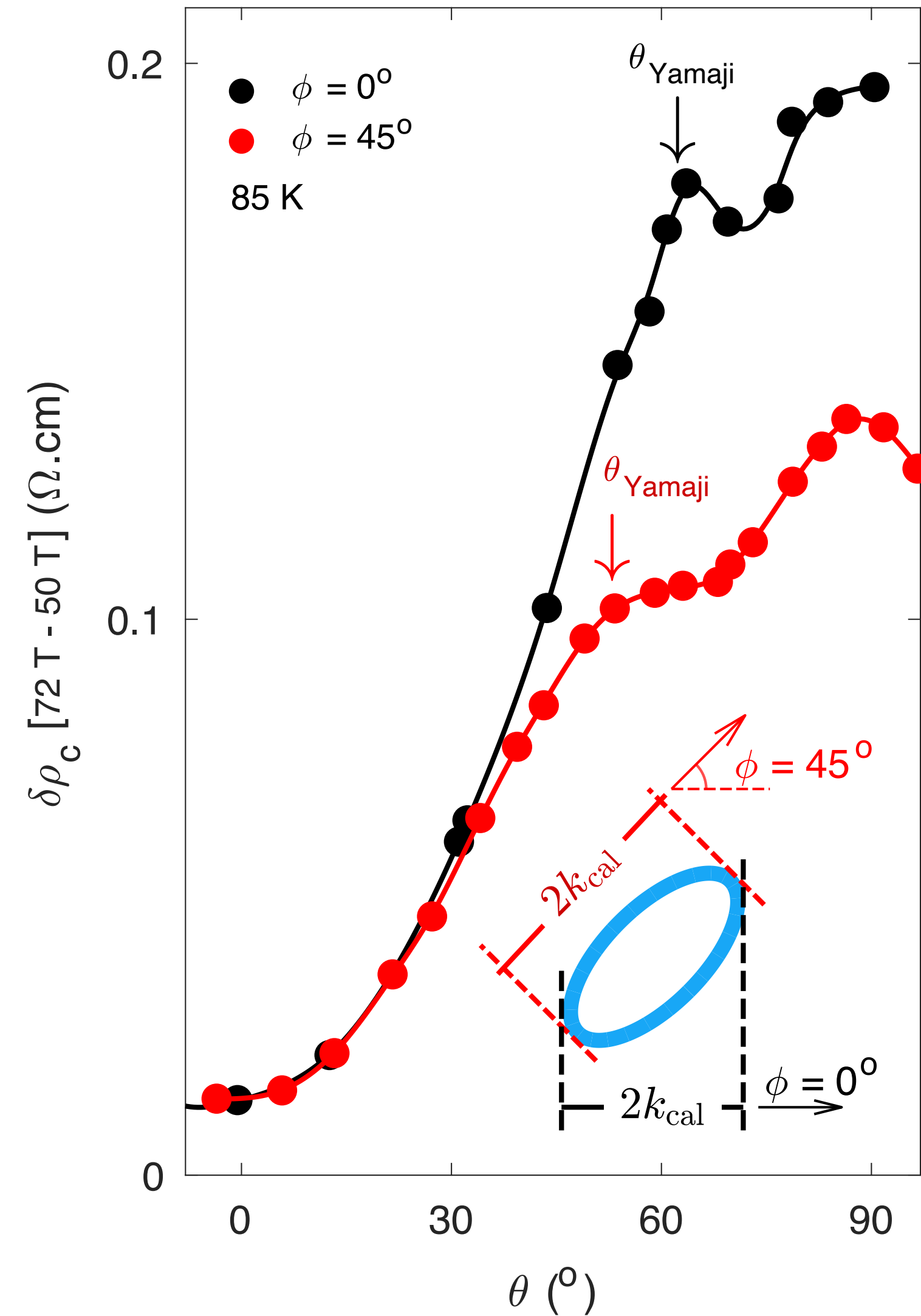
21, 1753 (2025)

superconductor

Mun K. Chan¹, Katherine A. Schreiber¹, Oscar E. Ayala-Valenzuela¹,

Eric D. Bauer², Arkady Shekhter¹ & Neil Harrison¹

Published online: 16 September 2025



Doping
 $p = 0.1$

The observation of the Yamaji peak is evidence for small Fermi-surface pockets in the normal state of the pseudogap phase. The small size of the pockets, each estimated to occupy only 1.3% of the Brillouin zone area, is not expected given the absence of long-range broken translational symmetry.

Predicted FL* pocket fraction = $p/8 = 1.25\%$!

Fluctuating AF metal fraction = $p/4 = 2.5\%$.

($p/8$ also in YRZ ansatz, Peter Johnson photoemission, and Jenny Hoffman and Seamus Davis STMs; Stanescu-Kotliar)

Jing-Yu Zhao, S. Chatterjee, S. S., Ya-Hui Zhang, arXiv:2510.13943

Observation of the Yamaji effect in a cuprate superconductor

nature physics

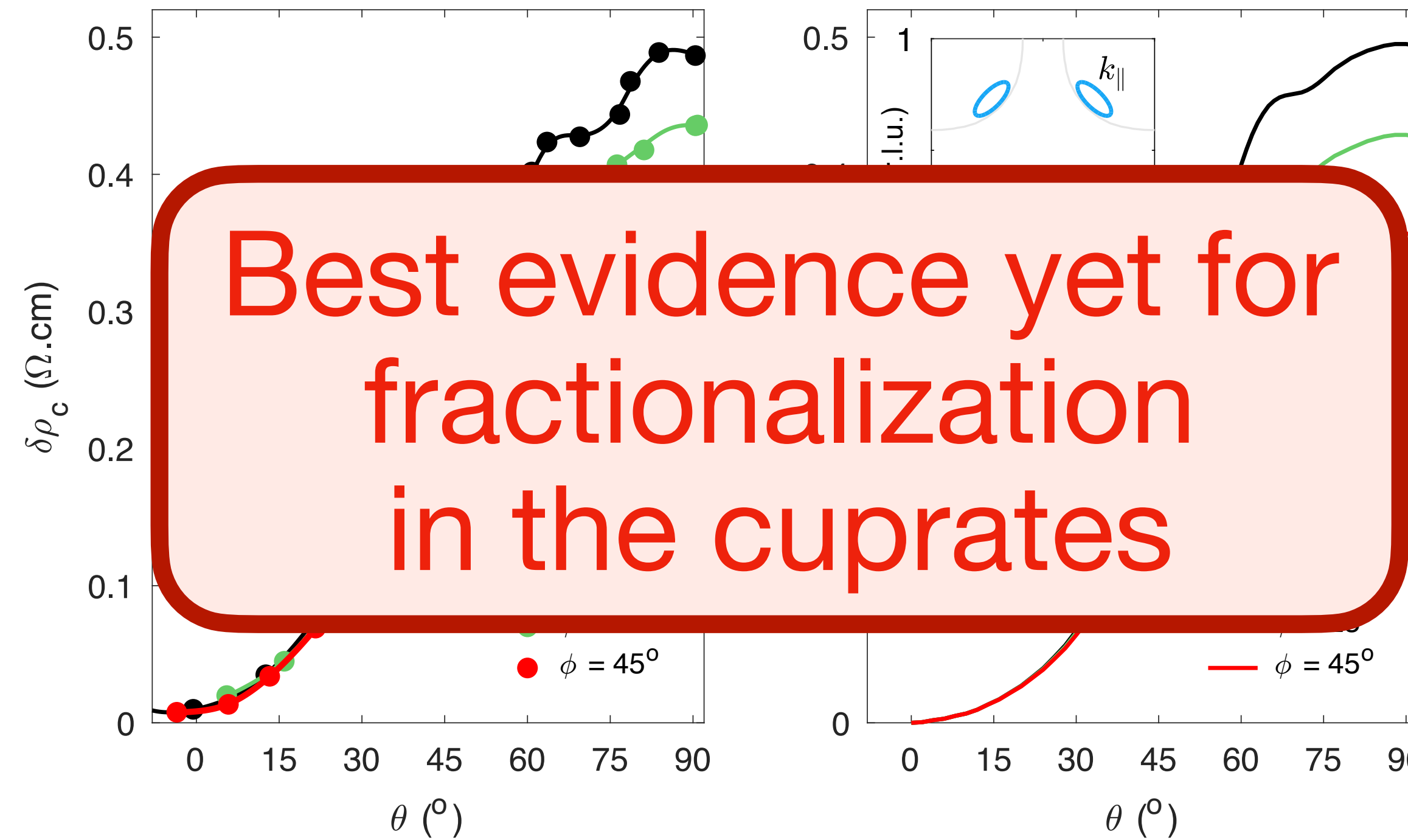
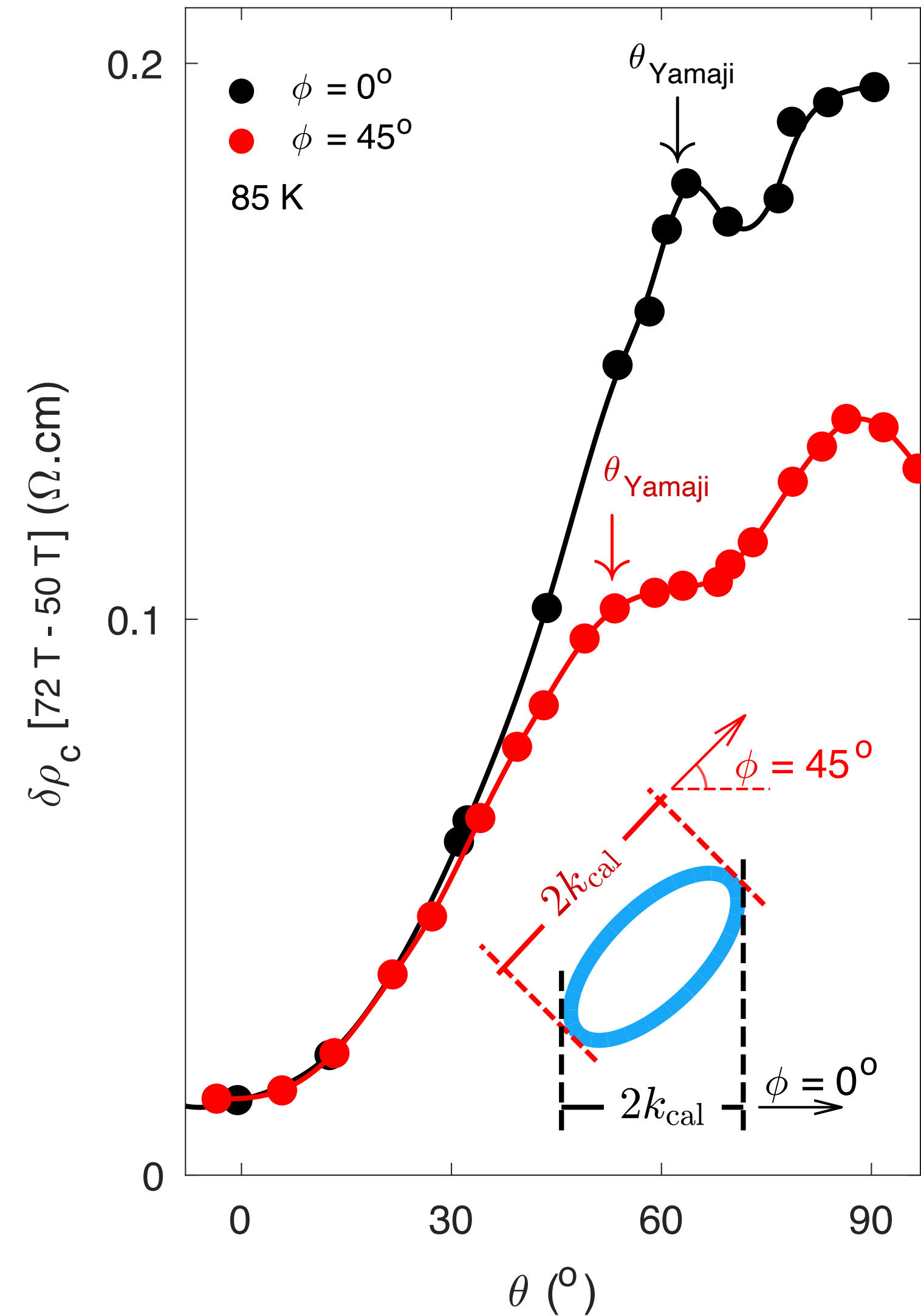
21, 1753 (2025)

superconductor

Mun K. Chan¹, Katherine A. Schreiber¹, Oscar E. Ayala-Valenzuela¹,

Eric D. Bauer², Arkady Shekhter¹ & Neil Harrison¹

Published online: 16 September 2025



Best evidence yet for fractionalization in the cuprates

Doping $p = 0.1$

The observation of the Yamaji peak is evidence for small Fermi-surface pockets in the normal state of the pseudogap phase. The small size of the pockets, each estimated to occupy only 1.3% of the Brillouin zone area, is not expected given the absence of long-range broken translational symmetry.

Predicted FL* pocket fraction = $p/8 = 1.25\%$!

Fluctuating AF metal fraction = $p/4 = 2.5\%$.

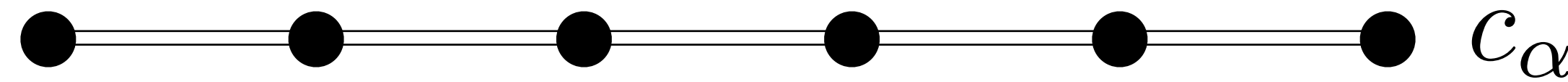
($p/8$ also in YRZ ansatz, Peter Johnson photoemission, and Jenny Hoffman and Seamus Davis STMs; Stanescu-Kotliar)

Jing-Yu Zhao, S. Chatterjee, S. S., Ya-Hui Zhang, arXiv:2510.13943

Ancilla Layer Model (ALM) of FL^*

Ancilla Layer Model of the Hubbard model

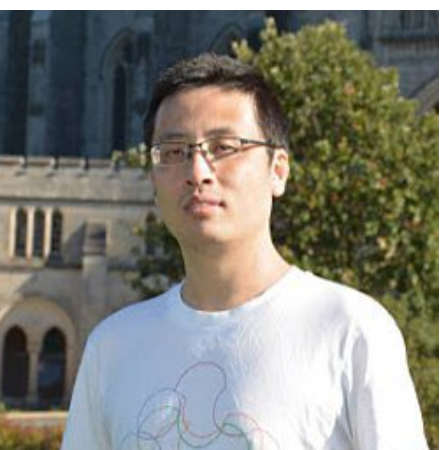
(Foolproof method to satisfy the Oshikawa anomaly)



Hubbard
model of
hole density
 $1+p$

$$\mathcal{H}_{\text{Hubbard}} = - \sum_{i,j} t_{ij} c_{i\alpha}^\dagger c_{j\alpha} + U \sum_i (c_{i\uparrow}^\dagger c_{i\uparrow}) (c_{i\downarrow}^\dagger c_{i\downarrow})$$

Ya-Hui
Zhang

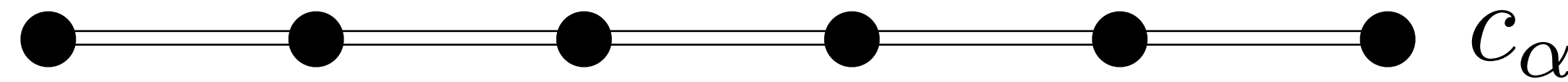


Ya-Hui Zhang and S. S., PRR **2**, 023172 (2020)

A. Nikolaenko, M. Tikhanovskaya, S. S., and Ya-Hui Zhang, PRB **103**, 235138 (2021)

Ancilla Layer Model of the Hubbard model

(Foolproof method to satisfy the Oshikawa anomaly)

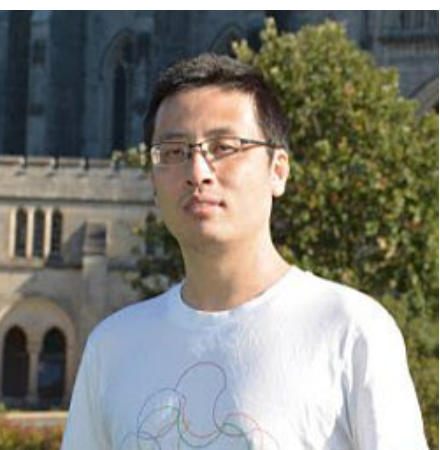


Hubbard
model of
hole density
 $1+p$

$$\mathcal{H}_{\text{Hubbard}} = - \sum_{i,j} t_{ij} c_{i\alpha}^\dagger c_{j\alpha} + \sum_i \left[\frac{3U}{8} \mathcal{P}_i^2 + U \mathcal{P}_i \cdot c_{i\alpha}^\dagger \frac{\boldsymbol{\sigma}_{\alpha\beta}}{2} c_{i\beta} \right].$$

$\mathcal{P}_i \Rightarrow$ Paramagnon

Ya-Hui
Zhang

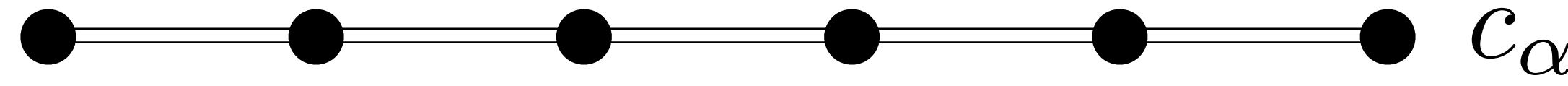


Ya-Hui Zhang and S. S., PRR **2**, 023172 (2020)

A. Nikolaenko, M. Tikhanovskaya, S. S., and Ya-Hui Zhang, PRB **103**, 235138 (2021)

Ancilla Layer Model of the Hubbard model

(Foolproof method to satisfy the Oshikawa anomaly)

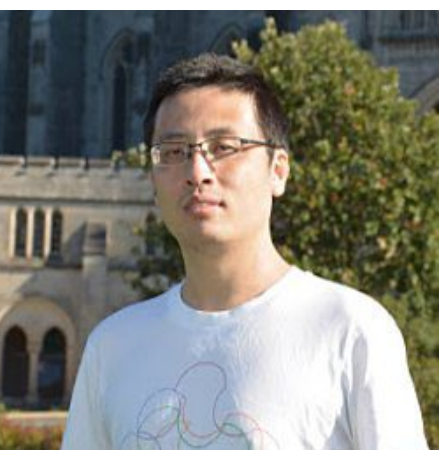


Hubbard
model of
hole density
 $1+p$

$$\mathcal{H}_{\text{Hubbard}} = - \sum_{i,j} t_{ij} c_{i\alpha}^\dagger c_{j\alpha} + \sum_i \left[\frac{3U}{8} \mathcal{P}_i^2 + U \mathcal{P}_i \cdot c_{i\alpha}^\dagger \frac{\boldsymbol{\sigma}_{\alpha\beta}}{2} c_{i\beta} + \frac{m\mathcal{P}}{2} (\partial_\tau \mathcal{P}_i)^2 \right].$$

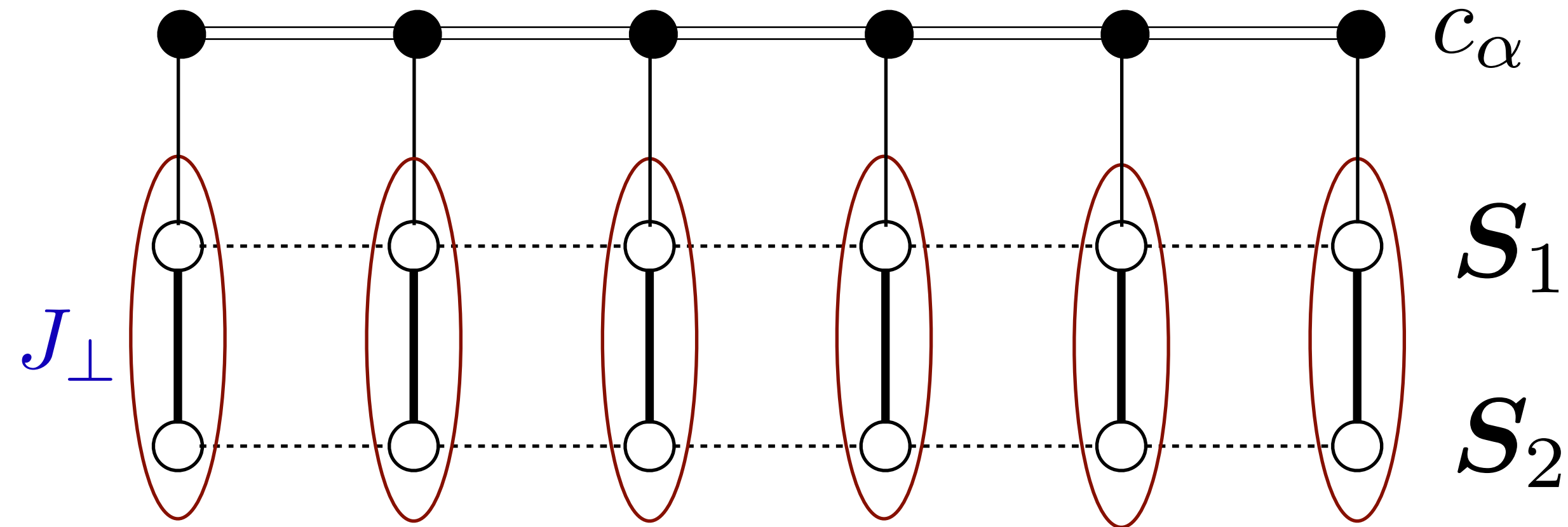
$\mathcal{P}_i \Rightarrow$ Paramagnon

Ya-Hui
Zhang



Ancilla Layer Model of the Hubbard model

(Foolproof method to satisfy the Oshikawa anomaly)



Free holes of density $1+p$

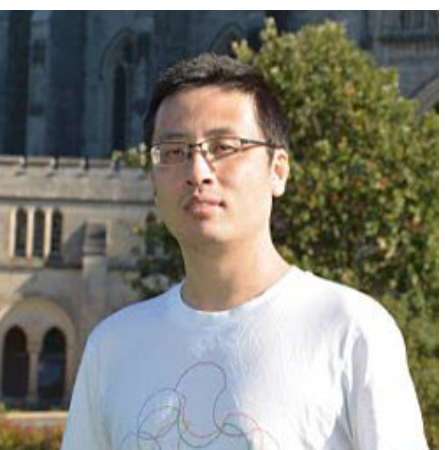
$$\mathcal{H}_{\text{Hubbard}} = - \sum_{i,j} t_{ij} c_{i\alpha}^\dagger c_{j\alpha} + \sum_i \left[\frac{3U}{8} \mathcal{P}_i^2 + U \mathcal{P}_i \cdot c_{i\alpha}^\dagger \frac{\boldsymbol{\sigma}_{\alpha\beta}}{2} c_{i\beta} + \frac{m\mathcal{P}}{2} (\partial_\tau \mathcal{P}_i)^2 \right]$$

3 \mathcal{P} oscillators' states: $|0, 0, 0\rangle, |1, 0, 0\rangle, |0, 1, 0\rangle, |0, 0, 1\rangle$

$\mathcal{S}_{1,2}$ ancilla qubits states : $(|\uparrow\downarrow\rangle - |\downarrow\uparrow\rangle)/\sqrt{2}, |\uparrow\uparrow\rangle, (|\uparrow\downarrow\rangle + |\downarrow\uparrow\rangle)/\sqrt{2}, |\downarrow\downarrow\rangle$

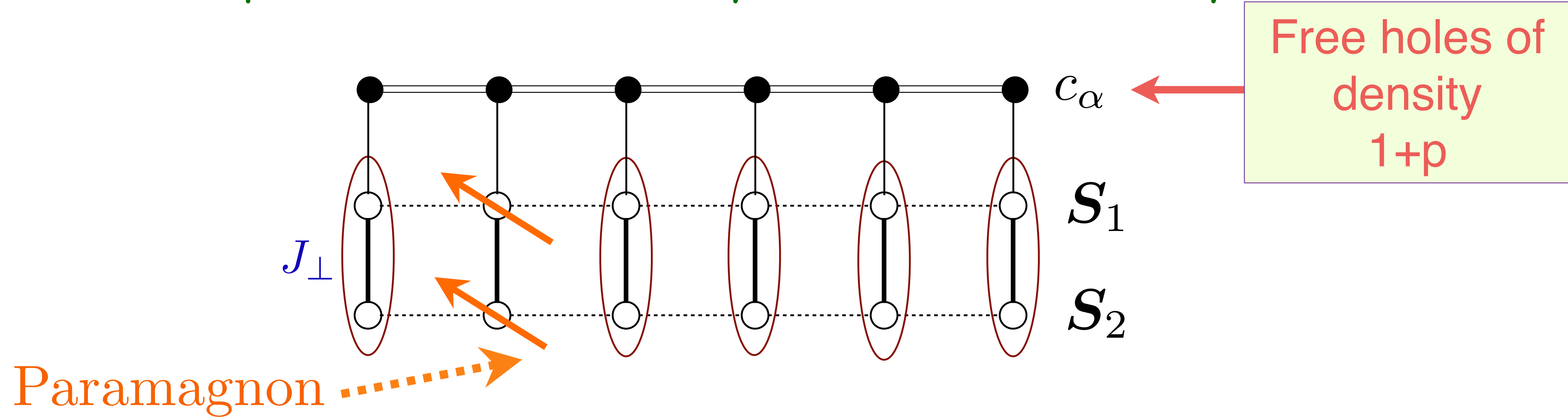
$$\mathcal{P} \sim \mathcal{S}_1 - \mathcal{S}_2$$

Ya-Hui
Zhang



Ancilla Layer Model of the Hubbard model

(Foolproof method to satisfy the Oshikawa anomaly)



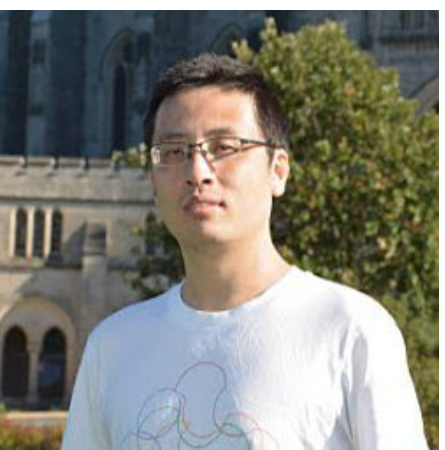
$$\mathcal{H}_{\text{Hubbard}} = - \sum_{i,j} t_{ij} c_{i\alpha}^\dagger c_{j\alpha} + \sum_i \left[\frac{3U}{8} \mathcal{P}_i^2 + U \mathcal{P}_i \cdot c_{i\alpha}^\dagger \frac{\boldsymbol{\sigma}_{\alpha\beta}}{2} c_{i\beta} + \frac{m\mathcal{P}}{2} (\partial_\tau \mathcal{P}_i)^2 \right]$$

3 \mathcal{P} oscillators' states: $|0, 0, 0\rangle, |1, 0, 0\rangle, |0, 1, 0\rangle, |0, 0, 1\rangle$

$\mathcal{S}_{1,2}$ ancilla qubits states : $(|\uparrow\downarrow\rangle - |\downarrow\uparrow\rangle)/\sqrt{2}, |\uparrow\uparrow\rangle, (|\uparrow\downarrow\rangle + |\downarrow\uparrow\rangle)/\sqrt{2}, |\downarrow\downarrow\rangle$

$$\mathcal{P} \sim \mathcal{S}_1 - \mathcal{S}_2$$

Ya-Hui
Zhang

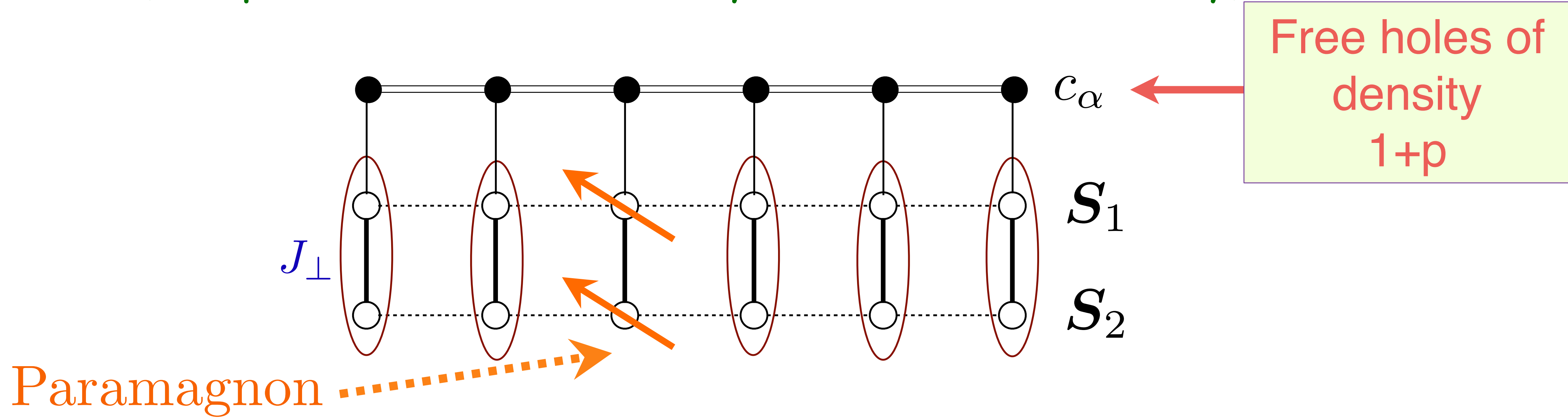


Ya-Hui Zhang and S. S., PRR **2**, 023172 (2020)

A. Nikolaenko, M. Tikhanovskaya, S. S., and Ya-Hui Zhang, PRB **103**, 235138 (2021)

Ancilla Layer Model of the Hubbard model

(Foolproof method to satisfy the Oshikawa anomaly)



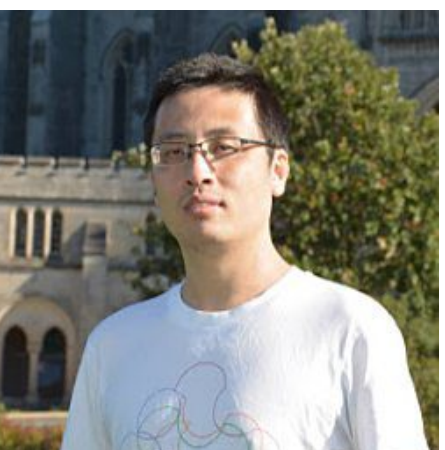
$$\mathcal{H}_{\text{Hubbard}} = - \sum_{i,j} t_{ij} c_{i\alpha}^\dagger c_{j\alpha} + \sum_i \left[\frac{3U}{8} \mathcal{P}_i^2 + U \mathcal{P}_i \cdot c_{i\alpha}^\dagger \frac{\boldsymbol{\sigma}_{\alpha\beta}}{2} c_{i\beta} + \frac{m\mathcal{P}}{2} (\partial_\tau \mathcal{P}_i)^2 \right]$$

3 \mathcal{P} oscillators' states: $|0, 0, 0\rangle, |1, 0, 0\rangle, |0, 1, 0\rangle, |0, 0, 1\rangle$

$\mathcal{S}_{1,2}$ ancilla qubits states : $(|\uparrow\downarrow\rangle - |\downarrow\uparrow\rangle)/\sqrt{2}, |\uparrow\uparrow\rangle, (|\uparrow\downarrow\rangle + |\downarrow\uparrow\rangle)/\sqrt{2}, |\downarrow\downarrow\rangle$

$$\mathcal{P} \sim \mathcal{S}_1 - \mathcal{S}_2$$

Ya-Hui
Zhang

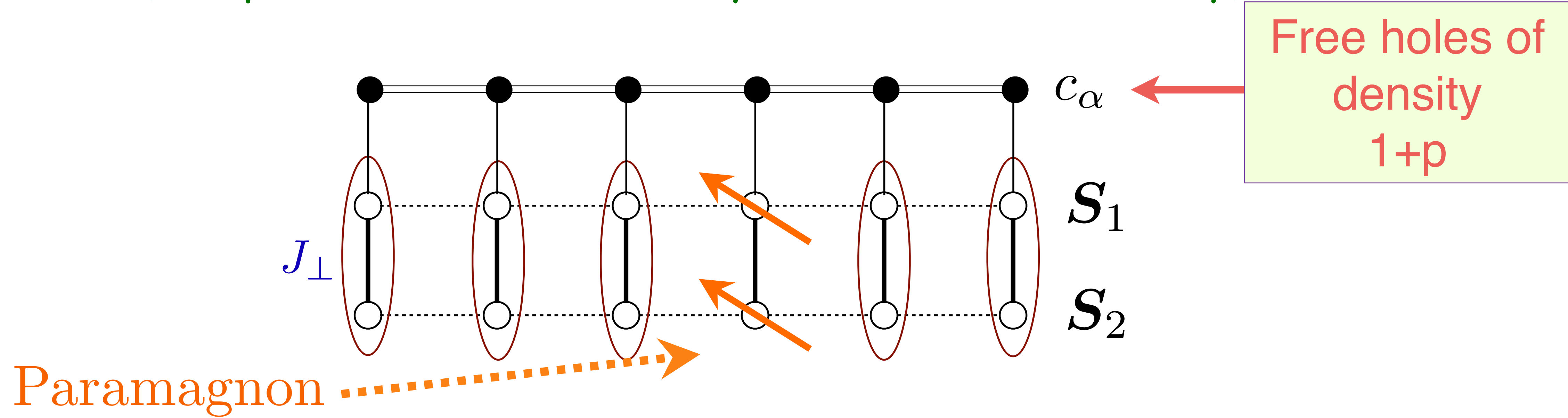


Ya-Hui Zhang and S. S., PRR **2**, 023172 (2020)

A. Nikolaenko, M. Tikhanovskaya, S. S., and Ya-Hui Zhang, PRB **103**, 235138 (2021)

Ancilla Layer Model of the Hubbard model

(Foolproof method to satisfy the Oshikawa anomaly)



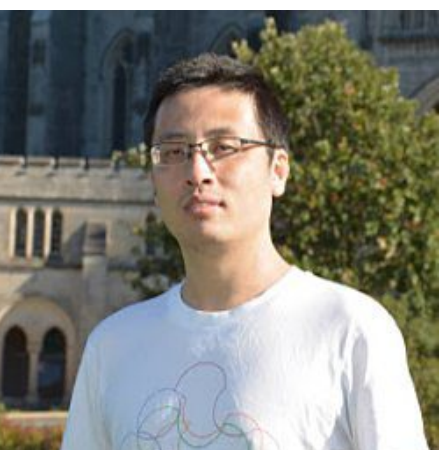
$$\mathcal{H}_{\text{Hubbard}} = - \sum_{i,j} t_{ij} c_{i\alpha}^\dagger c_{j\alpha} + \sum_i \left[\frac{3U}{8} \mathcal{P}_i^2 + U \mathcal{P}_i \cdot c_{i\alpha}^\dagger \frac{\boldsymbol{\sigma}_{\alpha\beta}}{2} c_{i\beta} + \frac{m\mathcal{P}}{2} (\partial_\tau \mathcal{P}_i)^2 \right]$$

3 \mathcal{P} oscillators' states: $|0, 0, 0\rangle, |1, 0, 0\rangle, |0, 1, 0\rangle, |0, 0, 1\rangle$

$\mathbf{S}_{1,2}$ ancilla qubits states : $(|\uparrow\downarrow\rangle - |\downarrow\uparrow\rangle)/\sqrt{2}, |\uparrow\uparrow\rangle, (|\uparrow\downarrow\rangle + |\downarrow\uparrow\rangle)/\sqrt{2}, |\downarrow\downarrow\rangle$

$$\mathcal{P} \sim \mathbf{S}_1 - \mathbf{S}_2$$

Ya-Hui
Zhang



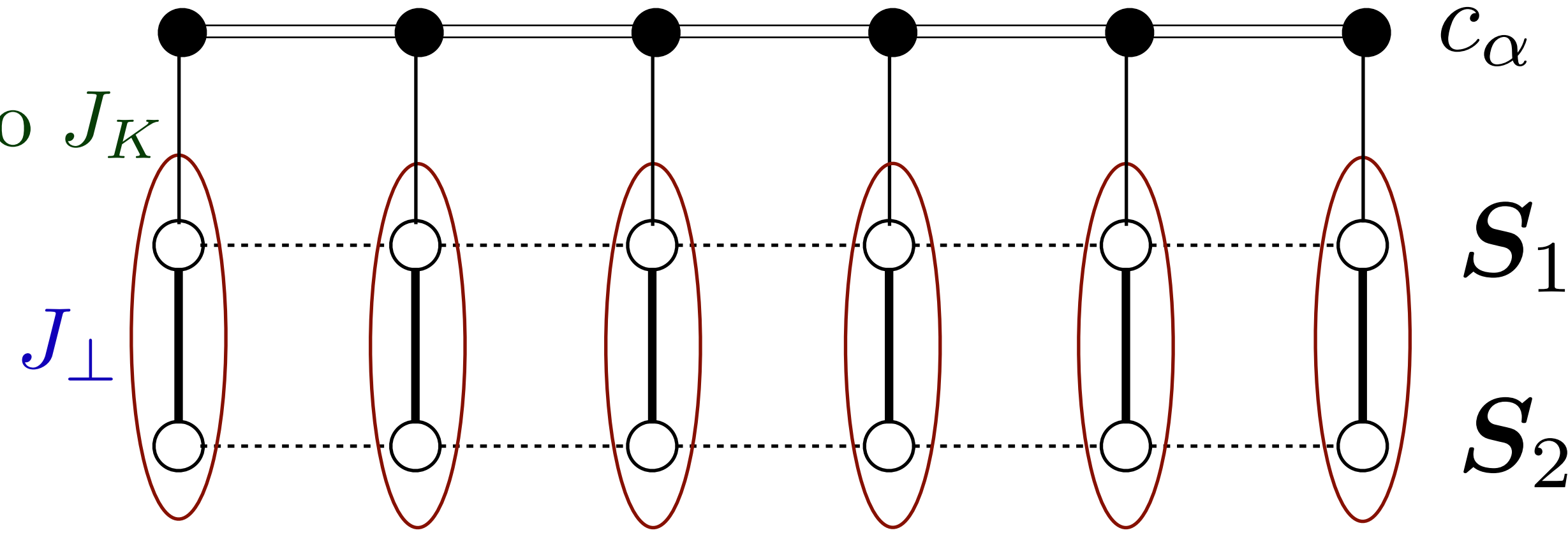
Ya-Hui Zhang and S. S., PRR **2**, 023172 (2020)

A. Nikolaenko, M. Tikhanovskaya, S. S., and Ya-Hui Zhang, PRB **103**, 235138 (2021)

Ancilla Layer Model of the Hubbard model

(Foolproof method to satisfy the Oshikawa anomaly)

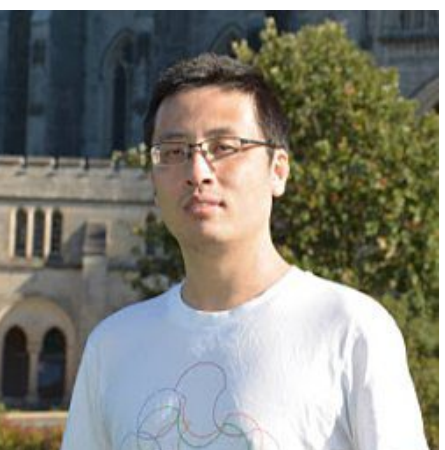
Antiferromagnetic Kondo J_K



Free holes of density $1+p$

$$\mathcal{H}_{\text{ALM}} = - \sum_{i,j} t_{ij} c_{i\alpha}^\dagger c_{j\alpha} + \sum_i \frac{J_K}{2} \mathbf{S}_{1i} \cdot c_{i\alpha}^\dagger \boldsymbol{\sigma}_{\alpha\beta} c_{i\beta} + J_\perp \sum_i \mathbf{S}_{1i} \cdot \mathbf{S}_{2i} .$$

Ya-Hui
Zhang



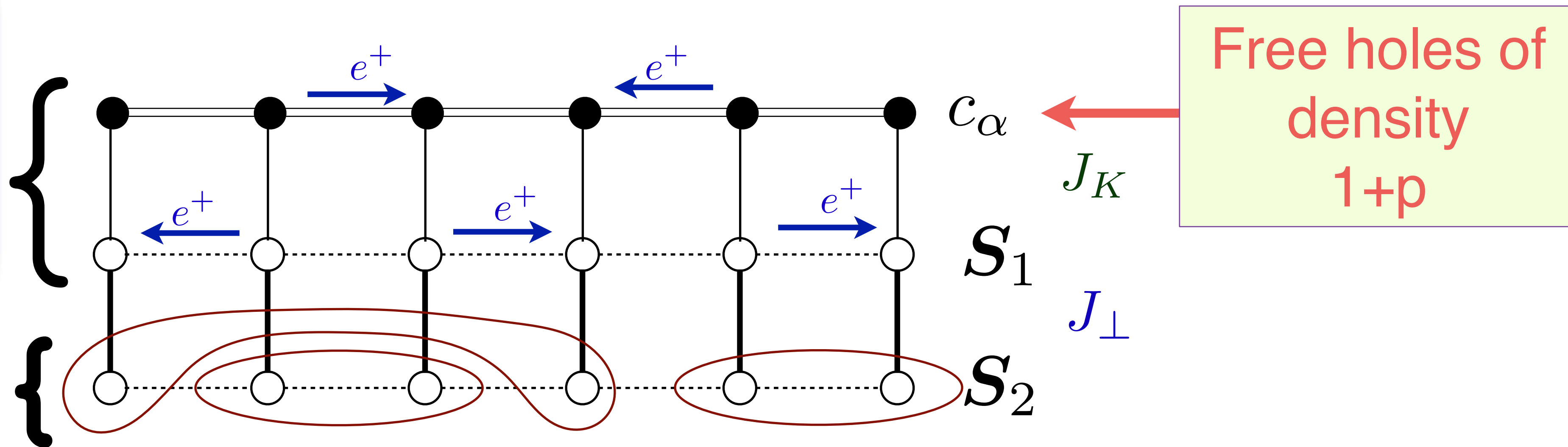
Ya-Hui Zhang and S. S., PRR **2**, 023172 (2020)

A. Nikolaenko, M. Tikhanovskaya, S. S., and Ya-Hui Zhang, PRB **103**, 235138 (2021)

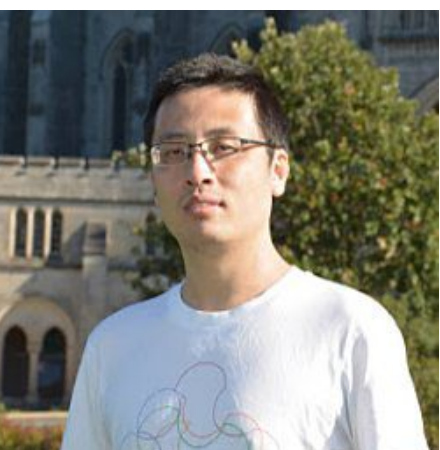
ALM of FL* of Hubbard model

Kondo lattice heavy Fermi liquid.
Area $(1 + p + 1)/2 = p/2 \pmod{1}$.
Small Fermi surface!

Your favorite spin liquid



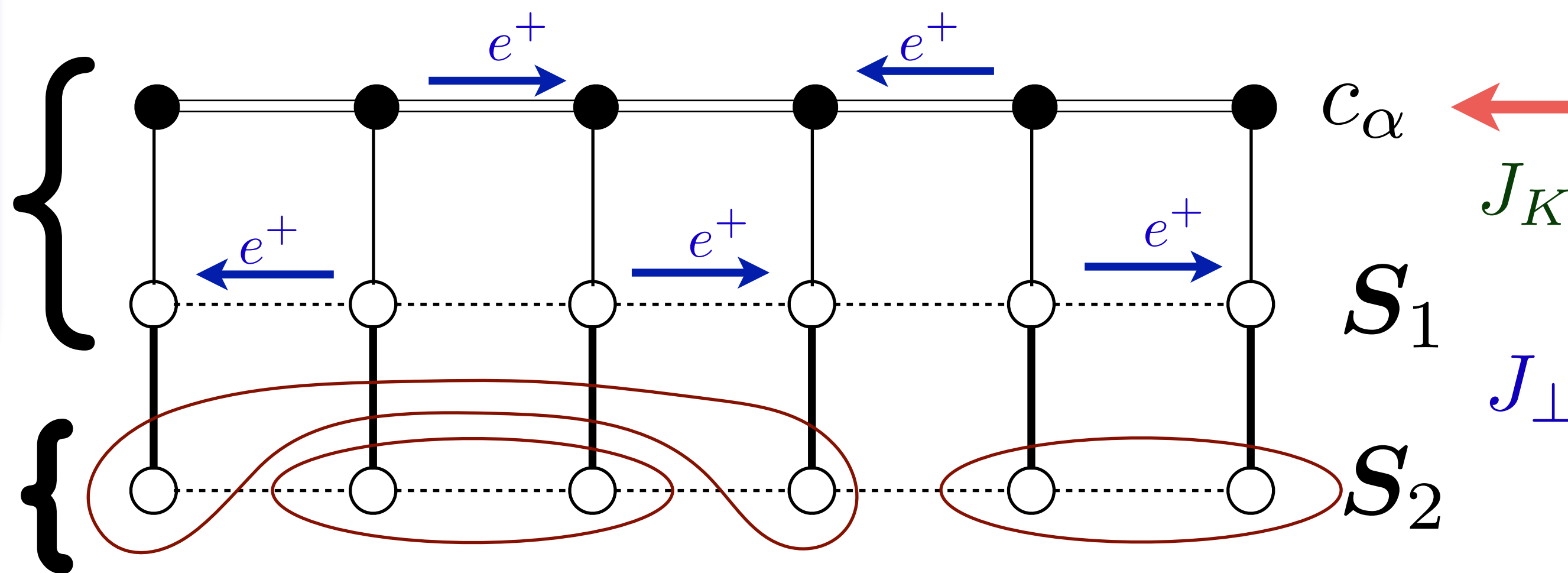
Ya-Hui
Zhang



ALM of FL* of Hubbard model

Kondo lattice heavy Fermi liquid.
 Area $(1 + p + 1)/2 = p/2 \pmod{1}$.
Small Fermi surface!

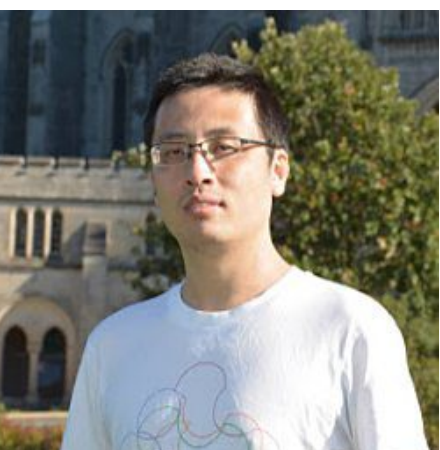
Your favorite spin liquid



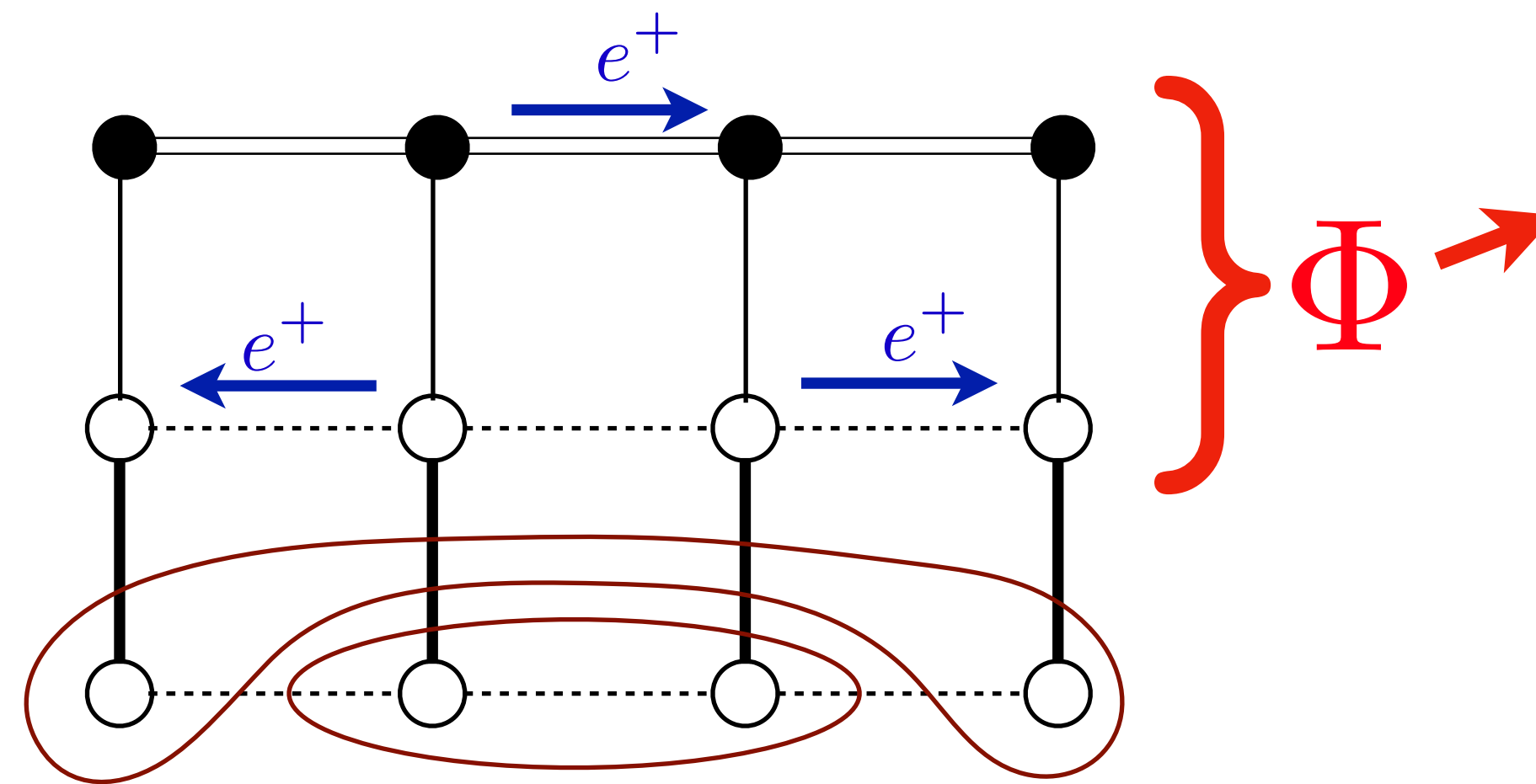
Free holes of density $1+p$

Kondo Lattice FL of c_α and S_1
 Pseudogap metal = \oplus
 Spin Liquid of S_2

Ya-Hui Zhang



Ancilla Layer Model of the Hubbard model

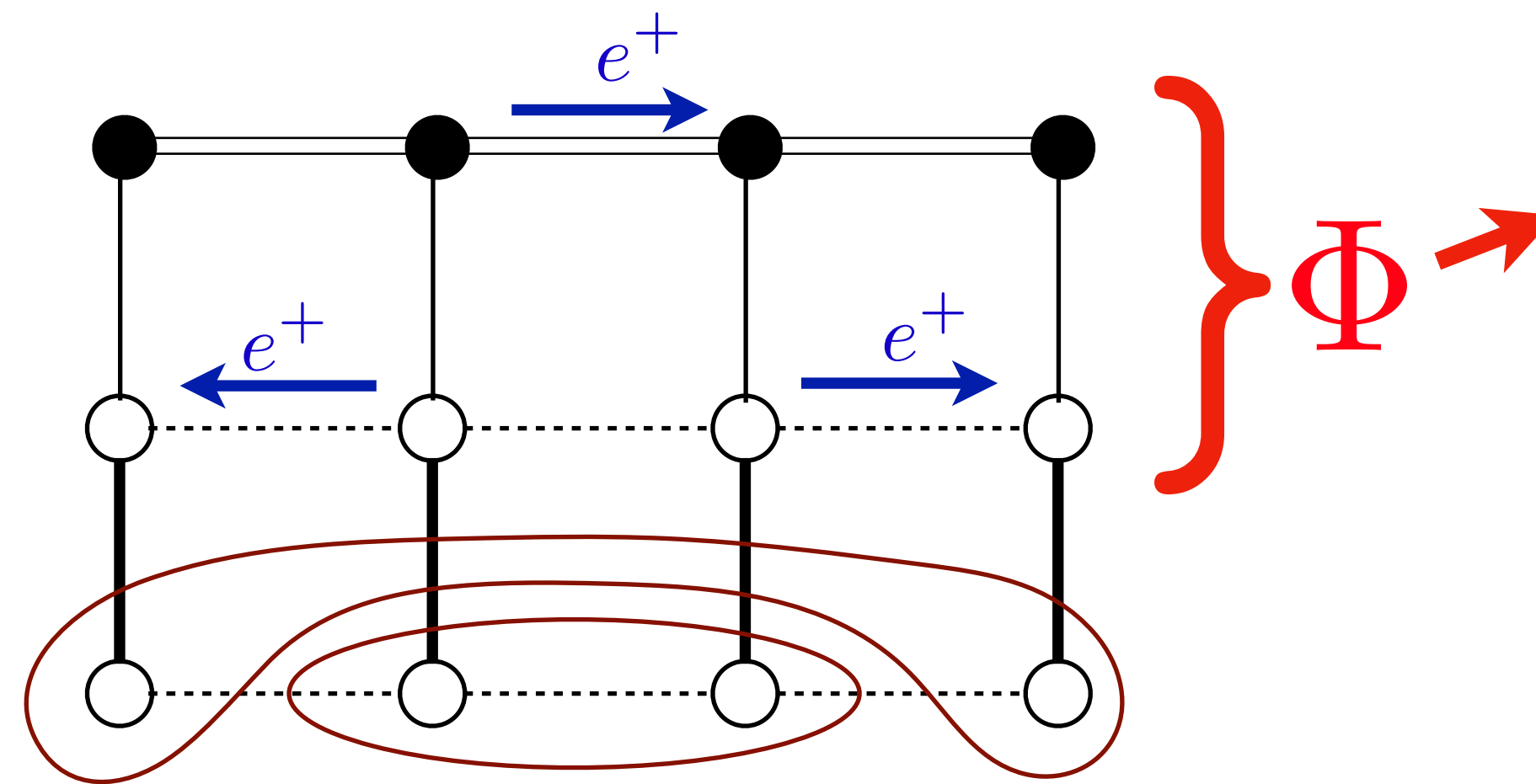


Higgs field Φ determines the pseudogap.
In FL* $\langle \Phi \rangle \neq 0$, antinodal pseudogap is determined by $\langle \Phi \rangle$, and electrons c_α are in 4 area $p/8$ hole pockets.

$|\text{FL}^*\rangle =$

$|\text{Slater determinant of top two layers with hybridization } \Phi\rangle$

Ancilla Layer Model of the Hubbard model



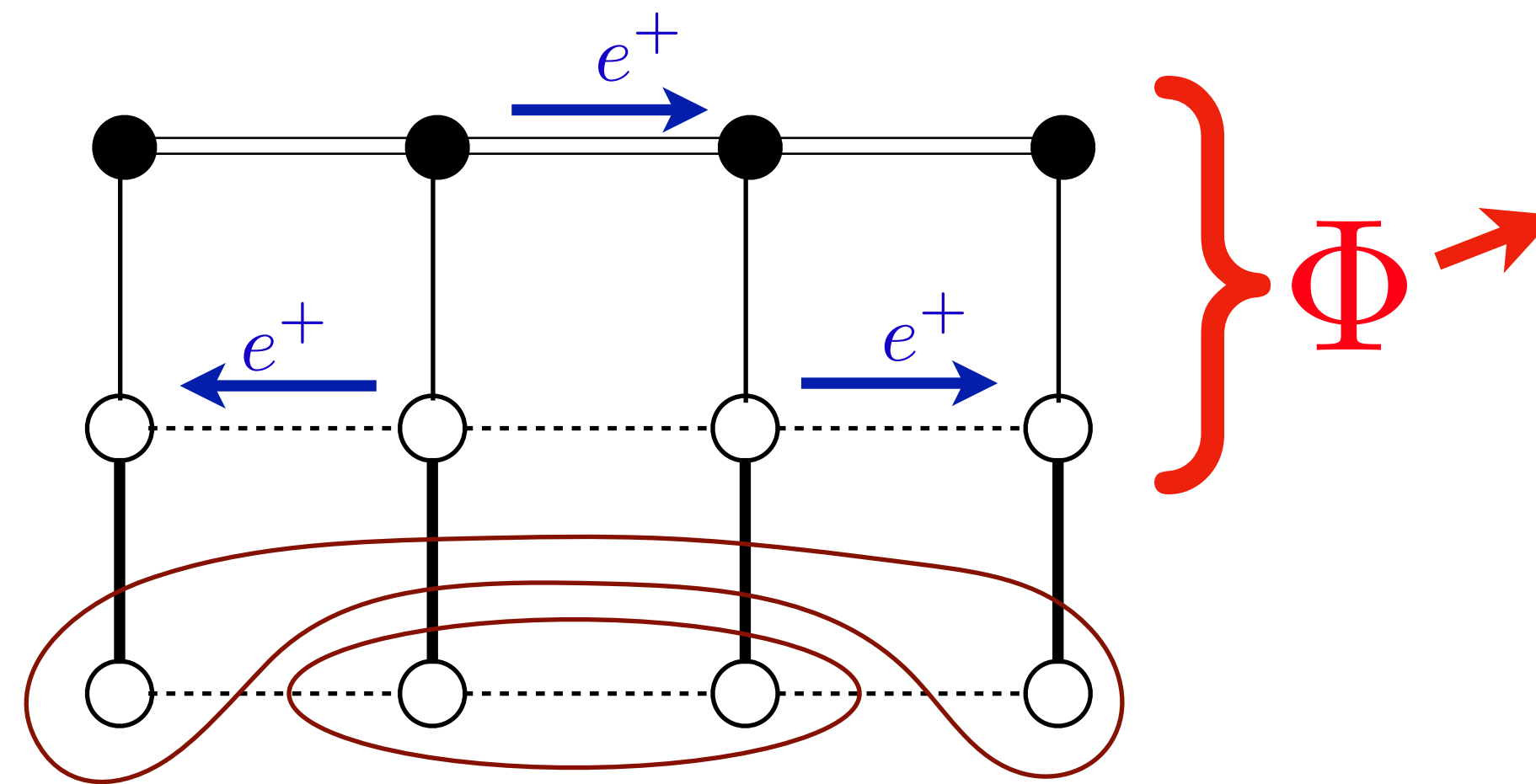
Higgs field Φ determines the pseudogap.
 In FL* $\langle \Phi \rangle \neq 0$, antinodal pseudogap is determined by $\langle \Phi \rangle$, and electrons c_α are in 4 area $p/8$ hole pockets.

- Spinons f_α in bottom layer are in a π -flux spin liquid

$|\text{FL}^*\rangle =$

\boxtimes |Slater determinant of top two layers with hybridization Φ
 \otimes |Slater determinant to spinons f_α

Ancilla Layer Model of the Hubbard model



Higgs field Φ determines the pseudogap.
 In FL* $\langle \Phi \rangle \neq 0$, antinodal pseudogap is determined by $\langle \Phi \rangle$, and electrons c_α are in 4 area $p/8$ hole pockets.

- Spinons f_α in bottom layer are in a π -flux spin liquid

$|\text{FL}^*\rangle = [\text{Projection onto rung singlets of } \mathcal{S}_1, \mathcal{S}_2]$

\boxtimes |Slater determinant of top two layers with hybridization Φ

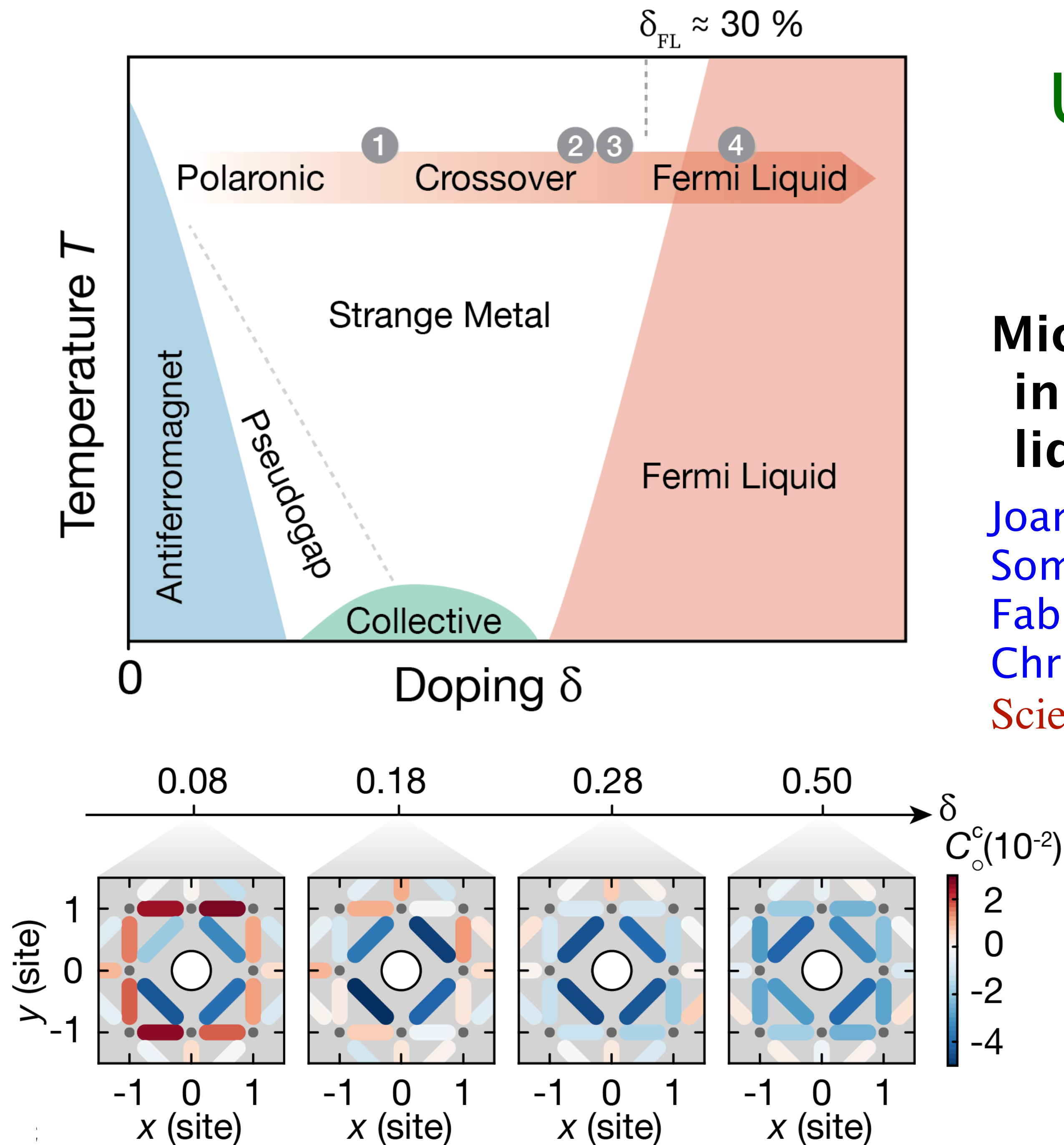
\otimes |Slater determinant to spinons f_α

Ultracold fermionic atoms in optical lattices

Microscopic evolution of doped Mott insulators from polaronic metal to Fermi liquid

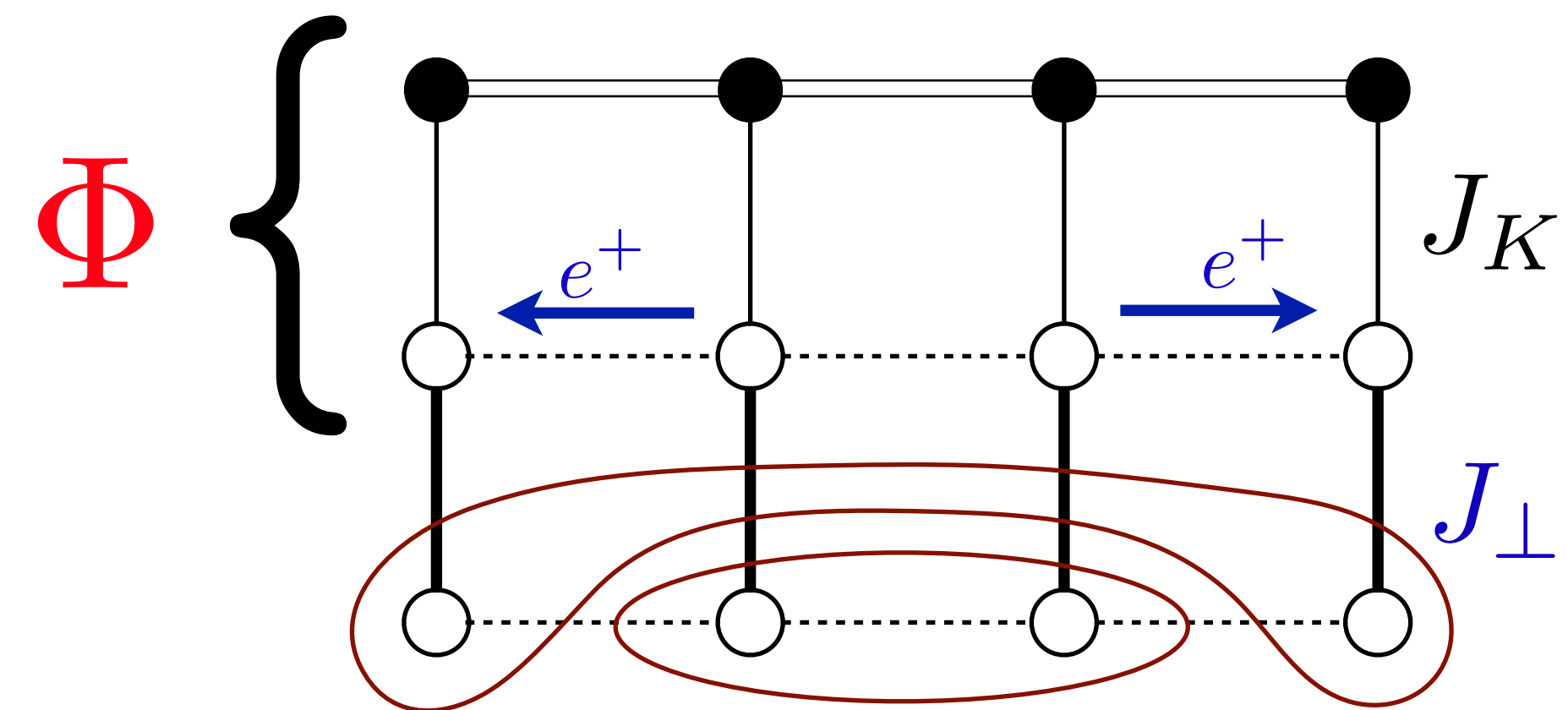
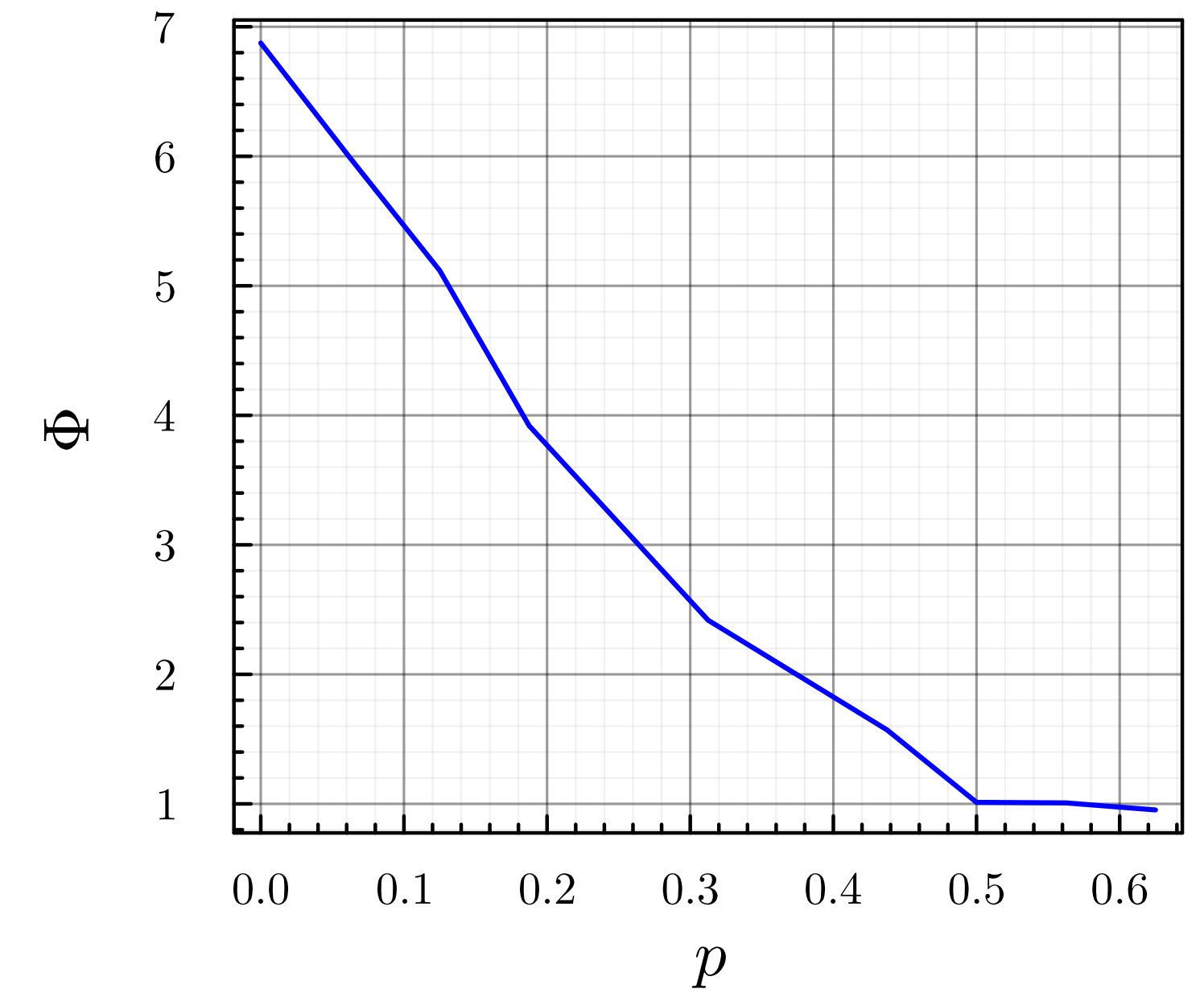
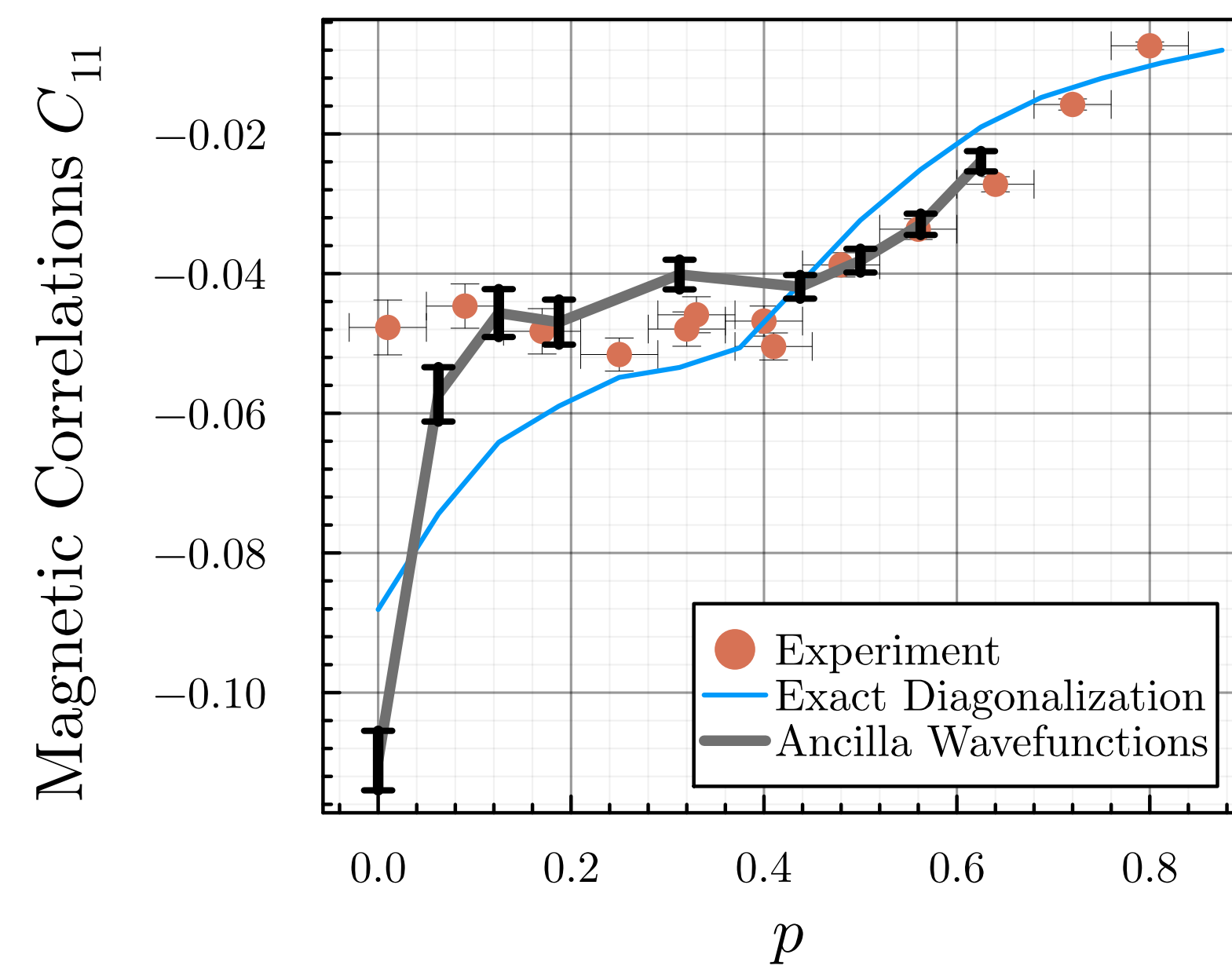
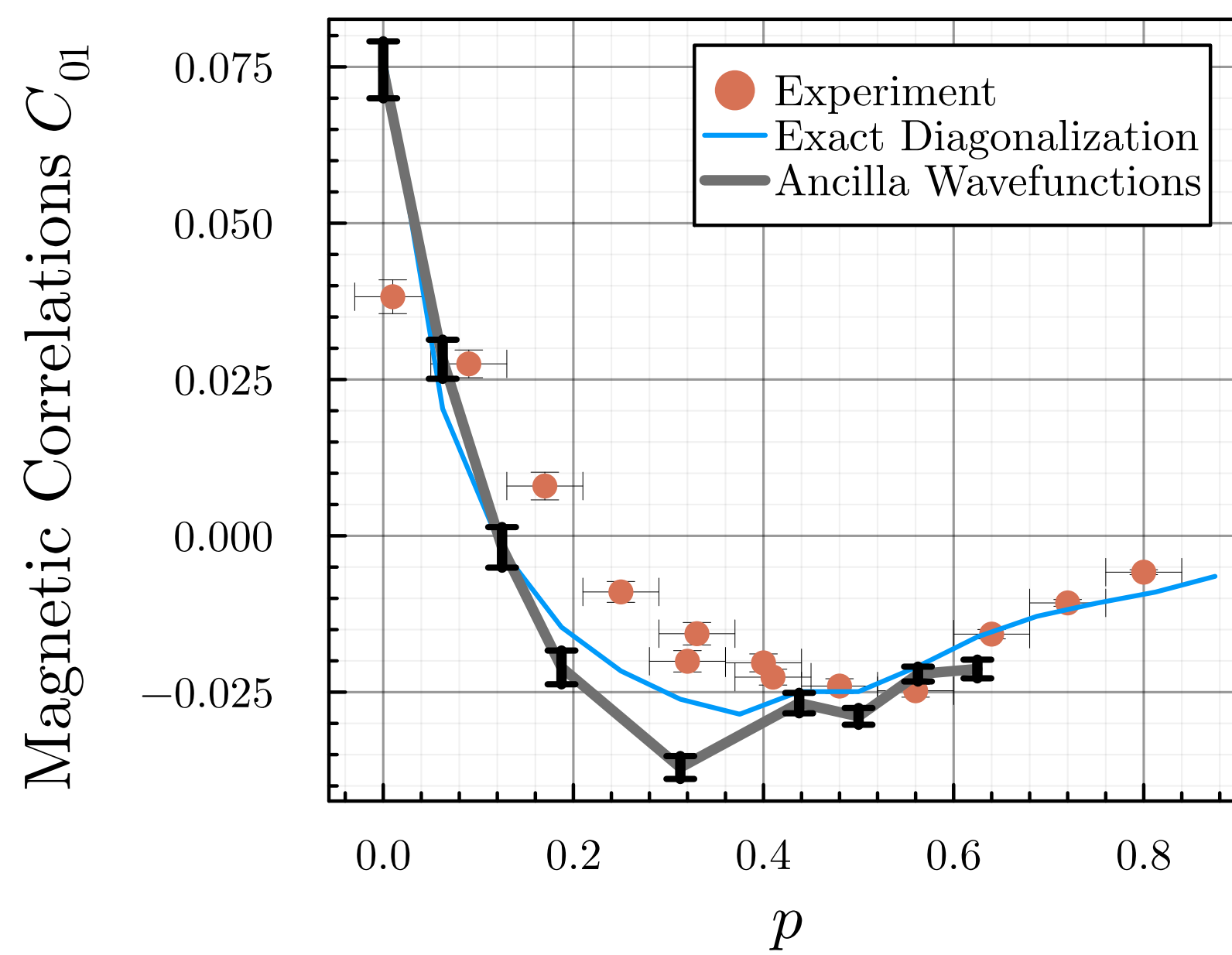
Joannis Koepsell, Dominik Bourgund, Pimonpan Sompet, Sarah Hirthe, Annabelle Bohrdt, Yao Wang, Fabian Grusdt, Eugene Demler, Guillaume Salomon, Christian Gross, Immanuel Bloch

Science **374** (2021) 82



Max Planck Institute of
Quantum Optics,
Garching

Trial wavefunction for FL* of Hubbard model

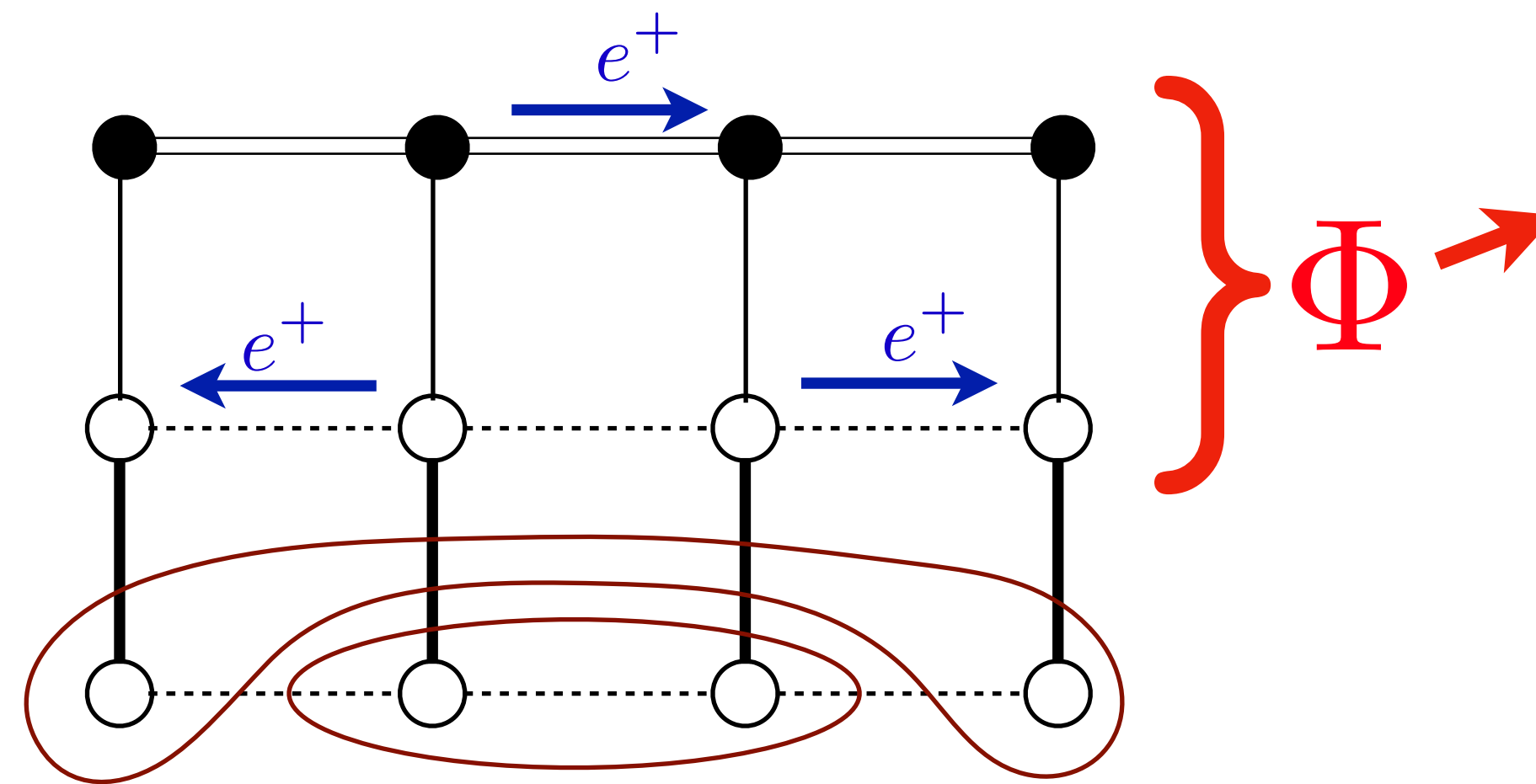


L. Shackleton and Shiwei Zhang, arXiv:2408.02190

Tobias Müller, Yasir Iqbal, S.S., Ronny Thomale, PNAS **122**, e2504261122 (2025)

From FL^* to
d-wave superconductivity
and charge order
in the ALM

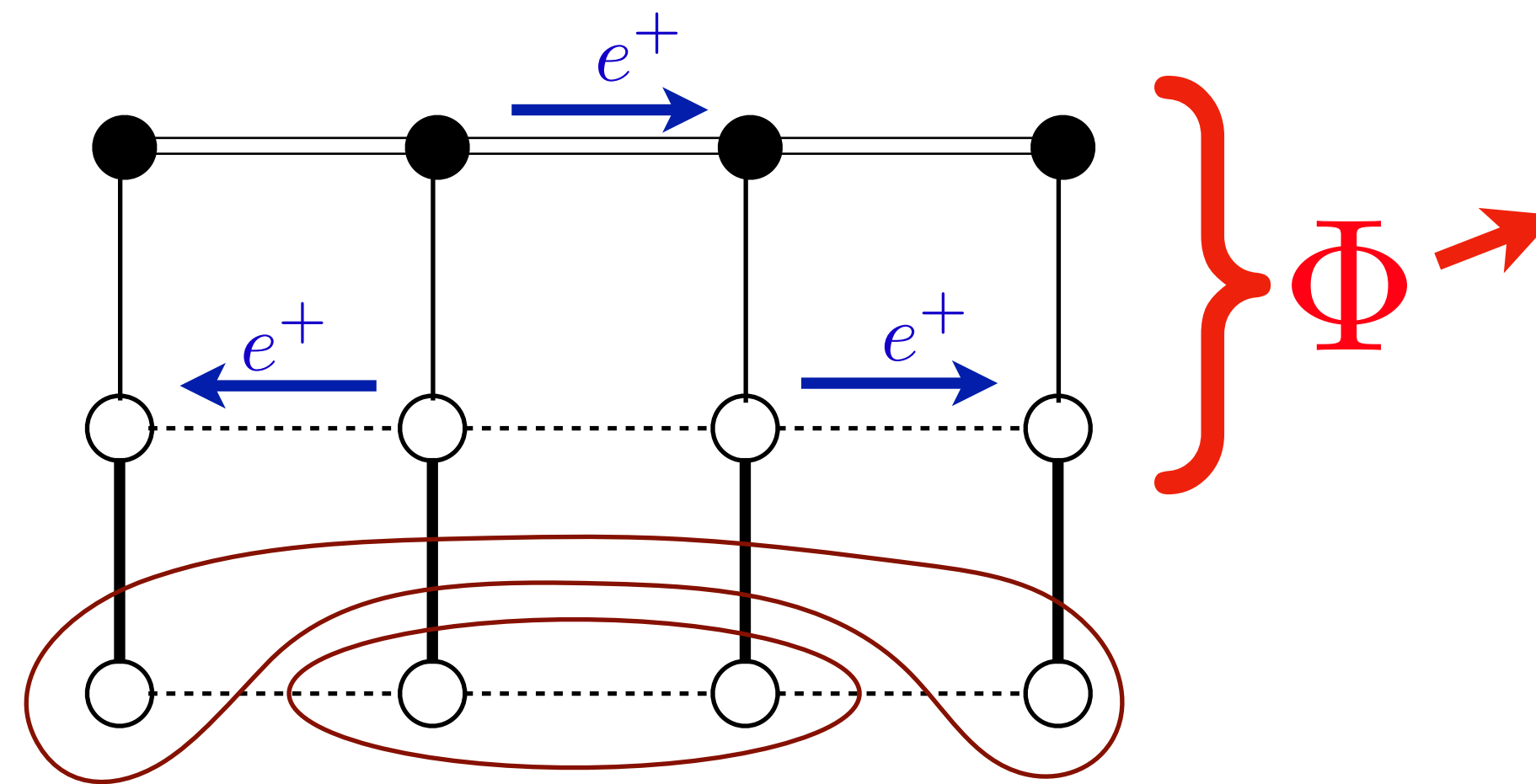
Ancilla Layer Model of the Hubbard model



Higgs field Φ determines the pseudogap.
In FL* $\langle \Phi \rangle \neq 0$, antinodal pseudogap is determined by $\langle \Phi \rangle$, and electrons c_α are in 4 area $p/8$ hole pockets.

- Spinons f_α in bottom layer are in a π -flux spin liquid

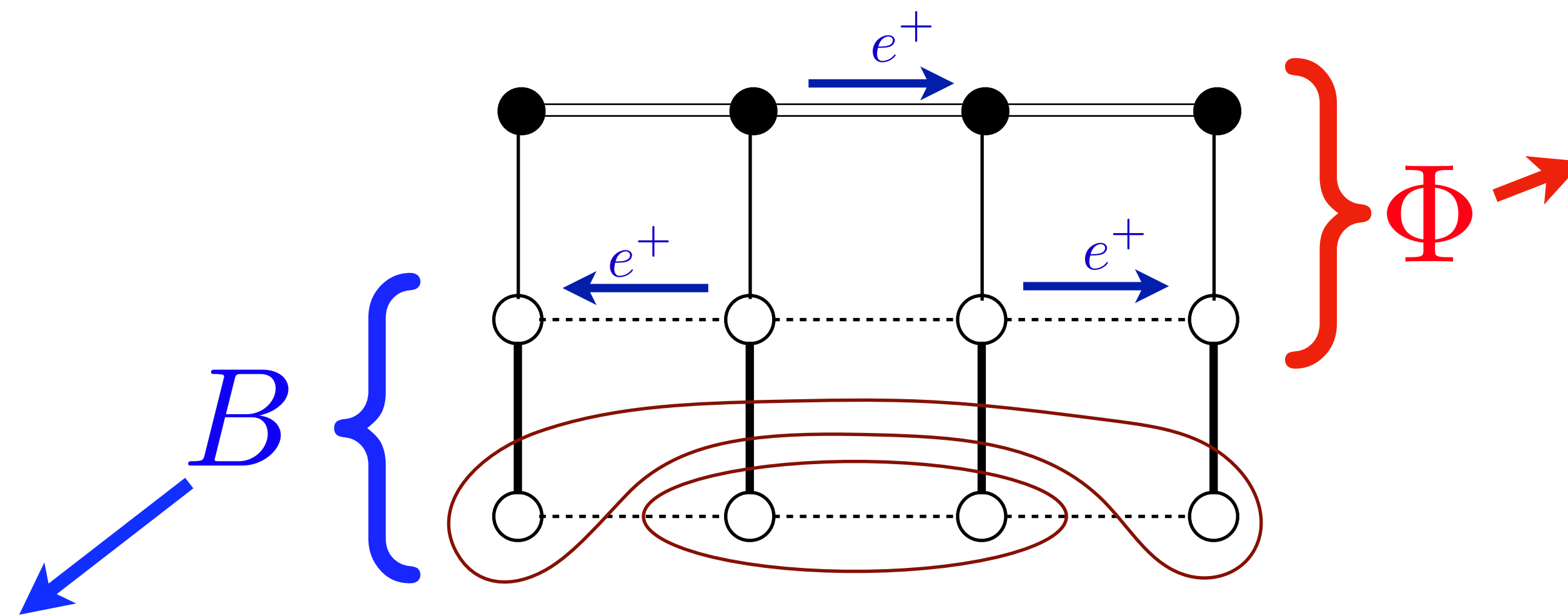
Ancilla Layer Model of the Hubbard model



Higgs field Φ determines the pseudogap.
In FL* $\langle \Phi \rangle \neq 0$, antinodal pseudogap is determined by $\langle \Phi \rangle$, and electrons c_α are in 4 area $p/8$ hole pockets.

- Spinons f_α in bottom layer are in a π -flux spin liquid with a SU(2) gauge field U .

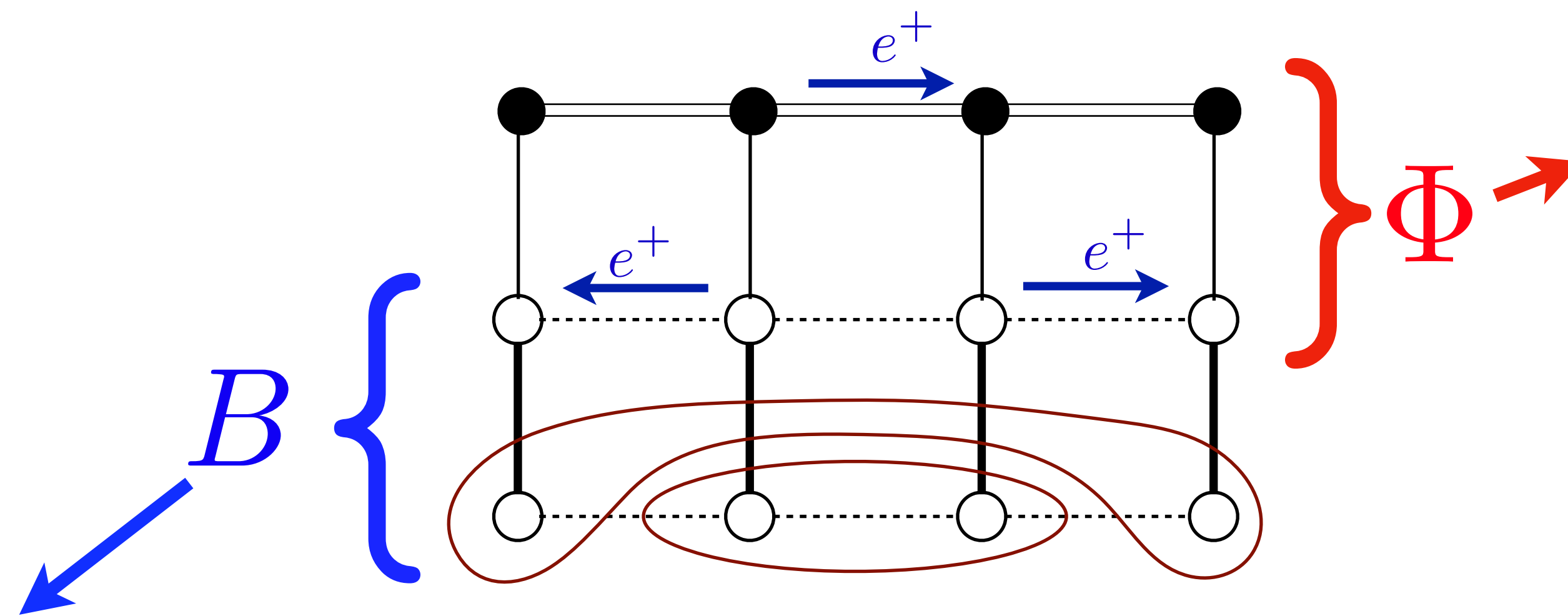
Ancilla Layer Model of the Hubbard model



Higgs field Φ determines the pseudogap.
In FL* $\langle \Phi \rangle \neq 0$, antinodal pseudogap is determined by $\langle \Phi \rangle$, and electrons c_α are in 4 area $p/8$ hole pockets.

- Spinons f_α in bottom layer are in a π -flux spin liquid with a SU(2) gauge field U .
- Higgs boson B has charge e , and is a SU(2) fundamental.

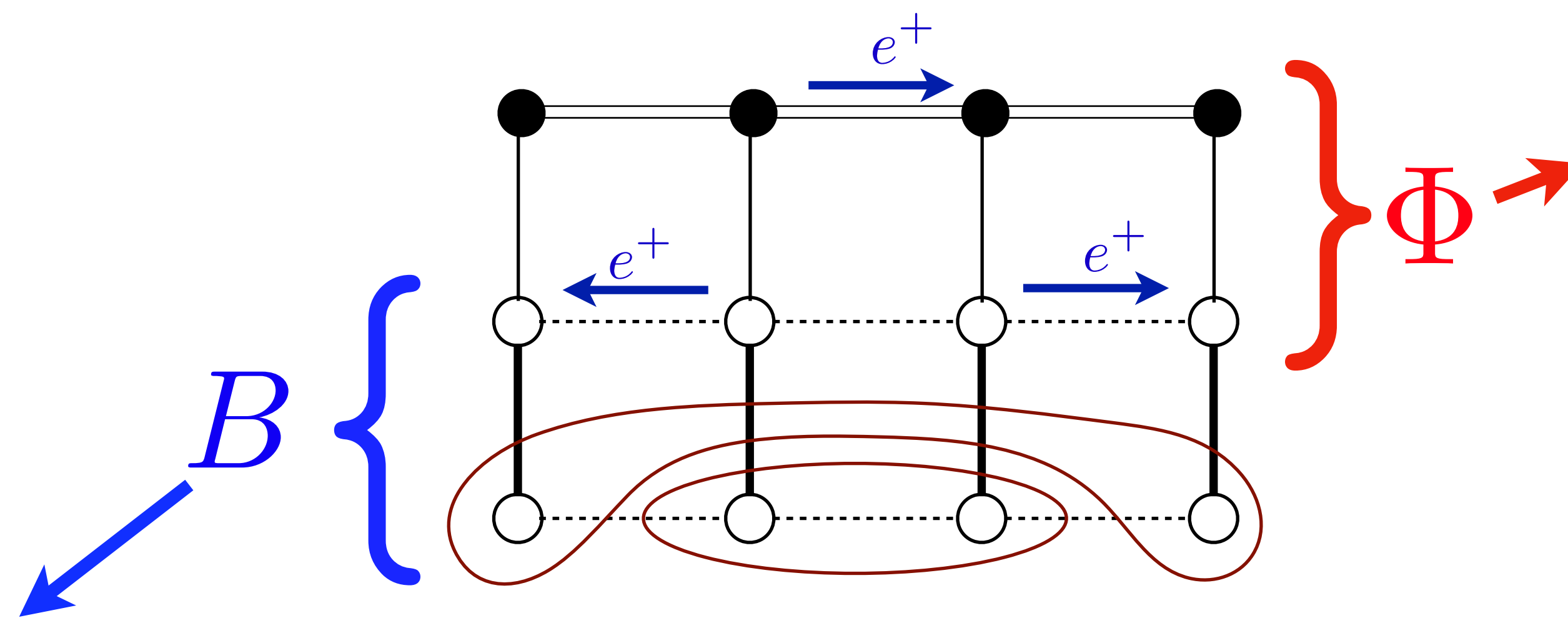
Ancilla Layer Model of the Hubbard model



Higgs field Φ determines the pseudogap.
In FL* $\langle \Phi \rangle \neq 0$, antinodal pseudogap is determined by $\langle \Phi \rangle$, and electrons c_α are in 4 area $p/8$ hole pockets.

- Spinons f_α in bottom layer are in a π -flux spin liquid with a SU(2) gauge field U .
- Higgs boson B has charge e , and is a SU(2) fundamental.
- Yukawa coupling between c_α , f_α and B .

Ancilla Layer Model of the Hubbard model



Higgs field Φ determines the pseudogap.
In FL* $\langle \Phi \rangle \neq 0$, antinodal pseudogap is determined by $\langle \Phi \rangle$, and electrons c_α are in 4 area $p/8$ hole pockets.

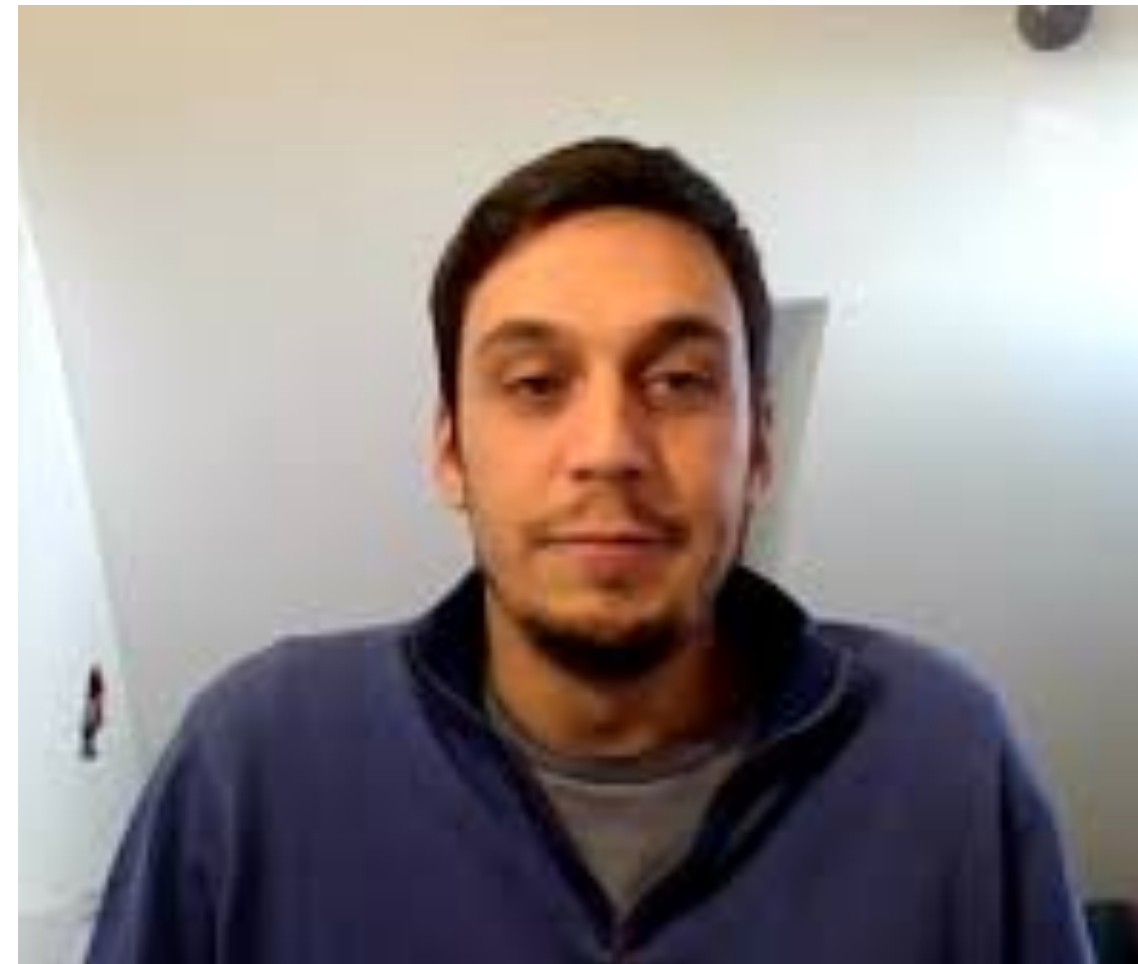
- Spinons f_α in bottom layer are in a π -flux spin liquid with a SU(2) gauge field U .
- Higgs boson B has charge e , and is a SU(2) fundamental.
- Yukawa coupling between c_α , f_α and B .
- B is a **fractionalized order parameter**, whose composites describe numerous superconducting and charge order parameters!

Monte-Carlo of
Born-Oppenheimer approx.

Classical B, U , quantum c_α, f_α .



Maine Christos
Caltech



Pietro Bonetti

Thermal $SU(2)$ lattice gauge theory of the cuprate pseudogap: reconciling Fermi arcs and hole pockets

H. Pandey, M. Christos, P.M. Bonetti, R. Shanker,
S. Sharma, S.S., arXiv:2507.05336



Harshit Pandey



Ravi Shanker



Sayantan Sharma

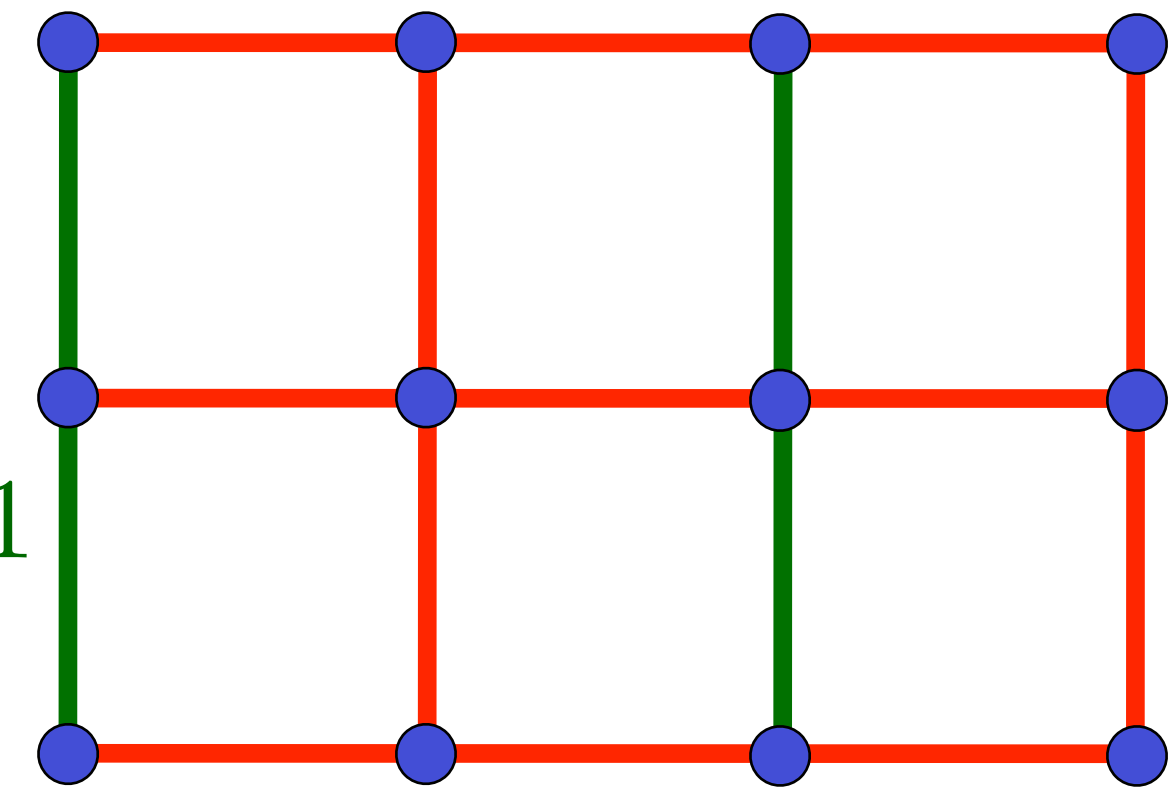
The Institute of Mathematical Sciences, Chennai

f_α and B both move in π -flux

Symmetry	f_α	B_a
T_x	$(-1)^y f_\alpha$	$(-1)^y B_a$
T_y	f_α	B_a
P_x	$(-1)^x f_\alpha$	$(-1)^x B_a$
P_y	$(-1)^y f_\alpha$	$(-1)^y B_a$
P_{xy}	$(-1)^{xy} f_\alpha$	$(-1)^{xy} B_a$
\mathcal{T}	$(-1)^{x+y} \varepsilon_{\alpha\beta} f_\beta$	$(-1)^{x+y} B_a$

$$e_{ij} = -1$$

$$e_{ij} = 1$$



Projective transformations of the f spinons and B chargons on lattice sites $\mathbf{i} = (x, y)$ under the symmetries

$$T_x : (x, y) \rightarrow (x + 1, y); T_y : (x, y) \rightarrow (x, y + 1);$$

$$P_x : (x, y) \rightarrow (-x, y); P_y : (x, y) \rightarrow (x, -y);$$

$$P_{xy} : (x, y) \rightarrow (y, x); \text{ and time-reversal } \mathcal{T}.$$

The indices α, β refer to global SU(2) spin, while the index $a = 1, 2$ refers to gauge SU(2).

f_α and B both move in π -flux

Symmetry	f_α	B_a
T_x	$(-1)^y f_\alpha$	$(-1)^y B_a$
T_y	f_α	B_a
P_x	$(-1)^x f_\alpha$	$(-1)^x B_a$
P_y	$(-1)^y f_\alpha$	$(-1)^y B_a$
P_{xy}	$(-1)^{xy} f_\alpha$	$(-1)^{xy} B_a$
\mathcal{T}	$(-1)^{x+y} \varepsilon_{\alpha\beta} f_\beta$	$(-1)^{x+y} B_a$

Projective transformations of the f spinons and B chargons on lattice sites $\mathbf{i} = (x, y)$ under the symmetries

$$T_x : (x, y) \rightarrow (x + 1, y); T_y : (x, y) \rightarrow (x, y + 1);$$

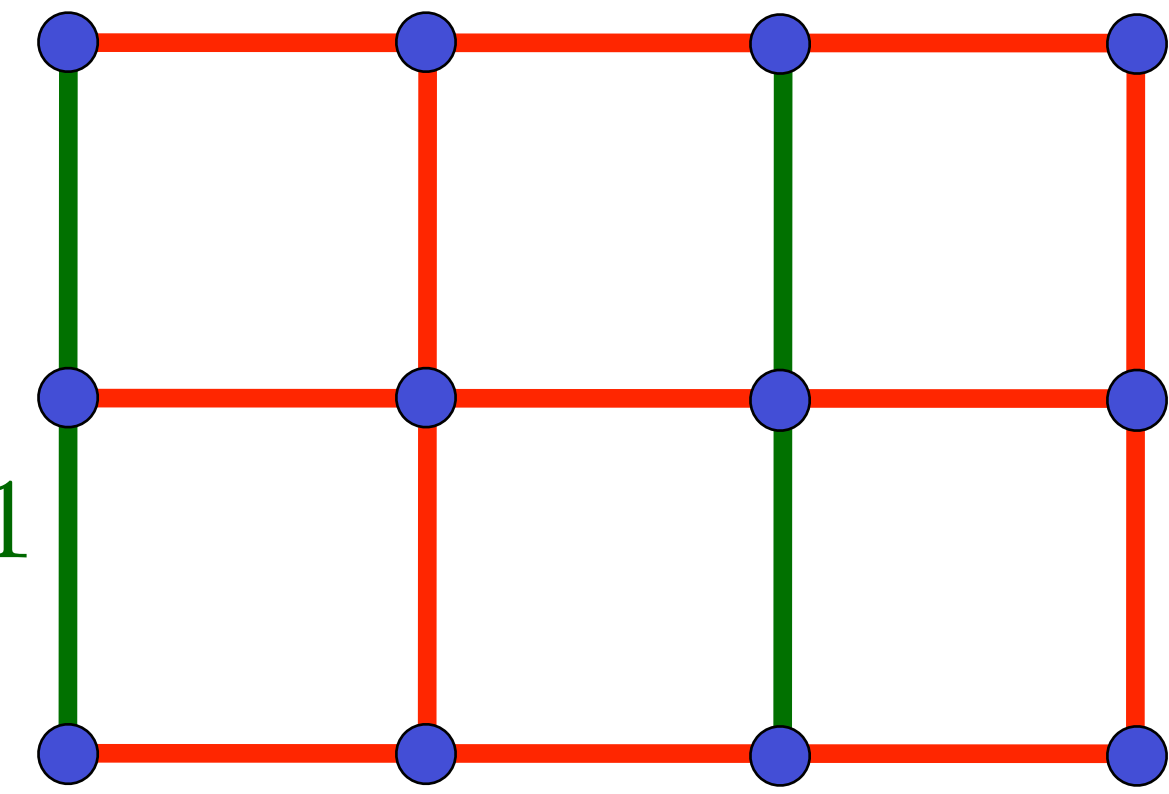
$$P_x : (x, y) \rightarrow (-x, y); P_y : (x, y) \rightarrow (x, -y);$$

$$P_{xy} : (x, y) \rightarrow (y, x); \text{ and time-reversal } \mathcal{T}.$$

The indices α, β refer to global SU(2) spin, while the index $a = 1, 2$ refers to gauge SU(2).

$$e_{ij} = -1$$

$$e_{ij} = 1$$



Pairing: $\langle \varepsilon_{\alpha\beta} c_{i\alpha} c_{j\beta} \rangle \sim$

$$\Delta_{ij} = \Delta_{ji} = \varepsilon_{ab} B_{ai} e_{ij} U_{ij} B_{bj}$$

site charge density: $\langle c_{i\alpha}^\dagger c_{i\alpha} \rangle \sim \rho_i = B_i^\dagger B_i$

bond density: $\langle c_{i\alpha}^\dagger c_{j\alpha} + c_{j\alpha}^\dagger c_{i\alpha} \rangle$

$$\sim Q_{ij} = Q_{ji} = \text{Im} \left(B_i^\dagger e_{ij} U_{ij} B_j \right)$$

bond current: $i \langle c_{i\alpha}^\dagger c_{j\alpha} - c_{j\alpha}^\dagger c_{i\alpha} \rangle$

$$\sim J_{ij} = -J_{ji} = \text{Re} \left(B_i^\dagger e_{ij} U_{ij} B_j \right)$$

Energy functional for B and U : $\mathcal{E}[B, U] = \mathcal{E}_2[B, U] + \mathcal{E}_4[B, U] + \mathcal{E}_{YM}[U]$

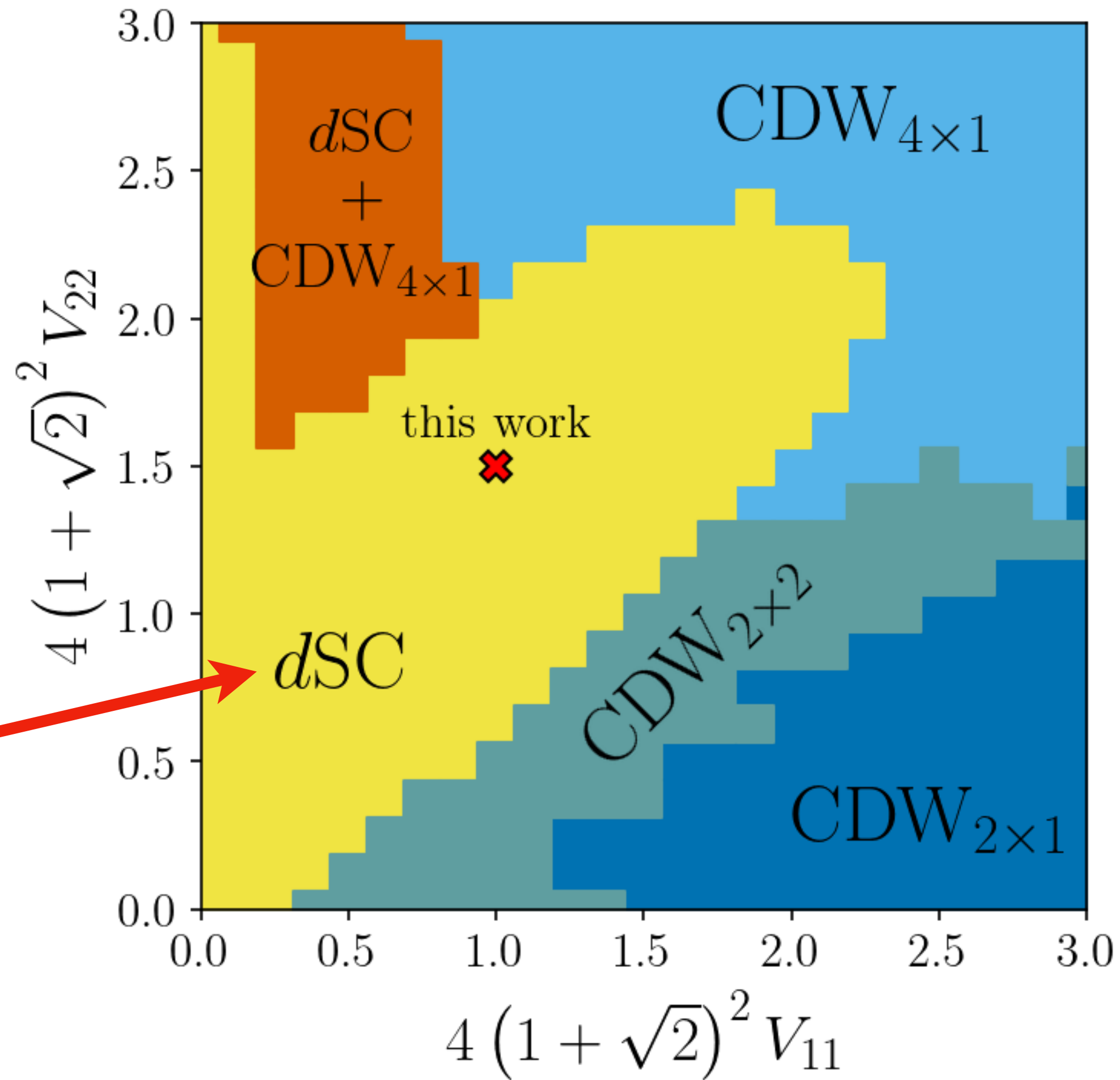
$$\mathcal{E}_2[B, U] = (r + 2\sqrt{2}w) \sum_i B_i^\dagger B_i + iw \sum_{\langle ij \rangle} e_{ij} \left(B_i^\dagger U_{ij} B_j - B_j^\dagger U_{ji} B_i \right)$$

$$\begin{aligned} \mathcal{E}_4[B, U] = & \frac{u}{2} \sum_i \rho_i^2 + V_1 \sum_i \rho_i (\rho_{i+\hat{x}} + \rho_{i+\hat{y}}) + g \sum_{\langle ij \rangle} |\Delta_{ij}|^2 + J_1 \sum_{\langle ij \rangle} Q_{ij}^2 + K_1 \sum_{\langle ij \rangle} J_{ij}^2 \\ & + V_{11} \sum_i \rho_i (\rho_{i+\hat{x}+\hat{y}} + \rho_{i+\hat{x}-\hat{y}}) + V_{22} \sum_i \rho_i (\rho_{i+2\hat{x}+2\hat{y}} + \rho_{i+2\hat{x}-2\hat{y}}) \end{aligned}$$

$$\mathcal{E}_{YM}[U] = \kappa \sum_{\square} \left[1 - \frac{1}{2} \text{ReTr} \prod_{ij \in \square} U_{ij} \right]$$

At $T = 0$, minimize $\mathcal{E}[B, U]$.

d -SC with
4 nodal quasiparticles
and $v_F \gg v_\Delta$.



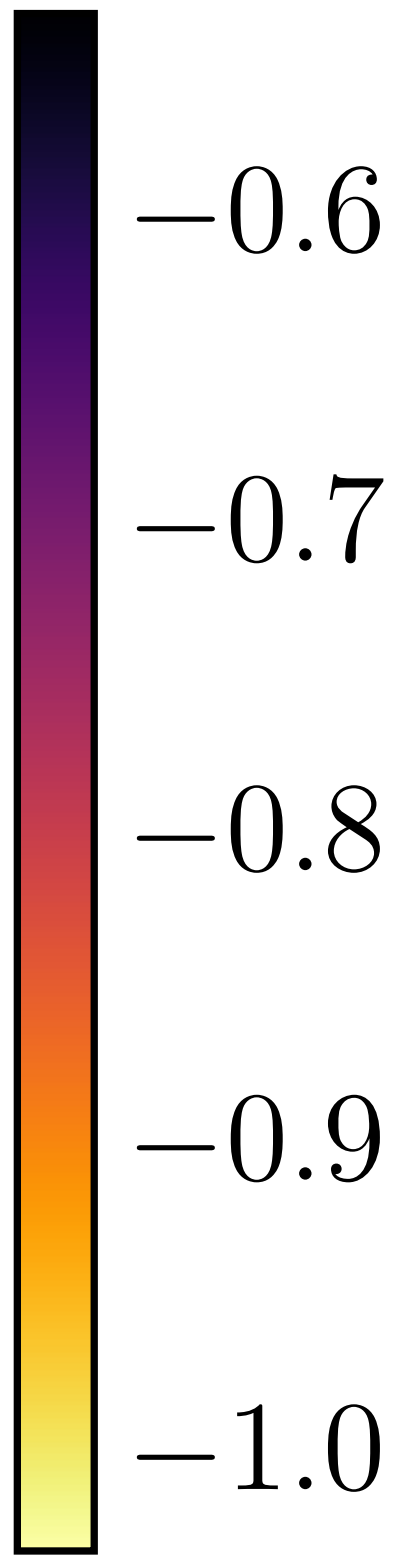
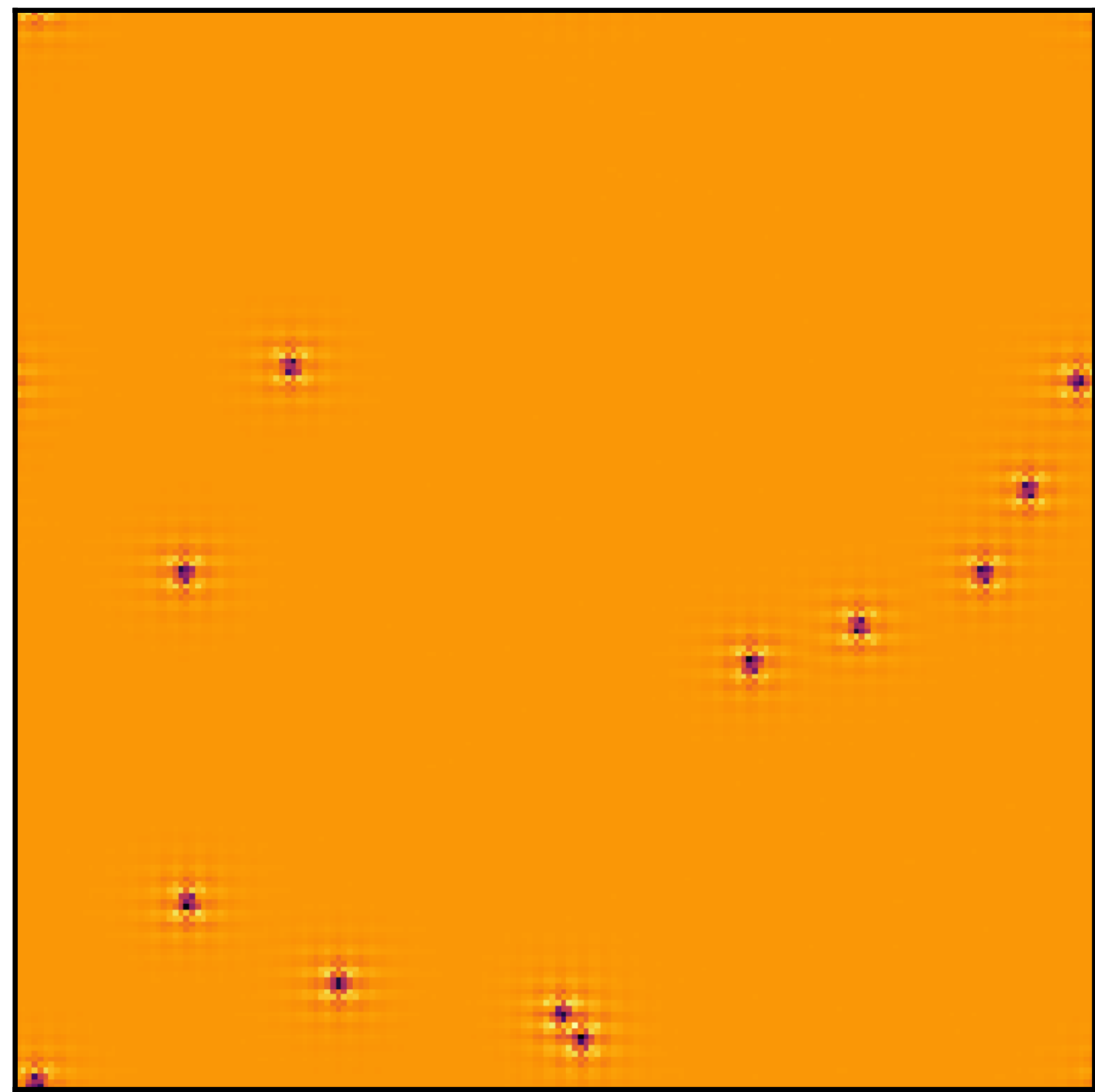
Parameters chosen so that the ground state is a d -wave superconductor,
and second best state is a period-4 stripe.

Monte Carlo at a temperature T

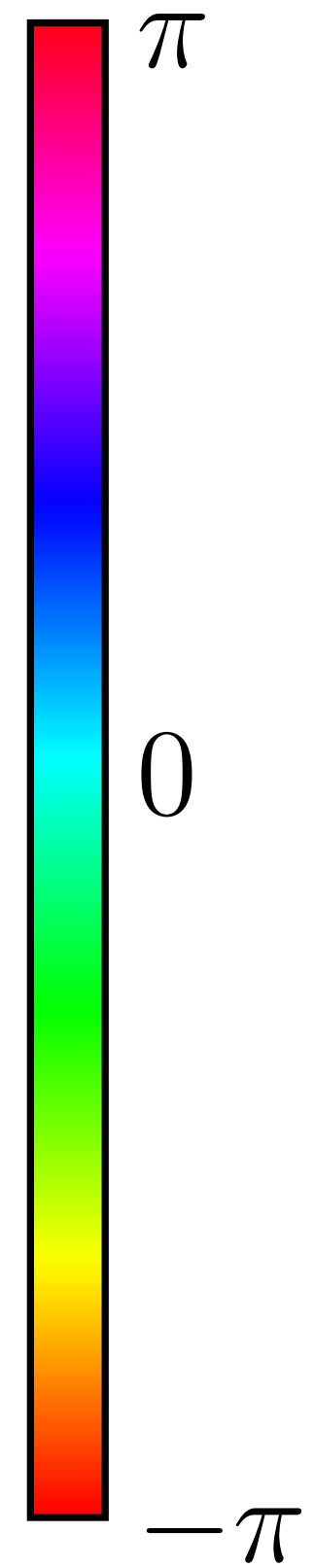
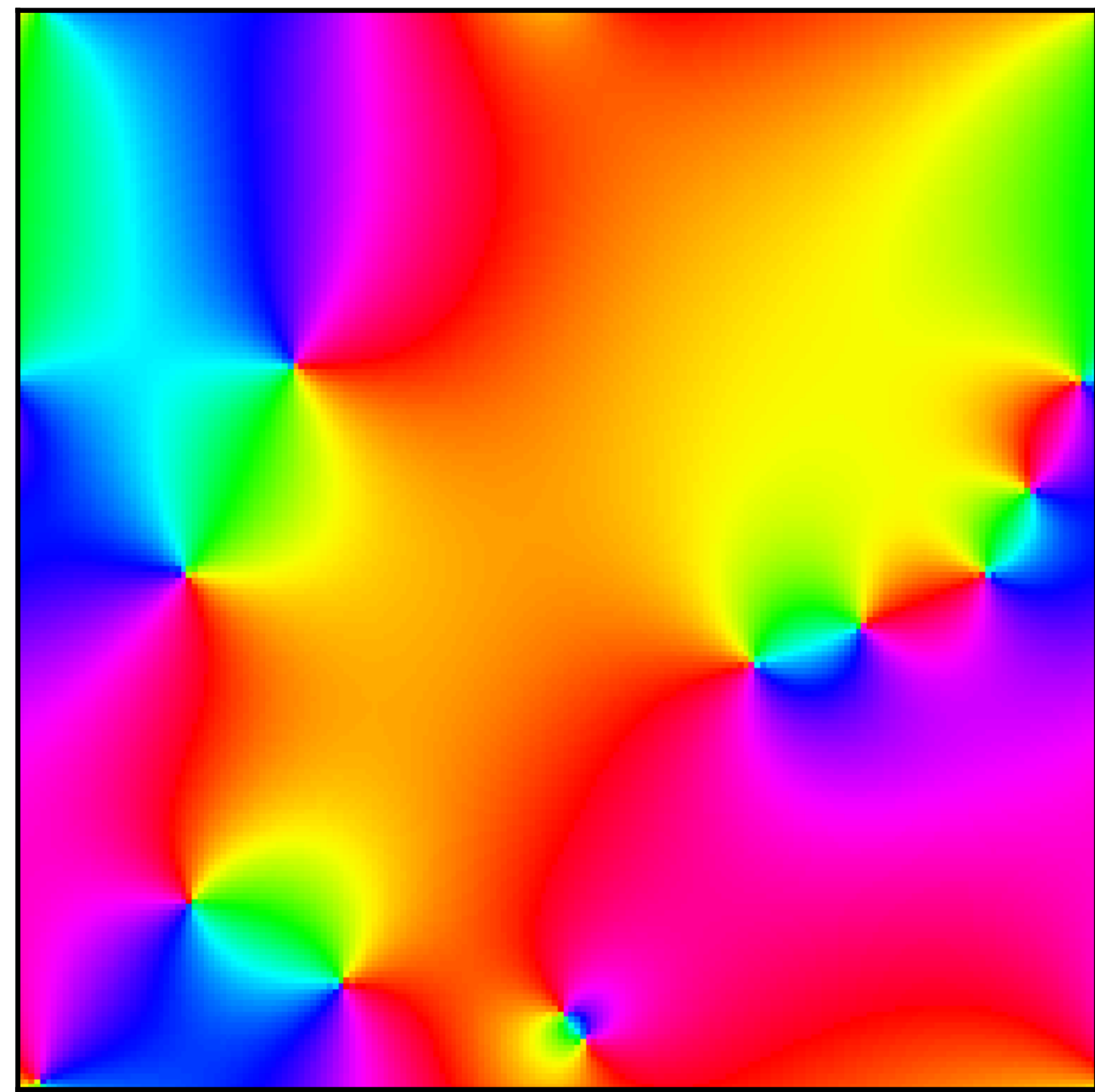
$$\mathcal{Z}_{2+0} = \int \prod_i \mathcal{D}B_i \int \prod_{\langle ij \rangle} \mathcal{D}U_{ij} \exp[-\mathcal{E}[B, U]/T]$$

- Simulation of classical, thermal theory for bosons B, U defined by \mathcal{Z}_{2+0}
- Diagonalize 3-layer fermion Hamiltonian for c, f_1, f for each snapshot of B, U , and average.

Monte Carlo at a temperature T

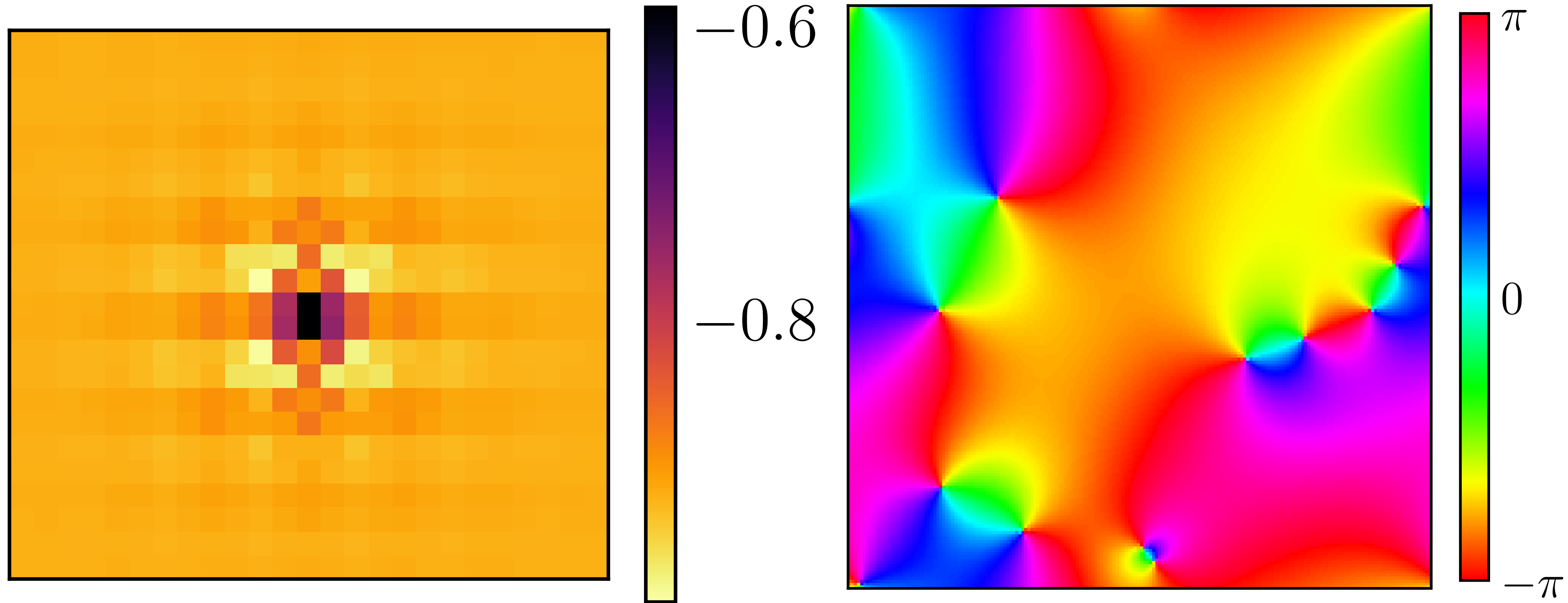


Bond density



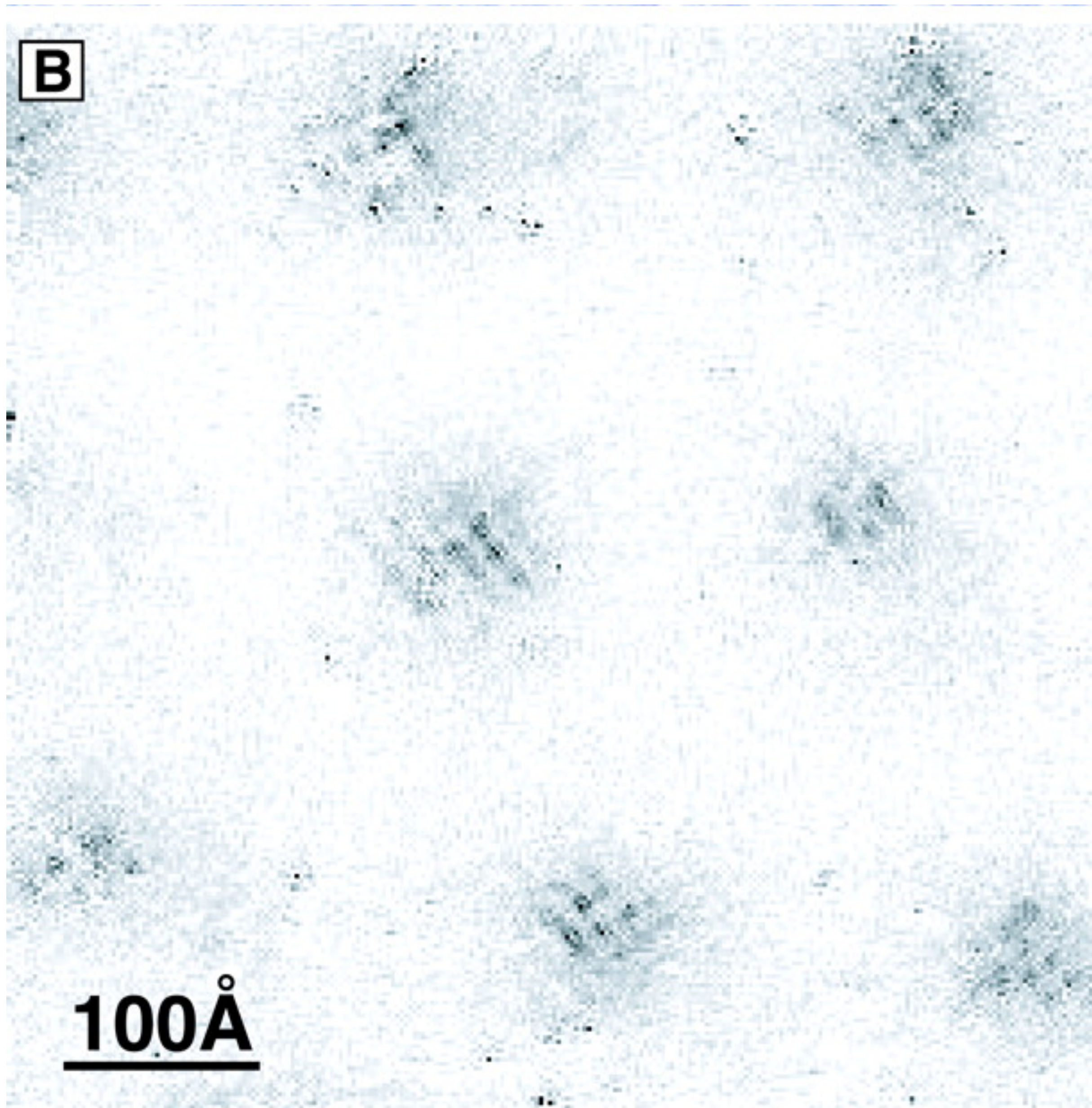
Phase of pairing amplitude

Monte Carlo at a temperature T



Bond density

Phase of pairing amplitude



A Four Unit Cell Periodic Pattern of Quasi-Particle States Surrounding Vortex Cores in $\text{Bi}_2\text{Sr}_2\text{CaCu}_2\text{O}_{8+\delta}$

J. E. Hoffman, E. W. Hudson,
K. M. Lang, V. Madhavan,
H. Eisaki, S. Uchida, J.C. Davis
Science **295**, 466 (2002)

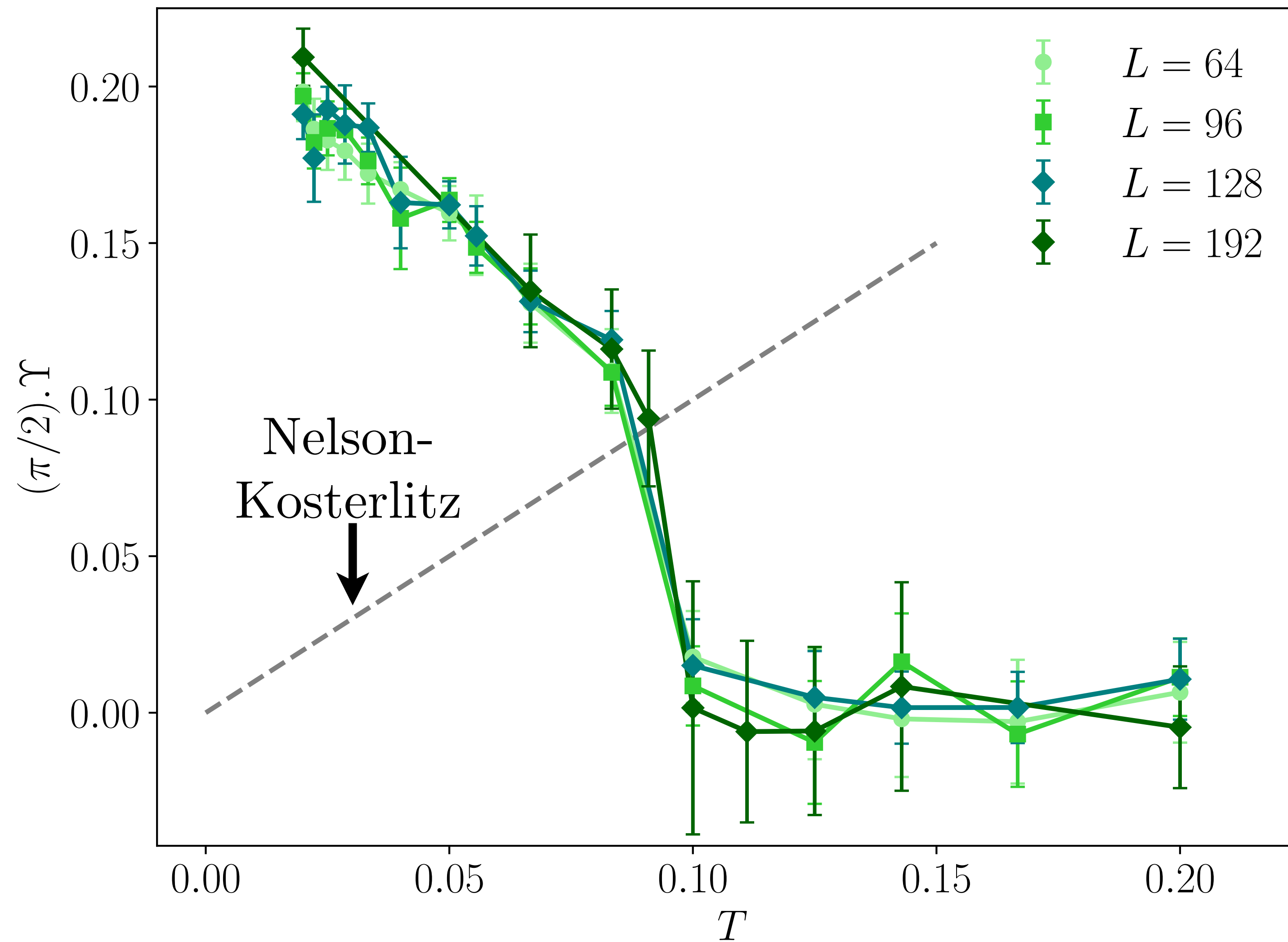
0 pA

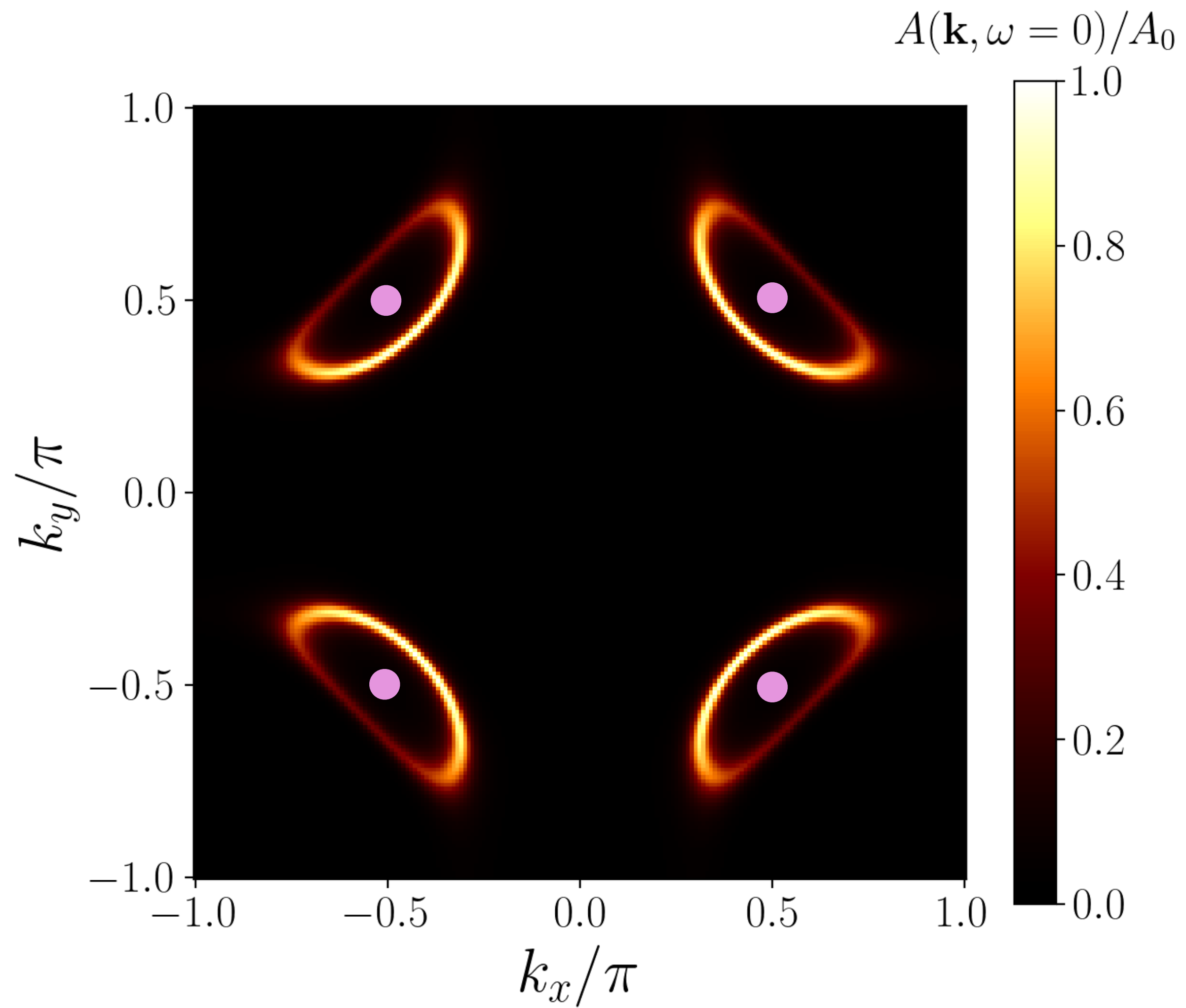


2 pA

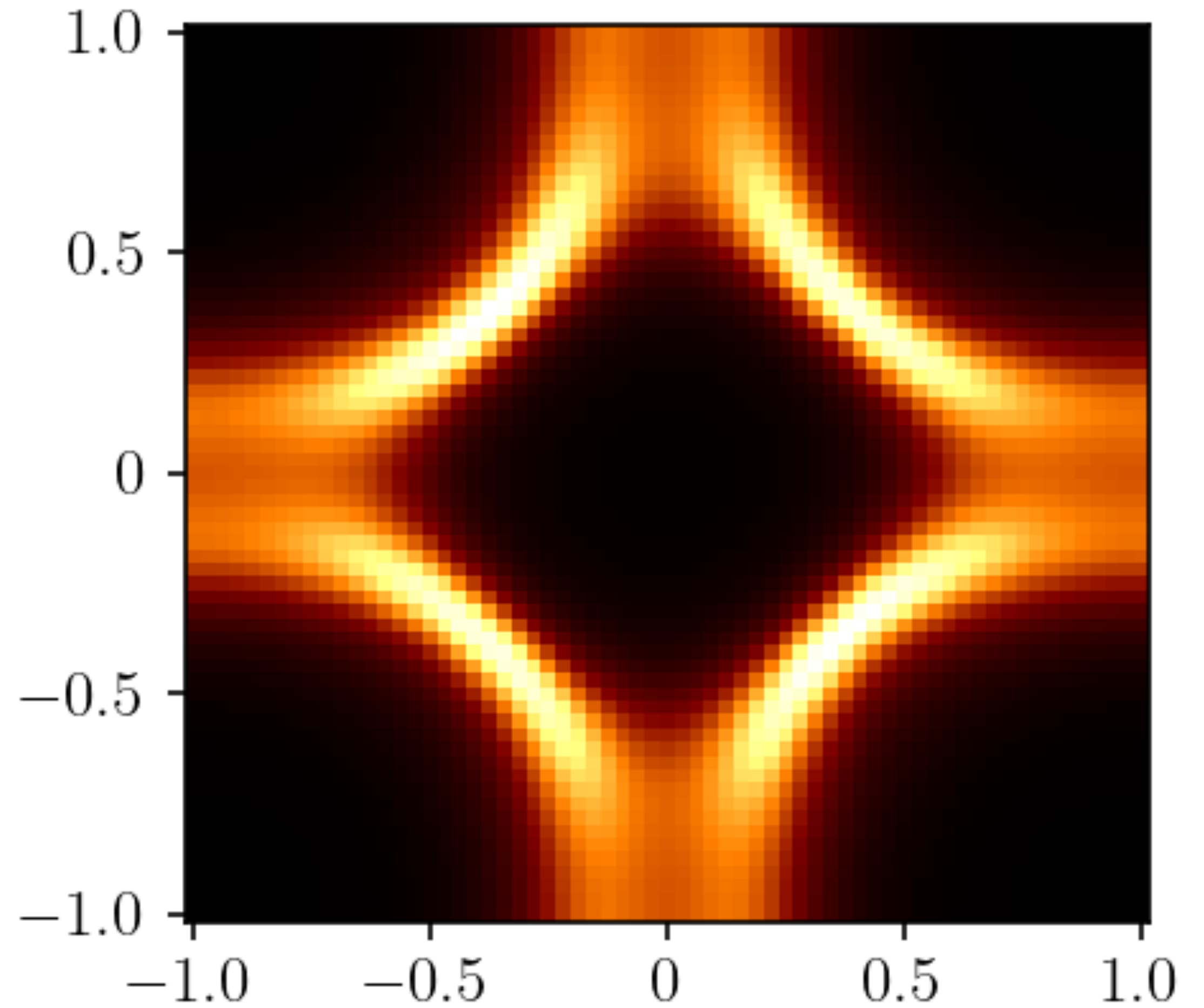
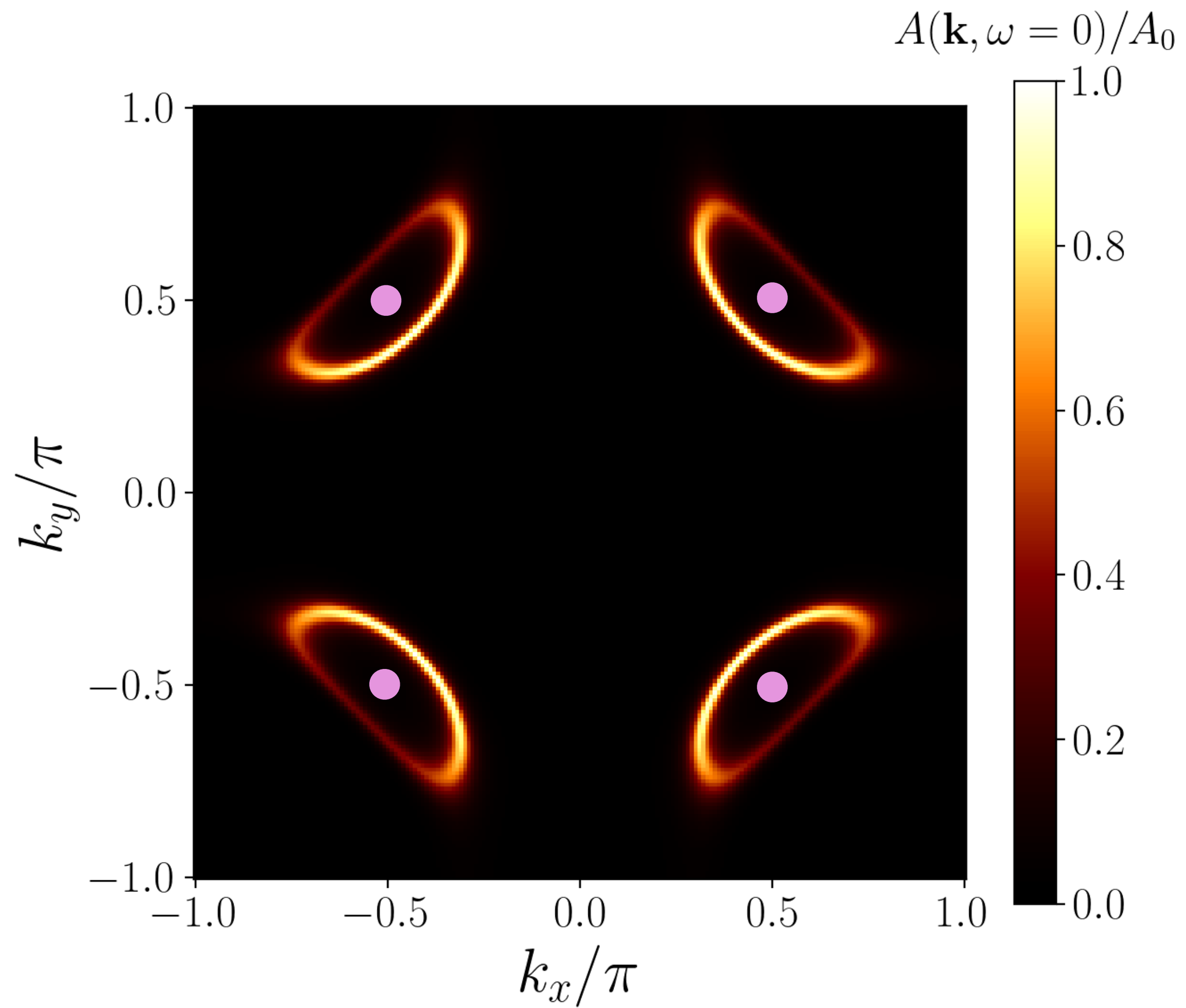
Monte Carlo at a temperature T

$\Upsilon =$
Helicity
Modulus



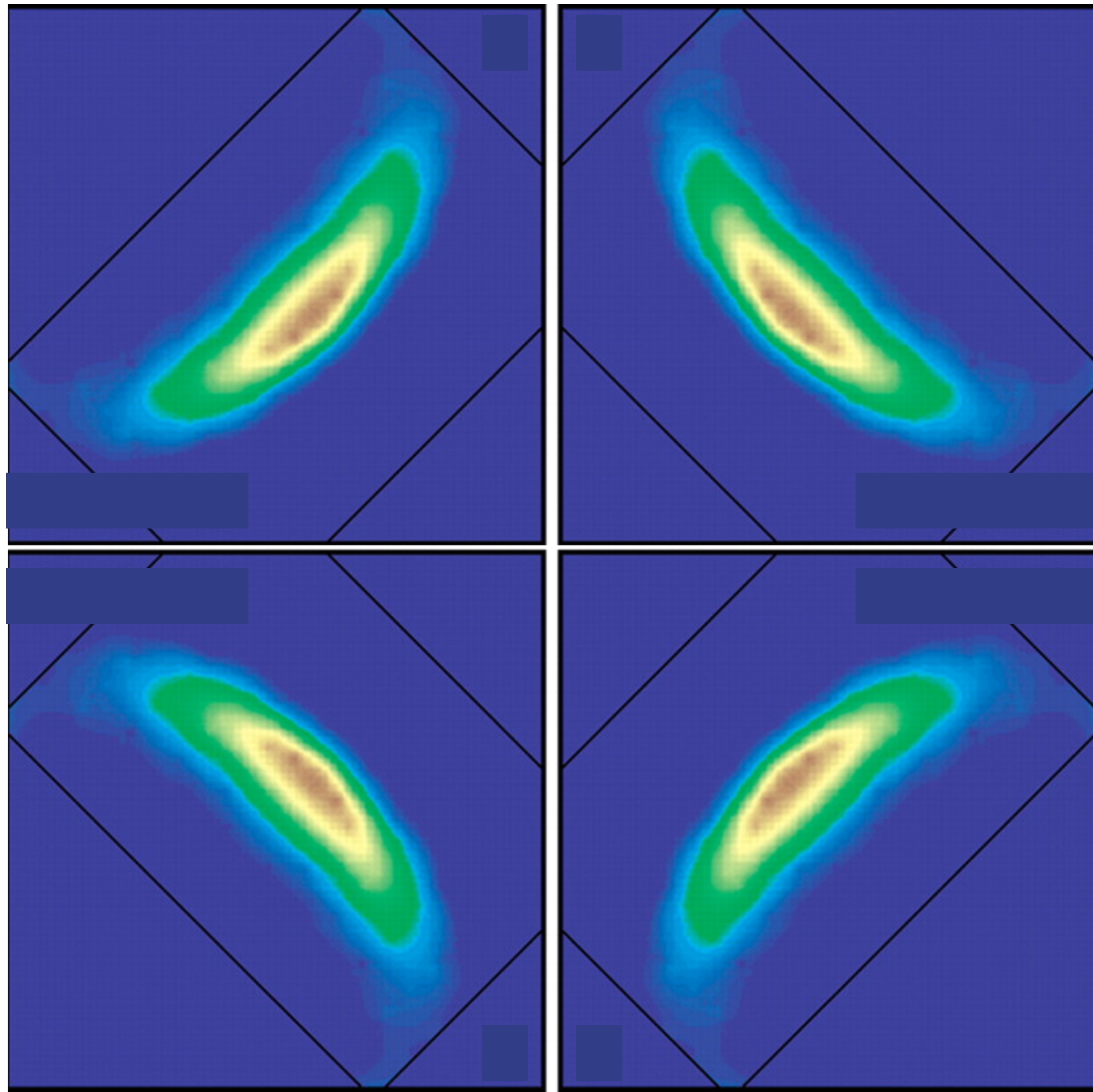


FL* fermionic spectrum with $B = 0$, $U = 1$
4 holes pockets of size $p/8$;
4 nodal spinons



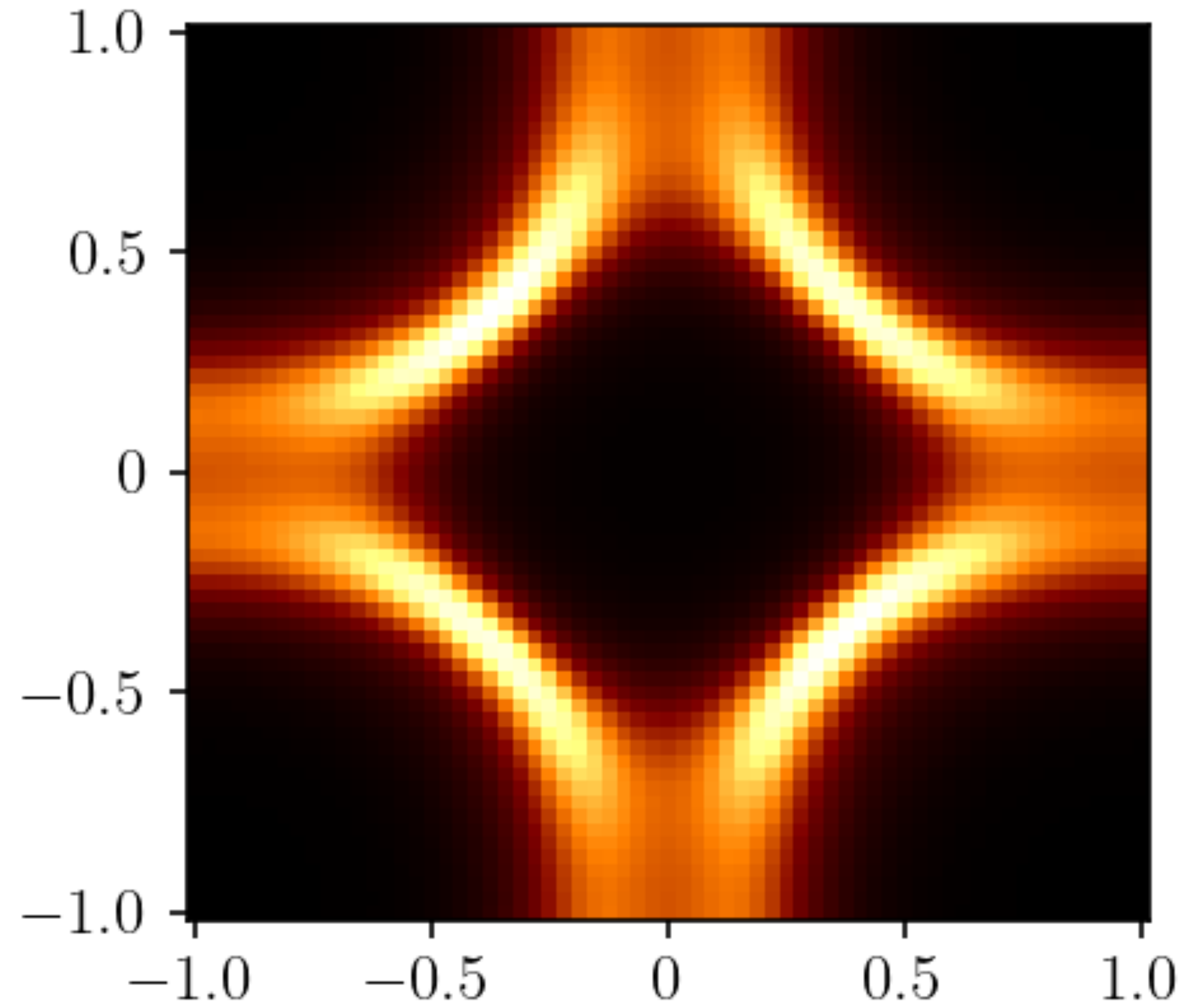
FL* fermionic spectrum with $B = 0$, $U = 1$
 4 holes pockets of size $p/8$;
 4 nodal spinons

Monte Carlo at a
 temperature $T > T_{KT}$



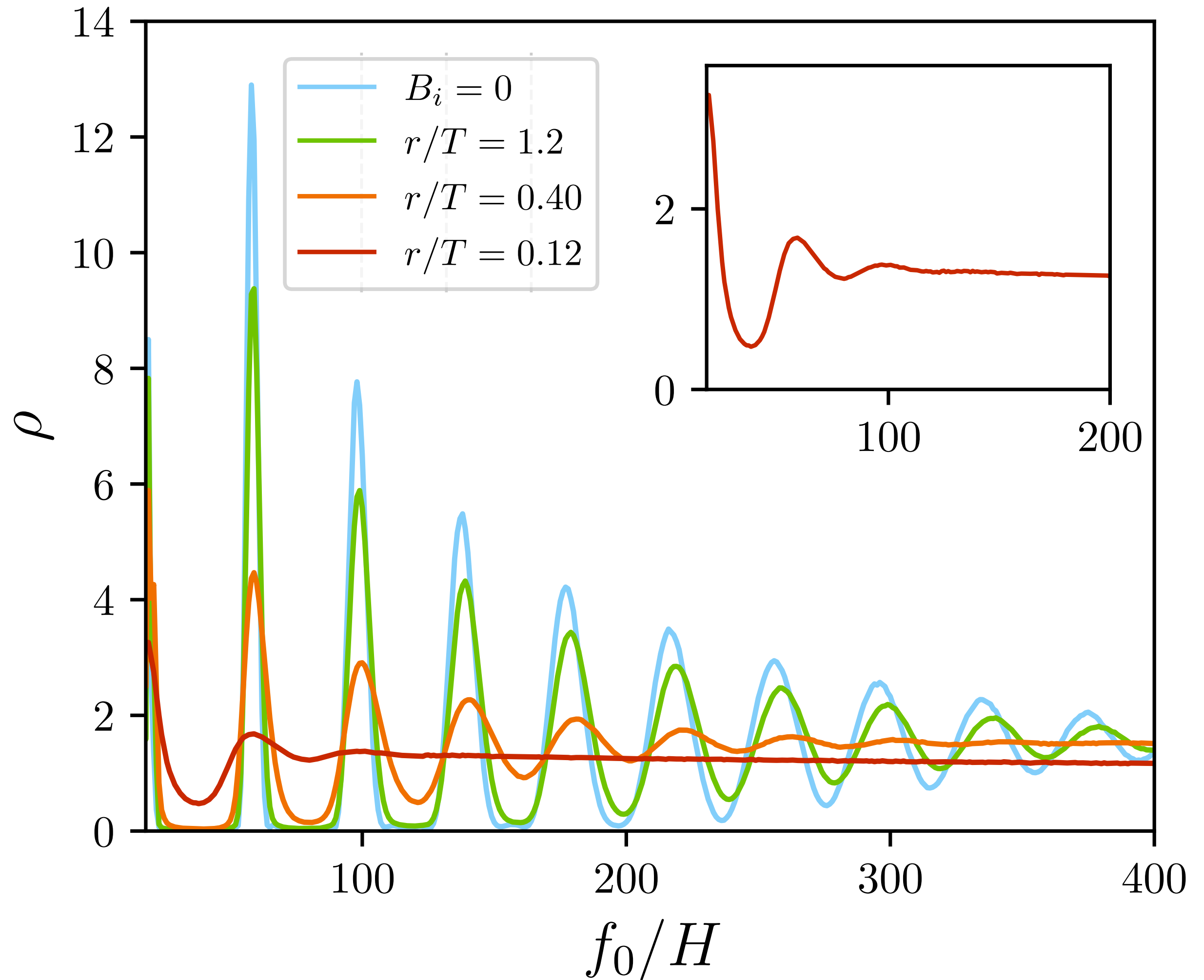
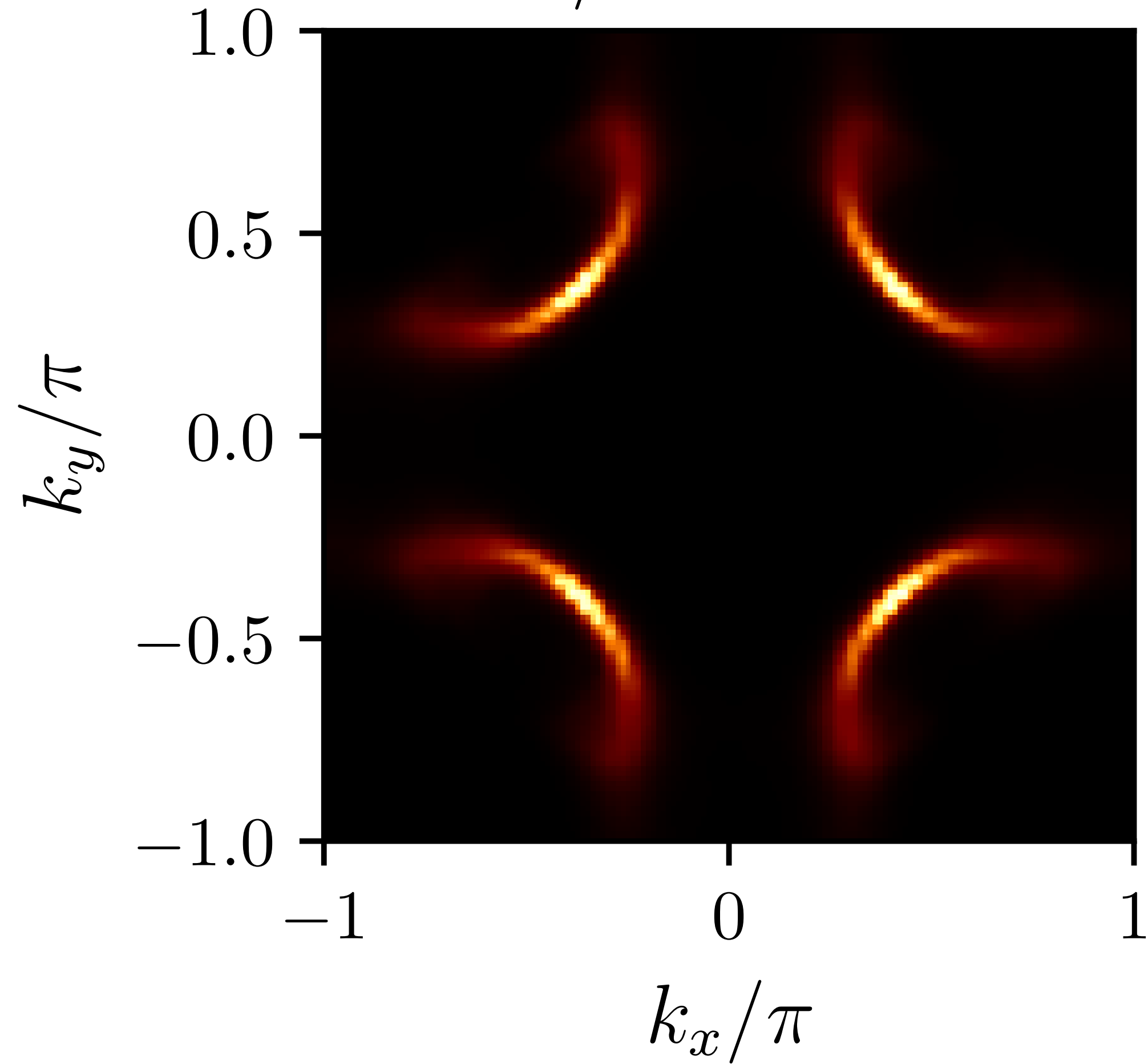
Kyle M. Shen, ... Z.-X. Shen, Science **307**, 901 (2005)

Photoemission observations



Monte Carlo at a
temperature $T > T_{KT}$

$$r/T = 0.12$$

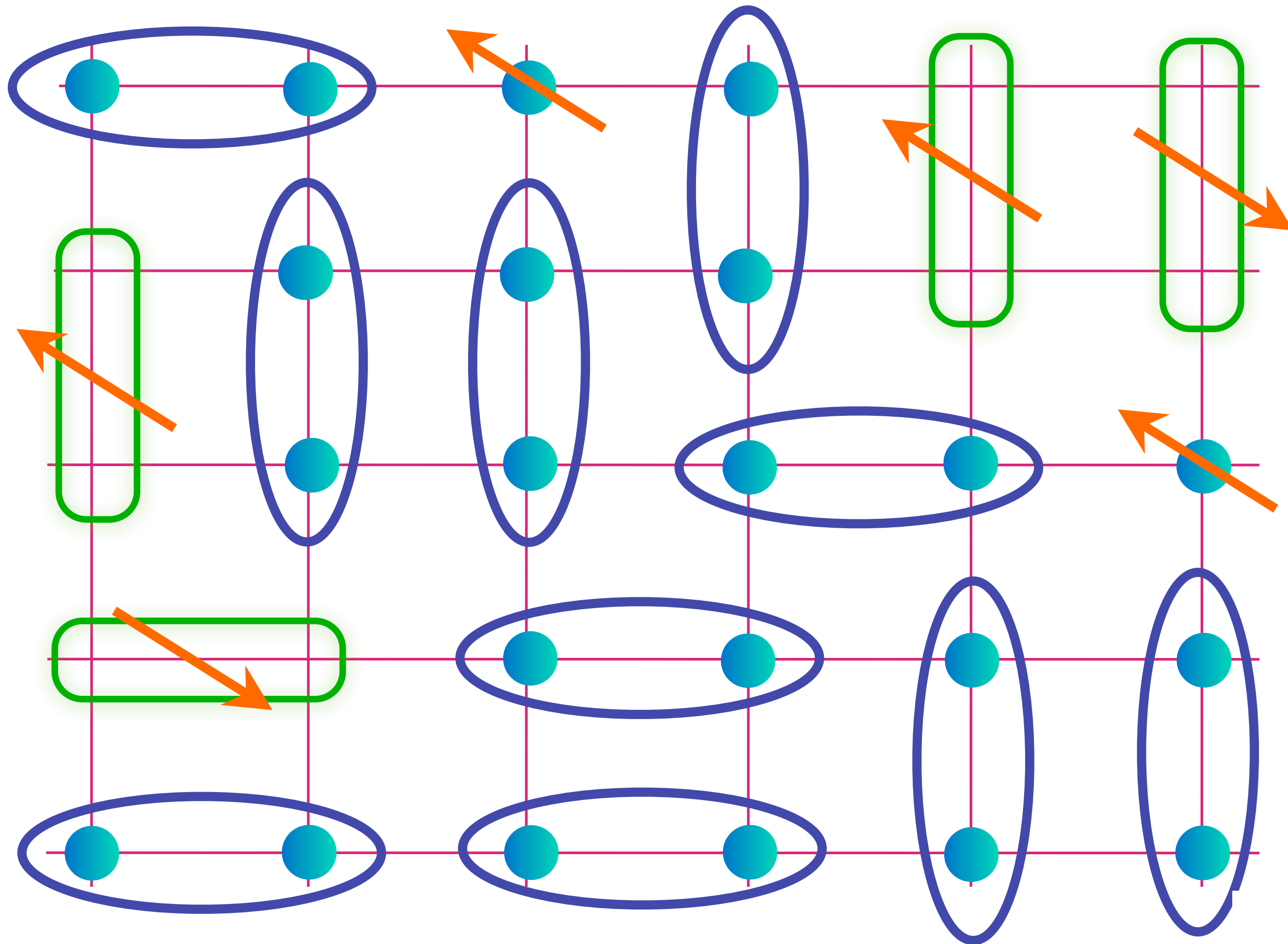


Thermal SU(2) gauge theory of mixing between holes and spinons mediated by Yukawa couplings to a SU(2) fundamental, charge $+e$ Higgs boson B .

Quantum oscillations survive even when pockets have turned to arcs in photoemission.

The cuprate phase diagram

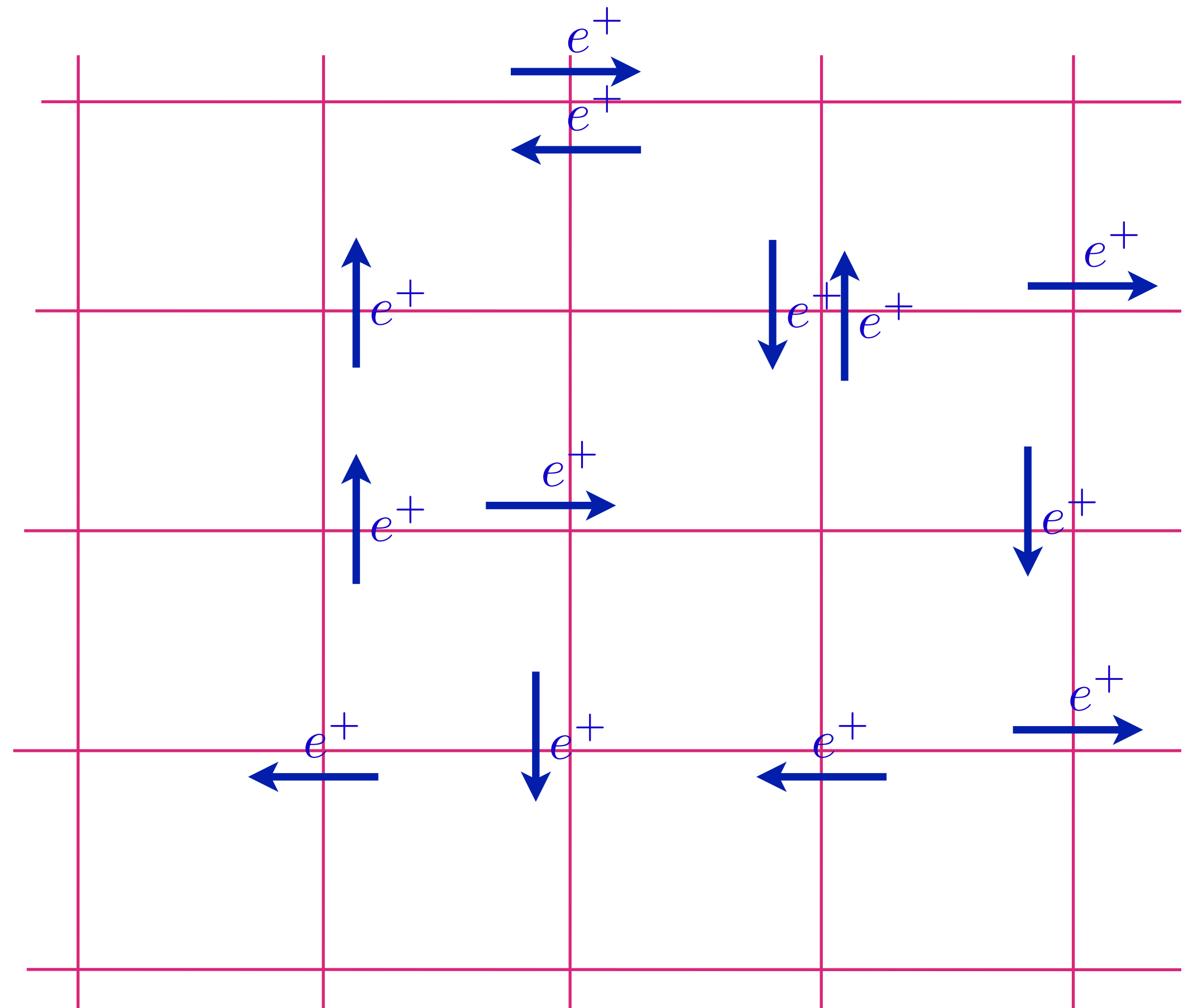
FL*



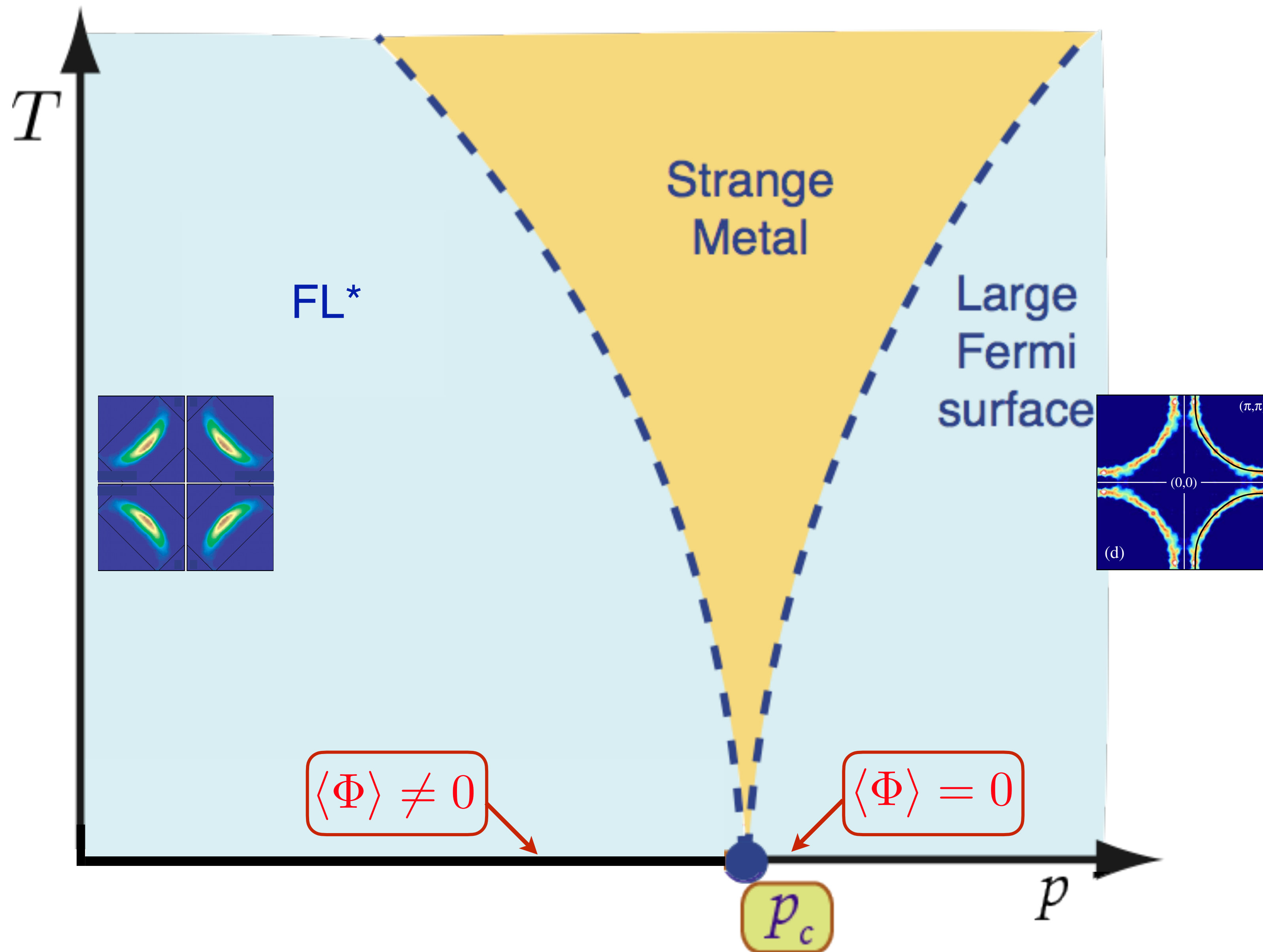
$$\text{Blue oval} = (|\uparrow\downarrow\rangle - |\downarrow\uparrow\rangle) / \sqrt{2}$$

$$\text{Green oval with arrow} = (|\uparrow\circ\rangle + |\circ\uparrow\rangle) / \sqrt{2}$$

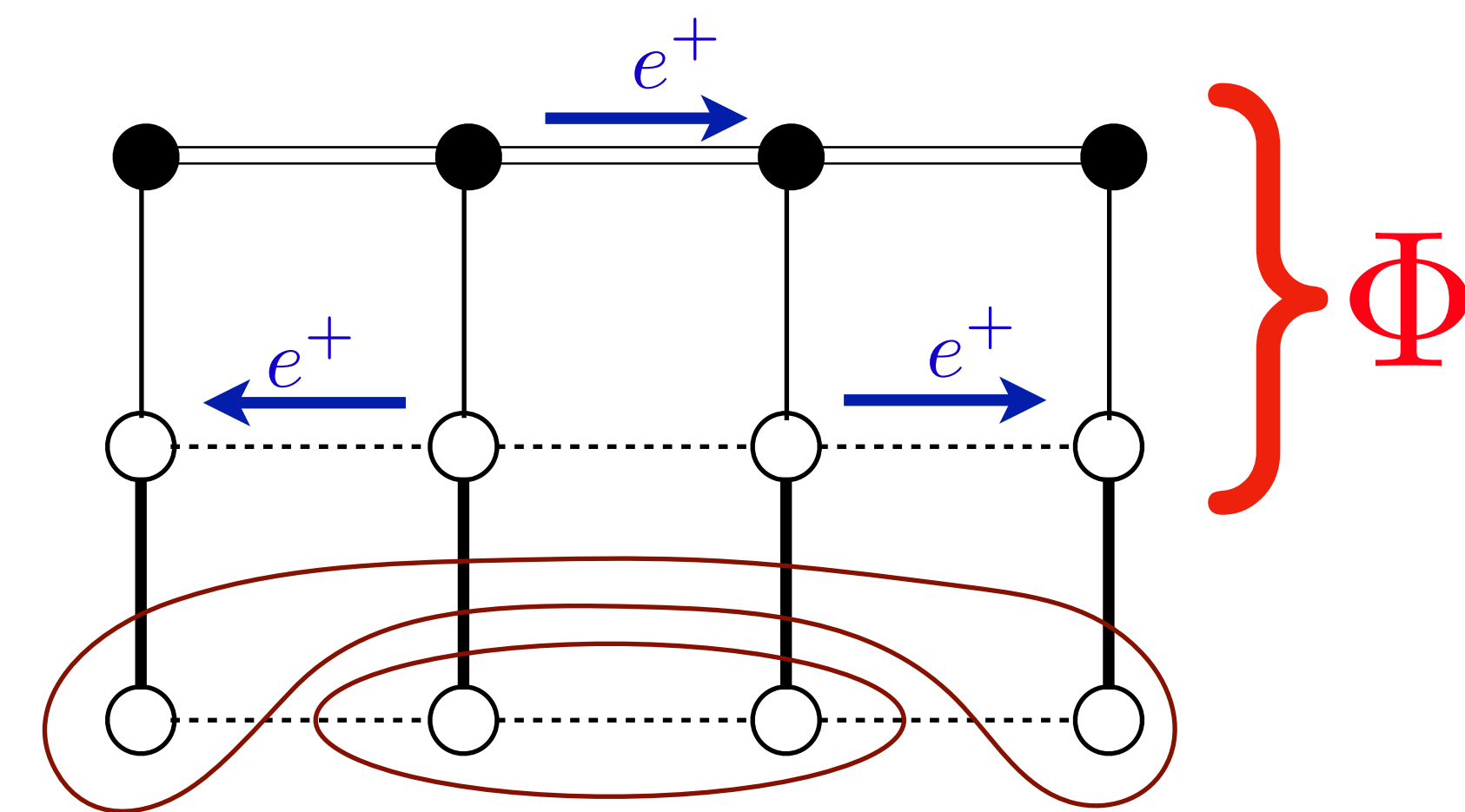
Ordinary metal

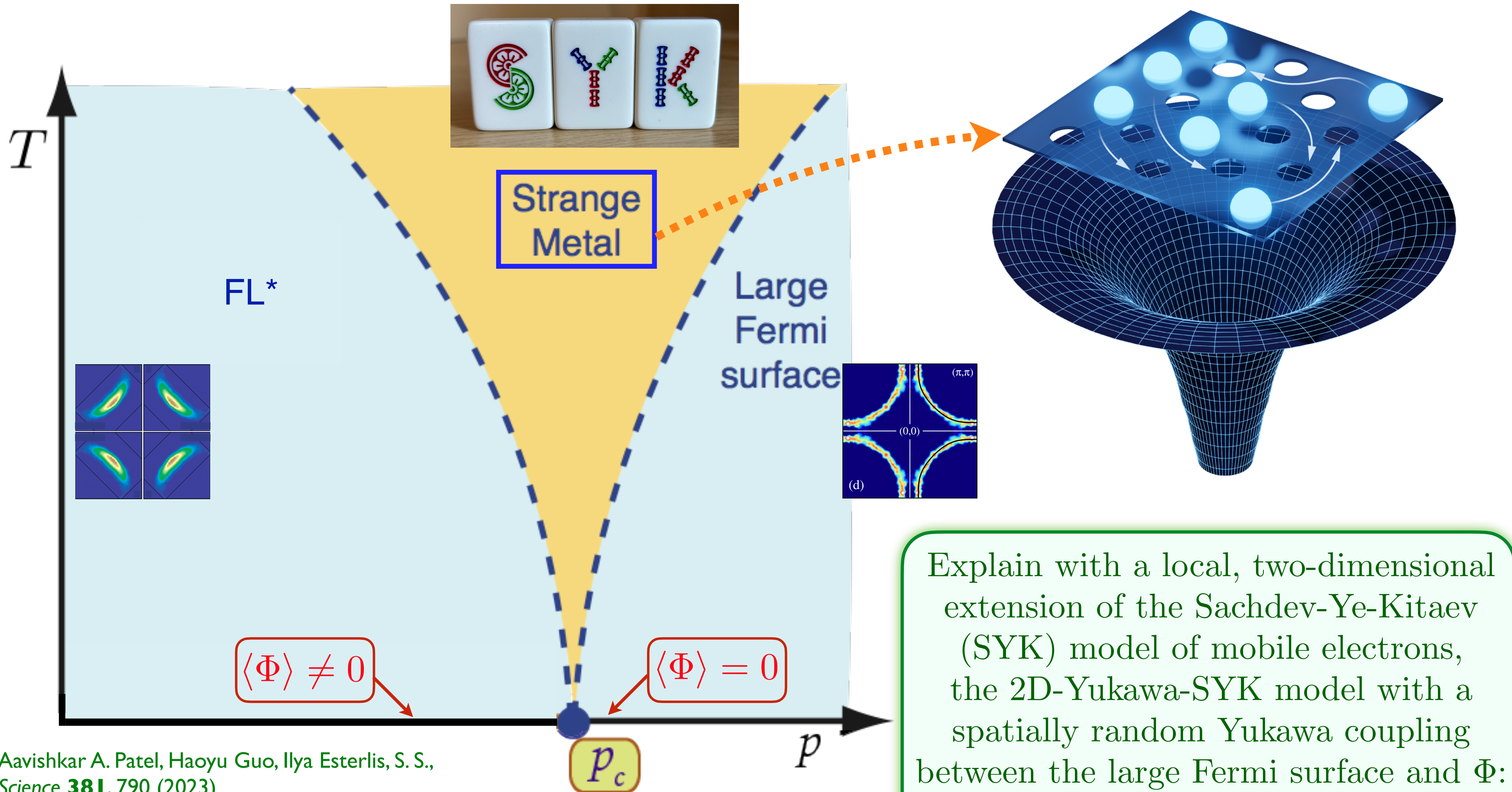


At large p , we obtain a gas of nearly free fermionic holes of density $1+p$ (relative to the filled band with 2 electrons per site)



Quantum-criticality of a quantum phase transition between two metals (FL* and FL) at $p = p_c$, with no symmetry breaking.

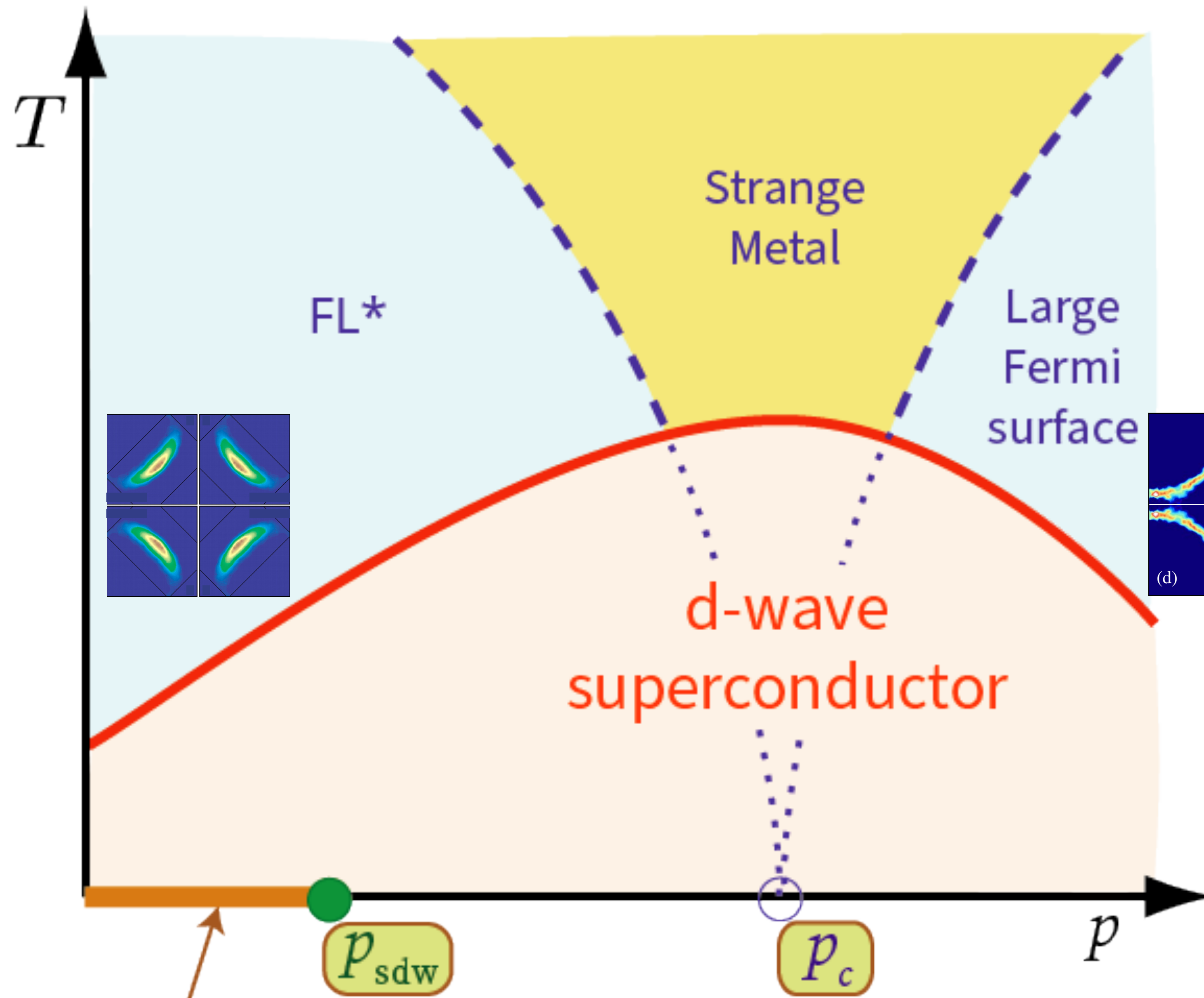




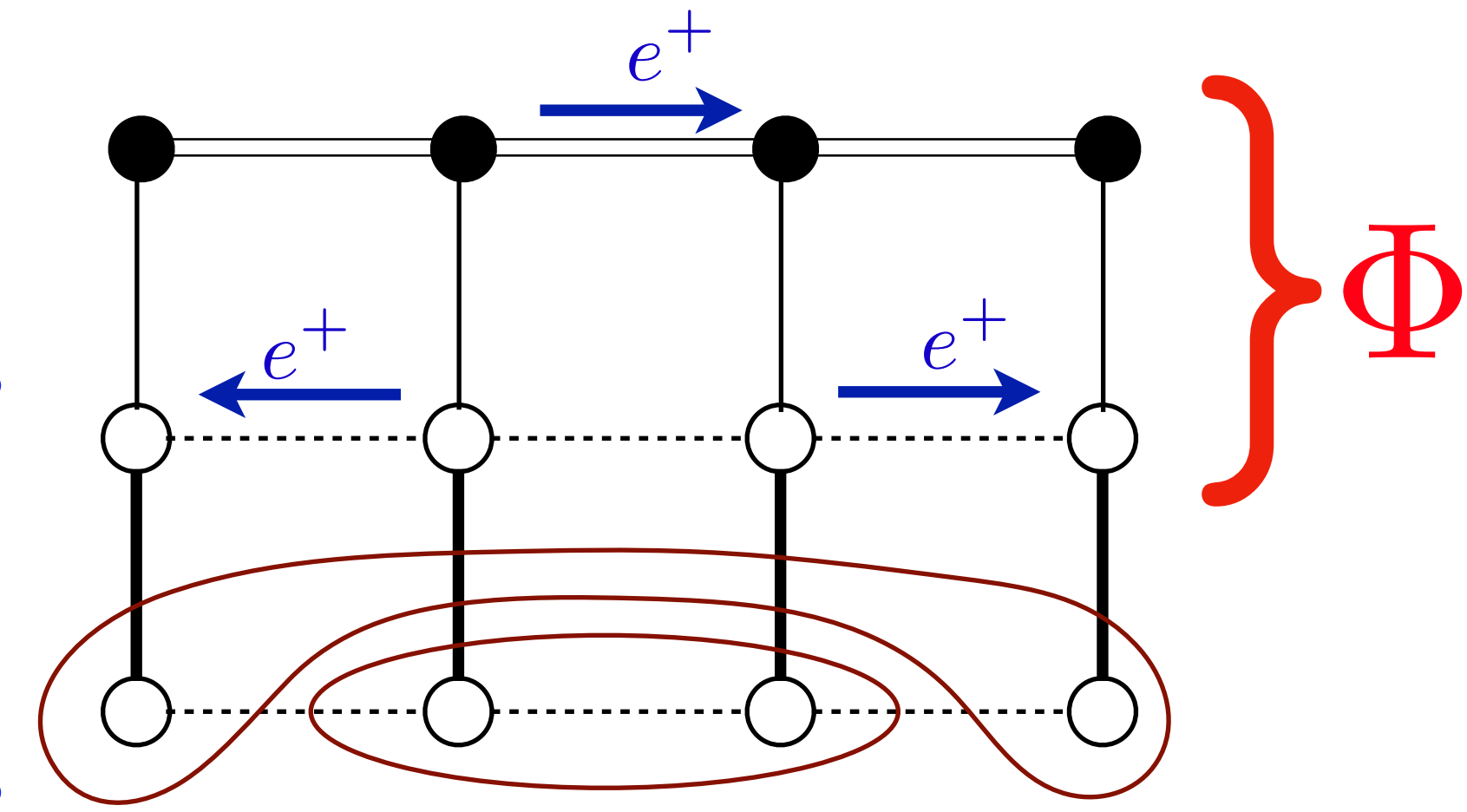
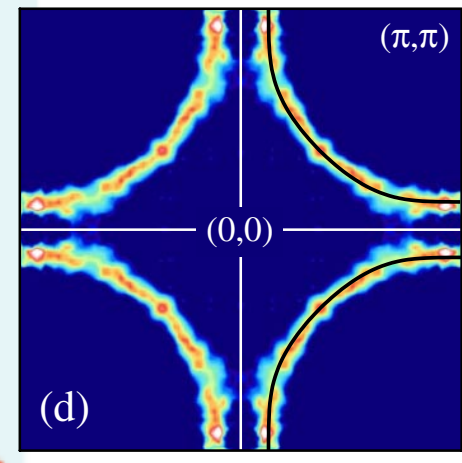
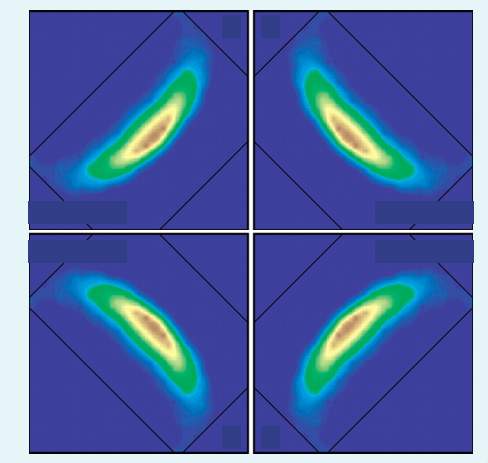
Aavishkar A. Patel, Haoyu Guo, Ilya Esterlis, S. S.,
Science **381**, 790 (2023)

Chenyuan Li, Aavishkar A. Patel, Haoyu Guo, Davide Valentini,
 Jorg Schmalian, S.S., Ilya Esterlis, *PRL* **133**, 186502 (2024)

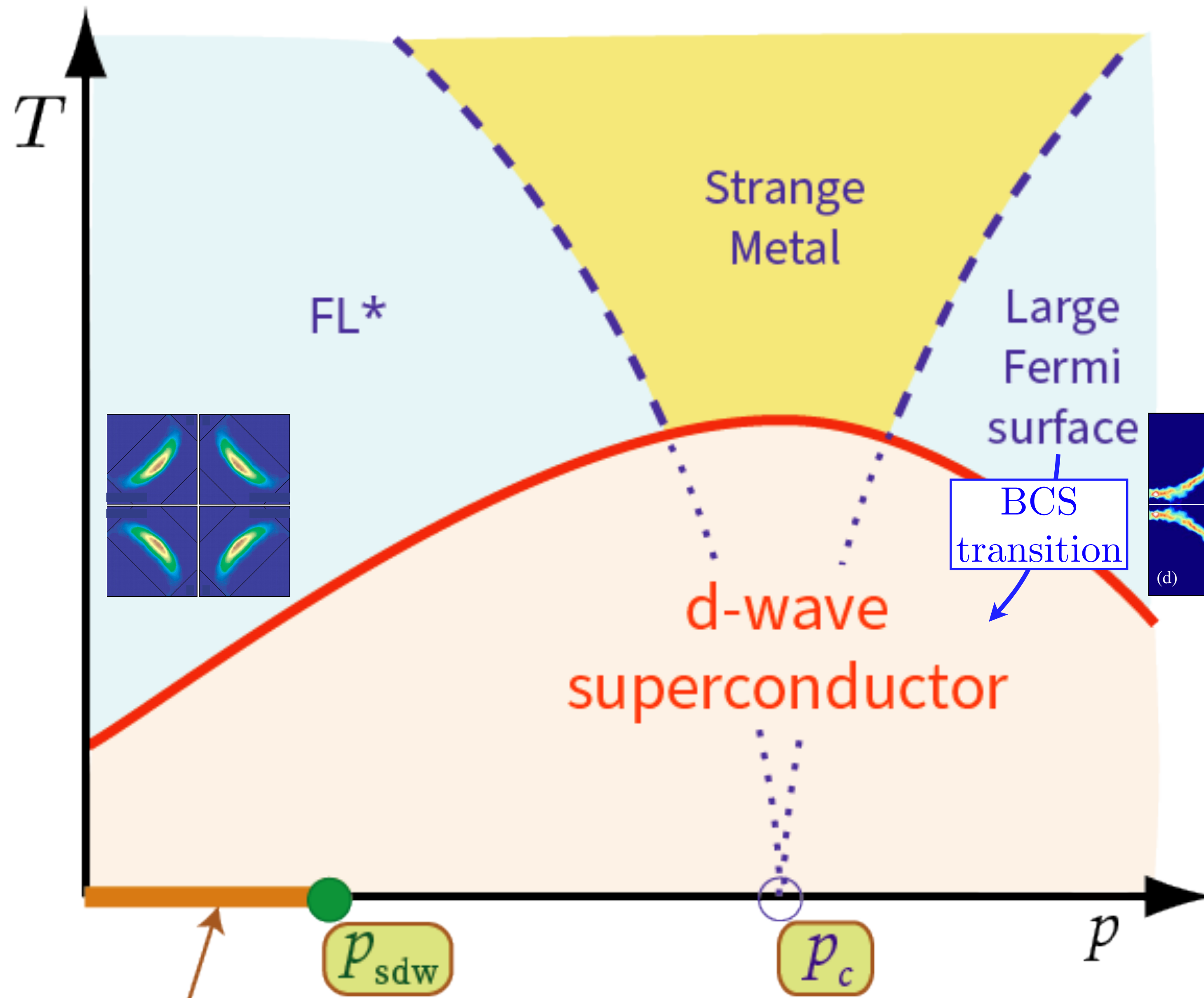
Explain with a local, two-dimensional extension of the Sachdev-Ye-Kitaev (SYK) model of mobile electrons, the 2D-Yukawa-SYK model with a spatially random Yukawa coupling between the large Fermi surface and Φ : a critical charge liquid



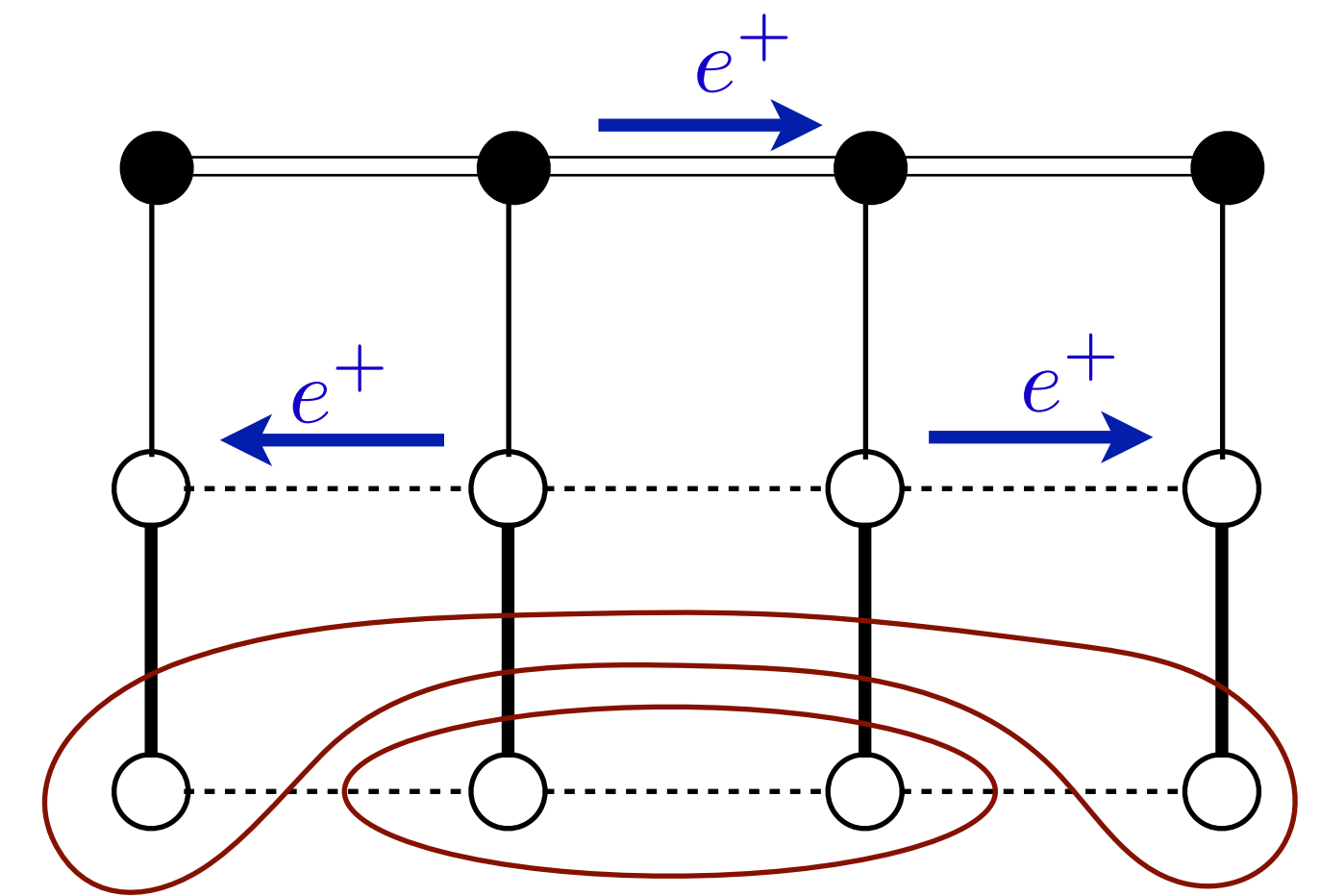
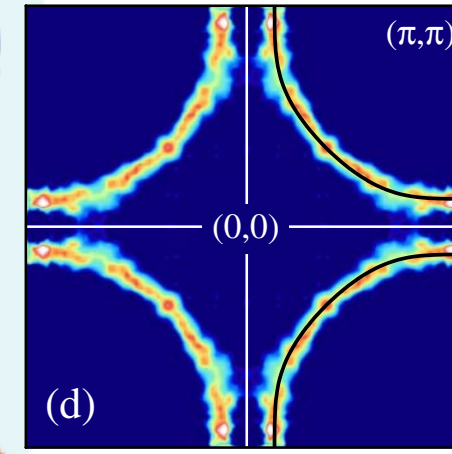
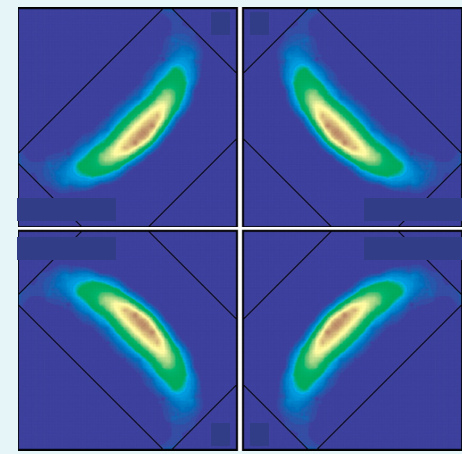
Both metals lead to the same *d*-wave superconductor at lower temperatures, and so there is no transition at $p = p_c$ within the superconducting state.



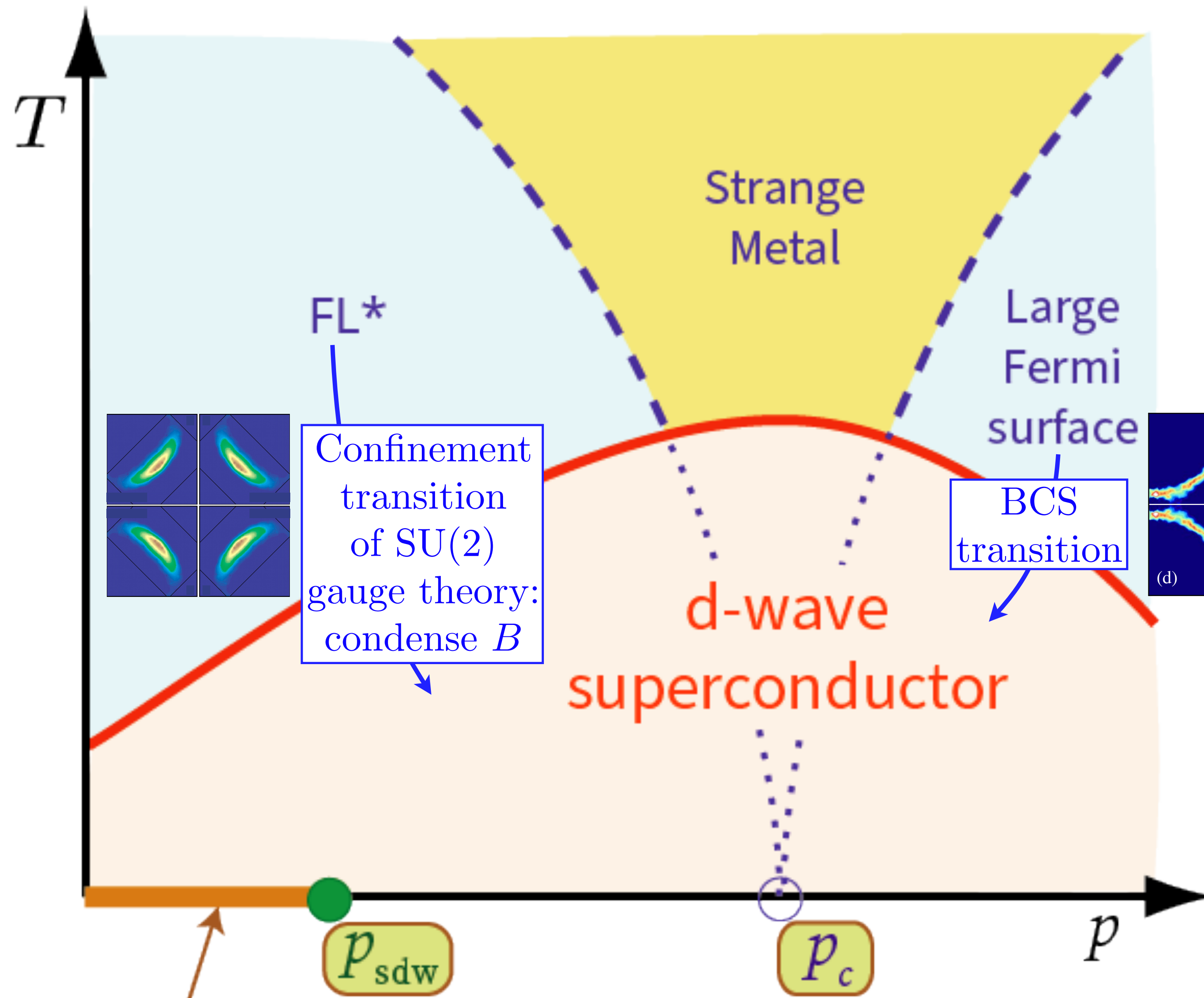
Spin density wave (SDW)



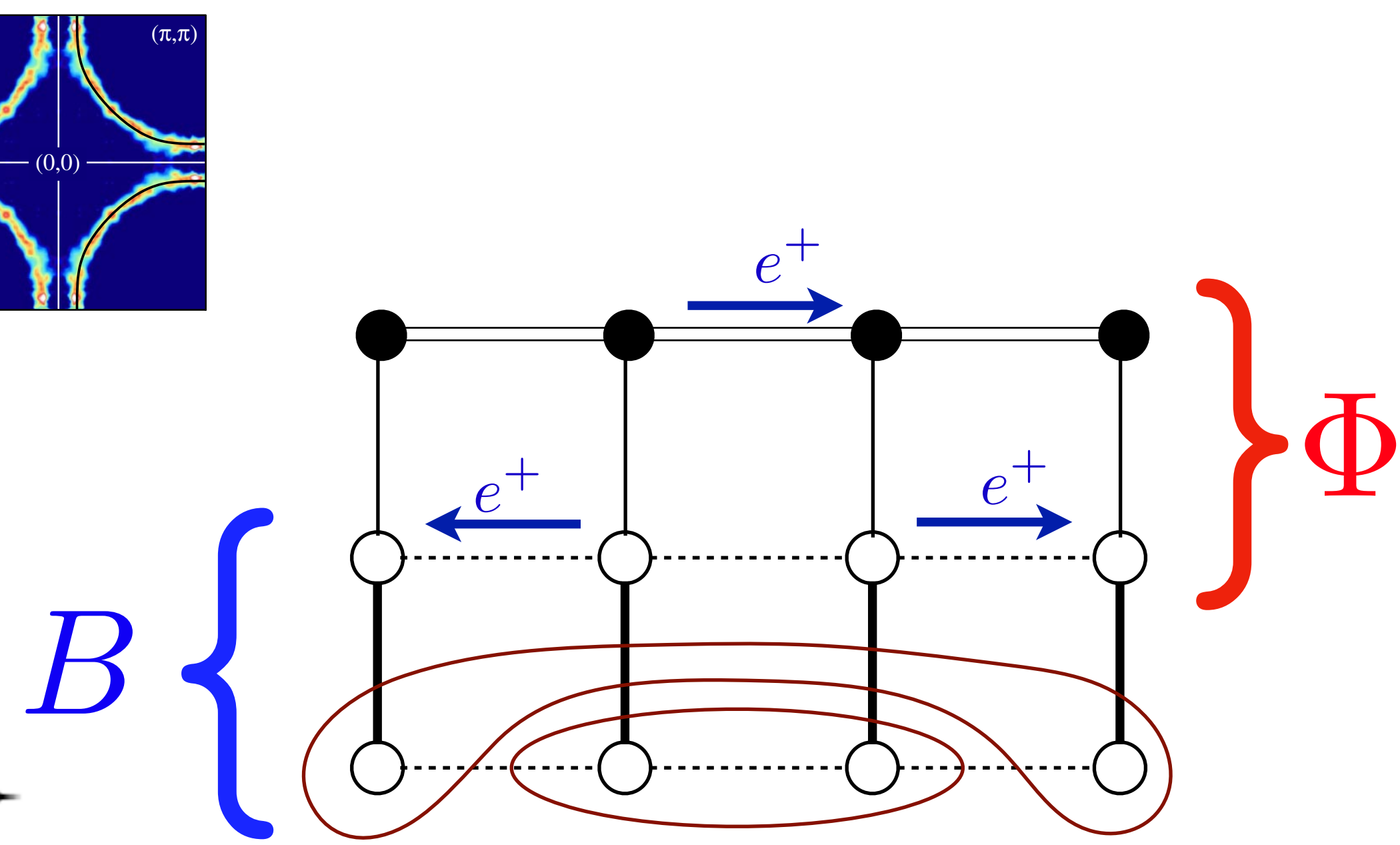
Both metals lead to the same *d*-wave superconductor at lower temperatures, and so there is no transition at $p = p_c$ within the superconducting state.



Spin density wave (SDW)



Both metals lead to the same *d*-wave superconductor at lower temperatures, and so there is no transition at $p = p_c$ within the superconducting state.



Spin density wave (SDW)